Uncovering novel biomarkers for Parkinson's disease and its prodromal stages

Marta Soto Gimeno

Biomedicine PhD program of the Universitat de Barcelona

Uncovering novel biomarkers for Parkinson's disease and its prodromal stages

This thesis has been realised in the laboratory of Parkinson's disease and other movement disorders of the Institut d'Investigacions Biomèdiques August Pi i Sunyer (IDIBAPS) – Hospital Clínic de Barcelona

PhD Student: Marta Soto Gimeno

Supervisors: Dr. Mario Ezquerra Trabalón & Dr. Rubén Fernández-Santiago

Tutor: Dr. Cristina Malagelada Grau

M. Soto Dr. M. Ezquerra Dr. R. Fernández-Santiago Dr. C. Malagelada

CLÍNIC BARCELONA Hospital Universitari

IDIBAPS

Universitat de Barcelona

CERTIFICATE OF DIRECTION

Dr. Mario Ezquerra Trabalón and Dr. Rubén Fernández-Santiago

CERTIFY: That the work "*Uncovering novel biomarkers for Parkinson's disease and its prodromal stages*" written and presented by Marta Soto Gimeno to qualify for Doctor in Biomedicine for the University of Barcelona has been done under our direction and the supervision of her tutor Cristina Malagelada Grau and meets all requirements to be presented and defended in the presence of the corresponding thesis committee.

The original research articles that comprise this thesis in order of publication and their impact factor are the following:

[Article 1]. Serum MicroRNAs Predict Isolated Rapid Eye Movement Sleep Behavior Disorder and Lewy Body Diseases. Mov Disord. 2022; 37: 2086-2098. (JCR'21 IF: 9.698 Q1)

[Article 2]. Differential serum microRNAs in premotor LRRK2 G2019S carriers from Parkinson's disease. NPJ Parkinsons Dis. Status: accepted (JCR'21 IF: 9.304 Q1)

[Article 3]. Combined CSF α-SYN RT-QuIC, CSF NFL and midbrain-pons planimetry in degenerative parkinsonisms: From bedside to bench, and back again. Parkinsonism Relat Disord. 2022; 99: 33-41. (JCR'20 IF:4.891 Q1)

Article 1 and 2 have not been included in any other thesis, nor will they in the future. Article 3 will also be part of the future thesis of Cèlia Painous Martí supervised by Dr. Yaroslau Compta Hirnyj. In that study the PhD candidate of the current thesis, Marta Soto Gimeno, set up and performed the RT-QuIC experiments and NFL ELISAs and strictly the methodological aspects of these techniques are the topics included in the current thesis; for her part Cèlia Painous Martí collected the demographic and clinical data, took part in the lab experiments and performed the statistical analysis in that article, with the clinical aspects of the differential diagnosis between parkinsonisms using these biomarkers in combination, along with their clinical and imaging correlates being the focus of her impending thesis.

Dr. M. Ezquerra Dr. R. Fernández-Santiago Dr. C. Malagelada

ACKNOWLEDGMENTS

Realitzar aquesta tesis no m'hagués estat possible sense l'ajuda i el suport de totes les persones que han estat al meu voltant durant aquests 4 anys, tant a nivell professional com personal.

En primer lugar, quiero agradeceros, Mario y Rubén, la oportunidad que me habéis dado y el apoyo continuo durante todo este tiempo. Agradezco mucho vuestra dedicación e implicación que me está permitiendo cerrar este proyecto cumpliendo todos mis objetivos y con muy buenos resultados. Teneros a los dos como directores y trabajar con vuestros puntos de vista complementarios ha sido muy enriquecedor y me ha ayudado a crecer como científica. Vull agrair també a la meva tutora, Cristina Malagelada, l'eficiència amb que sempre m'ha respost.

També vull agrair a totes les persones que han contribuït a fer-me un petit lloc a la unitat de Parkinson i altres trastorns del moviment. Al Dr. Compta per haver-me brindat l'oportunitat de reenganxar-me al laboratori quan semblava complicat i per la confiança que has dipositat en mi des del primer dia. A la Dra. Martí pel suport continuat durant tots aquests anys. Al Dr. Iranzo, l'Alicia i la Cèlia, perquè el treball conjunt ha estat una part fonamental d'aquests projectes i una experiència molt enriquidora. A la Laura Maragall, gràcies per fer-me un cop de mà sempre que pots i ajudar-me a desxifrar informació impossible. A la Marina, la Donina i després la Carlota, l'Ana, la Sandra i l'Almudena per tots els moments de bon rollo quan veniu al vostre moment "zen" al laboratori.

A la familia del 3B. La verdad que lo pienso y que paciencia habéis tenido todos para aguantar todas mis quejas e indignaciones, por la tesis, pero también por la RENFE, el metro, los patinetes, el gas, la burocracia, los alquileres de pianos, y cualquier cosa, vaya.

Los primos de AD. Cris, parece que queda muy lejos cuando estabas aquí de compi de mesa. Gracias por amenizarme los días durante los primeros años de tesis, gracias por inculcarme la importancia de comer a la hora, por no dejarme sola ante las tomaduras de pelo de Paqui y Manel, por los viernes *to guapos* y

todas las clases de yoga. Guada, gracias por ese *hoooooolaaa!* característico trayendo siempre alegría y buen rollo al laboratorio. Óscar, mi compi de doctorado, dicen que mal de muchos, consuelo de tontos ¡y nosotros muy tontos! Muchas gracias por todos los consejos y el apoyo diario.

También quiero dar las gracias a Paula Melón, por haber sufrido conmigo las extracciones de los dichosos microRNAs y haberte fiado de que te enseñase. A Jésica, siempre poniendo una sonrisa al día con tu carácter alegre y buen sentido del humor. A Idoia, con los del labo que pareces ya una más de lo que te gusta venir a vernos. Gracias por los cafés, las reformas compartidas, los momentos de hacernos perder el tiempo mutuamente y también los de escucharnos con nuestras rayadas.

A las nuevas incorporaciones que, aunque hayamos coincidido tarde, no habéis dudado en echarme una mano en esta última etapa. Lorena, gracias por compartir tu sabiduría y experiencia desde el primer día. Guillem, gracias por saber escuchar y transmitir esta despreocupación que unas veces pone nerviosa, pero otras es tan necesaria. Dani, *jozú, poz que te voy a decí a ti*, gracias por dejarme imitarte mal y hacernos sesiones de risoterapia diarias, pero también por ayudar siempre que puedes. Y las *supernenas*, gracias por habernos distraído a mí y a mi cabeza prácticamente a diario con chorrocientas actividades durante esta última etapa, me ha dado mucha fuerza, ya lo sabéis. Ana, gracias por compartir mis indignaciones y estreses, pero siempre poniendo templanza. Laura, gracias por estar siempre dispuesta a lo que haga falta y por tu característica de alegría (y buen día).

Manel y Paqui, ya debe hace más de 5 años que me tenía que ir la primera vez y aquí sigo, unas cuantas quejas y pinchos de tortilla después. ¡ni con agua caliente! Paqui, me adoptaste como hija del lab antes incluso de aprenderte mi nombre, cuando aún era *la niña*, gracias por todos los momentos compartidos, el apoyo y las risas diarias. Manel, desde el día cero cuando me encontraste en la

puerta sin poder entrar no has dejado de ayudarme en todo lo que has podido, gracias, creo que no hubiese llegado a hacer esta tesis sin tu ayuda.

Esti y Jon, gracias por los cafés, masajes y visitas tan reconfortantes. Marc Espina, Anna Sancho, Anika, Laura, Mattia gràcies per totes els moments de respir a les converses de passadís donant suport quan cal i creant sempre bon ambient.

I a la vida més enllà de la feina, però no patint menys el doctorat, Laia, Xavi, Arnau i l'AMCV en general, gràcies per donar-me lucidesa al kebab cada divendres i per la paciència i el suport a "l'altra feina". Les meves *Vaquetes (VP)* gràcies per estar sempre presents tot i les dificultats per coincidir, sembla que ara estaré una mica més disponible.

I per acabar, com no, a la meva família. Carlitos, gràcies per recolzar-me, entendre'm i escoltar totes les meves xapes durant tot el doctorat i sobretot en aquest últim any de convivència. Joan, gràcies pel suport i aguantar els meus atabalaments cada vegada que li passa alguna cosa a l'ordinador. Mama i papa, gràcies per animar-me sempre a seguir treballant i esforçar-me i per posar-m'ho tot més fàcil per poder tirar el doctorat endavant.

Per acabar, vull dedicar aquest treball a la iaia Eusebia que segur que estaria molt contenta i molt orgullosa de veure on soc.

TABLE OF CONTENT

SUMMARY

Parkinson's disease (PD) is the most common neurodegenerative movement disorder characterised by loss of dopaminergic neurons and the accumulation of aggregated α-synuclein. Clinical diagnosis is based on the appearance of the cardinal motor symptoms, yet neurodegeneration begins years before. In addition, any imaging or laboratory test can diagnose PD or discriminate PD from other parkinsonisms conclusively. In this work, we investigated candidate diagnostic and early progression biomarkers of PD and related parkinsonisms with a particular focus on the early stages of the disease. More specifically, we explored microRNA expression levels as early progression biomarkers in serum samples from two longitudinal cohorts of premotor PD and PD at-risk subjects to assess their potential applicability. In addition, we also set up an α-synuclein real-time quacking-induced conversion (RT-QuIC) assay to investigate the presence of misfolded α-synuclein aggregates in cerebrospinal fluid of PD and related parkinsonisms. In PD at-risk and premotor PD cohorts, we identified specific serum miRNAs that hold potential as early PD progression or pheno-conversion biomarkers. In addition, we implemented the α-synuclein RT-QuIC technique in our laboratory with high diagnostic accuracy for PD. Altogether, our findings advance the current state-of-the-art in the development of early PD biomarkers and have implications for disease prediction and early detection, even at premotor stages.

ABBEVIATIONS

ABBREVIATIONS

α-SYN	alpha-synuclein
APs	Atypical parkinsonisms
AUC	Area-under-the-curve
CBD	Corticobasal degeneration
CNS	Central nervous system
CSs	Control subjects
CSF	Cerebrospinal fluid
DAn	Dopaminergic neurons
DaT-SPECT	Dopamine transporter single-photon emission computed tomography
DaT(-) L2NMC	DaT-negative L2NMC (normal dopaminergic function)
DaT(+) L2NMC	DaT-positive L2NMC (abnormal dopaminergic function)
DEmiR	Differentially expressed miRNA
DLB	Dementia with Lewy bodies
EMG	Electromyogram
GBA	*β-glucocerebrosidase gene*
GnRH	Gonadotropine-releasing hormone
GPi	Globus pallidus internus
GWAS	Genome-wide association study
iPD	Idiopathic PD
iRBD	Idiopathic RBD
KEEG	Kyoto Encyclopedia of Genes and Genomes
GO	Gene Ontology
LB	Lewy body
LBD	Lewy body diseases
LRRK2	*Leucine-rich repeat kinase 2 gene*
L2NMC	*LRRK2* mutations non-manifesting carriers

L2PD	*LRRK2* mutations associated PD
MCI	Mild cognitive impairment
miRNA	microRNA
MPTP	1-methyl-4-phenyl-1,2,3,6-tetrahydropyridine
MRI	Magnetic resonance imaging
MSA	Multiple system atrophy
MDS	Movement Disorders Society
NFL	Neurofilament light chain
NPV	Negative predictive value
PD	Parkinson's disease
PD-1	Programmed cell death 1
PD-L1	Programmed cell death ligand 1
PMCA	Protein misfolded cyclic amplification
PPV	Positive predictive value
PRS	Polygenic risk score
PSP	Progressive supranuclear palsy
RBD	REM-sleep behaviour disorder
REM-sleep	Rapid-eye-movement sleep
ROC	Ras-of-complex
ROC curve	Receiver operating characteristic curve
RT-QuIC	Real-time quaking-induced conversion
RT-qPCR	Real-time quantitative polymerase chain reaction
SNCA	*α-synuclein gene*
SNpc	Substantia nigra *pars compacta*
SAA	Seeding aggregation assays
TCS	Transcranial sonography
TGF-β	Transforming growth factor β
TNF	Tumor necrosis factor
TRAIL	Tumor necrosis factor-related apoptosis-inducing ligand

INTRODUCTIO

1. INTRODUCTION

1.1 Parkinson's disease - a growing disease

Parkinson's disease (PD) is the most common age-related[1] neurodegenerative movement disorder, with a prevalence of 2-3% among the population over 65 years.[2] Ageing is indeed considered the principal risk factor,[3] and the incidence is higher in men than women (ratio 1.37).[1,4] Nowadays, PD is the fastest-growing neurological disorder.[5] Over the past two decades, worldwide PD prevalence has more than doubled[4] and is expected to still increase, exceeding 12 million people by 2040.[6] Besides the increase in life expectancy and the longer disease duration, other environmental factors could be contributing to the increment of PD cases. Furthermore, PD entails a large economic burden, estimated at €17.000 per year per patient in Spain in 2013,[7] and a total of $51.9 billion in the US in 2017.[8]

PD was first described by the English apothecary-surgeon, geologist, palaeontologist, and political activist Mr James Parkinson in *An Essay on the Shaking Palsy* (1817). Parkinson made a description of 6 cases of 'paralysis agitans', a long-duration nervous disorder characterised by resting tremor of limbs, decreased muscular strength, and a stooped posture associated with gait impairment,[9] which remains valid today. Later, Jean-Martin Charcot coined the term 'Parkinson's disease' and described the disease more deeply, distinguishing bradykinesia as a separate cardinal symptom and recognising a cognitive component.[10] In 1957, Arvid Carlsson discovered the functional role of dopamine[11] but it was not until three years later that Oleh Hornykiewicz's laboratory linked a deep dopamine deficit to PD and introduced dopamine replacement through intravenous injections of levodopa as therapy.[12] After this discovery, the clinical trial with orally administered levodopa by George Cotzias in 1967 introduced the chronic oral levodopa treatment, which remains the cornerstone of symptomatic treatment of PD.[13]

Nowadays, PD is considered a progressive neurodegenerative disorder clinically characterised by both motor and non-motor features resulting from the early prominent death of midbrain dopaminergic neurons (DAn) in the substantia nigra *pars compacta* (SNpc).[14] The causes of the disease are still largely unknown, and no treatment is currently available that changes the natural history of the disease.

1.2 Parkinson's - clinicopathological spectrum

The characteristic neuropathological hallmarks of PD are midbrain SNpc depigmentation due to progressive loss of DAn and accumulation of aggregated α-synuclein into Lewy bodies into the few surviving neurons (**Figure 1a-b**). The striatal dopamine deficit in PD leads to increased inhibitory GABAergic outputs from basal ganglia (GPi) to the thalamus by two mechanisms: reduced activity of the direct pathway from the striatum to GPi and increased activity of the indirect pathway.[15] The overstimulation of the subthalamic nucleus in the indirect pathway and the over-inhibition of the thalamus to the cortex due to the lack of dopamine are associated with the PD cardinal motor symptoms of bradykinesia, muscular rigidity, and resting tremor.[16,17] Yet, by the time motor symptoms emerge, the neural loss has been estimated at 30% of the DAn and 60% of their axon terminals.[18] Other neurotransmitter systems beyond the dopaminergic, i.e., the cholinergic, noradrenergic, glutamatergic or serotonergic, are also affected in PD and have been related to non-motor features[19,20] such as hyposmia, rapid eye movement (REM)-sleep behaviour disorder (RBD), constipation or depression.

PD diagnosis can only be confirmed by neuropathological post-mortem evaluation. However, in clinical practice, the diagnosis is based on neurological examination following the International Parkinson and Movement Disorders Society (MDS) diagnostic criteria.[21] The prerequisite to applying the MDS-PD criteria to establish PD is the diagnosis of parkinsonism, i.e., bradykinesia with rigidity and/or resting tremor. Yet, comorbidities and the misclassification between parkinsonisms can hinder an accurate PD diagnosis, estimated at 80%,[22] reaching 90% in specialised services.[23] Overall diagnostic accuracy of all parkinsonisms, i.e., multiple system atrophy (MSA) progressive supranuclear palsy (PSP) and corticobasal degeneration (CBD) is estimated at 71%,[24] with a particularly challenging differential diagnosis at the early stages when the overlap of symptoms is high.[17] To date, any imaging or laboratory test can diagnose PD or discriminate between parkinsonisms conclusively.

Neuropathologically, in 2003, Braak and colleagues proposed a staging model for the progressive nature of PD that hypothesises a cauda-rostral spread of the Lewy pathology performed in 6 different stages (**Figure 1c**). According to Braak et al., Lewy body lesions begin in the enteric nervous system and the dorsal motor nucleus of the vagus, and the anterior olfactory nucleus in the olfactory bulb (stage 1), progress to the locus coeruleus and Raphe in the pons (stage 2) and reach the DAn of the SNpc in the midbrain (stage 3). Later, pathology affects the basal forebrain, amygdala, and medial temporal lobe structures (stage 4) and extends to multiple cortical regions, including the association cortex and primary motor cortex areas (steps 5 and 6).[25] In addition, Braak's staging model reflects the clinical course of the disease. First, the apparition of the premotor symptoms of autonomic dysfunction and hyposmia corresponding with stage 1, followed by RBD and depression in stage 2.[26] Then, stages 3 and 4 when cardinal motor features appear, and finally, with the presence of significant gait symptoms and dementia at stages 5 and 6, relating to severe PD. However, Braak's staging model is mainly valid for PD cases with young onset and long duration with motor symptoms but does not explain other PD cases such as those with late-onset and rapid curse or those of individuals without neurological signs in life that show Braak stage 6 postmortem.[27,28]

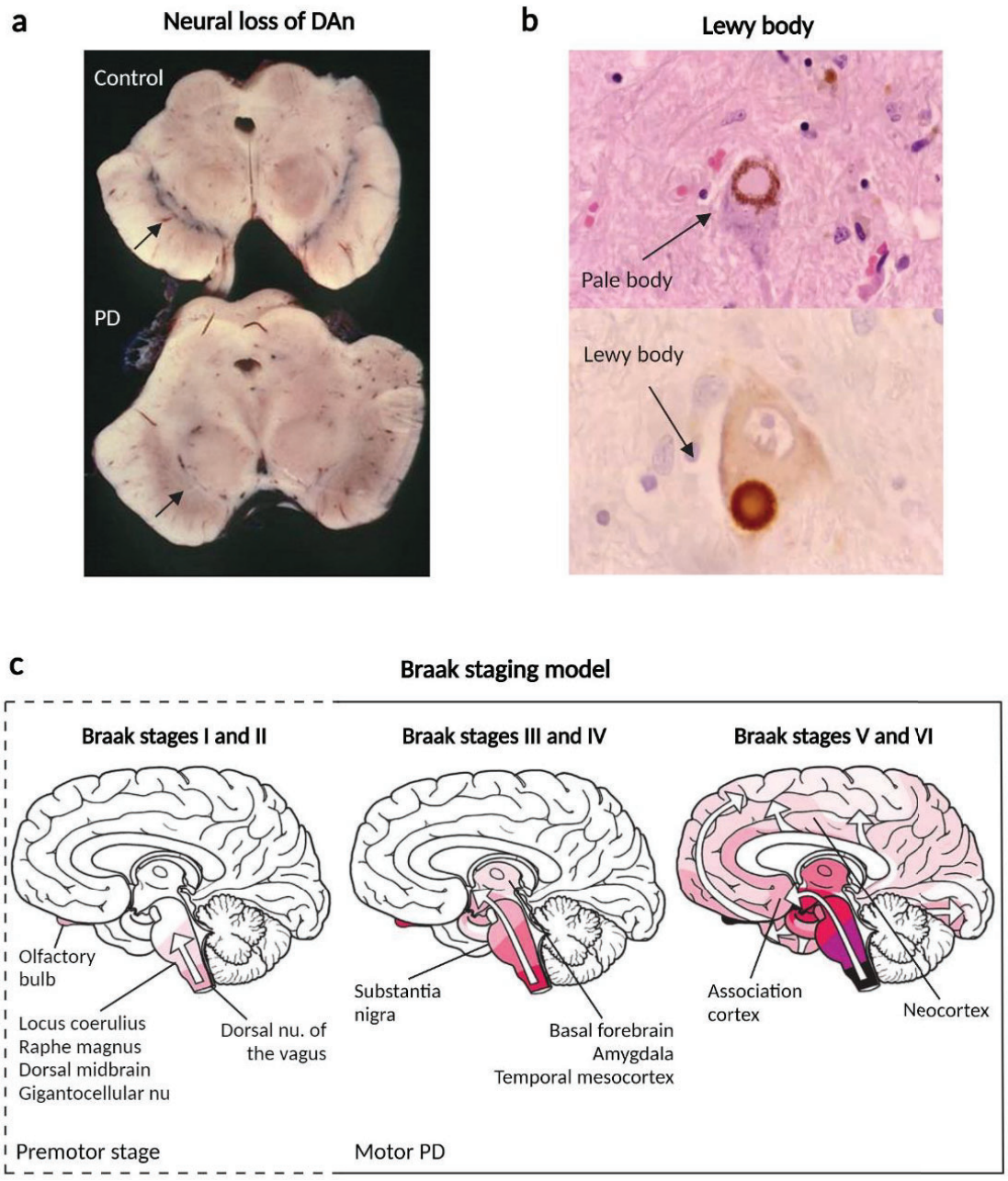

Figure 1 | Neuropathology of Parkinson's disease. (a) Macroscopical transverse section of the midbrain, showing depigmentation of the SNpc due to the neural loss of DAn. (b) Hematoxylin eosin-stained section of SNpc with a pigmented Pale body surrounded by neuromelanin and α-synuclein immunostained section of SNpc with a Lewy body. *Images courtesy of the Neurological Tisue Bank (BTN) of the Hospital Clínic de Barcelona*. (c) Progression of Parkinson's disease brain pathology according to Braak staging model. *Adapted from Neurobiol Aging. 2003; 24: 197-211.* DAn = dopaminergic neurons; SNpc = substantia nigra pars compacta.

1.3 Parkinson's disease – as an α-synucleinopathy

The accumulation of misfolded α-synuclein is a central pathogenic process in PD. The α-synuclein protein consists of three regions: the N-terminal domain, comprising an amphipathic region which contains the three known missense mutations causing familial PD; the central hydrophobic region associated with the capacity to form fibrils; and the acidic C-terminal tail containing negatively charged residues in which post-translational modifications can influence the propensity of the protein to aggregate.[29] The α-synuclein protein is located at presynaptic terminals, where it regulates neurotransmitter release, synapsis formation and plasticity.[30] Physiologically, native α-synuclein exist as monomers and protective α-helical tetramers,[31] whereas pathological forms occur as toxic oligomers with β-sheet structure and subsequent fibrils or strains.[32]

Lewy pathology is characterised by misfolded α-synuclein aggregates in the cell body, Lewy bodies, and the neural process, Lewy neurites, producing proteinaceous inclusions.[33] The α-synuclein aggregated species seems to be capable of initiating PD pathological processes.[34] Thus, cell culture and animal model studies revealed that the aggregation capacity of α-synuclein spread in a prion-like manner.[35–37] This concept has been reinforced with the advent of the new α-synuclein seeding aggregation assays (SAA) that exploit the aggregating properties of α-synuclein to detect pathogenic species.[38,39] Lewy pathology has been detected in different brain regions but also in the spinal cord and peripheral organs, e.g., retina, skin, submandibular glands, or bowels, indicating systematic pathology.[40] Yet, neurons containing neuromelanin, such as DAn, are particularly susceptible.[41] Neuromelanin is a derivative of oxidised dopamine that stores iron and other toxins, apparently as a neuroprotective response.[41,42] However, abnormally high levels of intracellular neuromelanin have been associated with dopaminergic death and motor phenotypes in rodents,[43,44] possibly caused by the increased levels of neuromelanin-bound iron.[45] Thus, age-dependent neuromelanin accumulation could be another cause of neural loss in PD.

Beyond PD, the accumulation of misfolded α-synuclein involves a spectrum of disorders known as α-synucleinopathies, i.e., dementia with Lewy bodies (DLB) and MSA.[46] Comparatively, in PD and DLB, misfolded α-synuclein is located in the neuronal cytoplasm and axonal processes, while in MSA, affects most prominently the oligodendroglia.[47] Remarkably, a recent study revealed different conformational strains of pathogenic α-synuclein in PD and MSA.[48] Phenotypically, all α-synucleinopathies share common symptoms, including parkinsonism but also prodromal signs such as RBD, often with clinical heterogeneity. Thus, DLB begins with dementia, also present in 45% of PD cases within ten years from the diagnosis,[49] and later progresses to parkinsonism.[50] Per contrary, MSA is characterised by autonomic dysfunction with motor subtypes of predominant parkinsonism or cerebellar.[51] Collectively, a deeper understanding of the pathophysiology underlying α-synucleinopathies is crucial for the development of biochemical markers that allow their differential diagnosis.

In addition, α-synucleinopathies and specific tauopathies share parkinsonian symptoms and are classified altogether as atypical parkinsonisms, yet the neuropathological substrate is different. Thus, PSP and CBD are tauopathies involving abnormal deposition of 4-repeat tau in neurons, oligodendrocytes, and astrocytes, differing in the astrocytic tau morphology.[52] PSP usually presents with supranuclear gaze palsy and early postural instability. Yet, in early stages, cases without gaze or with clear parkinsonism, sometimes with response to levodopa, can be misdiagnosed as PD. CBD features asymmetrical parkinsonism with apraxia or cortical sensory disturbance, with cognitive deficits ranging from aphasia to multidomain dementia being possible. In clinical practice, the misdiagnose of parkinsonisms is common even by movement disorders specialists (15%),[23] particularly during early disease stages, and no specific biomarker for conclusive diagnosis is yet available.[22] Thus, developing new tools for an accurate diagnosis is critical for predicting prognosis and planning particular treatments.

1.4 Parkinson's genetics - driving mechanistic discovery

For long, PD was considered an environmental disease with little familial segregation. For instance, in 1982, exposure to the synthetic heroin, 1-methyl-4-phenyl-1,2,3,6-tetrahydropyridine (MPTP) was identified as a cause of PD-inducing[53] dopaminergic loss by oxidative stress, mitochondrial apoptosis, inflammation and excitotoxicity.[54] However, in 1997, mutations in the *SNCA* gene were identified for the first time as the first genetic cause of PD.[55,56] This discovery was instrumental for understanding the aetiology of PD, allowing the identification of α-synuclein as the main component of the Lewy bodies,[33] and the subsequent development of the Braak progression model.[25] After *SNCA* identification, pesticides such as rotenone or paraquat,[57] extended exposure to manganese,[58] or traumatic brain injury,[59] were subsequently linked to PD. Yet, the genetic discovery in PD has also continued. Currently, PD is considered a complex multifactorial disease, in which idiopathic PD (iPD) represents 90-95% of the cases, whereas 5-10% are monogenic forms linked to mutations that segregate with the disease.

Despite its marginal percentage of cases, the monogenic discovery has been key to modelling disease mechanisms, which might share common traits with iPD. In addition, monogenic forms represent an exceptional opportunity to establish a definitive diagnosis in life, expand our knowledge of the pathophysiology of PD, and develop new therapeutic strategies.[60] To date, 23 PD-causative genes have been associated with inherited forms of parkinsonism (**Table 1**).[61] Thus, mutations in *SNCA*, *LRRK2* (*leucine-rich repeat kinase 2*) and *VPS35* genes have been unequivocally associated with autosomal dominant PD, whereas mutations in *PRKN*, *PINK-1* and *DJ-1* cause early-onset autosomal recessive PD. In addition, mutations at the GBA gene, which encodes for the lysosomal enzyme β-glucocerebrosidase, are considered the most significant genetic risk factor for sporadic PD.[62]

Gene symbol	Full gene name	Disease mechanism	Inheritance	Onset	Type	Ref
SNCA	Synuclein alpha	Gain of function	AD	EO/LO		[56]
PRKN	Parkin RBR E3 ubiquitin protein ligase	Loss of function	AR	EO		[63]
UCHL1	Ubiquitin C-terminal hydrolase L1	Loss of function	AD	EO/LO		[64]
PARK7 (DJ-1)	Parkinsonism associated deglycase	Loss of function	AR	EO		[65,66]
PINK1	PTEN-induced putative kinase 1	Loss of function	AR	EO		[67,68]
LRRK2	Leucine rich repeat kinase 2	Gain of function	AD	LO		[69,70]
POLG	DNA polymerase gamma, catalytic subunit	Loss of function	AD	EO	Atypical PD	[71]
HTRA2	HtrA serine peptidase 2	Loss of function	AD	LO		[72]
ATP13A2	ATPase cation transporting 13A2	Loss of function	AR	EO	Atypical PD	[73]
GIGYF2	GRB10 interacting GYF protein 2	Unclear	AD	LO		[74]
FBXO7	F-box protein 7	Loss of function	AR	EO	Atypical PD	[75]
PLA2G6	Phospholipase A2 group VI	Loss of function	AR	EO	Atypical PD	[76]
VPS35	VPS35 retromer complex component	Loss of function	AD	LO		[77]
EIF4G1	Eukaryotic translation initiation factor 4 gamma 1	Unclear	AD	LO		[78]
DNAJC6	DnaJ heat shock protein family (Hsp40) member C6	Loss of function	AR	EO	Atypical PD	[79]
SYNJ1	Synaptojanin 1	Loss of function	AR	EO	Atypical PD	[80]
DNAJC13	DnaJ heat shock protein family (Hsp40) member C13	Unclear	AD	LO		[81]
CHCHD2	Coiled-coil-helix-coiled-coil-helix domain containing 2	Loss of function	AD	LO		[82]
VPS13C	Vacuolar protein sorting 13 homolog C	Loss of function	AR	EO	Atypical PD	[83]
TMEM230	Transmembrane protein 230	Loss of function	AD	LO		[84]
RIC3	RIC3 acetylcholine receptor chaperone	Unclear	AD	LO		[85]
LRP10	LDL receptor related protein 10	Loss of function	AD	LO		[86]
ARSA	Arylsulfatase A	Unclear	AD	LO		[87]

Table 1 | Genes associated with monogenic Parkinson's disease. Gene symbol and full gene name provided by HGNC. AD = autosomal dominant; AR = autosomal recessive; EO = early-onset; LO = late-onset.

Among the monogenic PD forms, *LRRK2*-associated PD is of high research interest since it is the most frequently known cause of late-onset genetic PD and clinically closely resembles iPD. Thus, findings in the disease mechanisms or therapeutic strategies in *LRRK2*-associated PD could also apply to iPD. Interestingly, *LRRK2* mutations are detected not only in a relatively large number of autosomal dominant familial PD cases,[69,70] but also in apparently sporadic PD.[88] This is explained by mechanisms of incomplete penetrance influenced by still largely unknown additional genetic or environmental modifying factors.[89,90] From the mechanistic point of view, pathogenic missense variants identified in the gene are consistent with a toxic gain of function mechanism related to a hyperactivation of the kinase activity of the protein.[91] A total of 7 *LRRK2* variants (p.N1437H, p.R1441C/G/H, p.Y1699C, p.S1761R, p.G2019S, p.I2012T and p.I2020T), located at the enzymatic core of the protein, have been established as pathogenic by linkage and biochemical studies.[88,92]

LRRK2 gene encodes a 2.527-amino acid protein whose enzymatic core comprises two distinct domains, a Ras-of-complex (ROC) GTPase with its C-terminal domain (COR) and a serine/threonine kinase domain. The most frequent *LRRK2* mutation is p.G2019S which is responsible for up to 6% familial and 3% sporadic PD cases in Europeans,[93,94] up to 20% of the total cases among Ashkenazy Jews[95] or 40% in North African Berbers.[96] The founder event of the G2019S mutation, associated with the most common haplotype, was probably 3.800 years ago in North Africa.[97] The penetrance of G2019S is reduced but increases with age, being estimated at 25%-42% at the age of 80.[98,99] Clinically, *LRRK2* G2019S-associated PD is characterised by initial asymmetric tremor, good response to levodopa and slow and benign progression, thus largely resembling common iPD.[100] Recently, the reduction of *LRRK2* expression and activity has been identified as neuroprotective. Consequently, current therapeutic approaches for *LRRK2*-associated PD, which could also be applied to iPD, are exploring the use of LRRK2 kinase inhibitors as neuroprotective drugs.[101]

Given its high frequency, *LRRK2* non-manifesting mutation carriers represent an exceptional condition for studying individuals at-high-risk of PD before the onset of motor symptoms and the ideal window to administrate neuroprotective therapies. However, the variability and uncertainty in *LRRK2* mutation penetrance represent an obstacle to identifying asymptomatic LRRK2 carriers who will end up developing PD. Further hampering the prediction of PD development, non-motor symptoms preceding the motor manifestation of the disease seem to be scarce in *LRRK2*-associated PD,[102,103] and there are still no other predictive markers available.

Beyond the rare variants with high effect sizes, causative of familial or monogenic PD forms, the genetic contribution to PD also involves common variants with small effect sizes, commonly identified in iPD and considered genetic risk-modifying factors.[104,105] The advent of genome-wide association studies (GWAS) has transformed the understanding and detection of the genetic risk factors in PD by identifying multiple genetic risk loci. A recent PD GWAS meta-analysis in individuals of European ancestry has identified 90 significant independent risk signals that explained 16-36% of the heritable risk of PD.[106] Statistically compiling the effect of multiple genetic markers from GWAS, polygenic risk scores (PRS) estimate the genetic propensity of an individual for the disease or a particular characteristic.[107] PRS holds the potential for classifying individuals according to their disease risk, identifying those with a high predisposition to PD, and predicting age-dependent clinical outcomes. In addition, searching for epistatic interactions involving polymorphism that could be hidden in conventional analyses offers new possibilities, specifically in PD.[108,109] The interaction-based prediction model could also be used to outperform the PRS.[110] Yet, to successfully implement PRS in clinical practice, further investigation is needed.[111]

1.5 Premotor Parkinson's - novel opportunities for the early intervention

Premotor PD is recognised as an early disease phase in which neurodegeneration is already in progress, but cardinal motor symptoms have not yet appeared.[112] By the time of clinical PD diagnosis, approximately 30% of the DAn has already been lost.[18] Early non-motor symptoms include constipation, RBD, hyposmia, or depression,[113,114] and can appear ten or even twenty years before the onset of motor symptoms (**Figure 2**).[113,115,116] Thus, the premotor stage represents an opportunity to explore the molecular and physiological mechanisms underlying PD onset and to understand the earliest events of the disease progression. Nowadays, premotor PD is closely linked to disease prediction ahead of motor manifestation.[117–119] Ultimately, the premotor stage offers an exclusive and time-limited window to stop the neurodegeneration and prevent the development of more disabling and potentially irreversible motor symptoms when most DAn are still preserved. Therefore, the premotor periods are the ideal targets for testing disease-modifying therapies to prevent or delay the neurodegenerative process. However, identifying individuals at the premotor PD stage is complex due to the wide range of premotor symptoms and their low specificity in most cases.

In recent years, more than 15 PD prodromal symptoms and signs have been described in prospective studies.[114,120] Despite showing predictive value for PD appearance, the sensitivities of all these markers are highly variable, and the specificity is low in most cases. Thus, hyposmia exhibits the highest sensitivity of more than 80%, followed by autonomic dysfunction (50-80%), RBD (40%), and depression (30%).[112] Symptoms such as RBD, constipation or hyposmia are considered premotor signs of α-synucleinopathies, mainly PD and DLB but also MSA.[121,122] Yet, RBD is the premotor symptom with the highest risk of developing manifest α-synucleinopathy and is therefore considered the strongest prodromal PD predictor nowadays.[112] Presence of other prodromal PD symptoms, such as hyposmia, depression and constipation, have also been concomitantly described in RBD cases.[123]

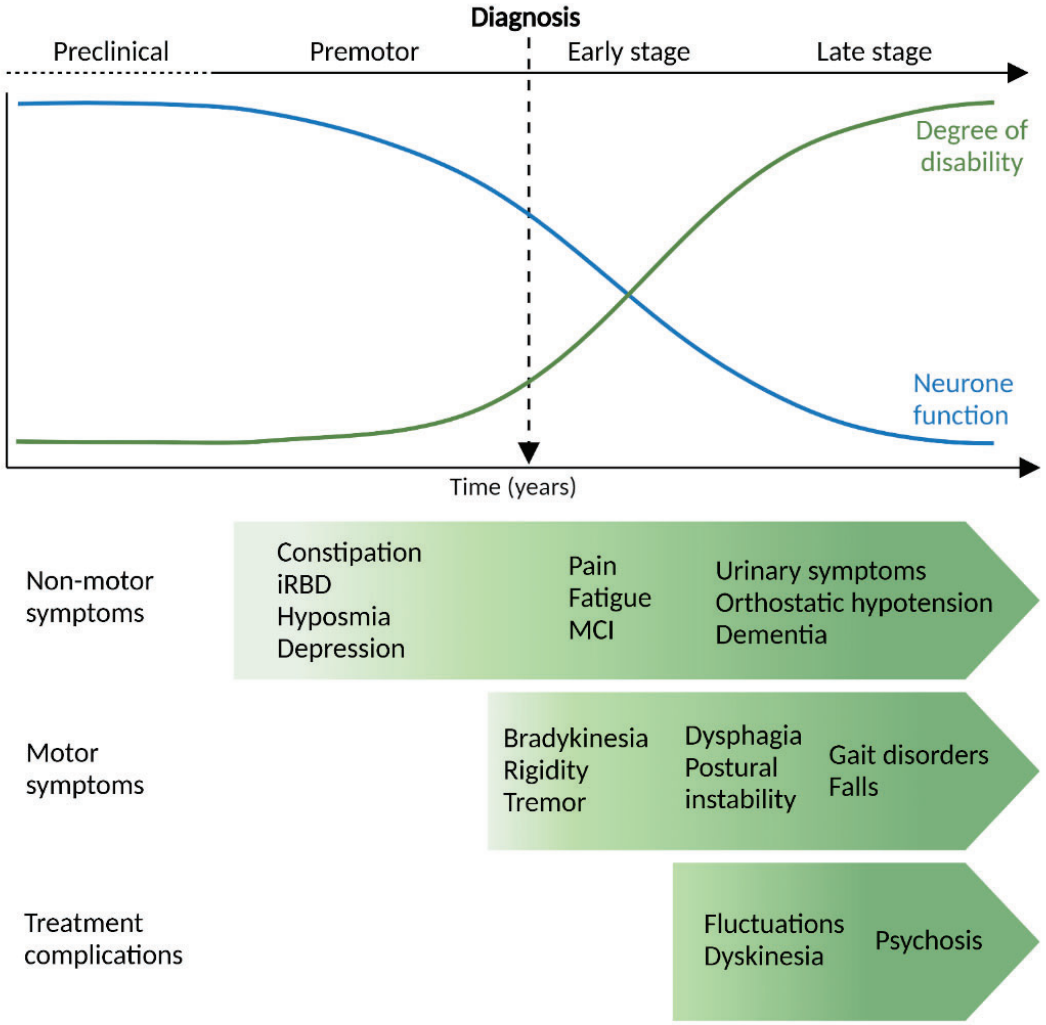

Figure 2 | Progression of Parkinson's disease clinical symptoms. Diagnosis of Parkinson's disease is based on the onset of the cardinal motor symptoms, yet the preclinical and premotor stages precede it. The premotor stage is characterised by non-motor symptoms, which still emerge in the manifested disease. In more advanced stages, besides axial motor symptoms, long-term treatment complications appear, increasing the disability. MCI = mild cognitive impairment

RBD is a widely studied clinical marker of the premotor stage of PD and related α-synucleinopathies, specifically MSA or DLB.[124–126] Thus, investigating RBD can help to understand early disease mechanisms and identify early progression and pheno-conversion biomarkers. Idiopathic RBD (iRBD) is a rare parasomnia characterised by a pronounced motor activity during REM sleep due to the absence of REM sleep-related muscle atonia.[127] More specifically, iRBD activity involves dreaming enactment behaviours, such as talking, gesturing, grabbing, or punching, that may cause physical damage to either the patient or the bed partner. The diagnosis of RBD requires altered polysomnography (PSG), measuring muscle activity by electromyogram (EMG) during REM sleep, and ruling out mimics.[128] In an average of 14 years from iRBD diagnosis, longitudinal studies revealed that more than 80% of the patients develop an α-synucleinopathy, mainly Lewy pathology spectrum (with PD and DLB as two ends of this spectrum), but also MSA, a non-Lewy glial predominant synucleinopathy.[116,129] Yet, only 30% of PD patients have iRBD at the onset of motor symptoms, and neither the time to pheno-conversion nor the specific clinical outcome could be predicted before the development of motor symptoms.

In normal sleep, skeletal motoneurons are tonically hyperpolarised during REM sleep, leading to muscular atonia. Functional and pharmacological studies showed that GABA and glycine induce the hyperpolarisation of the motoneurons and their consequent inhibition. Moreover, atonia is also mediated by decreased motoneuron excitation due to diminished glutamatergic, noradrenergic, serotoninergic, dopaminergic and hypocretinergic activity. Therefore, abnormal motor activity in RBD could be explained by the breakdown of inhibitory GABA and glycine circuit function, reinforced by activation of the typically silent excitatory mechanisms.[130] Neuroanatomically, distinct brainstem structures such as subcoeruleus complex (glutamatergic activity), gigantocellularis reticular nucleus (GABAergic activity), dorsal raphe nucleus, and pedunculopontine nucleus are affected in iRBD.[131,132]

Genetically, there is a partial overlap between iRBD and α-synucleinopathies. Of the two genes most commonly associated with PD, *GBA* and *LRRK2*, mutations in *GBA* have been described as the strongest genetic factor associated with iRBD,[133,134] while mutations in *LRRK2* are not related to iRBD.[135] Indeed, *LRRK2*-associated PD is negatively associated with prodromal features of iPD, such as iRBD or hyposmia. In addition, diverse variants in the SNCA gene have been associated with iRBD and PD.[136] Both iRBD and *GBA*-associated PD are linked to a gait impairment phenotype with more severe autonomic dysfunction and dementia.[137–139] These differences in the genetics of PD and iRBD, and particularly the absence of *LRRK2* mutations in iRBD patients, highlight the possibility that independent processes could ultimately converge into a typical PD motor phenotype. Still, the study of iRBD could improve the prognostic accuracy at prodromal stages of the different parkinsonisms associated with RBD (PD, MSA and DLB), ultimately aimed at effective and personalised management of the disease.

1.6 Parkinson's biomarkers - a contextualised synopsis

Early detection is essential in PD for implementing early neuroprotective interventions to slow, prevent or halt disease progression. In this context, a biomarker is defined as 'a characteristic that is objectively measured and evaluated as an indicator of normal biological processes, pathogenic processes, or pharmacological response to a therapeutic intervention'.[140] Besides the interest as clinical and diagnostic tools, biomarkers also have a key role as surrogate endpoints in clinical trials.[141] Early PD detection in the premotor phases is not yet possible since there is a long latency between the onset of neurodegeneration and motor manifestation. Therefore, searching for reliable diagnostic or early progression PD biomarkers has become a focus of increasing interest. Current candidate biomarkers of PD include neuroimaging, olfactory testing, genetic susceptibility, and tissue and biofluid molecular compounds.[142] Nevertheless, there is still no definitive biomarker to predict or conclusively diagnose PD or atypical parkinsonisms.[143]

Neuroimaging biomarkers, including single-photon emission computed tomography (SPECT), positron emission tomography (PET), magnetic resonance imaging (MRI) and transcranial sonography (TCS), have been evaluated to distinguish PD and atypical parkinsonisms.[144] None of these tests can discriminate among degenerative parkinsonisms, yet they can aid as adjuvant tools for the diagnosis.[145] For example, while dopamine levels cannot be determined directly, SPECT or PET allow the testing for dopaminergic innervation.[146] SPECT using dopamine transporter (DaT) ligands (DaT-SPECT) can measure the decline in DaT density, which strongly correlates with the loss of striatal dopamine nerve terminal function. Therefore, DaT imaging is informative of presynaptic dopaminergic deficit and is considered an imaging marker of nigrostriatal degeneration. Thus, DaT imaging differentiates degenerative parkinsonism from secondary causes, such as vascular or drug-induced parkinsonism and essential tremor.[147,148] Indeed, a reduced striatal uptake has been observed by DaT-SPECT

in *LRRK2*-associated PD and iRBD cases, even antedating the motor manifestation.[149,150] In addition, the DaT deficit appears less intense in iRBD than in manifest PD, supporting DaT-SPECT as a valuable tool to measure disease progression.[151,152] However, not all iRBD patients show concordance with these findings. On the other hand, MRI has exhibited reduced midbrain and pons areas in PSP and MSA, respectively, contributing to the distinction between parkinsonisms. Overall, imaging markers are used as adjuvant tools for the differential diagnosis of parkinsonism, yet with some controversies, mainly when correlating neuroimaging with clinical changes over time in early disease.[153,154]

Regarding molecular biomarkers, peripheral tissue and biofluids are suitable sources given the minimally invasive sampling procedure.[155] Beyond the central nervous system, α-synuclein pathological changes have been described in several PD tissues, such as skin, colon, and salivary glands, even in early stages, providing new diagnostic approaches.[40] Given its significant role in PD, levels of α-synuclein in plasma and cerebrospinal fluid (CSF) have been widely studied, yet with a lack of discrimination power and specificity in some cases.[156–158] Recently, SAA, which exploits self-aggregation properties of the prion proteins, have been successfully implemented as a diagnostic test for prion diseases.[159] As aggregated α-synuclein propagates in a prion-like manner,[35] α-synuclein SAA aim at the clinical assessment of α-synucleinopathies using CSF and peripheral tissues such as skin[160,161] or olfactory mucosa.[162,163] SAA include the protein misfolded cyclic amplification (PMCA) assay[38] and the real-time quaking-induced conversion (RT-QuIC) assay.[39] Overall, CSF α-synuclein RT-QuIC discriminant analysis (**Figure 3**) in PD showed high sensitivity and specificity, 89% and 96%, respectively, while results in MSA are more inconsistent.[119,164,165] Despite the good perspectives, the methodology needs standardisation, especially regarding the recombinant substrate, which may be the main limitation of the technique nowadays.

Other candidate molecular biomarkers are also under investigation. For instance, the neurofilament light chain (NFL) concentration has been extensively studied in CSF as an unspecific biomarker of aggressiveness of neurodegeneration. Increased levels of NFL demonstrated high accuracy in discriminating PD from atypical parkinsonism but are unspecific among atypical parkinsonism.[166] Mounting evidence supports the measurement of NFL in blood as its plasma levels significantly correlate with CSF NFL levels.[167]

In addition, in blood and its derivatives, cumulative evidence has revealed that the expression levels of circulating microRNAs (miRNAs), which are small non-coding RNAs regulating gene expression by mRNA cleavage or translation repression,[168] are altered in PD.[169–173] MiRNAs are considered promising candidate biomarkers for neurodegenerative diseases as they are easily accessible, well preserved in fresh frozen specimens, less expensive and time-consuming than other markers, and applicable with standard laboratory equipment.[174] However, the overlap of differentially expressed miRNAs between studies is still limited, owing to methodological differences and population-specific effects.[175] Thus, circulating miRNAs are promising biomarkers for PD, but further efforts are required to improve our knowledge and to be able to apply it in clinical practice.

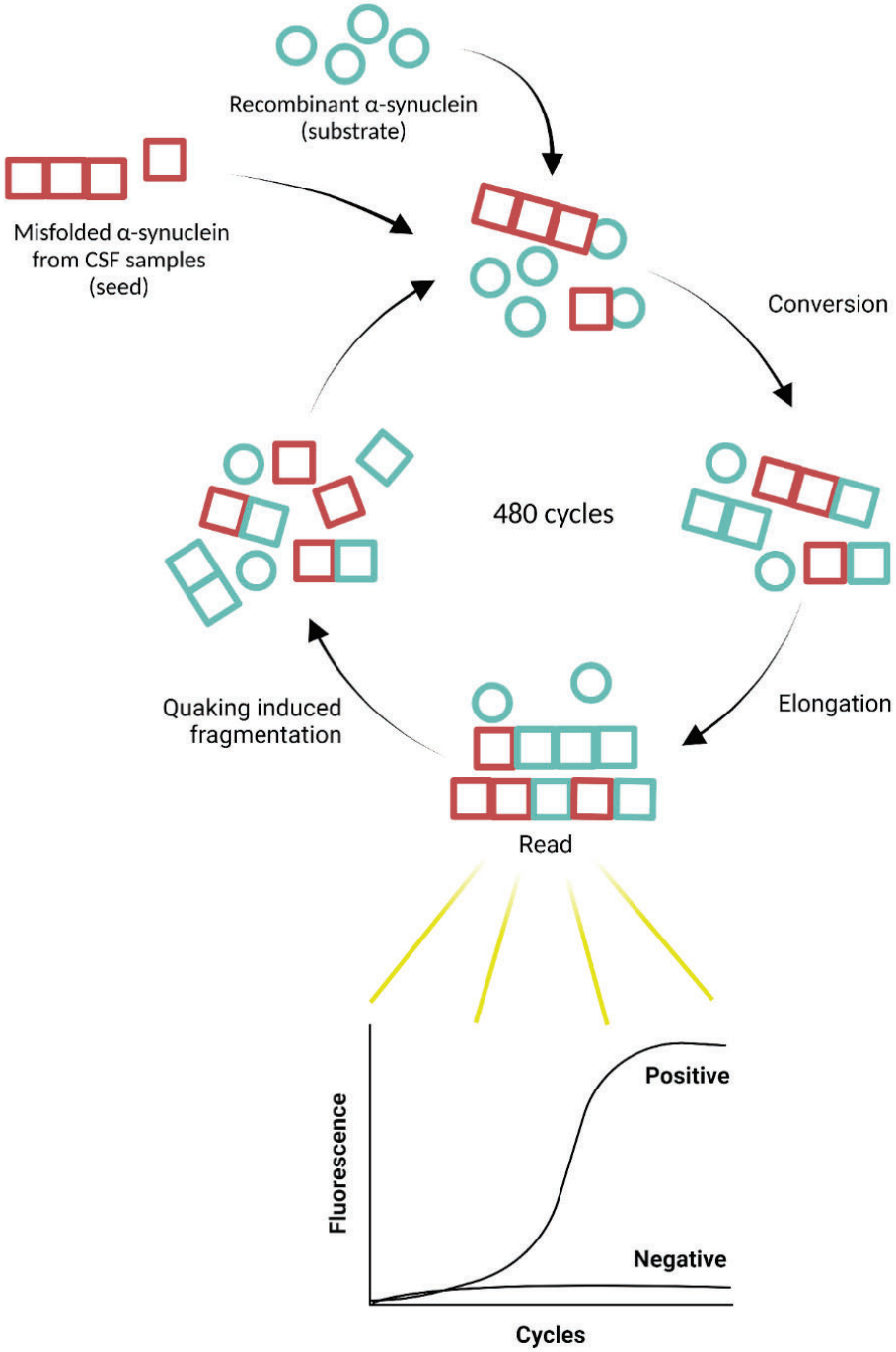

Figure 3 | Amplification cycle of α-synuclein real-time quaking-induced conversion (RT-QuIC) assay. Test CSF samples (seed) are added to the solution of recombinant monomeric α-synuclein (substrate) and fibril-sensitive dye thioflavin T. The seeds bind the substrate and induce their conformational conversion into misfolded oligomers and the subsequent fibrils formation. Thioflavin T binds the fibrils and emits fluorescence that is read by the plate reader. Then, a quacking event fragment the longer fibrils into new seeding surfaces, responsible for the exponential growth kinetics. *Inspired in Nat Protoc 2016; 11: 2233-2242.*

OBJECTIVES

2. OBJECTIVES

In this work, I investigated candidate PD diagnostic and progression biomarkers using biofluids from PD and other related α-synucleinopathies, with a special focus on the early stages of these diseases. The main objectives of this thesis included:

1. To elucidate whether serum miRNA deregulation in iRBD can antedate the diagnosis of PD by performing a longitudinal study in different progression stages of RBD characterised by DaT-SPECT imaging and assessing the predictive performance of differentially expressed miRNAs.
2. To assess serum miRNA expression in a longitudinal cohort of PD at-risk *LRRK2* G2019S non-manifesting carriers stratified by DaT-SPECT status, with a special focus on identifying miRNAs related to pheno-conversion into *LRRK2*-associated PD.
3. To set up the CSF α-synuclein RT-QuIC technique to investigate the presence of misfolded α-synuclein aggregates in PD and related α-synucleinopathies.

PUBLICATIONS

3. PUBLICATIONS

[Article 1]. Serum microRNAs predict isolated REM sleep behaviour disorder and Lewy body diseases.

Soto, M.*, Iranzo, A.*, Lahoz, S., Fernández, M., Serradell, M., Gaig, C., Melón, P., Martí, M.-J., Santamaría, J., Camps, J., Fernández-Santiago, R. and Ezquerra, M. (2022), Serum MicroRNAs Predict Isolated Rapid Eye Movement Sleep Behavior Disorder and Lewy Body Diseases. **Mov Disord**, 37: 2086-2098. DOI: 10.1002/mds.29171 (JCR'21 IF: 9.698 Q1)

[Article 2]. Differential serum microRNAs in premotor *LRRK2* G2019S carriers from Parkinson's disease.

Soto, M., Fernández, M., Bravo, P., Lahoz, S., Garrido, A., Sánchez-Rodríguez, A., Rivera-Sánchez, M., Sierra, M., Melón, P., Roig-García, A., Naito, A., Casey, B., Camps, J., Tolosa, E., Martí, M.J., Infante, J., Ezquerra, M., and Fernández-Santiago, R. Differential serum microRNAs in premotor LRRK2 G2019S carriers from Parkinson's disease. **NPJ Parkinsons Dis**. Status: accepted 20.12.2022 (JCR'21 IF: 9.304 Q1)

[Article 3]. Combined CSF α-SYN RT-QuIC, CSF NFL and midbrain-pons planimetry in degenerative parkinsonisms: From bedside to bench, and back again.

Compta, Y.*, Painous, C.*, Soto, M.*, Pulido-Salgado, M., Fernández, M., Camara, A., Sánchez, V., Bargalló, N., Caballol, N., Pont-Sunyer, C., Buongiorno, M., Martin, N., Basora, M., Tio, M., Giraldo, D.M., Pérez-Soriano, A., Zaro, I., Muñoz, E., Martí M.J., and Valldeoriola, F. (2022), Combined CSF α-SYN RT-QuIC, CSF NFL and midbrain-pons planimetry in degenerative parkinsonisms: From bedside to bench, and back again. **Parkinsonism Relat. Disord.** 99: 33-41. DOI: 10.1016/j.parkreldis.2022.05.006 (JCR'20 IF:4.891 Q1)

3.1 Article 1

RESEARCH ARTICLE

Serum MicroRNAs Predict Isolated Rapid Eye Movement Sleep Behavior Disorder and Lewy Body Diseases

Marta Soto, MSc,[1,2†] Alex Iranzo, MD,[2,3†] Sara Lahoz, MSc,[4,5] Manel Fernández, BTech,[1,2] Mónica Serradell, BSc,[2,3] Carles Gaig, MD,[2,3] Paula Melón, MSc,[1,2] Maria-Jose Martí, MD,[1,2,6] Joan Santamaría, MD,[2,3] Jordi Camps, PhD,[4,5] Rubén Fernández-Santiago, PhD,[1,2‡*] and Mario Ezquerra, PhD[1,2‡]

[1]*Laboratory of Parkinson Disease and Other Neurodegenerative Movement Disorders, Institut d'Investigacions Biomèdiques August Pi i Sunyer (IDIBAPS)-Hospital Clínic de Barcelona, University of Barcelona, Barcelona, Spain*
[2]*Centro de Investigación Biomédica en Red de Enfermedades Neurodegenerativas (CIBERNED), Barcelona, Spain*
[3]*Sleep Center, Department of Neurology, Hospital Clínic de Barcelona, Institut d'Investigacions Biomèdiques August Pi i Sunyer (IDIBAPS), University of Barcelona, Barcelona, Spain*
[4]*Gastrointestinal and Pancreatic Oncology Team, Institut d'Investigacions Biomèdiques August Pi i Sunyer (IDIBAPS)-Hospital Clínic de Barcelona, Barcelona, Spain*
[5]*Centro de Investigación Biomédica en Red de Enfermedades Hepáticas y Digestivas (CIBERehd), Madrid, Spain*
[6]*Movement Disorders Unit, Department of Neurology, Hospital Clínic de Barcelona, Institut d'Investigacions Biomèdiques August Pi i Sunyer (IDIBAPS), University of Barcelona, Barcelona, Spain*

ABSTRACT: Background: Isolated rapid eye movement sleep behavior disorder (IRBD) is a well-established clinical risk factor for Lewy body diseases (LBDs), such as Parkinson's disease (PD) and dementia with Lewy bodies (DLB).
Objective: To elucidate whether serum microRNA (miRNA) deregulation in IRBD can antedate the diagnosis of LBD by performing a longitudinal study in different progression stages of IRBD before and after LBD diagnosis and assessing the predictive performance of differentially expressed miRNAs by machine learning–based modeling.
Methods: Using genome-wide miRNA analysis and real-time quantitative polymerase chain reaction validation, we assessed serum miRNA profiles from patients with IRBD stratified by dopamine transporter (DaT) single-photon emission computed tomography into DaT-negative IRBD (n = 17) and DaT-positive IRBD (n = 21), IRBD phenoconverted into LBD (n = 13), and controls (n = 20). Longitudinally, we followed up the IRBD cohort by studying three time point serum samples over 26 months.
Results: We found sustained cross-sectional and longitudinal deregulation of 12 miRNAs across the RBD continuum, including DaT-negative IRBD, DaT-positive IRBD, and LBD phenoconverted IRBD (let-7c-5p, miR-19b-3p, miR-140, miR-22-3p, miR-221-3p, miR-24-3p, miR-25-3p, miR-29c-3p, miR-361-5p, miR-425-5p, miR-4505, and miR-451a) (false discovery rate $P < 0.05$). Age- and sex-adjusted predictive modeling based on the 12 differentially expressed miRNA biosignatures discriminated IRBD and PD or DLB from controls with an area under the curve of 98% (95% confidence interval: 89–99%).
Conclusions: Besides clinical diagnosis of IRBD or imaging markers such as DaT single-photon emission computed tomography, specific miRNA biosignatures alone hold promise as progression biomarkers for patients with IRBD for predicting PD and DLB clinical outcomes. Further miRNA studies in other PD at-risk populations, such as LRRK2 mutation asymptomatic carriers or hyposmic subjects, are warranted. © 2022 The Authors. *Movement Disorders* published by Wiley Periodicals LLC on behalf of International Parkinson and Movement Disorder Society

Key Words: isolated REM-sleep behavior disorder (IRBD); dopamine transporter single-photon emission computed tomography (DaT-SPECT); biomarkers; disease prediction; Parkinson's disease (PD)

***Correspondence to:** Dr. R. Fernández-Santiago, Laboratory of Parkinson Disease and Other Neurodegenerative Movement Disorders, IDIBAPS-Hospital Clínic de Barcelona, Faculty of Medicine (University of Barcelona), CELLEX Building, Casanova 143, Floor 3B, 08036 Barcelona, Spain; E-mail: ruben.fernandez.santiago@gmail.com

[†]Marta Soto and Alex Iranzo contributed equally to this work as co-first authors.

[‡]Rubén Fernández-Santiago and Mario Ezquerra contributed equally to this work as co-last authors.

Relevant conflicts of interest/financial disclosures: Nothing to report.

Full financial disclosures and author roles may be found in the online version of this article.

Received: 24 February 2022; **Revised:** 9 June 2022; **Accepted:** 10 July 2022

Published online 12 August 2022 in Wiley Online Library (wileyonlinelibrary.com). DOI: 10.1002/mds.29171

Rapid eye movement (REM) sleep behavior disorder (RBD) is characterized by the lack of REM sleep–related muscle atonia, disinhibited motor activity, and dream-enacting behaviors. The isolated form of RBD (IRBD) represents the prodromal state of the synucleinopathies because, after 14 years of follow-up, 91% of the patients with IRBD are diagnosed with Parkinson's disease (PD) and dementia with Lewy bodies (DLB), collectively known as Lewy body disorders (LBDs), and rarely with multiple system atrophy (MSA).[1] Yet, predicting disease progression in IRBD is challenging given that time to phenoconversion is variable and the resulting clinicopathological phenotype is heterogeneous, being DLB and MSA rapidly progressive diseases compared with PD. Thus, investigating IRBD can help assess the earliest molecular changes occurring at prodromal stages of α-synucleinopathies and identify potential diagnostic or prognostic biomarkers for these diseases.

MicroRNAs (miRNAs) are small noncoding RNAs that regulate gene expression by mRNA cleavage and translation repression.[2] Cumulative evidence showed serum or plasma miRNA deregulation in patients with PD and related α-synucleinopathies,[3-8] including its prodromal phases such as IRBD.[9,10] Yet, miRNA studies in premotor cohorts are still scarce, and longitudinal follow-ups in seriated IRBD progression stages are needed. In this study, we characterized the serum miRNA expression profiles of a Spanish IRBD cohort without motor and cognitive impairment and segregated by dopamine transporter single-photon emission computed tomography (DaT-SPECT) into DaT-negative IRBD, DaT-positive IRBD, IRBD phenoconverted into PD and DLB, and controls. We used this method to stratify IRBD into successive disease progression stages, given that abnormal DaT-SPECT represents a short-term marker for developing PD and DLB in less than 5 years.[11-13] Cross-sectionally, we identified novel differentially expressed miRNAs (DEmiRs) associated with IRBD and α-synucleinopathy, which we subsequently validated using three longitudinal follow-up serum samples from DaT-negative and DaT-positive IRBD. Lastly, by applying machine learning modeling algorithms, we assessed the disease prediction ability of the identified DEmiR to discriminate IRBD and PD or LBD patients from controls alone. The goal of the study was to investigate potential miRNAs as prognostic biomarkers for α-synucleinopathies.

Subjects and Methods

Subjects

All subjects provided written informed consent, and the Ethics Committee of Institut d'Investigacions Biomèdiques August Pi i Sunyer (IDIBAPS)-Hospital Clínic de Barcelona approved the study. The IRBD diagnosis required a history of dream-enacting behaviors, audiovisual-polysomnographic confirmation of excessive electromyographic activity in REM sleep, and absence of motor and cognitive impairment.[1] All the participating IRBD subjects were characterized by dopamine transporter single-photon emission computed tomography (DaT-SPECT) imaging using ^{123}I-2β-carbomethoxy-3β-(4-iodophenyl)-N-(3-fluoropropyl)-nortropane as previously described.[13] Overall, the cross-sectional cohort consisted of 51 patients with IRBD recruited and diagnosed at the Sleep Centre of the Neurology Service at the Hospital Clínic de Barcelona, Spain. Of these, 38 patients with IRBD were free of neurodegenerative disease, 17 of which had normal DaT-SPECT (DaT-negative IRBD) and 21 abnormal DaT-SPECT (DaT-positive IRBD). The remaining 13 patients were initially diagnosed with IRBD, and clinical follow-up showed the phenoconversion into LBD, PD (n = 8), and DLB (n = 5), fulfilling accepted criteria.[14,15] The study included 20 healthy control patients without evidence of neurological or sleep disorders from the Parkinson's Disease and Movement Disorders Unit at the Hospital Clínic de Barcelona (Table 1). Basal RBD and LBD medication is summarized in Table S1. All patients with IRBD were clinically followed up every 3–12 months, and serum samples were collected for at least three time points over 26 months (Table S2). During this period, three DaT-positive IRBD subjects (14%) were diagnosed with PD, one between the first and the second time point and two between the second and the third.

Serum miRNA Isolation

For each subject, we collected 5 mL peripheral blood in tubes with a clot activator (#366468; BD Vacutainer), preserved it for 30 minutes at room temperature, and centrifuged at 1500*g* for 10 minutes at 4°C. Serum volumes of 2 mL were removed from the supernatant, aliquoted in polypropylene CryoTubes (#121263; Greiner Bio-One), and stored at −80°C. We mixed 200 μL serum from each sample with 2 μL of yeast transfer RNA (tRNA) (#AM7119; Invitrogen) at a final concentration of 10 μg/mL as a carrier for nucleic acid precipitation. Following the manufacturer's instructions, total RNA enriched in miRNAs was isolated using the miRNeasy Serum/Plasma Kit (#217184; QIAGEN). The RNA concentration was determined on a NanoDrop ND-3300 fluorospectrometer (Thermo Scientific). We performed an electropherogram analysis using an Agilent Small RNA Kit in n = 22 random samples as quality control for 6- to 40-bp miRNA-enriched fractions and observed high-quality miRNA enrichment for all studied samples (Fig. S1).

TABLE 1 *Clinicodemographics of the study subjects*

Group	No. of subjects	Sex (M/F)	Age at IRBD onset (y)	Age at sampling (y)	Time from IRBD onset to sampling (y)	Interval from baseline (mo)	No. converted to PD	Age at PD diagnosis	No. converted to DLB	Age at DLB diagnosis (y)
Controls	20	16/4	–	70.10 ± 6.19	–	–	–	–	–	–
DaT(−) IRBD	17	14/3	63.65 ± 8.73	71.12 ± 8.21	7.12 ± 5.57	–	–	–	–	–
Time point 2	16	11/2	64.06 ± 8.84	72.50 ± 8.14	8.38 ± 5.80	10.13 ± 2.68	–	–	–	–
Time point 3	14	10/1	65.29 ± 8.79	74.50 ± 7.81	9.00 ± 5.66	19.57 ± 4.82	–	–	–	–
DaT(+) IRBD	21	16/4	61.38 ± 7.98	70.57 ± 5.73	8.86 ± 7.58	–	–	–	–	–
Time point 2	19	13/4	61.84 ± 8.26	71.95 ± 5.79	9.58 ± 7.71	10.84 ± 2.14	1	76	–	–
Time point 3	19	14/4	61.84 ± 8.26	72.39 ± 6.12	10.32 ± 7.72	20.00 ± 4.00	3	72.67 ± 4.93	–	–
LBD	13	7/6	60.15 ± 9.26	76.77 ± 5.34	16.62 ± 8.30	–	8	73.88 ± 5.77	5	76.40 ± 4.83

Clinicodemographic data from DaT-negative IRBD, DaT-positive IRBD, IRBD phenoconverted into LBD (PD and DLB), and healthy controls.
M, male; F, female; IRBD, isolated rapid eye movement sleep behavior disorder; PD, Parkinson's disease; DLB, dementia with Lewy bodies; LBD, Lewy body disease (PD and DLB); DaT, dopamine transporter-single-photon emission computed tomography imaging; DaT(−) IRBD, dopamine transporter-negative IRBD patients; DaT(+) IRBD, dopamine transporter-positive IRBD patients.

Genome-Wide miRNA Profiling

We explored the genome-wide miRNA expression profiles in serum using the Affymetrix GeneChip miRNA 4.0 Array, which interrogates the levels of 4603 human miRNAs, including 2578 mature miRNAs and 2025 pre-miRNAs (#902413; Thermo Fisher) (Product datasheet: https://www.thermofisher.com/). Serum miRNAs from individual subjects were hybridized onto the probe set separate arrays for 42 hours and scanned using an Affymetrix GeneChip Scanner 3000 7G following the manufacturer's instructions. Data files generated by the Affymetrix GeneChip Command Console were processed with the Expression Console software to determine the data quality. Expression raw data were analyzed using the Partek Genomic Suite v7.0 software (Partek Inc.) applying the robust multiarray average background correction model, which permits the relative comparison of miRNA abundance in different arrays. Only miRNAs with detection values greater than 2.4 arbitrary luminescence units in at least 50% of all samples, patients, and controls and a significant expression value above the background signal ($P < 0.05$) were considered as expressed in serum. In line with previous reports,[16] we observed that approximately 10% of the mature human screened miRNAs were expressed in serum from our cohort. Adjusting by sex and age, we used the global mean of all expressed serum miRNAs as a reference to define candidate differentially expressed miRNAs (DEmiRs) and the sign of the fold-change difference. Under a 2-tailed Student *t* test, we applied the criteria of a combination of a fold-change > |1.5| and $P < 0.05$ to select candidate miRNAs from the array for subsequent real-time quantitative polymerase chain reaction (RT-qPCR) validation (Table S3).

RT-qPCR Validation

miRNA samples were reverse transcribed into cDNA and preamplified using the TaqMan Advanced miRNA cDNA Synthesis Kit (#A28007; Thermo Fisher Scientific) in a Veriti 96-well Thermal Cycle (Applied Biosystems). cDNA preamplified products were quantified per duplicate using TaqMan Fast Advanced Master Mix (4444557; Thermo Fisher Scientific) and TaqMan Advanced miRNA Assays (A25576; Thermo Fisher Scientific) (Table S4). Reactions were plated with evenly balanced group samples in 96-well RT-qPCR plates at a final volume of 10 µL on a TaqMan StepOnePlus RT-qPCR System (Applied Biosystems). We used two endogenous and one exogenous miRNA simultaneously for normalization in all RT-qPCR comparisons.[17,18] As endogenous normalizers, we selected hsa-miR-320a-3p and hsa-miR-6727-5p among the most stable miRNAs from the array across all samples as identified using the NormFinder software[19] in other α-synucleinopathies

TABLE 2 *RT-qPCR assessment of microRNA expression levels in serum samples from DaT-negative IRBD, DaT-positive IRBD, and LBD patients (PD and DLB) as compared with healthy controls*

	DaT-negative IRBD						DaT-positive IRBD							
	Baseline		Time point 2		Time point 3		Baseline		Time point 2		Time point 3		LBD	
miRNA	**FC**	**Adj. *P***	**FC**	**Adj. *P***	**FC**	**Adj. *P***	**FC**	**Adj. *P***	**FC**	**Adj. *P***	**FC**	**Adj. *P***	**FC**	**Adj. *P***
miR-19b-3p	5.07	0.0002	11.59	$<1.0 \times 10^{-6}$	10.18	4.0×10^{-6}	5.45	0.0001	12.17	$<1.0 \times 10^{-6}$	14.00	$<1.0 \times 10^{-6}$	11.44	1.0×10^{-6}
miR-29c-3p	5.67	0.0002	11.24	$<1.0 \times 10^{-6}$	13.78	$<1.0 \times 10^{-6}$	5.17	0.0003	12.92	$<1.0 \times 10^{-6}$	15.15	$<1.0 \times 10^{-6}$	9.41	$<1.0 \times 10^{-6}$
miR-451a	6.00	0.0006	17.79	0.0007	16.66	4.6×10^{-5}	7.72	0.0003	44.54	$<1.0 \times 10^{-6}$	42.32	$<1.0 \times 10^{-6}$	18.42	$<1.0 \times 10^{-6}$
miR-425-5p	−4.22	0.0011	9.97	1.0×10^{-6}	5.93	0.0015	−3.64	0.0024	12.92	$<1.0 \times 10^{-6}$	12.41	$<1.0 \times 10^{-6}$	18.36	$<1.0 \times 10^{-6}$
miR-22-3p	3.41	0.0014	13.56	$<1.0 \times 10^{-6}$	14.14	2.0×10^{-6}	3.67	0.0005	14.04	$<1.0 \times 10^{-6}$	17.07	$<1.0 \times 10^{-6}$	12.86	$<1.0 \times 10^{-6}$
miR-24-3p	3.51	0.0017	17.99	$<1.0 \times 10^{-6}$	12.85	1.3×10^{-5}	3.85	0.0006	23.50	$<1.0 \times 10^{-6}$	21.37	$<1.0 \times 10^{-6}$	15.14	$<1.0 \times 10^{-6}$
miR-221-3p	2.47	0.0020	8.30	$<1.0 \times 10^{-6}$	7.08	0.0001	2.54	0.0012	10.81	$<1.0 \times 10^{-6}$	10.86	$<1.0 \times 10^{-6}$	8.44	$<1.0 \times 10^{-6}$
miR-1227-5p	−1.78	0.0064	−1.04	0.8443	−1.04	0.9069	−1.58	0.0365	1.06	0.7864	−1.23	0.2916	−1.20	0.4466
miR-25-3p	3.18	0.0108	15.34	$<1.0 \times 10^{-6}$	10.01	0.0003	4.16	0.0024	18.21	$<1.0 \times 10^{-6}$	20.97	$<1.0 \times 10^{-6}$	11.83	$<1.0 \times 10^{-6}$
miR-361-5p	2.48	0.0229	12.51	$<1.0 \times 10^{-6}$	7.51	0.0003	3.32	0.0033	17.93	$<1.0 \times 10^{-6}$	15.41	$<1.0 \times 10^{-6}$	10.94	$<1.0 \times 10^{-6}$
let-7c-5p	1.81	0.0454	5.38	$<1.0 \times 10^{-6}$	4.82	0.0008	2.25	0.0024	6.27	$<1.0 \times 10^{-6}$	7.70	$<1.0 \times 10^{-6}$	6.28	1.0×10^{-6}
miR-140-3p	1.82	0.2706	14.17	$<1.0 \times 10^{-6}$	9.02	0.0008	3.26	0.0034	17.65	$<1.0 \times 10^{-6}$	17.85	$<1.0 \times 10^{-6}$	14.56	1.0×10^{-6}
miR-4505	−1.15	0.6917	2.21	0.0068	2.41	0.0020	1.24	0.4253	3.16	0.0007	3.46	5.0×10^{-6}	1.89	0.0011
miR-1207-5p	−1.55	0.2706	1.40	0.2978	1.36	0.3792	−1.47	0.2305	1.61	0.1666	1.15	0.6314	1.06	0.8236
miR-3613-5p	1.06	0.8772	1.23	0.4684	1.46	0.3140	1.16	0.5718	1.23	0.4471	1.48	0.1314	1.20	0.5155

RT-qPCR, real-time quantitative polymerase chain reaction; DaT, dopamine transporter single-photon emission computed tomography imaging; IRBD, isolated rapid eye movement sleep behavior disorder; LBD, Lewy body disease (PD and DLB); PD, Parkinson's disease; DLB, dementia with Lewy bodies; FC, fold change; Adj. *P*, false discovery rate multiple-test adjusted *P* value.

studies in our population, i.e., MSA[20] and LRRK2-associated PD (Marta Soto, Manel Fernández, Paloma Bravo, Alicia Garrido, Antonio Sánchez-Rodríguez, María Rivera-Sánchez, María Sierra, Paula Melón, Anna Naito, Bradford Casey, Eduardo Tolosa, María-José Martí, Jon Infante, Mario Ezquerra and Rubén Fernández-Santiago). As an exogenous normalizer, we used the *Caenorhabditis elegans* miRNA cel-miR-39-3p added to all serum samples at a final concentration of 5 pM.[18] To assess miRNA relative expression, we used the DataAssist v3.0 software (Applied Biosystems), setting the maximum allowable cycle threshold value at 35 cycles. Statistical significance levels for DEmiRs were set at a fold-change > |1.5| and a false discovery rate (FDR) adjusted $P < 0.05$ under a 2-tailed Student *t* test. Using commercially available assays, we tested 22 miRNAs and discarded 7, which did not show an amplification signal. Of the remaining 15 miRNAs (Table S4), 10 were selected among the top candidate miRNAs found by array (let-7c-5p, miR-1207-5p, miR-1227-5p, miR-140-3p, miR-24-3p, miR-25-3p, miR-361-5p, miR-3613-5p, miR-425-5p, and miR-451a) (Table S5). The remaining five miRNAs were candidates earlier reported in PD alone (miR-22-3p, miR-29c-3p, miR-221-3p, and miR-4505)[7,21,22] or both PD and IRBD (miR-19b-3p).[8,9] Lastly, as quality control, we repeated the entire RT-qPCR experiment in all samples for three of the identified DEmiRs (miR-140-3p, miR-19b-3p, and miR-29c-3p) to discard potentially confounding effects of cDNA synthesis or preamplification (Table S6) and found a Pearson correlation of 78% ($P = 1.36 \times 10^{-4}$), thus validating findings.

Predictive Modeling Through Machine Learning Analysis

To predict each patient's probability of having the disease (ie, IRBD, DLB, or PD) versus being a control, we computed binary classification analyses using the caret framework in R, specifying age, sex, and RT-qPCR expression values of the 12 validated serum DEmiRs as predictors. Multifold imputations of missing data were performed by the predictive mean matching method implemented in the mouse R package. Numerical variables were centered and normalized, resulting in a standard distribution of mean 0 and variance 1. The gradient boosting machine (GBM) algorithm in the gbm package (v.2.1.8) was employed to classify patients in the two groups (disease vs control), using leave-one-out cross-validation to cut for potential overfitting. Variable selection was applied to each training dataset using the least absolute shrinkage and selection operator (Lasso) method in the glmnet package (v.2.0-18) (Table S7) so that only those features with a regression Beta greater than 0 were subsequently downstreamed to the GBM classifier. To address imbalanced class distributions, we performed random upsampling of the minority class on each training data fold so that the two classes acquired the same frequency using the upSample function from the caret. To evaluate the predictive performance of this model classifier, we inferred the accuracy, sensitivity, specificity, and positive and negative predictive values using the crossval package. We assessed discriminative ability by calculating the area under the curve (AUC) on a receiver operating characteristic (ROC) curve using the pROC package.

Biological Enrichment Analysis

To investigate the biological functions and localization of the identified DEmiR, we performed a restrictive overrepresented biological enrichment analysis using only the 12 DEmiRs that were deregulated at all longitudinal time points of both DaT-negative and DaT-positive IRBD and also in LBD (let-7c-5p, miR-19b-3p, miR-425-5p, miR-140-3p, miR-22-3p, miR-4505, miR-221-3p, miR-24-3p, miR-25-3p, miR-29c-3p, miR-361-5p, and miR-451a). To this end, we used the GeneOntology option from the miEAA 2.0 software, applying gene annotations from the miRTarBase database as earlier described[23] and the localization (RNALocate) (https://ccb-compute2.cs.uni-saarland.de/mieaa2).

Results

We first profiled overall miRNA levels in serum samples from patients with IRBD and healthy control patients as an approach to screen global miRNA expression variation and identify specific candidate miRNAs for validation. Compared with control patients, by genome-wide miRNA expression analysis, we found 116 candidate miRNAs in DaT-negative IRBD patients and 50 miRNAs in DaT-positive IRBD patients, which surpassed the fold-change threshold greater than |1.5| and a *P* value <0.05 (Table S3, Fig. S2). Given the higher sensitivity of RT-qPCR,[24,25] we defined DEmiRs based only on the stringent criteria of RT-qPCR validation with a fold-change > |1.5| and an FDR adjusted $P < 0.05$. To this end, we selected a total of 10 miRNAs among the topmost deregulated miRNAs identified at the genome-wide profiling, including seven miRNAs from DaT-positive IRBD patients (let-7c-5p, miR-140-3p, miR-24-3p, miR-25-3p, hsa-miR-361-5p, miR-425-5p, and miR-451a) and three from DaT-negative IRBD patients (miR-1207-5p, miR-1227-5p, and miR-3613-5p).

Next, by RT-qPCR, we quantified the relative expression levels of the selected miRNAs in DaT-negative IRBD, DaT-positive IRBD, and LBD phenoconverted patients (PD and DLB), all compared with healthy controls (Table 2). Of these, we validated seven DEmiRs in DaT-negative and DaT-positive IRBD patients (let-7c-

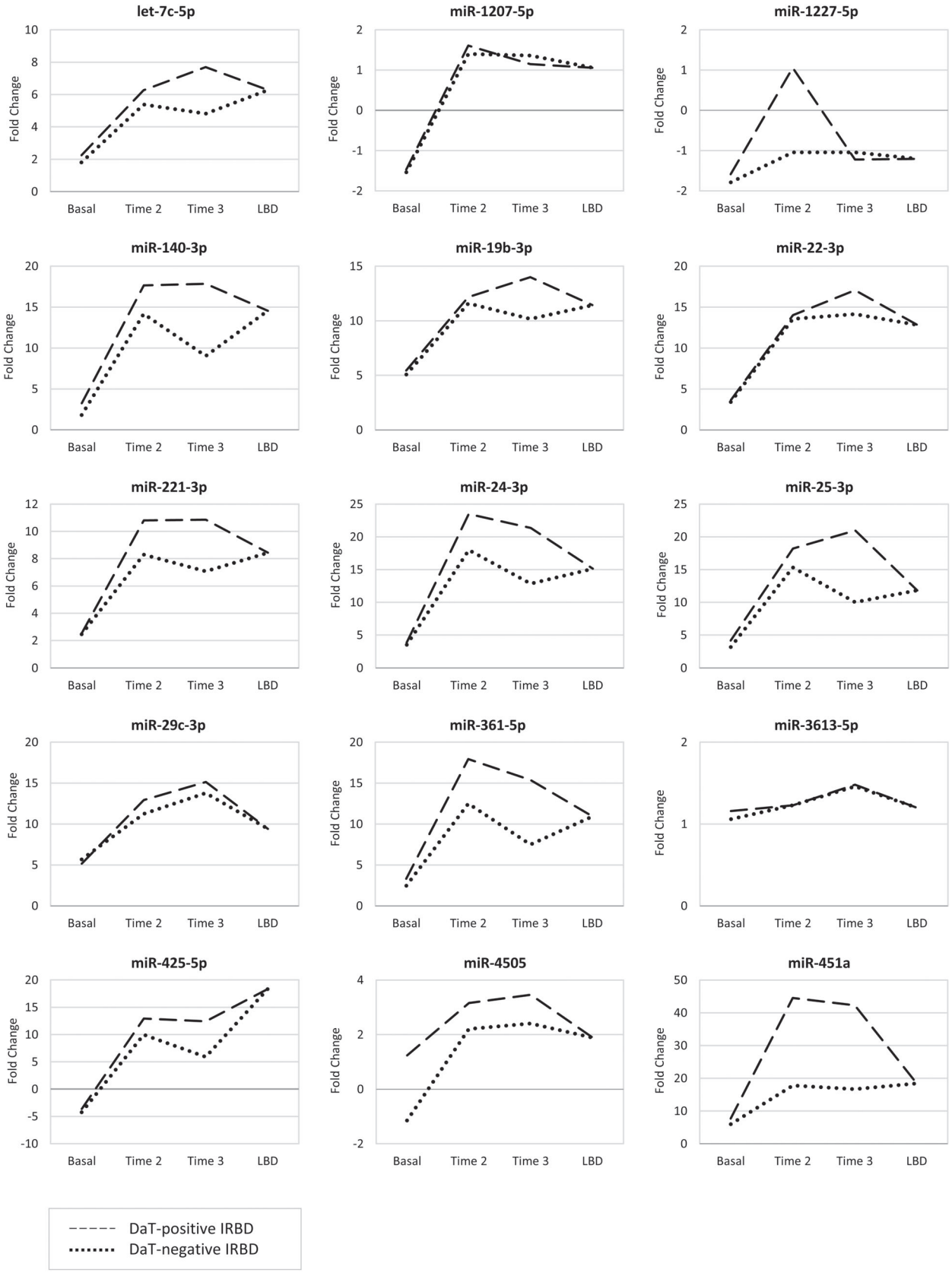

FIG. 1. Longitudinal microRNA (miRNA) expression levels in serum from patients with dopamine transporter (DaT)-negative idiopathic rapid eye movement sleep behavior disorder (IRBD), DaT-positive IRBD, and LBD compared with healthy controls. Dashed line, DaT-positive IRBD; dotted line, DaT-negative IRBD. LBD, Lewy body disease (Parkinson's disease and dementia with Lewy bodies).

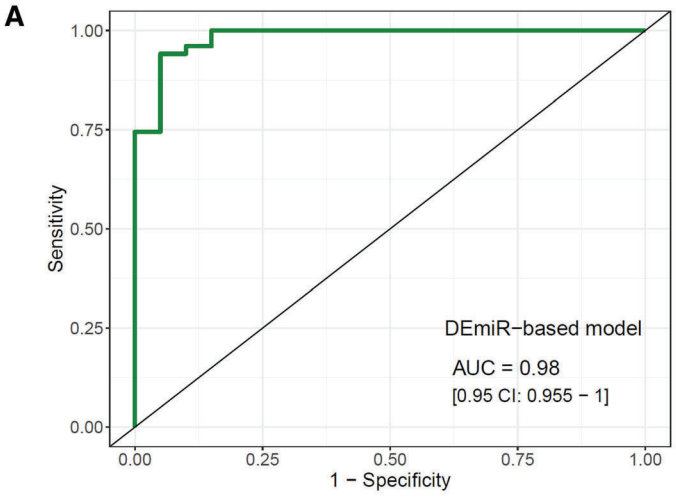

DEmiR discriminative features	C vs. IRBD & PD / DLB (N=71)
AUC (0.95 CI)	0.98 (0.96 - 1)
Sensitivity (0.95 CI)	0.98 (0.91 - 1)
Specificity (0.95 CI)	0.86 (0.68 - 0.96)
PPV (0.95 CI)	0.95 (0.88 - 0.98)
NPV (0.95 CI)	0.94 (0.76 - 0.99)
Accuracy (0.95 CI)	0.94 (0.89 - 0.99)

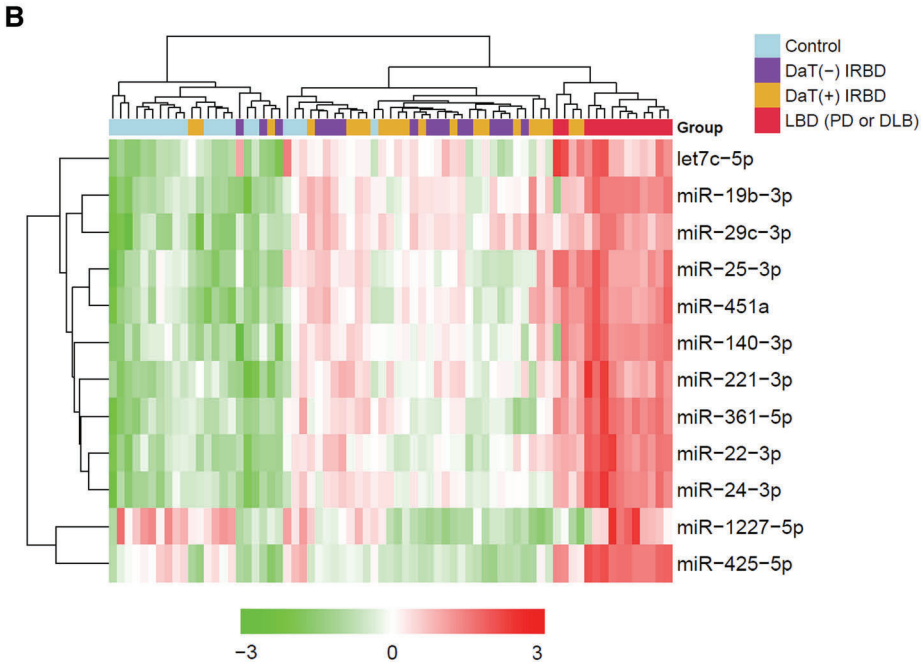

FIG. 2. Differential expression and diagnostic accuracy of the 12 miRNA biosignatures. (**A**) Receiver operating characteristic (ROC) curve showing the discriminative ability from the 12 miRNA biosignatures to predict the subject probability of disease, IRBD, or PD/DLB versus being a healthy control subject (n = 71). Table showing performance metrics obtained through machine learning analysis for binary classification of individuals within the disease or control groups. (**B**) Unsupervised hierarchical clustering displaying real-time quantitative polymerase chain reaction expression levels of the 12 miRNA signatures. Red pixels indicate miRNA overexpression, and green decreased expression levels. AUC, area under the curve; CI, confidence interval; DEmiR, differentially expressed microRNA; DLB, dementia with Lewy bodies; IRBD, idiopathic rapid eye movement sleep behavior disorder; LBD, Lewy body disease (PD and DLB); NPV, negative predictive value; PD, Parkinson's disease; PPV, positive predictive value. [Color figure can be viewed at wileyonlinelibrary.com]

5p, miR-1227-5p, miR-24-3p, miR-25-3p, miR-361-5p, miR-425-5p, and miR-451a). All of these DEmiRs were also deregulated in LBD phenoconverted patients, except miR-1227-5p. Of the remaining three, miR-140-3p was differentially expressed in LBD and DaT-positive IRBD patients, but not in DaT-negative IRBD patients. In addition, miR-1207-5p and miR-3613-5p were not validated in any group. Besides candidates from the array, we also quantified the serum expression levels of five miRNA candidates earlier associated with PD alone (miR-22-3p, miR-221-3p, miR-29c-3p, and miR-4505)[7,21,22] or with PD and IRBD (miR-19b-3p).[8,9] We found that miR-19b-3p, miR-22-3p, miR-221-3p, and miR-29c-3p were DEmiRs in all DaT-negative IRBD, DaT-positive IRBD, and LBD patients. Of these, miR-19b-3p and miR-29c-3p were topmost deregulated in most comparisons (Table 2). In addition, miR-4505 was a DEmiR only in LBD, but not in IRBD. Globally, by cross-sectional analysis, we identified 13 DEmiRs showing continued deregulation across the entire RBD continuum, including DaT-negative IRBD, DaT-positive IRBD, and IRBD patients who phenoconverted into PD/DLB.

Subsequently, we performed a follow-up miRNA expression analysis by RT-qPCR using longitudinal serums from DaT-negative and DaT-positive IRBD patients. Beyond baseline, we used two additional sera covering 26 months (Table 2, Fig. S3). Compared with controls, we found consistent longitudinal miRNA deregulation of 10 DEmiRs in DaT-negative and DaT-positive IRBD patients (let-7c-5p, miR-19b-3p, miR-22-3p, miR-221-3p, miR-24-3p, miR-25-3p, miR-29c-3p, miR-361-5p, miR-425-5p, and miR-451a). Overall, fold-change expression values were larger at time points 2 and 3 than baseline, and expression differences were stronger in DaT-positive than DaT-negative IRBD (Fig. 1). We also observed that miR-140-3p and miR-4505, which were not deregulated at baseline, emerged as DEmiR in the longitudinal follow-up. Lastly, miR-1207-5p, miR-3613-5p, and miR-1227-5p did not show longitudinal expression differences, so we excluded these miRNAs from the enrichment analyses. Altogether, we found longitudinal miRNA expression changes of 12 DEmiRs in DaT-negative and DaT-positive IRBD, which had consistent deregulation in PD/DLB-converted patients (let-7c-5p, miR-19b-3p, miR-140, miR-22-3p, miR-221-3p, miR-24-3p, miR-25-3p, miR-29c-3p, miR-361-5p, miR-425-5p, miR-4505, and miR-451a).

With the goal of discerning patients with the disease (n = 51; i.e., IRBD and PD or DLB patients) from controls (n = 20) and evaluating the discriminative potential of miRNAs, we performed predictive modeling based on the serum expression levels of the 12 experimentally validated DEmiRs identified in the cross-sectional analysis, adjusted by age and sex. During leave-one-out cross-validation, predictor features selected by Lasso in 100% of the training sets were age, sex, miR-1227-5p, miR-425-5p, and miR-451a (Table S7). The 12-DEmiR-based model classified 67/71 patients in the correct group (94% accuracy; 95% confidence interval [CI]: 89–99%), with a sensitivity for true disease cases of 98% (95% CI: 91–100%) and a specificity for true controls of 86% (95% CI: 68–96%). In terms of discriminative ability, ROC curve analysis showed an AUC of 0.98 (95% CI: 0.96–1) (Fig. 2A). Regarding individual miRNAs, age- and sex-adjusted AUC values ranged from 0.54 up to 0.85 (Table S8), and the topmost discriminant individual miRNAs distinguishing IRBD or LBD were miR-29c-3p, miR-1227-5p, and miR-24-3p, with AUCs of 0.85, 0.76, and 0.76, respectively. In summary, by predictive modeling, we found a biosignature of 12 DEmiRs, which alone, without further clinical or DaT-SPECT imaging inputs, efficiently predicted IRBD and PD or DLB clinical outcomes.

To further test the miRNA biosignature discriminative power for unbiased subject classification, we performed an unsupervised hierarchical clustering analysis using R. Consistent with the clinical status, we observed clear segregation into three main subclusters, including controls, patients with IRBD, and PD/DLB phenoconverted patients (Fig. 2B). Driven by these results, we next interrogated specific miRNA differences occurring within the IRBD continuum. We found no miRNA level differences between DaT-negative and DaT-positive IRBD, indicating no main relation between miRNA levels and DaT-SPECT status. However, we observed statistically significant expression differences for all 12 biosignature miRNAs between DaT-positive IRBD and PD/DLB patients, thus suggesting an association between the identified 12 miRNAs and the clinical phenoconversion into α-synucleinopathy (Table S9). These findings indicate that IRBD exhibits differential serum miRNA profiles compared with controls and PD/DLB phenoconverted patients, supporting that the identified serum miRNA biosignature can be informative as a disease progression biomarker for IRBD-initiated α-synucleinopathies.

Lastly, we conducted a biological enrichment analysis to explore the functionality of the genes targeted by the miRNAs differentially expressed at all longitudinal time points. We found substantial deregulation at biological terms previously involved in clinically manifested PD, such as ubiquitin-dependent protein degradation, inositol triphosphate signaling, apoptosis,[26] myelin sheaths, synaptic transmission, postsynaptic assembly, synaptic maturation, and synaptic vesicles, among others. Regarding localization, we found exosomes, microvesicles, and extracellular vesicles among the top terms (Table 3).

TABLE 3 *Functional enrichment of the predicted genes targeted by the 12 differentially expressed microRNAs in patients with IRBD showing the 15 top enriched terms*

Enriched terms	*P* value	Adj. *P* value
Subcategory: Gene Ontology (GO) biological processes		
Positive regulation of ubiquitin-dependent protein catabolic process	5.8×10^{-9}	4.9×10^{-5}
Positive regulation of TRAIL-activated apoptotic signaling pathway	4.2×10^{-8}	1.9×10^{-4}
Inositol-1,3,4,5-tetrakisphosphate 3-phosphatase activity	3.8×10^{-7}	2.4×10^{-4}
Myelin sheath adaxonal region	2.9×10^{-7}	2.4×10^{-4}
Negative regulation of keratinocyte migration	2.9×10^{-7}	2.4×10^{-4}
Negative regulation of synaptic vesicle clustering	2.9×10^{-7}	2.4×10^{-4}
Neuron–neuron synaptic transmission	2.0×10^{-7}	2.4×10^{-4}
Phosphatidylinositol-3,4,5-trisphosphate 3-phosphatase activity	3.0×10^{-7}	2.4×10^{-4}
Phosphatidylinositol-3,4-bisphosphate 3-phosphatase activity	2.9×10^{-7}	2.4×10^{-4}
Postsynaptic density assembly	9.9×10^{-8}	2.4×10^{-4}
Prepulse inhibition	4.0×10^{-7}	2.4×10^{-4}
Regulation of cellular component size	2.9×10^{-7}	2.4×10^{-4}
Rhythmic synaptic transmission	4.0×10^{-7}	2.4×10^{-4}
Synapse maturation	3.4×10^{-7}	2.4×10^{-4}
Brain morphogenesis	7.2×10^{-7}	2.4×10^{-4}
Subcategory: KEGG pathways		
Amyotrophic lateral sclerosis (ALS)	1.3×10^{-4}	0.0112
Apoptosis—multiple species	1.5×10^{-4}	0.0112
Carbohydrate digestion and absorption	2.1×10^{-4}	0.0112
Epithelial cell signaling in *Helicobacter pylori* infection	2.5×10^{-4}	0.0112
Fc epsilon RI signaling pathway	2.1×10^{-4}	0.0112
GnRH secretion	1.5×10^{-4}	0.0112
Toll-like receptor signaling pathway	1.0×10^{-4}	0.0112
PD-L1 expression and PD-1 checkpoint pathway in cancer	3.6×10^{-4}	0.0145
Central carbon metabolism in cancer	6.7×10^{-4}	0.0238
African trypanosomiasis	0.0010	0.0247
C-type lectin receptor signaling pathway	9.5×10^{-4}	0.0247
Proteasome	0.0011	0.0247
Pyrimidine metabolism	0.0010	0.0247
Salmonella infection	8.3×10^{-4}	0.0247
TGF-ß signaling pathway	0.0012	0.0247
TNF signaling pathway	0.0012	0.0247
Subcategory: localization (RNALocate)		
Exosome	2.0×10^{-8}	2.0×10^{-7}
Cytoplasm	1.3×10^{-7}	6.5×10^{-7}
Microvesicle	6.9×10^{-7}	2.3×10^{-6}
Mitochondrion	1.4×10^{-5}	3.5×10^{-5}
Nucleus	2.2×10^{-5}	4.3×10^{-5}
Extracellular vesicle	2.8×10^{-5}	4.6×10^{-5}
Circulating	4.8×10^{-5}	6.9×10^{-5}
Nucleolus	1.5×10^{-4}	1.9×10^{-4}
Exosome	0.0167	0.0185
Microvesicle	0.0194	0.0194

IRBD, isolated rapid eye movement sleep behavior disorder; KEGG, Kyoto Encyclopedia of Genes and Genomes; TGF-ß, transforming growth factor ß; TNF, tumor necrosis factor; TRAIL, tumor necrosis factor-related apoptosis-inducing ligand; GnRH, Gonadotropin-Releasing Hormone; PD-L1, programmed cell death ligand 1; PD-1, programmed cell death 1.

Discussion

We profiled serum miRNA levels in a Spanish IRBD cohort stratified into the seriated disease progression stages of DaT-negative IRBD, DaT-positive IRBD with a dopaminergic deficit,[27] and PD/DLB phenoconverted patients in which the disease had been initiated with IRBD. We uncovered a 12-DEmiR biosignature that shows sustained and differential deregulation profiles across prodromal DaT-negative and DaT-positive IRBD (including their longitudinal follow-up), and patients with manifest PD or DLB (let-7c-5p, miR-1227-5p, miR-19b-3p, miR-140-3p, miR-22-3p, miR-221-3p, miR-24-3p, miR-25-3p, miR-29c-3p, miR-361-5p, miR-425-5p, and miR-451a). The identified miRNA biosignature exhibited high diagnostic accuracy for discriminating patients with IRBD and PD or DLB from controls, achieving an AUC of 98%.

To the best of our knowledge, this is the first miRNA study in patients with IRBD characterized by DaT-SPECT with longitudinal follow-up, but two previous studies explored miRNAs in IRBD. A first study using candidate miRNAs reported the deregulation of miR-19b-3p in IRBD serum (n = 104) up to 5 years before α-synucleinopathy diagnosis.[9] Another deep sequencing study using whole blood from a mixed cohort of IRBD and hyposmic subjects (n = 223) reported 500 miRNAs.[10] Four of the 12 biosignature miRNAs here were topmost deregulated in the earlier reports (miR-19b-3p, miR-29c-3p, miR-221-5p, and miR-140-5p).[9,10] Complementing these studies, we found a miRNA biosignature informative for all IRBD progression stages, including IRBD and PD/DLB phenoconverted patients. Our findings align with studies showing early molecular deregulation in prodromal stages of α-synucleinopathies. Thus, recent works in IRBD observed misfolded α-synuclein in the cerebrospinal fluid (CSF) before developing motor and cognitive impairment.[28] Another study in IRBD showed the presence of phosphorylated α-synuclein aggregates in the minor labial salivary glands.[29] Akin to these studies, our findings support that early molecular changes associated with α-synucleinopathies occur at early IRBD prodromal stages and can antedate the clinical manifestations of PD and DLB.

In PD and DLB, developing disease prediction strategies ahead of the motor and cognitive manifestations is a challenge for the early neuroprotective intervention.[30,31] By machine learning, we evaluated the disease prediction capacity of the combined expression levels from the 12 miRNA biosignatures adjusted by age and sex to estimate each proband's probability of disease, IRBD and PD/DLB versus being control and without any further clinical or imaging input. The miRNA biosignature achieved a high discriminative capacity with an AUC of 98% (95% CI: 89–99%) and distinguished prodromal and manifest PD or DLB from controls more accurately than other previously proposed candidate biomarkers, including α-synuclein.[8,32-35] The predictive model also accurately classified both positive and negative individuals (94% accuracy), specifically identifying true positives (98% sensitivity). However, while the fraction of false negatives was only 2%, the false-positive rate was 14% (86% specificity). Therefore, it is important to emphasize the need to develop more specific strategies to capture true negatives. In this sense, regarding the most clinically relevant miRNAs detected by the Lasso algorithm using a feature importance selection, only four of the six miRNAs selected in more than 90% of training folds displayed AUC scores greater than 75% at the individual level (miR-1227-5p, miR-425-5p, miR-451a, and miR-221-3p).[32,33] Altogether, these findings support the proof-of-principle that, beyond clinical or imaging markers such as DaT-SPECT, specific serum miRNA deregulation alone can be informative to predict the presence of IRBD and PD or DLB.

Based on our findings, an exciting interpretation is that the identified biosignature could hold potential as progression or phenoconversion biomarkers for patients within the LBD spectrum. Our miRNA findings are novel in IRBD but largely consistent with previous studies in manifest PD. Ten of the 12 biosignature miRNAs were earlier deregulated in different PD or DLB biospecimens. In LBD peripheral tissues, miR-19b-3p,[8,36,37] miR-29c-3p,[7,8,37,38] miR-221-3p,[6,7,37] miR-24-3p,[5,36] and miR-451a[37] were reported in PD serum; miR-19b-3p, miR-29c-3p, and miR-361 in PD or early-stage PD peripheral blood mononuclear cells[33,39,40]; miR-451 in PD leukocytes[41]; miR-25 in DLB platelets[42]; and miR-22,[21] miR-4505,[22] and miR-140-3p[10] in PD whole blood. Other biosignature miRNAs were described in the central nervous system (CNS), such as miR-19b-3p, miR-22, miR-29c,[43] and miR-24[44] in PD CSF; or miR-221 and miR-425-5p[45,46] in PD brain. Lastly, let-7c was not described in PD previously, but other members of the let-7 family showed deregulation in PD.[32,43,47-49] In summary, most of the 12 biosignature miRNAs were earlier reported in α-synucleinopathy.[5-7,10,21,22,33,36-42] This is relevant given that, if validated, our findings may have implications for other PD at-risk cohorts, such as individuals with hyposmia or LRRK2 or GBA asymptomatic mutation carriers.

Functionally, the target genes from the 12 longitudinal DEmiRs are involved in ubiquitin-dependent protein degradation, inositol triphosphate signaling, apoptosis,[26] and neural terms such as myelin sheaths, synaptic transmission, postsynaptic assembly, synaptic maturation, or synaptic vesicle. Although the function and origin of serum miRNAs are not clear,[50] the terms found collectively

support a plausible role in the CNS. Conceptually, brain-derived exosomes crossing the brain–blood barrier represent a potential biomarker source for neurodegenerative diseases,[51] which is in line with our finding of exosome as the top localization term. In this context, the biological enrichment analysis in our study pinpointed a plausible brain or CSF origin of at least some of the biosignature miRNAs, thus supporting the concept that minimally invasive serum miRNAs could mirror pathophysiological processes occurring at the CNS in α-synucleinopathies. Future neuronal exosome studies in PD serum should address this question, especially if interrogating PD prodromal stages. Illustratively, a recent study reported increased α-synuclein at neuronal exosomes from IRBD serum preceding the diagnosis of PD, persisting during disease progression, and predicting PD clinical outcomes versus atypical parkinsonisms.[52]

Despite the promising identification of a novel miRNA biosignature that is informative of different disease progression stages in α-synucleinopathies, our study has limitations. First, we performed a restrictive miRNA expression analysis filtering in only miRNAs validated by RT-qPCR, but additional candidates could also be nominated for validation. Second, our miRNA analyses have not been corrected for IRBD medication, such as melatonin, which has been shown to interact with specific miRNAs in mice.[53,54] Third, ours is the first serum miRNA longitudinal study in IRBD characterized by DaT-SPECT, but the follow-up (26 months) was limited. Fourth, the power to discriminate between subtypes of α-synucleinopathy in our predictive modeling requires larger LBD sample sizes. Indeed, given the retrospective character of this study, further validation analyses in independent, larger cohorts of patients are warranted to ensure the predictive ability of this serum miRNA biosignature. Lastly, it has to be mentioned that the reproducibility of PD miRNA to date has been limited because of ancestry differences, lack of gold standard normalization methods, and reduced cohort sizes. In the absence of gold standard normalizers across populations,[18] we applied both endogenous and exogenous controls[17,55] as an improved strategy that can increase cross-laboratory miRNA reproducibility.

In summary, we identified a serum miRNA biosignature that is informative in discriminating healthy controls, patients with IRBD, and patients with PD/DLB and holds potential as a disease progression biomarker. If validated, our findings may have implications for disease prediction strategies and early detection of α-synucleinopathies such as PD and DLB. Further studies in other prodromal PD/DLB or PD/DLB at-risk cohorts are warranted.

Acknowledgments: This work was supported by the Fundación Tatiana Pérez de Guzmán el Bueno (grant FundTatiana16_PROY03) to M.E. and R.F.-S. M.F. was supported through a María de Maeztu grant (MDM-2017-0729) to the Parkinson's Disease and Movement Disorders group of the Institut de Neurociències (Universitat de Barcelona). S.L. was beneficiary of a PFIS fellowship from Instituto de Salud Carlos III (ISCIII) and cofunded by the European Regional Development Fund (grant FI18/00221). J.C. was supported by a Miguel Servet grant from ISCIII cofunded by the European Union (grant CPII18/00026). R.F.-S. was supported by a Miguel Servet grant from the ISCIII cofunded by the European Union (grant CP19/00048), and a Jóvenes Investigadores (JIN) grant of the Spanish Ministry of Economy and Competitiveness (MINECO) and the Agencia Estatal de Investigación (AEI) (AEI/FEDER/UE) (grant SAF2015-73508-JIN). This work was supported by Secretara de Estado de Investigacin, Desarrollo e Innovacin. We thank the patients and their relatives for participating in this study. This research project was done at the CELLEX building from IDIBAPS. IDIBAPS receives support from the CERCA program of Generalitat de Catalunya. We also thank the support from the AGAUR program from the Generalitat de Catalunya (grant AGAUR#2017SGR1502) and the Spanish Network for Research on Neurodegenerative Disorders (CIBERNED) – ISCIII (CIBERNED: CB06/05/0018-ISCIII).

Data Availability Statement

Data available on request from the authors

References

1. Iranzo A, Tolosa E, Gelpi E, et al. Neurodegenerative disease status and post-mortem pathology in idiopathic rapid-eye-movement sleep behaviour disorder: an observational cohort study. Lancet Neurol 2013;12:443–453. https://doi.org/10.1016/S1474-4422(13)70056-5
2. Bartel DP. MicroRNAs: genomics, biogenesis, mechanism, and function. Cell 2004;116:281–297. https://doi.org/10.1016/s0092-8674(04)00045-5
3. Maciotta S, Meregalli M, Torrente Y. The involvement of microRNAs in neurodegenerative diseases. Front Cell Neurosci 2013;7:1–17. https://doi.org/10.3389/fncel.2013.00265
4. Cardo LF, Coto E, Ribacoba R, et al. MiRNA profile in the substantia Nigra of Parkinson's disease and healthy subjects. J Mol Neurosci 2014;54:830–836. https://doi.org/10.1007/s12031-014-0428-y
5. Vallelunga A, Ragusa M, Di Mauro S, et al. Identification of circulating microRNAs for the differential diagnosis of Parkinson's disease and multiple system atrophy. Front Cell Neurosci 2014;8:1–10. https://doi.org/10.3389/fncel.2014.00156
6. Ding H, Huang Z, Chen M, et al. Identification of a panel of five serum miRNAs as a biomarker for Parkinson's disease. Parkinsonism Relat Disord 2016;22:68–73. https://doi.org/10.1016/j.parkreldis.2015.11.014
7. Ma W, Li Y, Wang C, et al. Serum miR-221 serves as a biomarker for Parkinson's disease. Cell Biochem Funct 2016;34:511–515. https://doi.org/10.1002/cbf.3224
8. Botta-Orfila T, Morató X, Compta Y, et al. Identification of blood serum micro-RNAs associated with idiopathic and LRRK2 Parkinson's disease. J Neurosci Res 2014;92:1071–1077. https://doi.org/10.1002/jnr.23377
9. Fernández-Santiago R, Iranzo A, Gaig C, et al. MicroRNA association with synucleinopathy conversion in rapid eye movement behavior disorder. Ann Neurol 2015;77:895–901. https://doi.org/10.1002/ana.24384
10. Kern F, Fehlmann T, Violich I, et al. Deep sequencing of sncRNAs reveals hallmarks and regulatory modules of the transcriptome during Parkinson's disease progression. Nat Aging 2021;1:309–322. https://doi.org/10.1038/s43587-021-00042-6
11. Kägi G, Bhatia KP, Tolosa E. The role of DAT-SPECT in movement disorders. J Neurol Neurosurg Psychiatry 2010;81:5–12. https://doi.org/10.1136/jnnp.2008.157370
12. Scherfler C, Schwarz J, Antonini A, et al. Role of DAT-SPECT in the diagnostic work up of parkinsonism. Mov Disord 2007;22:1229–1238. https://doi.org/10.1002/mds.21505
13. Iranzo A, Santamaría J, Valldeoriola F, et al. Dopamine transporter imaging deficit predicts early transition to synucleinopathy in idiopathic rapid eye movement sleep behavior disorder. Ann Neurol 2017;82:419–428. https://doi.org/10.1002/ana.25026

14. Postuma RB, Berg D, Stern M, et al. MDS clinical diagnostic criteria for Parkinson's disease. Mov Disord 2015;30:1591–1601. https://doi.org/10.1002/mds.26424
15. McKeith IG, Dickson DW, Lowe J, et al. Diagnosis and management of dementia with Lewy bodies: third report of the DLB consortium. Neurology 2005;65:1863–1872. https://doi.org/10.1212/01.wnl.0000187889.17253.b1
16. Umu SU, Langseth H, Bucher-Johannessen C, et al. A comprehensive profile of circulating RNAs in human serum. RNA Biol 2018;15:242–250. https://doi.org/10.1080/15476286.2017.1403003
17. Schwarzenbach H, Da Silva AM, Calin G, et al. Data normalization strategies for microRNA quantification. Clin Chem 2015;61:1333–1342. https://doi.org/10.1373/clinchem.2015.239459
18. Marabita F, De Candia P, Torri A, et al. Normalization of circulating microRNA expression data obtained by quantitative real-time RT-PCR. Brief Bioinform 2016;17:204–212. https://doi.org/10.1093/bib/bbv056
19. Andersen CL, Jensen JL, Ørntoft TF. Normalization of real-time quantitative reverse transcription-PCR data: a model-based variance estimation approach to identify genes suited for normalization, applied to bladder and colon cancer data sets. Cancer Res 2004;64:5245–5250. https://doi.org/10.1158/0008-5472.CAN-04-0496
20. Pérez-Soriano A, Bravo P, Soto M, et al. MicroRNA deregulation in blood serum Identi fi es multiple system atrophy altered pathways. Mov Disord 2020;10:1873–1879. https://doi.org/10.1002/mds.28143
21. Margis R, Margis R, Rieder CRM. Identification of blood microRNAs associated to Parkinson's disease. J Biotechnol 2011;152:96–101. https://doi.org/10.1016/j.jbiotec.2011.01.023
22. Infante J, Prieto C, Sierra M, et al. Comparative blood transcriptome analysis in idiopathic and LRRK2 G2019S-associated Parkinson's disease. Neurobiol Aging 2015;38(214):e1–214.e5. https://doi.org/10.1016/j.neurobiolaging.2015.10.026
23. Kern F, Fehlmann T, Solomon J, et al. miEAA 2.0: integrating multi-species microRNA enrichment analysis and workflow management systems. Nucleic Acids Res 2020;48:W521–W528. https://doi.org/10.1093/nar/gkaa309
24. Chen C, Ridzon DA, Broomer AJ, et al. Real-time quantification of microRNAs by stem-loop RT-PCR. Nucleic Acids Res 2005;33:1–9. https://doi.org/10.1093/nar/gni178
25. Gan L, Denecke B. Profiling pre-microRNA and mature microRNA expressions using a single microarray and avoiding separate sample preparation. Microarrays 2013;2:24–33. https://doi.org/10.3390/microarrays2010024
26. Wang S, El-Deiry WS. TRAIL and apoptosis induction by TNF-family death receptors. Oncogene 2003;22:8628–8633. https://doi.org/10.1038/sj.onc.1207232
27. Saari L, Kivinen K, Gardberg M, et al. Dopamine transporter imaging does not predict the number of nigral neurons in Parkinson disease. Neurology 2017;88:1461–1467. https://doi.org/10.1212/WNL.0000000000003810
28. Iranzo A, Fairfoul G, Na Ayudhaya A, et al. Detection of α-synuclein in CSF by RT-QuIC in patients with isolated rapid-eye-movement sleep behaviour disorder: a longitudinal observational study. Lancet Neurol 2021;20:203–212. https://doi.org/10.2139/ssrn.3556635
29. Iranzo A, Borrego S, Vilaseca I, et al. α-Synuclein aggregates in labial salivary glands of idiopathic rapid eye movement sleep behavior disorder. Sleep 2018;41:1–8. https://doi.org/10.1093/sleep/zsy101
30. Noyce AJ, R'Bibo L, Peress L, et al. PREDICT-PD: an online approach to prospectively identify risk indicators of Parkinson's disease. Mov Disord 2017;32:219–226. https://doi.org/10.1002/mds.26898
31. Postuma RB, Gagnon JF, Montplaisir J. Clinical prediction of Parkinson's disease: planning for the age of neuroprotection. J Neurol Neurosurg Psychiatry 2010;81:1008–1013. https://doi.org/10.1136/jnnp.2009.174748
32. Dos Santos MCT, Barreto-Sanz MA, Correia BRS, et al. miRNA-based signatures in cerebrospinal fluid as potential diagnostic tools for early stage Parkinson's disease. Oncotarget 2018;9:17455–17465. https://doi.org/10.18632/oncotarget.24736
33. Behbahanipour M, Peymani M, Salari M, et al. Expression profiling of blood microRNAs 885, 361, and 17 in the patients with the Parkinson's disease: integrating interaction data to uncover the possible triggering age-related mechanisms. Sci Rep 2019;9:1–11. https://doi.org/10.1038/s41598-019-50256-3
34. Chahine LM, Beach TG, Brumm MC, et al. In vivo distribution of α-synuclein in multiple tissues and biofluids in Parkinson disease. Neurology 2020;95:e1267–e1284. https://doi.org/10.1212/WNL.0000000000010404
35. Mollenhauer B, Caspell-Garcia CJ, Coffey CS, et al. Longitudinal analyses of cerebrospinal fluid α-Synuclein in prodromal and early Parkinson's disease. Mov Disord 2019;34:1354–1364. https://doi.org/10.1002/mds.27806
36. Cao XY, Lu JM, Zhao ZQ, et al. MicroRNA biomarkers of Parkinson's disease in serum exosome-like microvesicles. Neurosci Lett 2017;644:94–99. https://doi.org/10.1016/j.neulet.2017.02.045
37. Schulz J, Takousis P, Wohlers I, et al. Meta-analyses identify differentially expressed micrornas in Parkinson's disease. Ann Neurol 2019;85:835–851. https://doi.org/10.1002/ana.25490
38. Bai X, Tang Y, Yu M, et al. Downregulation of blood serum microRNA 29 family in patients with Parkinson's disease. Sci Rep 2017;7:1–7. https://doi.org/10.1038/s41598-017-03887-3
39. Martins M, Rosa A, Guedes LC, et al. Convergence of mirna expression profiling, α-synuclein interacton and GWAS in Parkinson's disease. PLoS One 2011;6:e25443. https://doi.org/10.1371/journal.pone.0025443
40. Pasinetti GM. Role of personalized medicine in the identification and characterization of Parkinson's disease in asymptomatic subjects. J Alzheimers Dis Parkinsonism 2012;2:e118. https://doi.org/10.4172/2161-0460.1000e118
41. Chen YP, Wei QQ, Chen XP, et al. Aberration of miRNAs expression in leukocytes from sporadic amyotrophic lateral sclerosis. Front Mol Neurosci 2016;9:1–11. https://doi.org/10.3389/fnmol.2016.00069
42. Gámez-Valero A, Campdelacreu J, Vilas D, et al. Platelet miRNA bio-signature discriminates between dementia with Lewy bodies and Alzheimer. disease 2021;9:1272. https://doi.org/10.1101/2020.05.04.075713
43. Gui YX, Liu H, Zhang LS, et al. Altered microRNA profiles in cerebrospinal fluid exosome in Parkinson disease and Alzheimer disease. Oncotarget 2015;6:37043–37053. https://doi.org/10.18632/oncotarget.6158
44. Marques TM, Kuiperij HB, Bruinsma IB, et al. MicroRNAs in cerebrospinal fluid as potential biomarkers for Parkinson's disease and multiple system atrophy. Mol Neurobiol 2017;54:7736–7745. https://doi.org/10.1007/s12035-016-0253-0
45. Tatura R, Kraus T, Giese A, et al. Parkinson's disease: SNCA-, PARK2-, and LRRK2- targeting microRNAs elevated in cingulate gyrus. Parkinsonism Relat Disord 2016;33:115–121. https://doi.org/10.1016/j.parkreldis.2016.09.028
46. Nair VD, Ge Y. Alterations of miRNAs reveal a dysregulated molecular regulatory network in Parkinson's disease striatum. Neurosci Lett 2016;629:99–104. https://doi.org/10.1016/j.neulet.2016.06.061
47. Chen L, Yang J, Lü J, et al. Identification of aberrant circulating miRNAs in Parkinson's disease plasma samples. Brain Behav 2018;8:1–9. https://doi.org/10.1002/brb3.941
48. Briggs CE, Wang Y, Kong B, et al. Midbrain dopamine neurons in Parkinson's disease exhibit a dysregulated miRNA and target-gene network. Brain Res 2015;1618:111–121. https://doi.org/10.1016/j.brainres.2015.05.021
49. Chatterjee P, Roy D. Comparative analysis of RNA-seq data from brain and blood samples of Parkinson's disease. Biochem Biophys Res Commun 2017;484:557–564. https://doi.org/10.1016/j.bbrc.2017.01.121
50. Turchinovich A, Weiz L, Burwinkel B. Extracellular miRNAs: the mystery of their origin and function. Trends Biochem Sci 2012;37:460–465. https://doi.org/10.1016/j.tibs.2012.08.003
51. Hornung S, Dutta S, Bitan G. CNS-derived blood exosomes as a promising source of biomarkers: opportunities and challenges. Front Mol Neurosci 2020;13:1–16. https://doi.org/10.3389/fnmol.2020.00038

52. Jiang C, Hopfner F, Hopfner F, et al. Serum neuronal exosomes predict and differentiate Parkinson's disease from atypical parkinsonism. J Neurol Neurosurg Psychiatry 2020;91:720–729. https://doi.org/10.1136/jnnp-2019-322588

53. Che H, Li H, Li Y, et al. Melatonin exerts neuroprotective effects by inhibiting neuronal pyroptosis and autophagy in STZ-induced diabetic mice. FASEB J 2020;34:14042–14054. https://doi.org/10.1096/fj.202001328R

54. Wang K, Ru J, Zhang H, et al. Melatonin enhances the therapeutic effect of plasma exosomes against cerebral ischemia-induced Pyroptosis through the TLR4/NF-κB pathway. Front Neurosci 2020;14:1–16. https://doi.org/10.3389/fnins.2020.00848

55. Madadi S, Schwarzenbach H, Lorenzen J, et al. MicroRNA expression studies: challenge of selecting reliable reference controls for data normalization. Cell Mol Life Sci 2019;76:3497–3514. https://doi.org/10.1007/s00018-019-03136-y

Supporting Data

Additional Supporting Information may be found in the online version of this article at the publisher's web-site.

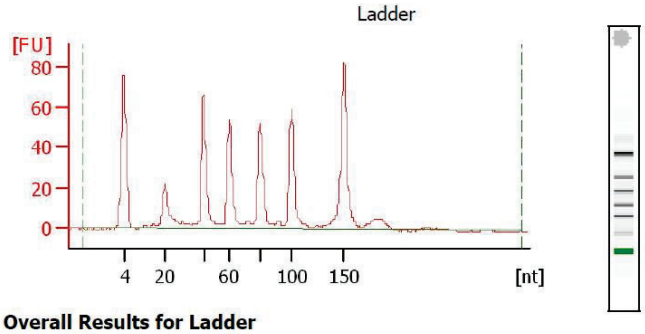

Overall Results for Ladder

Result Flagging Color:

Result Flagging Label: Number of Peaks: 6

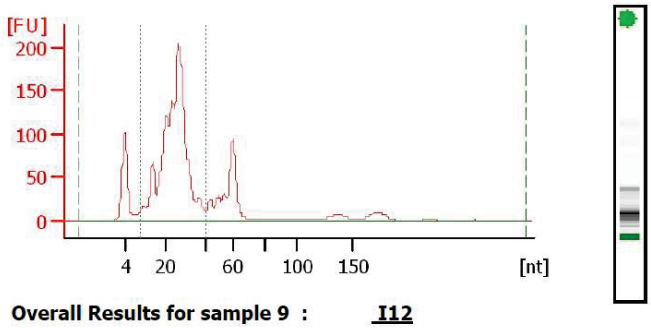

Overall Results for sample 9 : I12

Small RNA Concentration [pg/µl]: 10.005,7

miRNA Concentration [pg/µl]: 8.940,2

miRNA / Small RNA Ratio [%]: 89

Result Flagging Color:

Result Flagging Label: 89 % miRNA; Concentration: 8940.20 pg/µl

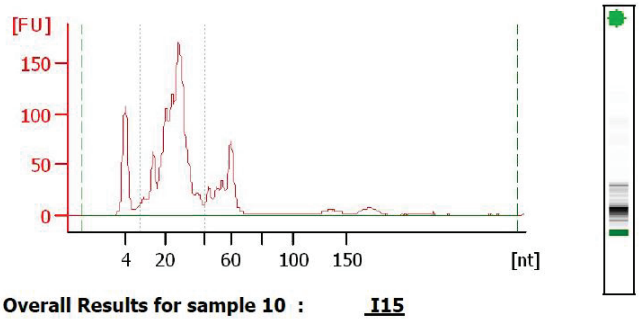

Overall Results for sample 10 : I15

Small RNA Concentration [pg/µl]: 8.243,6

miRNA Concentration [pg/µl]: 7.363,3

miRNA / Small RNA Ratio [%]: 89

Result Flagging Color:

Result Flagging Label: 89 % miRNA; Concentration: 7363.30 pg/µl

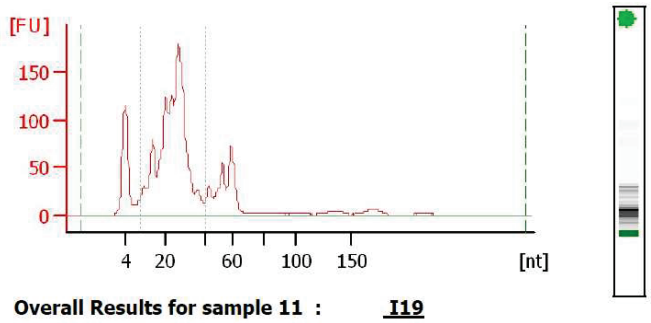

Overall Results for sample 11 : I19

Small RNA Concentration [pg/µl]: 7.796,2

miRNA Concentration [pg/µl]: 6.937,4

miRNA / Small RNA Ratio [%]: 89

Result Flagging Color:

Result Flagging Label: 89 % miRNA; Concentration: 6937.40 pg/µl

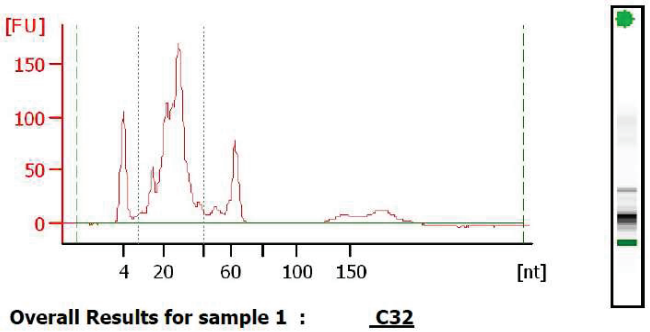

Overall Results for sample 1 : C32

Small RNA Concentration [pg/µl]: 7.862,2

miRNA Concentration [pg/µl]: 7.093,7

miRNA / Small RNA Ratio [%]: 90

Result Flagging Color:

Result Flagging Label: 90 % miRNA; Concentration: 7093.70 pg/µl

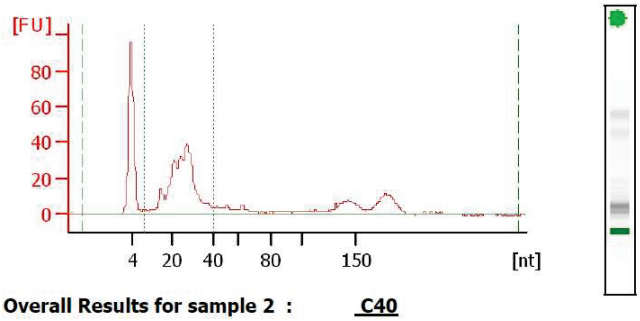

Overall Results for sample 2 : C40

Small RNA Concentration [pg/µl]: 2.369,4

miRNA Concentration [pg/µl]: 2.103,6

miRNA / Small RNA Ratio [%]: 89

Result Flagging Color:

Result Flagging Label: 89 % miRNA; Concentration: 2103.60 pg/µl

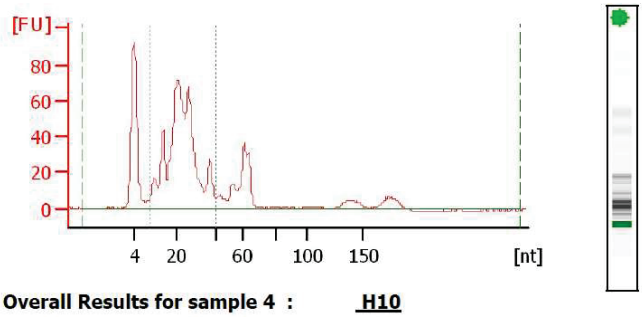

Overall Results for sample 4 : H10

Small RNA Concentration [pg/µl]: 4.684,8

miRNA Concentration [pg/µl]: 4.222,5

miRNA / Small RNA Ratio [%]: 90

Result Flagging Color:

Result Flagging Label: 90 % miRNA; Concentration: 4222.50 pg/µl

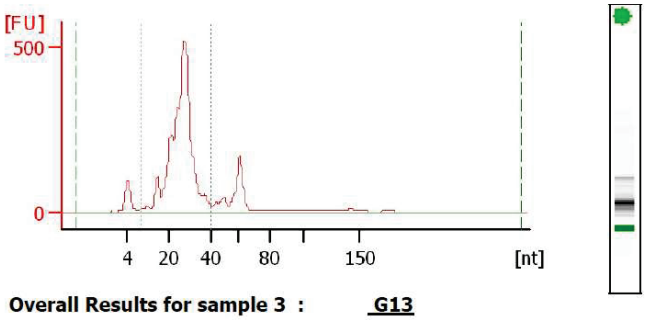

Overall Results for sample 3 : G13

Small RNA Concentration [pg/µl]: 22.296,2

miRNA Concentration [pg/µl]: 20.736,4

miRNA / Small RNA Ratio [%]: 93

Result Flagging Color:

Result Flagging Label: 93 % miRNA; Concentration: 20736.40 pg/µl

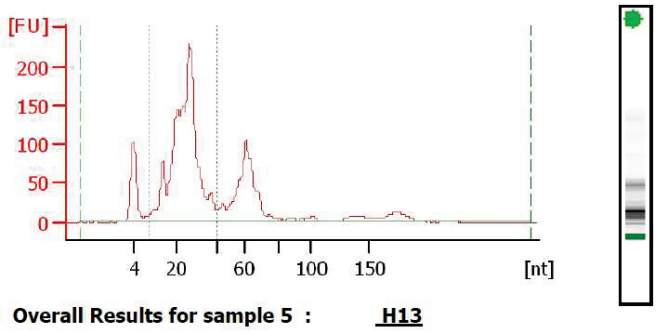

Overall Results for sample 5 : H13

Small RNA Concentration [pg/µl]:	11.061,4
miRNA Concentration [pg/µl]:	9.566,3
miRNA / Small RNA Ratio [%]:	86
Result Flagging Color:	
Result Flagging Label:	86 % miRNA; Concentration: 9566.30 pg/µl

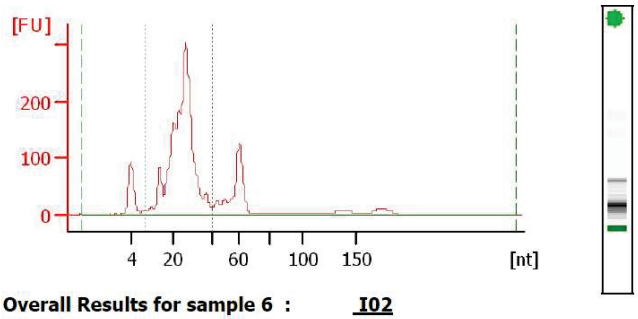

Overall Results for sample 6 : I02

Small RNA Concentration [pg/µl]:	14.327,6
miRNA Concentration [pg/µl]:	13.102,9
miRNA / Small RNA Ratio [%]:	91
Result Flagging Color:	
Result Flagging Label:	91 % miRNA; Concentration: 13102.90 pg/µl

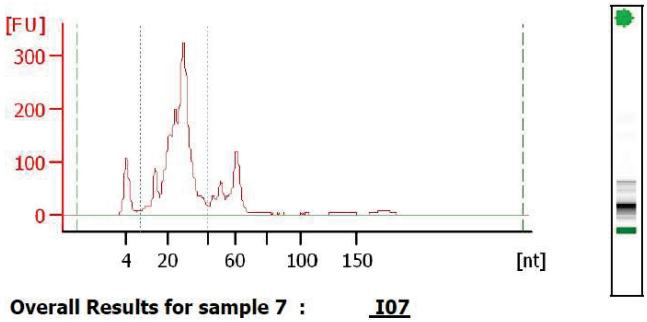

Overall Results for sample 7 : I07

Small RNA Concentration [pg/µl]:	13.185,8
miRNA Concentration [pg/µl]:	11.847,7
miRNA / Small RNA Ratio [%]:	90
Result Flagging Color:	
Result Flagging Label:	90 % miRNA; Concentration: 11847.70 pg/µl

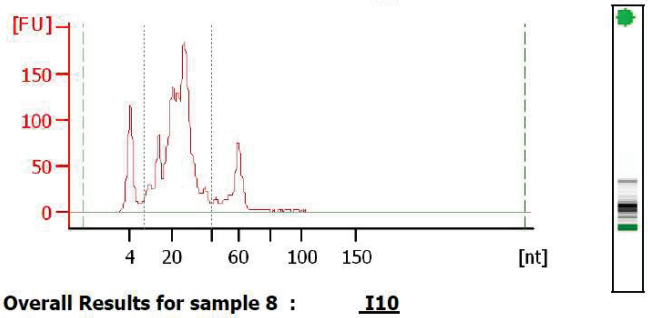

Overall Results for sample 8 : I10

Small RNA Concentration [pg/µl]:	7.945,7
miRNA Concentration [pg/µl]:	7.398,0
miRNA / Small RNA Ratio [%]:	93
Result Flagging Color:	
Result Flagging Label:	93 % miRNA; Concentration: 7398 pg/µl

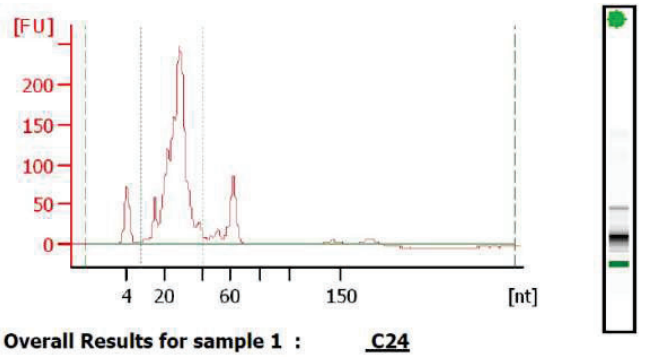

Overall Results for sample 1 : C24

Small RNA Concentration [pg/µl]:	12.374,7
miRNA Concentration [pg/µl]:	11.537,6
miRNA / Small RNA Ratio [%]:	93
Result Flagging Color:	
Result Flagging Label:	93 % miRNA; Concentration: 11537.60 pg/µl

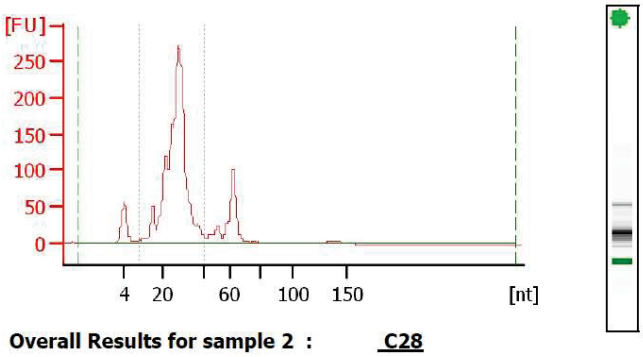

Overall Results for sample 2 : C28

Small RNA Concentration [pg/µl]:	16.768,4
miRNA Concentration [pg/µl]:	15.626,8
miRNA / Small RNA Ratio [%]:	93
Result Flagging Color:	
Result Flagging Label:	93 % miRNA; Concentration: 15626.80 pg/µl

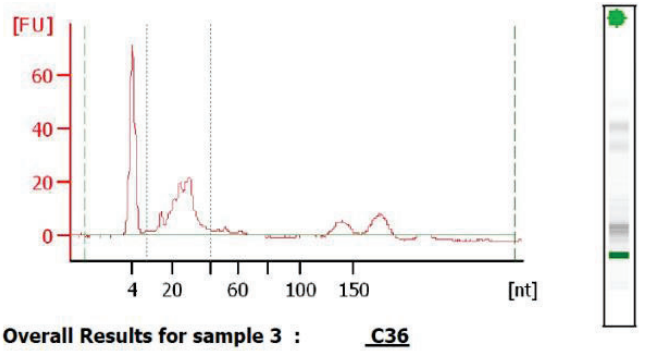

Overall Results for sample 3 : C36

Small RNA Concentration [pg/µl]:	1.553,2
miRNA Concentration [pg/µl]:	1.364,5
miRNA / Small RNA Ratio [%]:	88
Result Flagging Color:	
Result Flagging Label:	88 % miRNA; Concentration: 1364.50 pg/µl

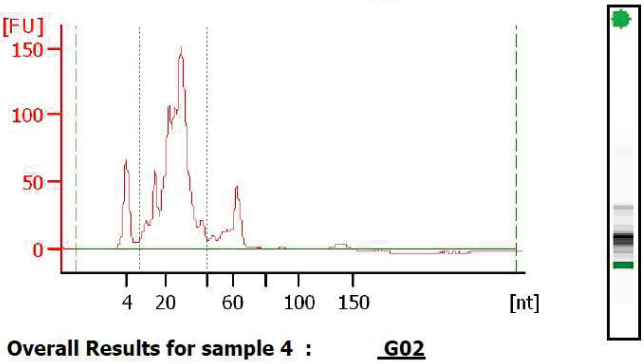

Overall Results for sample 4 : G02

Small RNA Concentration [pg/µl]:	9.559,0
miRNA Concentration [pg/µl]:	8.997,4
miRNA / Small RNA Ratio [%]:	94
Result Flagging Color:	
Result Flagging Label:	94 % miRNA; Concentration: 8997.40 pg/µl

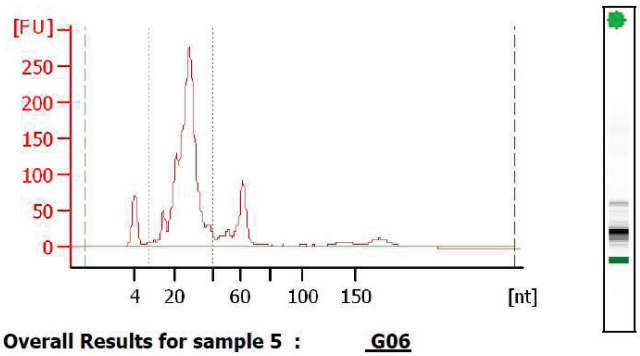

Overall Results for sample 5 : G06

Small RNA Concentration [pg/µl]:	13.888,0
miRNA Concentration [pg/µl]:	12.710,1
miRNA / Small RNA Ratio [%]:	92
Result Flagging Color:	
Result Flagging Label:	92 % miRNA; Concentration: 12710.10 pg/µl

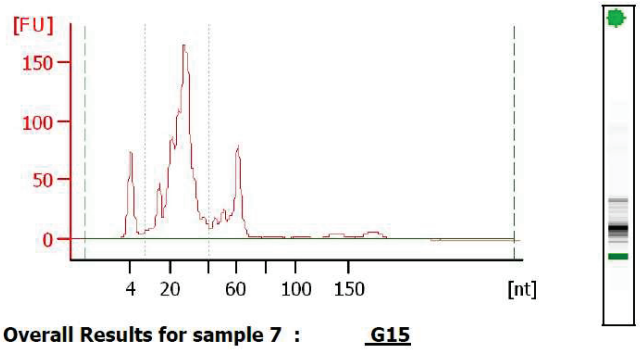

Overall Results for sample 7 : G15

Small RNA Concentration [pg/µl]:	9.109,0
miRNA Concentration [pg/µl]:	8.144,7
miRNA / Small RNA Ratio [%]:	89
Result Flagging Color:	
Result Flagging Label:	89 % miRNA; Concentration: 8144.70 pg/µl

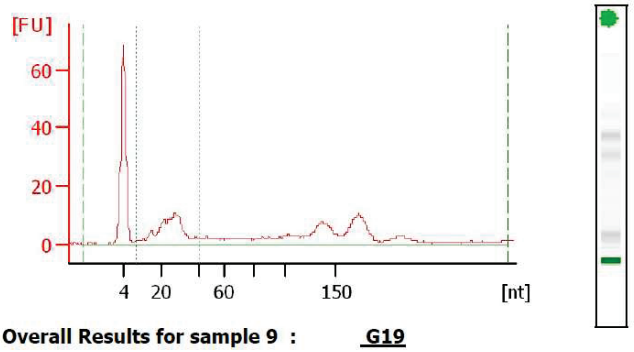

Overall Results for sample 9 : G19

Small RNA Concentration [pg/µl]:	1.271,3
miRNA Concentration [pg/µl]:	791,4
miRNA / Small RNA Ratio [%]:	62
Result Flagging Color:	
Result Flagging Label:	62 % miRNA; Concentration: 791.40 pg/µl

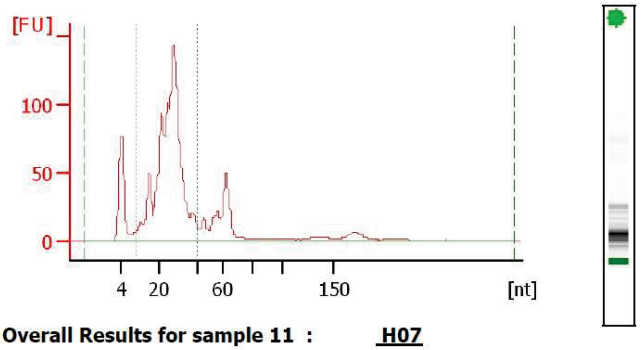

Overall Results for sample 11 : H07

Small RNA Concentration [pg/µl]:	7.798,3
miRNA Concentration [pg/µl]:	6.998,0
miRNA / Small RNA Ratio [%]:	90
Result Flagging Color:	
Result Flagging Label:	90 % miRNA; Concentration: 6998 pg/µl

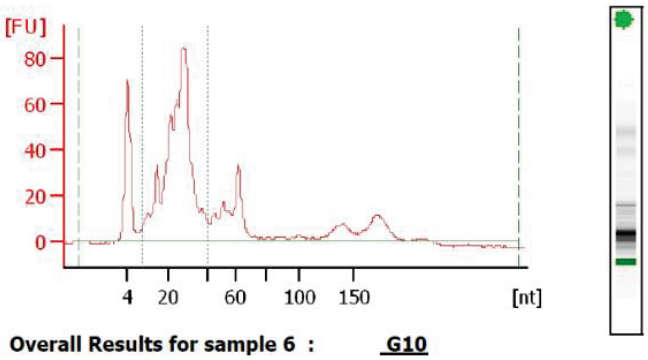

Overall Results for sample 6 : G10

Small RNA Concentration [pg/µl]:	5.815,4
miRNA Concentration [pg/µl]:	4.957,9
miRNA / Small RNA Ratio [%]:	85
Result Flagging Color:	
Result Flagging Label:	85 % miRNA; Concentration: 4957.90 pg/µl

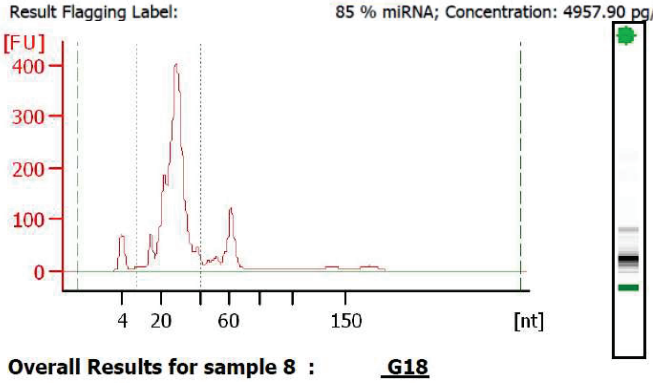

Overall Results for sample 8 : G18

Small RNA Concentration [pg/µl]:	20.041,1
miRNA Concentration [pg/µl]:	18.467,0
miRNA / Small RNA Ratio [%]:	92
Result Flagging Color:	
Result Flagging Label:	92 % miRNA; Concentration: 18467 pg/µl

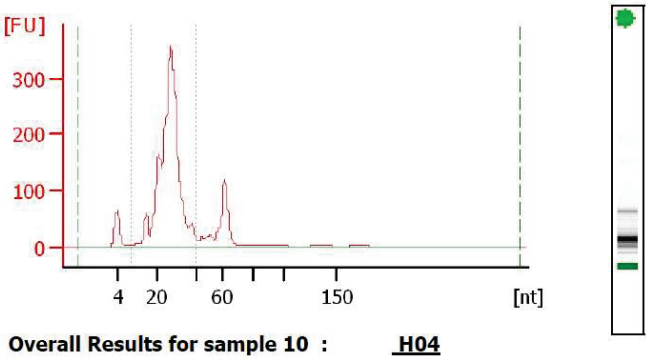

Overall Results for sample 10 : H04

Small RNA Concentration [pg/µl]:	19.632,5
miRNA Concentration [pg/µl]:	18.040,6
miRNA / Small RNA Ratio [%]:	92
Result Flagging Color:	
Result Flagging Label:	92 % miRNA; Concentration: 18040.60 pg/µl

Suppl. Fig. 1

Genome-wide candidate miRNA

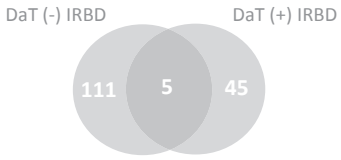

Groups	Total	miRNAs
DaT (+) IRBD vs. C DaT (-) IRBD vs. C	5	miR-8084 miR-6780b-5p miR-6741-5p miR-3201 miR-4701-3p
DaT (-) IRBD vs. C	111	miR-4707-5p miR-6126 miR-6848-5p miR-6816-5p miR-7108-5p miR-4758-5p miR-6716-5p miR-4486 miR-4539 miR-4689 miR-1275 miR-4710 miR-6763-5p miR-6729-5p miR-4793-3p miR-92b-5p miR-4505 miR-6771-5p miR-1228-5p miR-6786-5p miR-3960 miR-6779-5p miR-6752-5p miR-5093 miR-3197 mir-6089-1 miR-1343-5p miR-185-3p miR-1909-3p miR-595 mir-6089-2 miR-4498 miR-6775-5p miR-4466 miR-2861 miR-6727-5p miR-7110-5p miR-4492 miR-4507 miR-1587 miR-4695-5p miR-6891-5p miR-762 miR-3648 miR-1469 miR-149-3p miR-6756-5p miR-6821-5p miR-3621 miR-6769b-5p miR-3613-5p miR-328-5p miR-4632-5p miR-6858-5p miR-1268b mir-4679-1 miR-3656 miR-663a miR-6850-5p miR-7107-5p miR-4281 miR-6749-5p miR-8072 miR-3620-5p miR-6722-3p miR-6869-5p miR-4745-5p miR-3178 miR-1207-5p miR-6798-5p miR-1237-5p miR-6805-5p mir-1913 miR-4270 miR-6799-5p miR-4739 miR-1227-5p miR-7150 miR-4459 miR-6791-5p miR-5001-5p miR-4440 miR-3135b miR-4463 miR-6789-5p miR-4690-5p miR-937-5p miR-4484 mir-4466 miR-4649-5p miR-4651 miR-320d miR-4433b-3p miR-6824-5p miR-1225-5p miR-4429 mir-4281 miR-1908-5p miR-3141 miR-6743-5p miR-4508 miR-6860 miR-4462 miR-4763-3p miR-6787-5p miR-3940-5p miR-1268a miR-1233-5p miR-4433-3p miR-6724-5p miR-4734
DaT (+) IRBD vs. C	45	miR-151a-5p miR-361-5p miR-23a-3p miR-4454 miR-185-5p miR-150-5p miR-4530 miR-744-5p miR-22-3p miR-122-5p miR-17-5p miR-24-3p miR-4467 mir-550a-3 miR-26a-5p miR-342-3p miR-20a-5p miR-652-3p miR-25-3p let-7b-5p mir-550a-1 miR-6732-5p miR-23b-3p miR-193a-5p miR-877-5p miR-3128 let-7d-5p miR-297 let-7c-5p miR-4487 miR-191-5p miR-451a mir-7515 miR-638 miR-140-3p miR-106a-5p miR-7114-5p miR-16-5p miR-126-3p miR-425-5p miR-5787 miR-103a-3p miR-93-5p miR-107 mir-550a-2

Cross-sectional RT-qPCR DEmiR

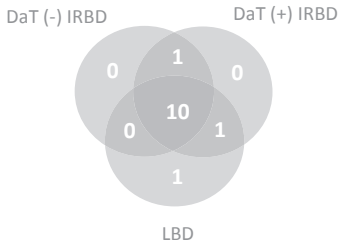

Groups	Total	miRNAs
DaT (+) IRBD vs. C DaT (-) IRBD vs. C LBD vs. C	10	miR-19b-3p miR-425-5p miR-24-3p miR-29c-3p miR-221-3p miR-25-3p miR-361-5p miR-451a let-7c-5p miR-22-3p
DaT (+) IRBD vs. C DaT (-) IRBD vs. C	1	miR-1227-5p
DaT (+) IRBD vs. C LBD vs. C	1	miR-140-3p
LBD vs. C	1	miR-4505

Longitudinal RT-qPCR DEmiR DAT (-) IRBD vs. C

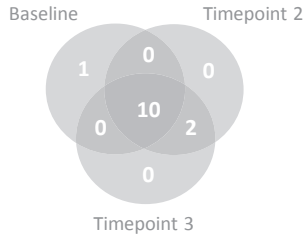

Groups	Total	miRNAs
Baseline Timepoint 1 Timepoint 2	10	miR-19b-3p miR-425-5p miR-24-3p miR-29c-3p miR-221-3p miR-25-3p miR-361-5p miR-451a let-7c-5p miR-22-3p
Timepoint 2 Timepoint 3	2	miR-140-3p miR-4505
Baseline	1	miR-1227-5p

Longitudinal RT-qPCR DEmiR DAT (+) IRBD vs. C

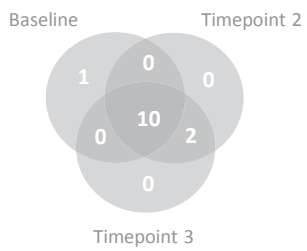

Groups	Total	miRNAs
Baseline Timepoint 1 Timepoint 2	11	miR-19b-3p miR-425-5p miR-24-3p miR-29c-3p miR-221-3p miR-140-3p miR-25-3p miR-361-5p miR-451a let-7c-5p miR-22-3p
Timepoint 1 Timepoint 3	1	miR-4505
Baseline	1	miR-1227-5p

Suppl. Fig. 2

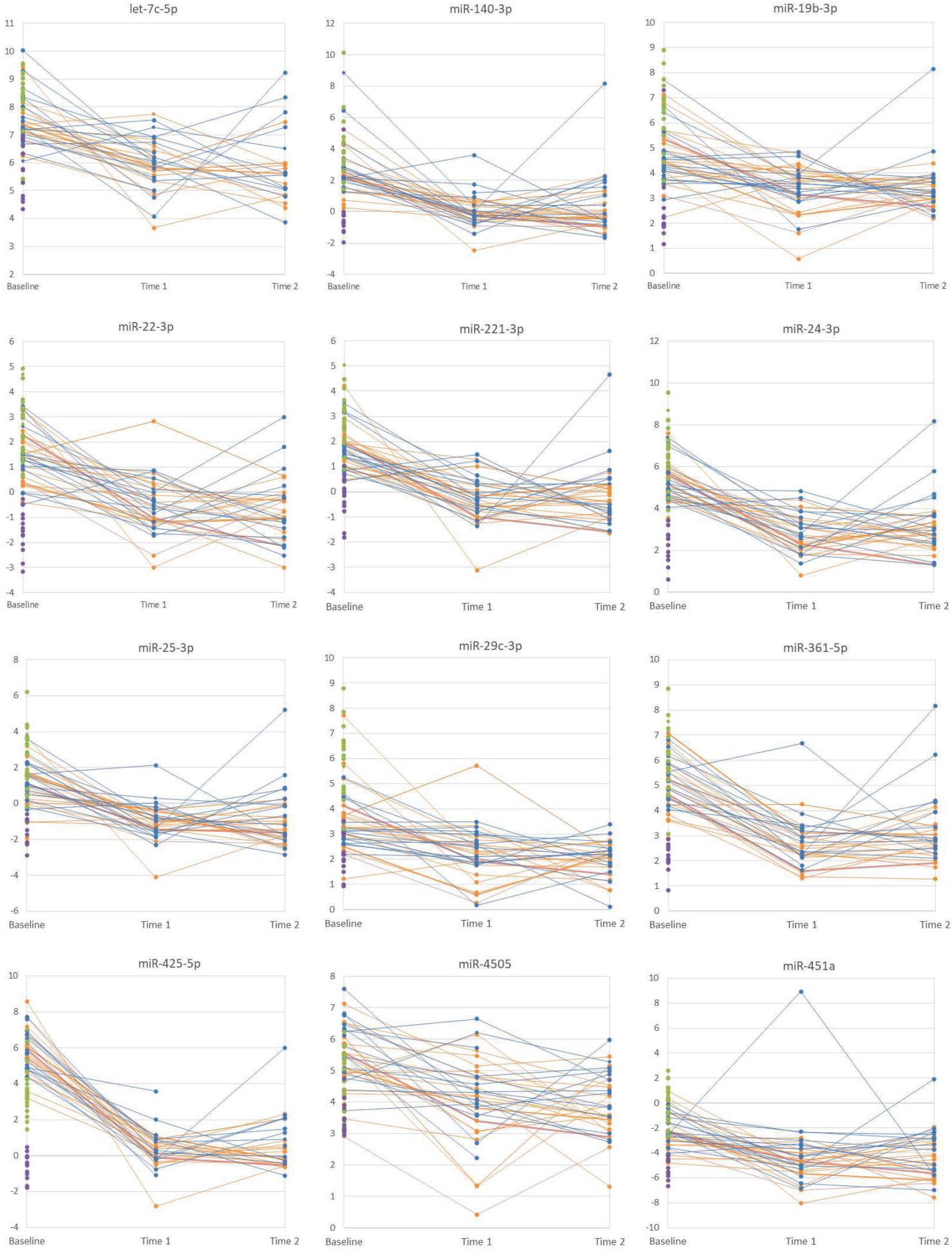
let-7c-5p
miR-140-3p
miR-19b-3p
miR-22-3p
miR-221-3p
miR-24-3p
miR-25-3p
miR-29c-3p
miR-361-5p
miR-425-5p
miR-4505
miR-451a
Baseline
Time 1
Time 2

Suppl. Fig. 3

SUPPLEMENTARY TABLE 1: Number of subjects treated for RBD and LBD and range of dose.

IRBD = isolated rapid eye movement sleep behaviour disorder; DaT = DaT-SPECT imaging; LBD = Lewy body disease (PD and LBD)

	RBD treatment				LBD treatment					
	Clonazepam		Melatonin		L-DOPA		Cholinesterase inhibitors			
							Rivastigmine		Donepezil	
	Treated Nr. (%)	Dose (mg)	Treated Nr. (%)	Dose (mg)	Treated Nr. (%)	LEDD	Treated Nr. (%)	Dose (mg)	Treated Nr. (%)	Dose (mg)
DaT(-) IRBD baseline (n=17)	12 (70.6)	0.25-2	1 (5.9)	4	0	-	0	-	0	-
Timepoint 2 (n=16)	15 (93.8)	0.25-3	1 (6.3)	2	0	-	0	-	0	-
Timepoint 3 (n=14)	13 (92.9)	0.25-3	0 (0.0)	-	0	-	0	-	0	-
DaT(+) IRBD baseline (n=21)	16 (76.2)	0.25-2	3 (14.3)	2-6	0	-	0	-	0	-
Timepoint 2 (n=19)	12 (63.2)	0.25-2	7 (36.8)	2-6	1 (5.3)	100	0	-	0	-
Timepoint 3 (n=19)	11 (57.9)	0.25-2	7 (36.8)	5-6	1 (5.3)	450	0	-	0	-
LBD (PD and DLB) (n=13)	9 (69.2)	0.5-2.5	2 (15.4)	2-9	5 (38.5)	300-450	2 (15.4)	4.6-13	1 (7.7)	10

SUPPLEMENTARY TABLE 2: Timepoint intervals between longitudinal follow-up sampling per each subject. Number of months between baseline sampling and timepoints 2 and 3 in DaT-negative and DaT-positive IRBD subjects. IRBD = isolated rapid eye movement sleep behaviour disorder; DaT= DaT-SPECT imaging

	DaT-negative IRBD																				
Subject	H01	H02	H03	H04	H05	H06	H07	H08	H09	H10	H11	H12	H13	H14	H15	H16	H17				
Timepoint 2	9	10	9	13	13	6	9	9	14	8	14	9	10	5	12	-	12				
Timepoint 3	15	16	16	24	26	-	20	15	25	21	19	13	29	17	18	-	-				
	DaT-positive IRBD																				
Subject	G01	G02	G03	G04	G05	G06	G07	G08	G09	G10	G11	G12	G13	G14	G15	G16	G17	G18	G19	G20	G21
Timepoint 2	13	5	14	11	11	11	10	10	11	10	12	12	10	10	14	-	14	10	9	9	-
Timepoint 3	25	11	26	17	20	20	20	18	18	23	18	17	22	19	26	-	26	21	15	18	-

SUPPLEMENTARY TABLE 3: Candidate differentially expressed miRNAs identified by genome-wide microRNA expression analysis. (**A**) DaT-negative IRBD vs. controls. (**B**) DaT-positive IRBD vs. controls. IRBD = isolated rapid eye movement sleep behaviour disorder; DaT = DaT-SPECT imaging; FC = Fold change

A

DaT-negative IRBD vs. controls

miRNA	P-value	FC	miRNA	P-value	FC
miR-1207-5p	0.0004	-3.4591	miR-6724-5p	0.0187	-5.2830
miR-3613-5p	0.0004	-4.8195	miR-1228-5p	0.0188	-6.5628
miR-6749-5p	0.0013	-3.8441	mir-4281	0.0191	-2.5978
miR-1225-5p	0.0015	-2.6884	mir-4466	0.0191	-2.3140
miR-3135b	0.0020	-3.3210	miR-4492	0.0191	-3.7386
miR-1268a	0.0020	-4.0370	miR-4508	0.0195	-4.3001
miR-4433-3p	0.0022	-2.8057	miR-5093	0.0198	-3.6453
miR-7107-5p	0.0030	-3.4487	miR-6860	0.0207	-1.6281
miR-4651	0.0031	-4.7370	miR-6798-5p	0.0228	-3.8951
miR-4632-5p	0.0043	-3.4045	miR-6850-5p	0.0230	-3.3948
miR-1275	0.0045	-2.6125	miR-6743-5p	0.0231	-3.8223
miR-6780b-5p	0.0049	-2.8125	miR-762	0.0235	-5.9579
miR-6787-5p	0.0053	-3.3145	miR-4710	0.0241	-1.9819
miR-6741-5p	0.0055	-2.7941	miR-1908-5p	0.0249	-3.8674
miR-6848-5p	0.0057	-2.2715	miR-4701-3p	0.0254	-3.3770
miR-4486	0.0059	-3.6694	mir-1913	0.0255	-2.1930
miR-1227-5p	0.0061	-4.5322	miR-4281	0.0257	-5.6829
miR-6775-5p	0.0062	-2.9418	mir-4679-1	0.0257	2.1690
miR-6126	0.0064	-11.6036	miR-8072	0.0266	-3.8344
miR-1268b	0.0065	-3.3554	miR-4462	0.0268	-2.3962
miR-937-5p	0.0067	-2.2224	miR-4429	0.0270	-2.6096
miR-7150	0.0067	-2.1668	miR-3197	0.0279	-2.9470
miR-4440	0.0071	-10.4155	miR-1469	0.0285	-2.4667
miR-4498	0.0074	-2.1742	miR-7108-5p	0.0292	-5.5311
miR-3141	0.0077	-3.7493	miR-663a	0.0297	-4.3441
miR-6756-5p	0.0081	-3.0460	miR-92b-5p	0.0301	-2.0062
miR-7110-5p	0.0083	-10.3706	miR-4539	0.0315	-1.6012
miR-4690-5p	0.0083	-1.7339	miR-6799-5p	0.0316	-2.1169
miR-4689	0.0088	-2.3884	miR-6805-5p	0.0328	-4.7530

miR-4463	0.0090	-6.2556	miR-149-3p	0.0330	-5.5593
miR-6716-5p	0.0092	-2.5374	miR-3656	0.0333	-4.8674
miR-4433b-3p	0.0092	-4.4368	miR-3960	0.0334	-3.2700
miR-4649-5p	0.0095	-3.5703	miR-6779-5p	0.0340	-2.0326
miR-3648	0.0097	-1.9334	mir-6089-1	0.0342	-5.0746
miR-6824-5p	0.0104	-2.8603	mir-6089-2	0.0342	-5.0746
miR-328-5p	0.0105	-5.2601	miR-6891-5p	0.0344	-1.8823
miR-4505	0.0105	-2.7027	miR-6786-5p	0.0360	-4.4784
miR-6752-5p	0.0110	-5.8512	miR-3201	0.0361	5.7072
miR-4758-5p	0.0111	-3.2209	miR-8084	0.0362	5.3057
miR-185-3p	0.0116	-5.0231	miR-2861	0.0362	-3.6982
miR-3178	0.0117	-5.8236	miR-5001-5p	0.0370	-3.4264
miR-3620-5p	0.0118	-3.6626	miR-6769b-5p	0.0380	-1.7772
miR-6763-5p	0.0123	-1.7206	miR-3621	0.0383	-3.6583
miR-4507	0.0123	-3.5668	miR-4793-3p	0.0407	-4.7293
miR-6821-5p	0.0125	-5.3855	miR-6729-5p	0.0408	-2.9794
miR-6771-5p	0.0125	-3.3738	miR-320d	0.0416	-4.6420
miR-1909-3p	0.0127	-2.9737	miR-4466	0.0431	-3.7586
miR-1587	0.0129	-2.5024	miR-6869-5p	0.0434	-4.0146
miR-4695-5p	0.0131	-2.3696	miR-1237-5p	0.0437	-5.0657
miR-6791-5p	0.0137	-3.9123	miR-4707-5p	0.0456	-2.7577
miR-4739	0.0139	-2.2166	miR-4745-5p	0.0459	-4.3048
miR-6722-3p	0.0145	-4.4306	miR-4459	0.0464	-2.1769
miR-4270	0.0147	-3.9392	miR-4734	0.0465	-3.9511
miR-6858-5p	0.0158	-3.9603	miR-4763-3p	0.0467	-2.7399
miR-1343-5p	0.0167	-3.6256	miR-595	0.0472	-2.6410
miR-6816-5p	0.0172	-7.3172	miR-6727-5p	0.0477	-3.6857
miR-3940-5p	0.0177	-6.5240	miR-4484	0.0491	-5.9006
miR-1233-5p	0.0186	-2.8683	miR-6789-5p	0.0497	-4.0448

B

DaT-positive IRBD vs. controls

miRNA	P-value	FC	miRNA	P-value	FC
miR-4530	3.23E-07	6.9268	miR-151a-5p	0.0037	3.3509
miR-122-5p	9.20E-06	17.1805	miR-126-3p	0.0042	2.5816
miR-425-5p	2.61E-05	10.2558	miR-22-3p	0.0043	3.6848
miR-361-5p	4.53E-05	3.1425	miR-3201	0.0053	-4.3733
miR-25-3p	4.97E-05	4.2740	miR-106a-5p	0.0064	3.5565
let-7c-5p	0.0001	3.8664	miR-342-3p	0.0064	3.1194
miR-193a-5p	0.0001	3.4711	miR-20a-5p	0.0066	2.9721
miR-140-3p	0.0003	6.4165	miR-5787	0.0100	-1.6947
miR-4487	0.0003	2.1046	let-7b-5p	0.0111	4.9079
miR-6732-5p	0.0008	-1.6071	miR-107	0.0125	3.3149
miR-23a-3p	0.0008	7.5698	mir-7515	0.0187	-3.0543
miR-191-5p	0.0009	7.9700	miR-7114-5p	0.0190	-2.0832
miR-24-3p	0.0009	6.7009	miR-451a	0.0201	2.8320
miR-8084	0.0011	-5.4270	miR-6780b-5p	0.0204	-2.0387
miR-26a-5p	0.0012	5.0407	miR-297	0.0220	-3.7245
miR-652-3p	0.0014	3.1623	miR-4454	0.0230	1.6804
miR-17-5p	0.0014	4.1517	miR-16-5p	0.0248	4.6549
miR-23b-3p	0.0017	3.2719	miR-6741-5p	0.0297	-1.9861
miR-185-5p	0.0020	5.2206	miR-4701-3p	0.0316	-2.5938
miR-93-5p	0.0022	5.3113	miR-877-5p	0.0402	1.5216
miR-4467	0.0024	3.0629	miR-638	0.0407	-1.4231
let-7d-5p	0.0032	2.3475	mir-550a-1	0.0431	-1.3283
miR-103a-3p	0.0032	4.8721	mir-550a-2	0.0431	-1.3283
miR-150-5p	0.0036	2.8061	mir-550a-3	0.0431	-1.3283
miR-744-5p	0.0037	2.5224	miR-3128	0.0447	-2.5953

SUPPLEMENTARY TABLE 4: Details of commercially available TaqMan Fast Advanced miRNA assays for assessment of miRNA expression levels by real-time quantitative PCR (RT-qPCR). (A) Assays used for RT-qPCR assessment of miRNA levels. **(B)** Assays discarded due to poor RT-qPCR amplification

A

miRNA	Assay ID	Catalog number	miRbase Accession Number	Type
hsa-miR-6727-5p	480235_mir	A25576	MI0022572	Endogenous Control
hsa-miR-320a-3p	478594_mir	A25576	MI0000542	Endogenous Control
cel-miR-39-3p	478293_mir	A25576	MI0000010	Exogenous Control
hsa-let-7c-5p	478577_mir	A25576	MI0000064	Target
hsa-miR-1207-5p	477873_mir	A25576	MI0006340	Target
hsa-miR-1227-5p	480789_mir	A25576	MI0006316	Target
hsa-miR-140-3p	477908_mir	A25576	MI0000456	Target
hsa-miR-19b-3p	478264_mir	A25576	MI0000074	Target
hsa-miR-22-3p	477985_mir	A25576	MI0000078	Target
hsa-miR-221-3p	477981_mir	A25576	MI0000298	Target
hsa-miR-24-3p	477992_mir	A25576	MI0000080	Target
hsa-miR-25-3p	477994_mir	A25576	MI0000082	Target
hsa-miR-29c-3p	479229_mir	A25576	MI0000735	Target
hsa-miR-361-5p	478056_mir	A25576	MI0000760	Target
hsa-miR-3613-5p	479424_mir	A25576	MI0016003	Target
hsa-miR-425-5p	478094_mir	A25576	MI0001448	Target
hsa-miR-4505	477842_mir	A25576	MI0016868	Target
hsa-miR-451a	478107_mir	A25576	MI0001729	Target

B

miRNA	Assay ID	Catalog number	miRbase Accession Number	Type
has-miR-185-3p	474832_mir	A25576	MI0000482	Did not amplify
hsa-miR-3619-5p	479689_mir	A25576	MI0016009	Did not amplify
has-miR-4530	478918_mir	A25576	MI0016897	Did not amplify
has-miR-4632-5p	479865_mir	A25576	MI0017259	Did not amplify
has-miR-6126	480186_mir	A25576	MI0021260	Did not amplify
hsa-miR-6741-3p	480259_mir	A25576	MI0022586	Did not amplify
has-miR-6749-5p	480272_mir	A25576	MI0022594	Did not amplify

SUPPLEMENTARY TABLE 5: RT-qPCR assessment of 10 selected miRNAs identified by genome-wide miRNA expression analysis. IRBD = isolated rapid eye movement sleep behaviour disorder; RT-qPCR = real-time quantitative PCR; FC = fold change. (*) Differentially expressed miRNAs (DEmiR) from the array validated by RT-qPCR with the same fold change direction and a statistically significant P-value

	Microarray		**RT-qPCR**	
	FC	**P-value**	**FC**	**Adj. P-value**
DaT-negative IRBD vs. controls				
miR-1207-5p	-3.46	0.0004	-1.55	0.2706
miR-1227-5p	-4.53	0.0061*	-1.78	0.0064*
miR-3613-5p	-4.82	0.0004	1.06	0.8772
DaT-positive IRBD vs. controls				
Let-7c-5p	3.87	0.0001*	2.25	0.0024*
miR-140-3p	6.42	0.0003*	3.26	0.0034*
miR-24-3p	6.70	0.0009*	3.85	0.0006*
miR-25-3p	4.27	4.97E-05*	4.16	0.0024*
miR-361-5p	3.14	4.53E-05*	3.32	0.0033*
miR-425-5p	10.25	2.61E-05	-3.64	0.0024
miR-451a	2.83	0.0201*	7.72	0.0003*

SUPPLEMENTARY TABLE 6: Technical validation of the real-time quantitative PCR (RT-qPCR) longitudinal analyses. Replication of the longitudinal RT-qPCR assessment of miRNA expression levels in serum samples from DaT-positive and DaT-negative IRBD patients as compared to controls. IRBD = isolated rapid eye movement sleep behaviour disorder; DaT = DaT-SPECT imaging; FC = fold change; adj. P = false discovery rate (FDR) multiple-testing adjusted P-values

	DaT-negative IRBD						**DaT-positive IRBD**					
	Baseline		**Timepoint 2**		**Timepoint 3**		**Baseline**		**Timepoint 2**		**Timepoint 3**	
	FC	**Adj. P**	**FC**	**Adj. P**	**FC**	**Adj. P**	**FC**	**Adj. P**	**FC**	**Adj. P**	**FC**	**Adj. P**
Initial analysis												
miR-140-3p	1.82	0.2706	14.17	$<1.0x10^{-6}$	7.51	0.0008	3.26	0.0034	17.65	$<1.0x10^{-6}$	17.85	$<1.0x10^{-6}$
miR-19b-3p	5.07	0.0002	11.59	$<1.0x10^{-6}$	4.82	$4.0x10^{-6}$	5.45	0.0001	12.17	$<1.0x10^{-6}$	14.00	$<1.0x10^{-6}$
miR-29c-3p	5.67	0.0002	11.24	$<1.0x10^{-6}$	1.36	$<1.0x10^{-6}$	5.17	0.0003	12.92	$<1.0x10^{-6}$	15.15	$<1.0x10^{-6}$
Replication												
miR-140-3p	1.77	0.0631	6.10	$5.5x10^{-5}$	5.60	$5.7x10^{-5}$	3.09	0.0014	14.19	$<1.0x10^{-6}$	12.68	$<1.0x10^{-6}$
miR-19b-3p	4.06	0.0005	10.19	$<1.0x10^{-6}$	9.44	$2.0x10^{-6}$	5.75	$3.2x10^{-5}$	14.32	$<1.0x10^{-6}$	17.19	$<1.0x10^{-6}$
miR-29c-3p	3.91	0.0014	9.09	$2.0x10^{-6}$	7.92	$1.3x10^{-5}$	4.65	0.0006	13.84	$<1.0x10^{-6}$	13.38	$<1.0x10^{-6}$

SUPPLEMENTARY TABLE 7: Frequency of selection by LASSO of each miRNA included in machine-learning analysis folds (N=71).

Variable	Nr. of folds	Frequency of folds (%)
Age at sampling	71	100
Gender	71	100
miR-1227-5p	71	100
miR-425-5p	71	100
miR-451a	71	100
miR-22-3p	70	98.59
miR-221-3p	70	98.59
miR-361-5p	67	94.37
miR-24-3p	42	59.15
let-7c-5p	11	15.49
miR-25-3p	8	11.27
miR-29c-3p	6	8.45
miR-19b-3p	1	1.41
miR-140-3p	0	0

SUPPLEMENTARY TABLE 8: Performance metrics achieved by machine-learning analysis for detection of IRBD, PD and DLB (N=71). (*) AUC values are adjusted by age and sex in the machine-learning classifier. (**) P-values obtained by Mann-Whitney U test. AUC = area under the curve; CI = confidence interval; Adj. P-value = FDR multiple testing adjusted P-value; IRBD = isolated rapid eye movement sleep behaviour disorder

	AUC* (0.95 CI)	Fold-change	P-value**	Adj. P-value	Regulation
let-7c-5p	0.68 (0.52 - 0.85)	2.63	<0.0001	<0.0001	Upregulated
miR-1227-5p	0.76 (0.60 - 0.91)	-1.84	0.0001	<0.0001	Downregulated
miR-140-3p	0.66 (0.48 - 0.83)	3.64	<0.0001	<0.0001	Upregulated
miR-19b-3p	0.74 (0.60 - 0.89)	5.20	<0.0001	<0.0001	Upregulated
miR-22-3p	0.58 (0.43 - 0.73)	3.51	<0.0001	0.0001	Upregulated
miR-221-3p	0.72 (0.57 - 0.87)	3.42	<0.0001	<0.0001	Upregulated
miR-24-3p	0.76 (0.62 - 0.89)	4.34	<0.0001	<0.0001	Upregulated
miR-25-3p	0.66 (0.51 - 0.81)	4.04	<0.0001	<0.0001	Upregulated
miR-29c-3p	0.85 (0.77 - 0.94)	5.55	<0.0001	<0.0001	Upregulated
miR-361-5p	0.54 (0.40 - 0.69)	3.34	<0.0001	<0.0001	Upregulated
miR-425-5p	0.75 (0.58 - 0.91)	-1.40	0.056	0.3496	Downregulated
miR-451a	0.75 (0.63-0.88)	6.68	<0.0001	<0.0001	Upregulated

SUPPLEMENTARY TABLE 9: RT-qPCR assessment of miRNA expression levels in serum samples within the IRBD continuum. IRBD = isolated rapid eye movement sleep behaviour disorder; LBD = Lewy body disease (PD and DLB); DaT = DaT-SPECT imaging; DaT(-) IRBD = DaT-negative IRBD patients; DaT(+) IRBD = DaT-positive IRBD patients; FC = fold change; Adj. P = FDR multiple-test adjusted P-value

	DaT(+) IRBD vs. DaT(-) IRBD		LBD vs. DaT(+) IRBD	
	FC	**Adj. P**	**FC**	**Adj. P**
let7c-5p	1.16	0.8624	3.00	0.0039
miR1227-5p	1.23	0.4361	2.67	0.0101
miR140-3p	1.56	0.4361	5.80	0.0006
miR19b-3p	1.11	0.8624	4.22	0.0002
miR22-3p	1.04	0.8624	7.36	0.0009
miR221-3p	1.04	0.8624	3.61	0.0037
miR24-3p	1.07	0.8624	7.87	0.0011
miR25-3p	1.62	0.4361	4.13	0.0006
miR29c-3p	1.09	0.8624	2.09	0.0067
miR361-5p	1.48	0.4361	5.63	0.0001
miR451a	1.69	0.4361	4.52	0.0016

3.2 Article 2

Differential serum microRNAs in premotor *LRRK2* G2019S carriers from Parkinson's disease

Marta Soto, MSc,[1,2,3] Manel Fernández,[1,2,3,4] Paloma Bravo, MSc,[1,2,3] Sara Lahoz, MSc,[5,6] Alicia Garrido, MD,[1,2,3] Antonio Sánchez-Rodríguez, MD,[7] María Rivera-Sánchez, MD,[7] María Sierra, MD,[7] Paula Melón, MSc,[1,2,3] Ana Roig-García, MSc,[1,2,3] Anna Naito, PhD,[8] Bradford Casey PhD,[8] Jordi Camps, PhD,[5,6] Eduardo Tolosa, MD, PhD,[1,2,3] María-José Martí, MD, PhD,[1,2,3] Jon Infante, MD, PhD,[3,7] Mario Ezquerra, PhD,[1,2,3,+,*], & Rubén Fernández-Santiago, PhD,[1,2,3,9,+,*]

[1] Lab of Parkinson Disease & Other Neurodegenerative Movement Disorders, Institut d'Investigacions Biomèdiques August Pi i Sunyer (IDIBAPS), Institut de Neurociències, Universitat de Barcelona, ES-08036 Barcelona, Catalonia, Spain. [2] Parkinson disease and Movement Disorders Unit, Neurology Service, Institut Clínic de Neurociències, Hospital Clínic de Barcelona, ES-08036 Barcelona, Catalonia, Spain. [3] Centro de Investigación Biomédica en Red sobre Enfermedades Neurodegenerativas (CIBERNED: CB06/05/0018-ISCIII), ES-08036 Barcelona, Catalonia. [4] Parkinson's disease and Movement Disorders group of the Institut de Neurociències (Universitat de Barcelona), ES-08036 Barcelona, Catalonia, Spain. [5] Gastrointestinal and Pancreatic Oncology Team, Institut d'Investigacions Biomèdiques August Pi i Sunyer (IDIBAPS)-Hospital Clínic de Barcelona, 08036 Barcelona, Spain. [6] Centro de Investigación Biomédica en Red de Enfermedades Hepáticas y Digestivas (CIBERehd), Madrid, Spain. [7] Movement Disorders Unit, Department of Neurology, Hospital Universitario Marqués de Valdecilla, Universidad de Cantabria, ES-39008 Santander, Cantabria, Spain [8] The Michael J. Fox Foundation for Parkinson's Research, Grand Central Station, P.O. Box 4777, New York, NY 10120, USA. [9] Histology Unit, Department of Biomedicine, Faculty of Medicine, Universitat de Barcelona, ES-08036 Barcelona, Catalonia, Spain.

Correspondence to: Dr. Rubén Fernández-Santiago & Dr. Mario Ezquerra
Lab of Parkinson Disease and Other Neurodegenerative Movement Disorders, IDIBAPS-Hospital Clínic de Barcelona, CELLEX Building, Casanova 143, Floor 3B, 08036 Barcelona, Catalonia, Spain.
Phone: +34 932 275 400 ext. 5785.
e-mail: ruben.fernandez.santiago@gmail.com; ezquerra@clinic.cat

Word count (4,000-4,500): 3,743

Abstract (typically 150 words): 223

(No abbreviations preferred)

Tables and/or figures (up to 10): 4 Tables / 5 Figures

Supplemental data: 4 Suppl. Tables

References (around 60): 67

Characters in the title: 87

Characters in the running title: 48

(Formatted in UK British English)

RUNNING TITLE: Longitudinal miRNA assessment in G2019S carriers

KEYWORDS: LRRK2-associated Parkinson's disease (L2PD); LRRK2 non-manifesting carriers (L2NMC); dopamine transporter single-photon emission computed tomography (DAT-SPECT); microRNA (miRNA); follow-up, biomarkers

FINANCIAL DISCLOSURE / CONFLICTS OF INTEREST: Nothing to report

FUNDING: This work was supported by the Michael J. Fox Foundation for Parkinson's Research (MJFF) to R.F.-S. and M.E. Subject recruitment was supported by the Michael J. Fox Foundation for Parkinson's Research (MJFF) (grant #11849) to M.J.-M., and E.T. M.F. was funded by the María de Maeztu program (grant #MDM-2017-0729) to the Parkinson's disease and Movement Disorders group of the Institut de Neurociències (Universitat de Barcelona). R.F.-S. was supported by the Miguel Servet (grant #CP19/00048), FIS (grant #FIS20-PI20/00659) and PFIS (grant #FI21/00104) programmes from the Instituto de Salud Carlos III (ISCIII) co-funded by the European Union, and also by a Jóvenes Investigadores (JIN) grant of the Spanish Ministry of Economy and Competitiveness (MINECO) and the Agencia Estatal de Investigación (AEI) (AEI/FEDER/UE) (grant #SAF2015-73508-JIN). IDIBAPS receives support from the CERCA program of Generalitat de Catalunya.

ABSTRACT

The *LRRK2* G2019S pathogenic mutation causes LRRK2-associated Parkinson's disease (L2PD) with incomplete penetrance. LRRK2 non-manifesting carriers (L2NMC) are at PD high risk but predicting pheno-conversion is challenging given the lack of progression biomarkers. To investigate novel biomarkers for PD premotor stages, we performed a longitudinal microRNA (miRNA) assessment of serum samples from G2019S L2NMC followed-up over 8 years. Our cohort consisted of G2019S L2NMC stratified by dopamine transporter single-photon emission computed tomography (DaT-SPECT) into DaT-negative (n=20) and DaT-positive L2NMC (n=20), pheno-converted G2019S L2PD patients (n=20), idiopathic PD (iPD) (n=19), and controls (n=40). We also screened a second cohort of L2PD patients (n=19) and controls (n=20) (Total n=158). Compared to healthy controls, we identified 8 deregulated miRNAs in DaT-negative L2NMC, 6 in DaT-positive L2NMC, and one in L2PD. Between groups, the highest miRNA differences, 24 candidate miRNAs, occurred between DaT-positive L2NMC and L2PD. Longitudinally, we found 11 common miRNAs with sustained variation in DaT-negative and DaT-positive L2NMCs compared to their baselines. Our study identifies novel miRNA alterations in premotor stages of PD co-occurring with progressive DaT-SPECT decline before motor manifestation, whose deregulation seems to attenuate after the diagnosis of L2PD. Moreover, we identified 4 miRNAs with relatively high discriminative ability (AUC=0.82) between non-pheno-converted DaT-positive G2019S carriers and pheno-converted L2PD patients (miR-4505, miR-8069, miR-6125, and miR-451a), which hold potential as early progression biomarkers for PD.

ABBREVIATIONS

(Minimal abbreviations to be used in the text)

miRNA: microRNA

PD: Parkinson's disease

iPD: idiopathic PD

L2PD: *LRRK2*-associated PD

LRRK2: leucine-rich repeat kinase 2 gene

L2NMC: disease non-manifesting *LRRK2* mutation carriers

DaT-SPECT: ^{123}I-FP-CIT dopamine transporter single-photon emission computed tomography

DaT(-) L2NMC: DaT-negative L2NMC (normal dopaminergic function)

DaT(+) L2NMC: DaT-positive L2NMC (abnormal dopaminergic function)

DEmiR: differentially expressed microRNA

INTRODUCTION

Parkinson's disease (PD) is an age-related neurodegenerative movement disorder[1] which is characterized by the loss of dopaminergic neurons (DAn) in the substantia nigra pars compacta and Lewy bodies containing α-synuclein in different brain areas.[2,3] The clinical diagnosis is based on motor symptoms (bradykinesia, rigidity, and resting tremor). Still, prodromal disease stages may course with non-motor symptoms such as REM sleep behaviour disorder (RBD), hyposmia, constipation, or depression.[4,5] Most PD cases are classified as idiopathic PD (iPD) patients, but 5-10% encompass monogenic forms.[6] Among these, mutations in the leucine-rich repeat kinase 2 gene (*LRRK2*) leading to LRRK2-associated PD (L2PD) are the most frequent monogenic cause of PD.[7,8] However, the penetrance of mutations in *LRRK2*, e.g., G2019S, is incomplete and varies across populations, suggesting the involvement of additional modulators.[9–13] Thus, LRRK2 non-manifesting carriers (L2NMC) are at a higher risk of PD, but predicting disease onset is challenging due to the lack of early progression biomarkers.

MicroRNAs (miRNAs) are small non-coding RNAs regulating gene expression by mRNA cleavage and translational repression.[14] MiRNA alterations have been associated with PD,[15,16] and some miRNAs have been proposed as non-invasive candidate biomarkers.[17,18] However, longitudinal studies are needed, especially in PD at-risk subjects. Thus, to explore early progression biomarkers, we profiled serum miRNA expression levels in a cohort of G2019S L2NMC from Spain, which we followed-up over 8 years.[19,20] Given that dopamine transporter single-photon emission computed tomography (DaT-SPECT) correlates with striatal PD DAn loss[21,22] and that L2NMC can show reduced striatal ligand uptake before the onset of the motor symptoms,[23] we stratified our cohort into DaT-positive and DaT-negative G2019S L2NMC.[20,24] By genome-wide miRNA discovery (2,578 miRNAs) and RT-qPCR validation, we investigated differentially expressed miRNAs (DEmiR) in G2019S L2NMC, L2PD patients, iPD, and healthy controls.[20] Overall, this study tackles early miRNA deregulation at PD premotor stages and evaluates the potential of miRNAs as candidate progression biomarkers for PD.

RESULTS

Cross-sectional genome-wide miRNA analysis

In our cohort of study (**Table 1**, **Fig. 1A**), by genome-wide discovery analysis and under a P-value below 0.05 and a fold-change above |1.5|, we identified 21 candidate miRNAs in DaT-negative L2NMC vs controls and 10 in DaT-positive L2NMC (**Fig. 1B-C**). We also found 11 candidate miRNAs in G2019S L2PD and 45 in iPD compared to controls. These findings indicate a more pronounced miRNA deregulation effect in iPD than L2PD (**Fig. 1D-E, Suppl. Table 1A**). In addition, across all four comparisons, we observed an overlap in two or more groups of only 10 (13%) out of the 76 unique miRNAs, thus illustrating that most of the deregulated miRNAs identified at the genome-wide level were group-specific (**Fig. 2A**). Moreover, in line with previous findings, in iPD cases we found miR-19b-3p as the top deregulated miRNA by the array.[25,26] Altogether, these results indicate that microRNA deregulation is more prominent in iPD than in L2PD and that specific miRNA changes occur across the continuum of progression stages in G2019S carriers including DaT-negative and DaT-positive L2NMC.

Cross-sectional RT-qPCR

By RT-qPCR, we assessed the expression levels of 10 candidate miRNAs found in the genome-wide analysis across different comparisons (**Suppl. Table 2**) and 2 additional candidate miRNA earlier reported in iPD (miR-29c-3p)[25,27] or PD prodromal stages (miR-451a).[28] Using the same serum samples, we validated 8 DEmiR, which were deregulated in one or more G2019S carrier groups (miR-122-5p, miR-16-5p, miR-185-5p, miR-221-3p, miR-3196, miR-4505, miR-451a, and miR-8069) (**Fig. 3, Table 2**). Of these, all 8 miRNAs were up-regulated in DaT-negative L2NMC, 6 in DaT-positive L2NMC (miR-122-5p, miR-16-5p, miR-185-5p, miR-3196, miR-4505 and miR-451a), and only one in L2PD (miR-3196). Thus, miR-3196 was the only DEmiR common for all G2019S carriers (**Fig. 2B**). Moreover, to confirm findings in L2PD, we tested an independent set of L2PD patients and controls of equal size (**Table 1**) and, in line with the initial results, we observed few differences between L2PD and controls (miR-122-5p) (**Suppl. Table 3**). Although miR-122-5p but not miR-3196 was the miRNA detected in the validation set, given our limited size, both miRNAs represent proposed candidates for subsequent studies in larger L2PD cohorts.

Altogether, these results support the concept of a progressive decline in the number of miRNAs deregulated across the successive progression stages in G2019S carriers. In addition, in iPD cases, we found 9 of the 12 studied miRNAs deregulated (miR-122-5p, miR-16-5p, miR-185-5p, miR-19b-3p, miR-22-3p, miR-221-3p, miR-29c-3p, miR-451a, and miR-8069), again detecting greater miRNA deregulation in iPD than in L2PD. Lastly, miR-19b-3p and miR-29c-3p, which were earlier reported as DEmiR in iPD and idiopathic RBD,[25–27,29,30] showed significant changes only in iPD but not in L2PD nor L2NMC, thus indicating differential miRNA deregulation between iPD and the continuum of progression stages in G2019S carriers, at least for these two specific miRNAs.

Comparison of progression stages in G2019S carriers

We next inquired about miRNA differences occurring across the continuum of progression stages in G2019S carriers. To this end, using genome-wide miRNA data, we first performed pair-wise comparisons among DaT-negative L2NMC, DaT-positive L2NMC, and L2PD (**Fig. 4A-C**, **Suppl. Table 1B**). We found modest miRNA changes between DaT-negative and DaT-positive L2NMC despite their different DaT-SPECT status (miR-7110-5p and miR-4445-3p). However, we observed that most miRNA differences occurred between DaT-positive L2NMC and L2PD patients with overt disease (24 miRNAs), thus suggesting specific miRNA deregulation occurring along with changes in disease status. Moreover, we exploratorily assessed potential miRNA changes related to pheno-conversion by comparing DaT-positive L2NMC non-pheno-converted after 8 years of follow-up (n=16) vs all pheno-converted subjects, i.e., L2PD discovery (n=20) and validation (n=19) sets, and DaT-positive L2NMC which pheno-converted during the study (n=4) (total n=43). We identified 4 miRNAs significantly associated with pheno-conversion including miR-4505 (adj. P=0.0006), miR-8069 (adj. P=0.0035), and miR-6125 (adj. P=0.0280) and a borderline trend for miR-451a (adj. P=0.0828) (**Suppl. Table 4**). Subsequently, when assessing the discriminative capacity of these 4 miRNAs to identify pheno-conversion, an area under the curve (AUC) of 0.82 (95% CI: 0.71-0.93) was observed to discern pheno-converted from non-pheno-converted G2019S carriers (**Fig. 5**). These 4 miRNAs hold potential as candidate pheno-conversion biomarkers and could be prioritized in subsequent studies.

Longitudinal RT-qPCR

To further assess specific miRNA changes across time before motor manifestation, by RT-qPCR, we assessed the longitudinal expression levels of the same 12 cross-sectional miRNA in L2NMC. To this end, we used the DaT-negative and DaT-positive L2NMC cross-sectional serum samples as the reference (baseline),[31] and compared it to their seriated samples after 4 (time point 2) and 8 years (time point 3) of follow-up. Compared to their respective baselines, longitudinal time points 2 and 3 from DaT-negative and DaT-positive L2NMC[20] showed significant miRNA variation for 11 of the 12 studied miRNAs (**Table 3, Fig. 6**). More specifically, 5 DEmiR showed continued expression variation which was consistent across both follow-up time points in DaT-negative and DaT-positive L2NMC (miR-16-5p, miR-19-5p, miR-22-3p, miR-451a, and miR-6125), indicating longitudinally sustained expression changes for some miRNAs. MiR-8069 was deregulated in the longitudinal assessment only in DaT-negative L2NMC but not in the DaT-positive group, thus suggesting early deregulation prior to DaT-SPECT decline for this miRNA. Other miRNAs showed expression variations in only one of the two follow-up time points (miR-122-5p, miR-185-5p, miR-221-3p, miR-29c-3p, and miR-4505) and require further investigation. Lastly, miR-3196, which was found differentially expressed in all G2019S carriers groups including L2PD in the cross-sectional analysis, did not show L2NMC longitudinal changes compared to baseline, thus indicating that the deregulation of miR-3196 was steady across all G2019S carrier stages and did not depend on DaT-SPECT status. Conversely, miR-122-5p was differentially expressed in the L2PD validation group but also in time point 3 from both DaT-positive and DaT-negative L2NMC of the longitudinal analysis, potentially suggesting dynamic levels of this miRNA which need further investigation. Altogether, we observed that, compared to DaT-negative and DaT-positive L2NMC baselines, the expression levels of miRNAs deregulated at PD premotor stages are dynamic and can vary across time, at least during the 8-year follow-up period of this study.

Biological enrichment analysis

Lastly, we performed a biological enrichment analysis exploring the functionality of only experimentally validated genes from the miRTarbase, which are described to be targeted by the candidate miRNAs associated with the G2019S mutation. To that end, we used the top 10 miRNAs

from each comparison from the discovery study. We found a higher number of target genes in iPD patients than in G2019S carriers, and iPD was also the only group surpassing the FDR-multiple testing adjustment (**Table 4**). Enriched biological functions in iPD differed from G2019S carriers and included gene expression, AKT, TGFb signalling, and senescence/TP53. In G2019S carriers, top deregulated pathways included Rho GTPases in DaT-negative and DaT-positive L2NMC and NOTCH signalling in DaT-positive L2NMC and L2PD. These pathways identified in G2019S carriers are involved in dendritic development and axonal arborization and have been extensively associated with LRRK2 biological functions before.[32–34]

DISCUSSION

The lack of informative biomarkers hampers the prediction of disease progression in G2019S L2NMC.[35] Here, we profiled serum miRNAs in a cohort of G2019S carriers from Spain stratified by DaT-SPECT. We observed dynamic miRNA expression profiles across the continuum of progression stages and identified 8 validated DEmiR in DaT-negative L2NMC, 6 in DaT-positive L2NMC, and one in L2PD. The strongest miRNA deregulation was in asymptomatic G2019S carriers, occurred along with the progressive DaT-SPECT decline before motor manifestation, and seemed to attenuate after the diagnosis of L2PD. Moreover, by an 8-year follow-up of DaT-negative and DaT-positive L2NMC, we detected sustained longitudinal variation of 11 DEmiR compared to their baselines. Our study identified specific miRNA changes in PD prodromal stages before motor manifestation, especially in DaT-positive L2NMC who are at a higher risk of PD compared to the general population. Moreover, we identified 4 miRNAs with a reasonable discriminative power to discern pheno-converted vs non-pheno-converted G2019S carriers, which hold promise as early progression biomarkers for L2PD.

In iPD, we found stronger miRNA deregulation than in G2019S carriers and a higher number of miRNA-targeted genes. These findings are relevant given that L2PD is used to model iPD based on their similar clinical features,[36] yet with a certain degree of motor and non-motor heterogeneity[37] and a slower progression described for L2PD.[38,39] Thus, at the molecular level, we also found different miRNA profiles between L2PD and iPD with a total of 46 DEmiR. As a possible interpretation, LRRK2 has been shown to directly interact with the Argonaute-2 component of the RNA-induced silencing complex (RISC).[40,41] Therefore, unlike iPD, miRNA deregulation in LRRK2 carriers could be partially mediated by changes in the miRNA machinery related to the pathogenic activity of mutant LRRK2. Similarly, two earlier studies showed distinct miRNA fingerprints in iPD and monogenic PD patients with *LRRK2*, *SNCA,* or *GBA* mutations.[31,42] In addition, miR-19b-3p and miR-29c-3p were previously associated with iPD[25,26,29,30,43,44] or idiopathic RBD,[27,28] and were also deregulated in our study only in iPD but not in G2019S carriers. Altogether, these results align with previous findings[31,42] indicating group-specific miRNA deregulation between iPD and L2PD and an overall greater miRNA deregulation effect in iPD than in L2PD, which is compliant with the complex multifactorial aetiology of iPD.[45,46]

Ours is the first study addressing miRNA changes in PD premotor stages, i.e., G2019S carriers with and without DaT-SPECT alterations, during an extended follow-up of 8 years. In G2019S carriers, we found that miRNA changes were more prominent in L2NMC than L2PD, suggesting an attenuation of miRNA deregulation after the diagnosis of PD. Specifically, we found 7 DEmiR deregulated in L2NMC both cross-sectional and longitudinally (miR-122-5p, miR-16-5p, miR-185-5p, miR-451a, miR-4505, miR-221-3p, and miR-8069). Apart from miR-8069, which is novel, six of these miRNAs were earlier described in PD patients with overt disease. Thus, a transcriptome study identified miR-4505 in L2PD blood.[47] Another RNA-seq study using PPMI cohorts found altered miR-122-5p, miR-16-5p, miR-185-5p, and miR-451a in monogenic PD with *LRRK2*, *SNCA*, or *GBA* mutations, and also, miR-16-5p and miR-451a in iPD.[31] Lastly, miR-185-5p and miR-221-3p are part of a 5-miRNA panel discriminating iPD serum from controls.[48] Collectively, these studies support the potential of miRNAs from our study as candidate biomarkers of early PD progression before motor manifestation.

In light of our findings, one hypothesis is that the G2019S pathogenic mutation, which leads to a toxic gain of kinase function of LRRK2,[49] is also associated with miRNA deregulation processes in early premotor stages, which attenuate after motor manifestation in L2PD. Other studies described early molecular deregulation in subjects at-risk of PD before the clinical diagnosis. Thus, several reports showed a higher transcriptomic deregulation in L2NMC than in L2PD[47] (L2NMC/L2PD ratio of 1.64) or in PD prodromal stages than in manifested PD (L2NMC/L2PD ratio of 2.36).[50] In our longitudinal miRNA assessment of DaT-negative and DaT-positive L2NMC, we also found progressive miRNA variation after 4 and 8 years compared to their respective baselines. These results align with a 3-year longitudinal RNA-seq study in a PPMI cohort including iPD and monogenic L2PD reporting dynamic miRNA levels across the progression of PD.[31] Similarly, our 8-year longitudinal follow-up in G2019S carriers indicates dynamic miRNA expression changes in premotor stages of PD.

Overall, exploring the prodromal stage of PD is essential to elucidate early disease mechanisms and identify early PD progression biomarkers.[51,52] Illustratively, a recent cerebrospinal fluid (CSF) study reported that levels of total and oligomeric α-synuclein and TNF-α discriminate L2NMC from L2PD and iPD, and controls,[53] thus proposing these candidates as risk

biomarkers in prodromal PD stages. Moreover, another study has recently identified specific phospho-protein changes associated with the G2019S mutation in L2NMC.[54] Similarly, here we found specific miRNA deregulation in G2019S carriers with and without DaT-SPECT decline before the diagnosis of PD. Thus, as earlier suggested,[54,55] a relevant implication of our findings is that initiation of LRRK2 inhibitors treatment in L2NMC before motor manifestation represents an attractive option to investigate in clinical trials. In this context, miRNAs detected in L2NMC before motor manifestation warrant further investigation as candidate early progression biomarkers. Specifically, we identified a combination of 4 miRNAs (miR-4505, miR-8069, miR-6125, and miR-451a) that exhibits an AUC of 0.82 in discriminating 8-year followed-up non-pheno-converted DaT-positive L2NMC from pheno-converted L2PD patients. Hence, these 4 miRNAs hold potential as candidate pheno-conversion biomarkers and could be prioritized in subsequent longitudinal studies on *LRRK2* G2019S carriers or other prodromic PD cohorts.

Lastly, we performed a restrictive functional enrichment analysis using experimentally validated target genes only from the top 10 deregulated miRNAs from each discovery group. We found that the biological enrichment in iPD was substantially different from G2019S carriers and targeted the AKT and TGF-beta pathways, which are mostly related to the immune system and inflammation.[56,57] In all G2019S carriers, we found consistent deregulation of Rho GTPases and NOTCH signalling. These pathways play a key role in axonal guidance by regulating neural arborization and dendritic development and are involved in neurodegenerative processes.[58,59] Moreover, the Rho GTPase RAC1 and NOTCH are functionally related to LRRK2, and can be affected by *LRRK2* mutations.[32,33] By mass-spectrometry phospho-proteome analysis, Rho GTPases were also reported among the top deregulated pathways in peripheral blood cells from G2019S carriers.[54] Lastly, Rho GTPases and NOTCH have also been proposed as therapeutic targets for PD.[60,61] Altogether, these studies further strengthen a plausible role for miRNA deregulation in G2019S carriers.

Despite some exciting observations on differential miRNA expression profiles in L2NMC, our study has limitations. First, we performed an extensive longitudinal study of L2NMC characterized by DaT-SPECT, but did not longitudinally followed-up L2PD, iPD, or controls. Second, during our 8-year follow-up period, only 4 out of 20 DaT-positive L2NMC (20%) pheno-

converted; therefore, more extended follow-up periods are needed in future studies. Third, given that not all L2NMC are expected to develop PD, our study did not explore other risk or protective factors modulating the penetrance of mutations in *LRRK2* beyond miRNAs. Fourth, no other PD-associated mutations other than in *LRRK2* gene were screened. Lastly, a limitation of many miRNA studies is the inter-lab variability regarding biospecimens, techniques, and normalizers and the lack of consensus guidelines, thus eventually limiting cross-lab reproducibility.

In summary, our study identifies novel miRNA alterations co-occurring with progressive DaT-SPECT decline in premotor stages of PD before the diagnosis of PD. If validated, some of the identified miRNAs hold potential as early progression biomarkers or pheno-conversion in premotor G2019S carriers. These findings may have implications for early PD detection or early neuroprotective strategies when available.

MATERIALS & METHODS

Subjects

All subjects provided written informed consent, and the Ethics Committees of IDIBAPS-Hospital Clínic de Barcelona and Hospital Marqués de Valdecilla approved the study. Serum samples and clinical data from probands were collected at the Movement Disorder units from Hospital Clínic de Barcelona and Hospital Marqués de Valdecilla in Santander (**Table 1**). By center and group, our cohort included n=20 DaT-negative G2019S L2NMC (7 from Barcelona/ 13 from Santander), n=20 DaT-positive G2019S L2NMC (7/13), n=20 G2019S L2PD patients (7/13), n=19 iPD cases (7/12), and n=40 healthy controls (27/13). We additionally recruited n=19 L2PD patients and n=20 controls, all from Barcelona, to further assess miRNA findings in a second L2PD cohort (total studied n=158). PD patients were clinically diagnosed according to the UK PD Society Brain Bank criteria, except for the fact that more than one affected relative with PD was not an exclusion criterion.[62] We genotyped all LRRK2 G2019S carriers and iPD patients for the LRRK2 G2019S and R1441G/C/H mutations using commercial Taqman SNP assays-on-demand on a Step One Plus Real-time PCR System as previously described.[63] No systematic sequencing was performed to exclude additional mutations causing monogenic PD. We characterized G2019S L2NMC by DaT-SPECT imaging using 123I-2β-carbomethoxy-3β-(4-iodophenyl)-N-(3-fluoropropyl)-nortropane (123I-FP-CIT) as earlier described in the Barcelona[64] and Santander[65] cohorts. L2NMC were accordingly dichotomized into DaT-negative (normal) and DaT-positive (abnormal dopaminergic function) SPECT status. For longitudinal assessment of L2NMC, subjects were clinically followed-up on average every 2 years and, beyond the baseline, donated two additional serum samples, thus covering a follow-up period above 8 years. In this period, 4 DaT-positive L2NMC (20%) from Santander developed motor symptoms and met the criteria for clinical PD diagnosis.

Serum miRNA isolation

A total of 5ml peripheral blood was collected in tubes without anticoagulant (BD Vacutainer) and centrifuged 10 minutes at 1500xg and 4°C. Serum was aliquoted into polypropylene CryoTubes (Greiner Bio-One) and kept at −80°C until use. Total miRNA enriched RNA was extracted using the miRNeasy Serum/Plasma Kit (QIAGEN #217184) following manufacturer recommendations. As a carrier for miRNA isolation, we added 2ul of diluted yeast tRNA (Invitrogen #AM7119) into

200ul of serum for a final concentration of 10ug/ml. RNA concentration was determined for all samples on a NanoDrop ND-3300 fluorospectrometer (Thermo Fisher Sci.), and miRNA quality was evaluated for a subset of randomly selected samples by electropherogram using an Bioanalizer Small RNA Kit (Agilent #5067-1548).

Genome-wide miRNA analysis

In the discovery genome-wide miRNA expression analysis, serum miRNA samples were hybridized individually and blind to operator for 42 hours onto Affymetrix GeneChip miRNA 4.0 Array (Applied Biosystems #902411; product datasheet), which contains probes for more than 4,603 human miRNAs (2,578 mature miRNAs and 2,025 pre-miRNAs). Images were scanned using an Affymetrix GeneChip Scanner 3,000 7G following the manufacturer's recommendations. Files generated by the Affymetrix GeneChip Command Console (AGCC) were processed with the Expression Console software to determine the data quality. Microarray raw data were analysed using Partek Genomic Suite v7.0 software applying the robust multi-array average (RMA) background correction model, which allows the relative comparison of miRNA abundance in different arrays. Only miRNAs with fluorescence detection values above 2.4 arbitrary units and a significant expression P-value below 0.05 compared to background were considered expressed in human serum samples. In line with previous reports, up to 10% of the mature human miRNA screened in the array were expressed in human serum.[66] For differential miRNA expression analysis, we used the global normalization method adjusting by gender, age, and hybridization date. We compared the miRNA expression levels of DaT-negative L2NMC, DaT-positive L2NMC, L2PD, or iPD with controls, or among study groups (DaT-negative vs. DaT-positive L2NMC, DaT-positive L2NMC vs. L2PD, and L2PD vs iPD) in a two-tailed Student´s T-test. We defined as candidate differentially expressed miRNAs for subsequent RT-qPCR assessment those miRNAs with a significance double criterion of a fold-change above |1.5| and a P-value below 0.05.

RT-qPCR miRNA analysis

Serum miRNA samples were reverse-transcribed and pre-amplified using TaqMan Advanced miRNA cDNA Synthesis Kit (Thermo Fisher Sci. #A28007) in a Veriti™ 96-well Thermal Cycle (Applied Biosystems #4375786). For each miRNA, cDNA pre-amplified products were quantified

using TaqMan Fast Advanced Master Mix (Thermo Fisher Sci. #4444557) and TaqMan Advanced miRNA Assays (Thermo Fisher Sci. #A25576). Reactions were performed per duplicate on a TaqMan® StepOnePlus™ Real-Time PCR System (Applied Biosystems) using 96-well real-time PCR plates at a final volume of 10µl. After discarding commercially available assays which did not amplify at a minimum quality level in serum samples, by real-time quantitative PCR (RT-qPCR) we tested a total of 12 candidate miRNAs. These included 10 candidate DEmiR detected by the array (miR-122-5p, miR-16-5p, miR-185-5p, miR-19b-3p, miR-22-3p, miR-221-3p, miR-29c-3p, miR-3196, miR-4505, miR-451a, miR-6125 and miR-8069), and 2 additional candidate miRNA earlier reported in iPD (miR-29c-3p)[25,27] or well-established PD prodromal stages (idiopathic RBD) (miR-451a).[28] Among the candidate miRNAs selected from the array, miR-185-5p, miR-6125, miR-3196, miR-4505, and miR-22-3p were detected in more than one comparison (**Suppl. Table 1**), and miR-19b-3p and miR-221-3p were previously reported as deregulated miRNAs in PD[25] and idiopathic RBD.[28] For normalization, we selected miR-320a-3p and miR-6727-5p as endogenous references. These miRNAs were unbiasedly nominated among the miRNAs showing the most stable expression across all samples using the NormFinder software.[67] For relative quantification, we applied the $\Delta\Delta C_T$ method using the DataAssist v3.0 software (Applied Biosystems). The maximum allowable C_T value was set at 35. Statistical significance levels for RT-qPCR validated differentially expressed miRNAs (DEmiR) were established at a fold-change difference above |1.5|, and a Benjamini-Hochberg FDR adjusted P-value below 0.05 under a two-tailed Student´s T-test.

ROC analysis

To infer the probability of each patient to undergo pheno-conversion based on miRNA expression values, logistic regression models were fitted by using the *caret* framework in R, and including leave-one-out cross-validation to reduce overfitting of predicted data. The discriminative ability of the differentially expressed miRNAs was assessed by means of the area under the curve (AUC) on a receiver operating characteristic (ROC) curve employing the *pROC* package.

Biological enrichment analysis

As a functional analysis, we selected only the 10 top miRNAs identified in each genome-wide discovery group as compared to controls and performed a miRNA target gene analysis using the

Mienturnet tool (link). Using the miRTarbase database, we further filtered-in only experimentally validated target genes which were targeted by one or more miRNAs. Lastly, we performed a biological enrichment analysis using the pathway database Reactome in Webgestalt online source (link) under the significance cut-off of a Benjamini-Hochberg FDR adjusted P-value below 0.05.

DATA AVAILABILITY

All data generated or analysed during this study are available from the corresponding author upon reasonable request.

ACKNOWLEDGEMENTS

We thank the patients and their relatives for their generous and continued collaboration in this project. M.F. was funded by María de Maeztu programme (grant #MDM-2017-0729) to the Parkinson's disease and Movement Disorders group of the Institut de Neurociènices (Universitat de Barcelona). S.L. was beneficiary of a PFIS fellowship from Instituto de Salud Carlos III (ISCIII) and co-funded by the European Regional Development Fund (ERDF) (grant #FI18/00221). J.C. was supported by a Miguel Servet grant from Instituto de Salud Carlos III (ISCIII) co-funded by the European Union (grant #CPII18/00026). R.F.-S. was supported by the Miguel Servet (grant #CP19/00048), FIS (grant #FIS20-PI20/00659) and PFIS (grant #FI21/00104) programmes from the Instituto de Salud Carlos III (ISCIII) co-funded by the European Union, and also by a Jóvenes Investigadores (JIN) grant of the Spanish Ministry of Economy and Competitiveness (MINECO) and the Agencia Estatal de Investigación (AEI) (AEI/FEDER/UE) (grant #SAF2015-73508-JIN). We also thank the support from the AGAUR program from the Generalitat de Catalunya (grant AGAUR#2017SGR1502) and the Spanish Network for Research on Neurodegenerative Disorders (CIBERNED) – ISCIII (CIBERNED: CB06/05/0018-ISCIII).

COMPETING INTERESTS STATEMENT

Nothing to report.

AUTHOR CONTRIBUTIONS

(1) Conception and design of the study: Conception (RFS, ME); Organization (RFS, ME); Execution (MS, MF, PB, PM); Patient recruitment (AG, ASR, MRS, MS, MJM, JI).

(2) Acquisition and analysis of data: Design (ME, RFS); Execution (MS, MF, PB, SL); Interpretation: (MS, SL, AG, AN, BC, JC, ET, MJM, ME, RFS); Review and Critique (all authors).

(3) Drafting of the manuscript or figures: Writing of the first draft (MS, ME, RFS); Draft editing (MS, AG, AN, BC, ET, MJM, ME, RFS); Review and Critique (all authors)

BIBLIOGRAPHY

1. A. Elbaz, L. Carcaillon, S. Kaba, F. M. Epidemiology of Parkinson' s disease. *Rev. Neurol. (Paris).* **172**, 14–26 (2016).
2. Spillantini, M. G. *et al.* α-Synuclein in Lewy bodies. *Nature* **388**, 839–840 (1997).
3. Dickson, D. W. *et al.* Neuropathological assessment of Parkinson's disease: refining the diagnostic criteria. *Lancet Neurol.* **8**, 1150–1157 (2009).
4. Sveinbjornsdottir, S. The clinical symptoms of Parkinson's disease. *J. Neurochem.* **139**, 318–324 (2016).
5. Postuma, R. B. *et al.* MDS clinical diagnostic criteria for Parkinson's disease. *Mov. Disord.* **30**, 1591–1601 (2015).
6. Lesage, S. & Brice, A. Parkinson's disease: From monogenic forms to genetic susceptibility factors. *Hum. Mol. Genet.* **18**, 48–59 (2009).
7. Paisán-Ruíz, C. *et al.* Cloning of the gene containing mutations that cause PARK8-linked Parkinson's disease. *Neuron* **44**, 595–600 (2004).
8. Zimprich, A. *et al.* Mutations in LRRK2 Cause Autosomal-Dominant Parkinsonism with Pleomorphic Pathology. *Neuron* **44**, 601–607 (2004).
9. Ruiz-Martínez, J. *et al.* Penetrance in Parkinson's disease related to the LRRK2 R1441G mutation in the Basque country (Spain). *Mov. Disord.* **25**, 2340–2345 (2010).
10. Sierra, M. *et al.* High frequency and reduced penetrance of lRRK2 g2019S mutation among Parkinson's disease patients in Cantabria (Spain). *Mov. Disord.* **26**, 2343–2346 (2011).
11. Hentati, F. *et al.* LRRK2 parkinsonism in Tunisia and Norway: a comparative analysis of disease penetrance. *Neurology* **83**, 568–569 (2014).
12. Marder, K. *et al.* Age-specific penetrance of LRRK2 G2019S in the Michael J. Fox Ashkenazi Jewish LRRK2 Consortium. *Neurology* **85**, 89–95 (2015).
13. Lee, A. J. *et al.* Penetrance estimate of LRRK2 p.G2019S mutation in individuals of non-Ashkenazi Jewish ancestry. *Mov. Disord.* **32**, 1432–1438 (2017).
14. Bartel, D. P. MicroRNAs: Genomics, Biogenesis, Mechanism, and Function. *Cell* **116**, 281–297 (2004).

15. Oliveira, S. R. *et al.* Circulating inflammatory mirnas associated with parkinson's disease pathophysiology. *Biomolecules* **10**, 1–13 (2020).
16. Hu, Y. B. *et al.* miR-425 deficiency promotes necroptosis and dopaminergic neurodegeneration in Parkinson's disease. *Cell Death Dis.* **10**, (2019).
17. Chen, X. *et al.* Characterization of microRNAs in serum: A novel class of biomarkers for diagnosis of cancer and other diseases. *Cell Res.* **18**, 997–1006 (2008).
18. Danborg, P. B., Simonsen, A. H., Waldemar, G. & Heegaard, N. H. H. The potential of microRNAs as biofluid markers of neurodegenerative diseases-a systematic review. *Biomarkers* **19**, 259–268 (2014).
19. Gaig, C., Ezquerra, M. & Marti, M J, et al. Mutations in Spanish Patients With Parkinson Disease. *Arch. Neurol.* **63**, 6–11 (2006).
20. Sánchez-Rodríguez, A. *et al.* Serial DaT-SPECT imaging in asymptomatic carriers of LRRK2 G2019S mutation: 8 years' follow-up. *Eur. J. Neurol.* **28**, 4204–4208 (2021).
21. Kägi, G., Bhatia, K. P. & Tolosa, E. The role of DAT-SPECT in movement disorders. *J. Neurol. Neurosurg. Psychiatry* **81**, 5–12 (2010).
22. Scherfler, C. *et al.* Role of DAT-SPECT in the Diagnostic Work Up of Parkinsonism. *Mov. Disord.* **22**, 1229–1238 (2007).
23. Sierra, M. *et al.* Prospective clinical and DaT-SPECT imaging in premotor LRRK2 G2019S-associated Parkinson disease. *Neurology* **89**, 439 LP – 444 (2017).
24. Iranzo, A. *et al.* Serial dopamine transporter imaging of nigrostriatal function in patients with idiopathic rapid-eye-movement sleep behaviour disorder: A prospective study. *Lancet Neurol.* **10**, 797–805 (2011).
25. Botta-Orfila, T. *et al.* Identification of blood serum micro-RNAs associated with idiopathic and LRRK2 Parkinson's disease. *J. Neurosci. Res.* **92**, 1071–1077 (2014).
26. Cao, X. Y. *et al.* MicroRNA biomarkers of Parkinson's disease in serum exosome-like microvesicles. *Neurosci. Lett.* **644**, 94–99 (2017).
27. Fernández-Santiago, R. *et al.* MicroRNA association with synucleinopathy conversion in rapid eye movement behavior disorder. *Ann. Neurol.* **77**, 895–901 (2015).
28. Soto, M. *et al.* Serum MicroRNAs Predict Isolated Rapid Eye Movement Sleep Behavior

Disorder and Lewy Body Diseases. *Mov. Disord.* **37**, 2086–2098 (2022).

29. Bai, X. *et al.* Downregulation of blood serum microRNA 29 family in patients with Parkinson's disease. *Sci. Rep.* **7**, 1–7 (2017).
30. Ma, W. *et al.* Serum miR-221 serves as a biomarker for Parkinson's disease. *Cell Biochem. Funct.* **34**, 511–515 (2016).
31. Kern, F. *et al.* Deep sequencing of sncRNAs reveals hallmarks and regulatory modules of the transcriptome during Parkinson's disease progression. *Nat. Aging* **1**, 309–322 (2021).
32. Chan, D., Citro, A., Cordy, J. M., Shen, G. C. & Wolozin, B. Rac1 protein rescues neurite retraction caused by G2019s leucine-rich repeat kinase 2 (LRRK2). *J. Biol. Chem.* **286**, 16140–16149 (2011).
33. Imai, Y. *et al.* The Parkinson's Disease-Associated Protein Kinase LRRK2 Modulates Notch Signaling through the Endosomal Pathway. *PLoS Genet.* **11**, 1–30 (2015).
34. Redmond, L. & Ghosh, A. The role of Notch and Rho GTPase signaling in the control of dendritic development. *Curr. Opin. Neurobiol.* **11**, 111–117 (2001).
35. Tolosa, E., Garrido, A., Scholz, S. W. & Poewe, W. Challenges in the diagnosis of Parkinson's disease. *Lancet Neurol.* **20**, 385–397 (2021).
36. Aasly, J. O. *et al.* Clinical features of LRRK2-associated Parkinson's disease in Central Norway. *Ann. Neurol.* **57**, 762–765 (2005).
37. Marras, C. *et al.* Motor and nonmotor heterogeneity of LRRK2-related and idiopathic Parkinson's disease. *Mov. Disord.* **31**, 1192–1202 (2016).
38. Saunders-Pullman, R. *et al.* Progression in the LRRK2-Associated Parkinson Disease Population. *JAMA Neurol.* **75**, 312–319 (2018).
39. Kestenbaum, M. & Alcalay, R. N. Clinical Features of LRRK2 Carriers with Parkinson's Disease. *Adv. Neurobiol.* **14**, 31–48 (2017).
40. Gonzalez-Cano, L., Menzl, I., Tisserand, J., Nicklas, S. & Schwamborn, J. C. Parkinson's Disease-Associated Mutant LRRK2-Mediated Inhibition of miRNA Activity is Antagonized by TRIM32. *Mol. Neurobiol.* **55**, 3490–3498 (2018).
41. Gehrke, S., Imai, Y., Sokol, N. & Lu, B. Pathogenic LRRK2 negatively regulates microRNA-mediated translational repression. *Nature* **466**, 637–641 (2010).

42. Ravanidis, S. *et al.* Circulating Brain-Enriched MicroRNAs for Detection and Discrimination of Idiopathic and Genetic Parkinson's Disease. *Mov. Disord.* **35**, 457–467 (2020).
43. Martins, M. *et al.* Convergence of mirna expression profiling, α-synuclein interacton and GWAS in Parkinson's disease. *PLoS One* **6**, e25443 (2011).
44. Gui, Y. X., Liu, H., Zhang, L. S., Lv, W. & Hu, X. Y. Altered microRNA profiles in cerebrospinal fluid exosome in Parkinson disease and Alzheimer disease. *Oncotarget* **6**, 37043–37053 (2015).
45. Ascherio, A. & Schwarzschild, M. A. The epidemiology of Parkinson's disease: risk factors and prevention. *Lancet Neurol.* **15**, 1257–1272 (2016).
46. Fernández-Santiago, R. & Sharma, M. What have we learned from genome-wide association studies (GWAS) in Parkinson's disease? *Ageing Res. Rev.* **79**, 101648 (2022).
47. Infante, J. *et al.* Comparative blood transcriptome analysis in idiopathic and LRRK2 G2019S-associated Parkinson's disease. *Neurobiol. Aging* **38**, 214.e1-214.e5 (2015).
48. Ding, H. *et al.* Identification of a panel of five serum miRNAs as a biomarker for Parkinson's disease. *Park. Relat. Disord.* **22**, 68–73 (2016).
49. Marchand, A., Drouyer, M., Sarchione, A., Chartier-Harlin, M. C. & Taymans, J. M. LRRK2 Phosphorylation, More Than an Epiphenomenon. *Front. Neurosci.* **14**, 1–21 (2020).
50. Craig, D. W. *et al.* RNA sequencing of whole blood reveals early alterations in immune cells and gene expression in Parkinson's disease. *Nat. Aging* **1**, 734–747 (2021).
51. Schapira, A. H. V. & Tolosa, E. Molecular and clinical prodrome of Parkinson disease: Implications for treatment. *Nat. Rev. Neurol.* **6**, 309–317 (2010).
52. Marek, K. & Jennings, D. Can we image premotor Parkinson disease? *Neurology* **72**, S21 LP-S26 (2009).
53. Majbour, N. K. *et al.* CSF total and oligomeric α-Synuclein along with TNF-α as risk biomarkers for Parkinson's disease: A study in LRRK2 mutation carriers. *Transl. Neurodegener.* **9**, 1–10 (2020).
54. Garrido, A. *et al.* Differential Phospho-Signatures in Blood Cells Identify LRRK2 G2019S Carriers in Parkinson's Disease. *Mov. Disord.* **37**, 1004–1015 (2022).
55. Tolosa, E., Vila, M., Klein, C. & Rascol, O. LRRK2 in Parkinson disease: challenges of clinical

trials. *Nat. Rev. Neurol.* **16**, 97–107 (2020).

56. Sangphech, N., Osborne, B. A. & Palaga, T. Notch signaling regulates the phosphorylation of Akt and survival of lipopolysaccharide-activated macrophages via regulator of G protein signaling 19 (RGS19). *Immunobiology* **219**, 653–660 (2014).
57. Villegas, S. N. *et al.* PI3K/Akt Cooperates with Oncogenic Notch by Inducing Nitric Oxide-Dependent Inflammation. *Cell Rep.* **22**, 2541–2549 (2018).
58. DeGeer, J. & Lamarche-Vane, N. Rho GTPases in neurodegeneration diseases. *Exp. Cell Res.* **319**, 2384–2394 (2013).
59. Ables, J. L., Breunig, J. J., Eisch, A. J. & Rakic, P. Not(ch) just development: Notch signalling in the adult brain. *Nat. Rev. Neurosci.* **12**, 269–283 (2011).
60. Musilli, M. *et al.* Therapeutic effects of the Rho GTPase modulator CNF1 in a model of Parkinson's disease. *Neuropharmacology* **109**, 357–365 (2016).
61. DeGeer, J. & Lamarche-Vane, N. Rho GTPases in neurodegeneration diseases. *Exp. Cell Res.* **319**, 2384–2394 (2013).
62. Hughes, A. J., Daniel, S. E., Kilford, L. & Lees, A. J. Accuracy of clinical diagnosis of idiopathic Parkinson ' s disease : a clinico-pathological study of 100 cases. *J. Neurol. Neurosurg. Psychiatry* **55**, 181–184 (1992).
63. Simón-Sánchez, J. *et al.* Parkinson's disease due to the R1441G mutation in Dardarin: A founder effect in the Basques. *Mov. Disord.* **21**, 1954–1959 (2006).
64. Garrido, A., Fairfoul, G., Tolosa, E. S., Martí, M. J. & Green, A. α-synuclein RT-QuIC in cerebrospinal fluid of LRRK2-linked Parkinson's disease. *Ann. Clin. Transl. Neurol.* **6**, 1024–1032 (2019).
65. Sierra, M., Martínez-, M. I., González-, I., Palacio, E. & Carril, J. M. Olfaction and imaging biomarkers in Parkinson disease. *Neurology* **80**, 621–626 (2013).
66. Umu, S. U. *et al.* A comprehensive profile of circulating RNAs in human serum. *RNA Biol.* **15**, 242–250 (2018).
67. Andersen, C. L., Jensen, J. L. & Ørntoft, T. F. Normalization of Real-Time Quantitative Reverse Transcription-PCR Data: A Model-Based Variance Estimation Approach to Identify Genes Suited for Normalization, Applied to Bladder and Colon Cancer Data Sets.

Cancer Res. **64**, 5245–5250 (2004).

1

TABLE 1: Clinico-demographic data of participants. UPDRS-III scaling is provided as a mean ± standard deviation (S.D.) with the number of subjects with available data specified in brackets. DaT = DaT-SPECT imaging; L2NMC = LRRK2 non-manifesting carriers; L2PD = LRRK2-associated PD patients; iPD = idiopathic PD patients; gender, M = males, F = females; LEDD = levodopa equivalent daily dose; MDS UPDRS-III = Unified Parkinson's Disease Rating Scale scoring of the Movement Disorders Society

Total n=158	**Nr. of studied subjects**	**Gender (M/F)**	**Age at PD onset ± SD (years)**	**Age at sampling ± SD (years)**	**Time from baseline ± SD (years)**	**Mean LEDD ± SD (mg)**	**Mean MDS UPDRS-III ± SD (Nr. of available from total)**	**Nr. of pheno-converted subjects**
Controls	40	28/12	-	65.48 ± 11.69	-	-	-	-
L2NMC DaT-	20	8/12	-	52.30 ± 10.12	-	-	0.39 ± 0.61 (n=18/20)	-
Time point 2	18	6/12	-	56.78 ± 11.60	4.32 ± 1.68	-	1.72 ± 1.79 (n=16/18)	0
Time point 3	16	7/9	-	59.50 ± 11.40	7.79 ± 2.22	-	2.33 ± 2.23 (n=12/16)	0
L2NMC DaT+	20	12/8	-	60.50 ± 14.49	-	-	3.10 ± 5.22 (n=20/20)	-
Time point 2	16	9/7	-	61.63 ± 13.26	5.02 ± 1.50	-	6.34 ± 10.26 (n=16/16)	3
Time point 3	13	8/5	-	63.85 ± 11.63	9.12 ± 1.68	-	5.19 ± 5.64 (n=8/13)	4
L2PD	20	12/8	58 ± 13.14	65 ± 10.90	-	802.47 ± 810.02	22.00 ± 13.10 (n=17/20)	-
iPD	19	12/7	56.16 ± 13.01	63.53 ± 11.77	-	420.13 ± 391.46	25.00 ± 16.37 (n=8/19)	-
L2PD 2nd cohort	19	8/11	53.47 ± 10.79	64.47 ± 11.34	-	708.68 ± 469.64	28.05 ± 13.87 (n=19/19)	-
Controls 2nd cohort	20	8/12	-	63.65 ± 10.75	-	-	-	-

TABLE 2: RT-qPCR assessment of miRNA levels in serum samples from DaT-negative and DaT-positive L2NMC, L2PD patients and iPD as compared to healthy controls. DaT = DaT-SPECT imaging; L2NMC = LRRK2 no manifesting carrier; L2PD = LRRK2 carrier with symptomatic Parkinson disease; iPD = idiopathic Parkinson disease; FC = fold change; Adj. P = FDR multiple-test adjusted P-value

microRNA	DaT (-) L2NMC (n=20)		DaT (+) L2NMC (n=20)		L2PD (n=20)		iPD (n=19)	
	FC	Adj. P	FC	Adj. P	FC	Adj. P	FC	Adj. P
miR-122-5p	7.07	$3.0x10^{-6}$	3.38	0.0269	2.01	0.1616	3.05	0.0025
miR-16-5p	3.42	0.0007	2.51	0.0237	1.66	0.2590	5.21	0.0003
miR-185-5p	3.68	$3.0x10^{-5}$	4.32	0.0004	1.49	0.3122	3.60	0.0028
miR-19b-3p	1.05	0.8394	1.25	0.5280	-2.05	0.1303	3.04	0.0018
miR-22-3p	1.66	0.0632	1.77	0.0759	1.64	0.1611	2.67	0.0025
miR-221-3p	2.06	0.0079	1.15	0.6263	1.37	0.3122	1.93	0.0076
miR-29c-3p	1.44	0.1435	1.93	0.0759	1.45	0.2741	2.67	0.0025
miR-3196	2.43	$1.0x10^{-5}$	1.98	0.0012	2.13	0.0001	1.11	0.6142
miR-4505	1.98	0.0016	3.51	0.0004	-1.06	0.7803	-1.28	0.3225
miR-451a	4.44	$1.1x10^{-5}$	4.16	0.0004	2.43	0.0629	4.76	0.0016
miR-6125	-1.47	0.1179	-1.26	0.3307	-1.01	0.9535	-1.32	0.2461
miR-8069	1.89	0.0006	1.44	0.0759	1.09	0.7352	-1.53	0.0145

TABLE 3: Longitudinal follow-up of serum miRNA levels during 8 years in DaT-negative and DaT-positive L2NMC with respect to their baselines. RT-qPCR analysis comparing time point 2 and 3 of DaT-negative and DaT-positive L2NMC groups with their respective baselines. DaT = DaT-SPECT imaging; L2NMC = LRRK2 non-manifesting carriers; L2PD = LRRK2-associated PD patients; iPD = idiopathic PD patients; FC = fold change; Adj. P = FDR multiple-test adjusted P-value

	DaT-negative L2NMC				DaT-positive L2NMC			
microRNA	**Time point 2 (n=18)**		**Time point 3 (n=16)**		**Time point 2 (n=16)**		**Time point 3 (n=13)**	
	FC	**Adj. P**	**FC**	**Adj. P**	**FC**	**Adj. P**	**FC**	**Adj. P**
miR-122-5p	1.30	0.5467	2.74	0.0117	1.66	0.3585	3.57	0.0190
miR-16-5p	6.12	$4.0x10^{-6}$	12.71	$<1.0x10^{-6}$	5.43	0.0002	17.94	$<1.0x10^{-6}$
miR-185-5p	1.40	0.1996	3.73	0.0002	-1.22	0.5354	3.35	0.0005
miR-19b-3p	5.60	$<1.0x10^{-6}$	15.40	$<1.0x10^{-6}$	3.25	0.0055	15.72	$<1.0x10^{-6}$
miR-22-3p	2.99	$3.5x10^{-5}$	7.48	$<1.0x10^{-6}$	2.39	0.0087	8.06	$<1.0x10^{-6}$
miR-221-3p	1.39	0.1996	2.90	0.0005	2.16	0.0273	5.39	$2.0x10^{-6}$
miR-29c-3p	3.02	0.0001	7.09	$<1.0x10^{-6}$	1.54	0.2551	7.55	$1.0x10^{-6}$
miR-3196	1.11	0.5663	-1.09	0.5548	1.46	0.1274	1.21	0.3083
miR-4505	-1.89	0.0015	-1.16	0.4436	-1.25	0.0068	-1.54	0.1144
miR-451a	2.85	0.0017	5.05	$2.5x10^{-5}$	2.42	0.0273	6.60	$3.0x10^{-6}$
miR-6125	6.75	$<1.0x10^{-6}$	5.81	$1.0x10^{-6}$	5.51	0.0002	5.46	$7.0x10^{-6}$
miR-8069	-1.72	0.0004	-1.89	0.0006	-1.43	0.0879	-1.47	0.0709

TABLE 4: Biological enrichment analysis of experimentally validated target genes from the top 10 DEmiR from discovery analysis in all main cross-sectional study groups. DaT = DaT-SPECT imaging; L2NMC = LRRK2 non-manifesting carriers; L2PD = LRRK2 carrier with symptomatic Parkinson disease; iPD = idiopathic PD; Adj. P = FDR multiple-test adjusted P-value

Reactome - DaT-negative G2019S L2NMC	**P-value**	**Adj. P**
Disinhibition of SNARE formation	0.0009	1
MECP2 regulates neuronal receptors and channels	0.0093	1
Response to elevated platelet cytosolic Ca2+	0.0103	1
Regulation of KIT signalling	0.0105	1
Signalling by Rho GTPases	0.0120	1
Rho GTPase effectors	0.0127	1
Signalling by ERBB2	0.0130	1
Innate immune system	0.0140	1
Antimicrobial peptides	0.0153	1
Axon guidance	0.0196	1

166 user IDs / **165** user IDs unambiguously mapped to **165** unique EntrezGene IDs / **1** unmapped

Reactome - DaT-positive G2019S L2NMC	**P-value**	**Adj. P**
Signalling by EGFR	0.0104	1
Collagen degradation	0.0221	1
Signalling by NOTCH1	0.0249	1
Constitutive signalling by NOTCH1	0.0249	1
Release of Hh-Np from the secreting cell	0.0285	1
Regulation of cytoskeletal remodelling and cell spreading by IPP complex	0.0285	1
Removal of aminoterminal propeptides from γ-carboxylated proteins	0.0354	1
GAB1 signalosome	0.0389	1
RHO GTPases activate KTN1	0.0389	1
γ-carboxylation, transport, and amino-terminal cleavage of proteins	0.0389	1

65 user IDs / **65** user IDs unambiguously mapped to **65** unique EntrezGene IDs

Reactome - G2019S L2PD	**P-value**	**Adj. P**
Estrogen-dependent gene expression	0.0006	0.5460
ESR-mediated signalling	0.0006	0.5460
Signalling by nuclear receptors	0.0013	0.7380
Pre-NOTCH transcription and translation	0.0048	0.8148
RUNX1 genes / megakaryocyte differentiation and platelet function	0.0052	0.8148
RUNX1 regulated expression of components of tight junctions	0.0057	0.8148
RUNX1 regulated transcription of genes involved in interleukin signalling	0.0057	0.8148
Pre-NOTCH expression and processing	0.0065	0.8148
Senescence-associated secretory phenotype	0.0066	0.8148
Generic transcription pathway	0.0067	0.8148

24 user IDs / **24** user IDs unambiguously mapped to **24** unique EntrezGene IDs

Reactome - iPD	**P-value**	**Adj. P**
Gene expression (transcription)	7.25E-13	1.25E-09
Generic transcription pathway	2.16E-11	1.87E-08
RNA polymerase II transcription	9.32E-11	5.37E-08
Transcriptional regulation by TP53	3.87E-08	1.67E-05
Oncogene induced senescence	4.89E-08	1.69E-05
Signalling by TGF-beta family members	3.80E-07	1.09E-04
PIP3 activates AKT signalling	5.40E-07	1.33E-04
Circadian clock	1.40E-06	3.02E-04
Intracellular signalling by second messengers	1.77E-06	3.05E-04
Cellular responses to external stimuli	1.95E-06	3.05E-04

1150 user IDs / **1139** user IDs unambiguously mapped to **1139** unique EntrezGene IDs/ **11** unmapped

a

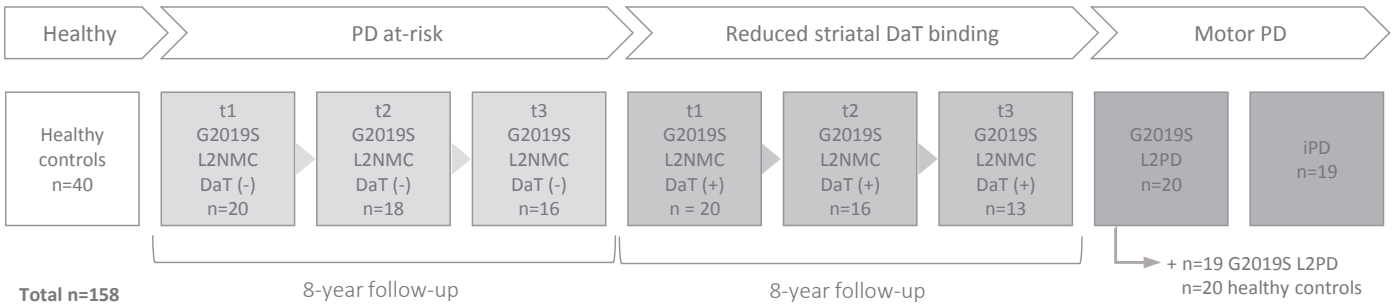
Healthy
PD at-risk
Reduced striatal DaT binding
Motor PD
Healthy controls n=40
t1 G2019S L2NMC DaT (-) n=20
t2 G2019S L2NMC DaT (-) n=18
t3 G2019S L2NMC DaT (-) n=16
t1 G2019S L2NMC DaT (+) n = 20
t2 G2019S L2NMC DaT (+) n=16
t3 G2019S L2NMC DaT (+) n=13
G2019S L2PD n=20
iPD n=19
Total n=158
8-year follow-up
8-year follow-up
+ n=19 G2019S L2PD
n=20 healthy controls

b

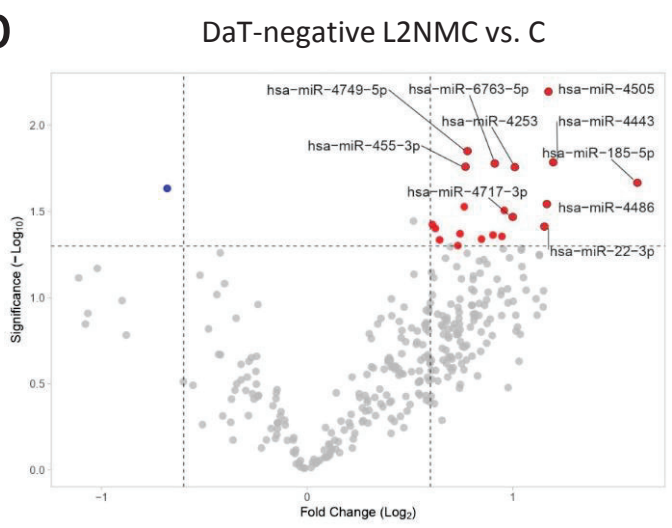
DaT-negative L2NMC vs. C
hsa-miR-4749-5p
hsa-miR-6763-5p
hsa-miR-4505
hsa-miR-4253
hsa-miR-4443
hsa-miR-455-3p
hsa-miR-185-5p
hsa-miR-4717-3p
hsa-miR-4486
hsa-miR-22-3p
Significance (−Log10)
Fold Change (Log2)

c

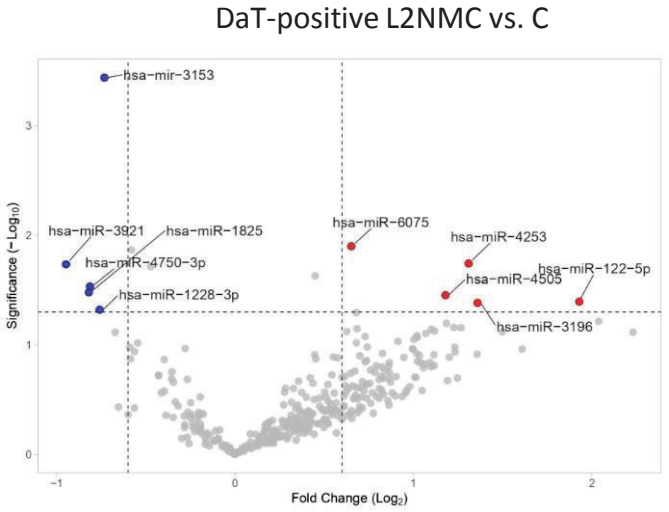
DaT-positive L2NMC vs. C
hsa-mir-3153
hsa-miR-3921
hsa-miR-1825
hsa-miR-4750-3p
hsa-miR-1228-3p
hsa-miR-6075
hsa-miR-4253
hsa-miR-122-5p
hsa-miR-4505
hsa-miR-3196
Significance (−Log10)
Fold Change (Log2)

d

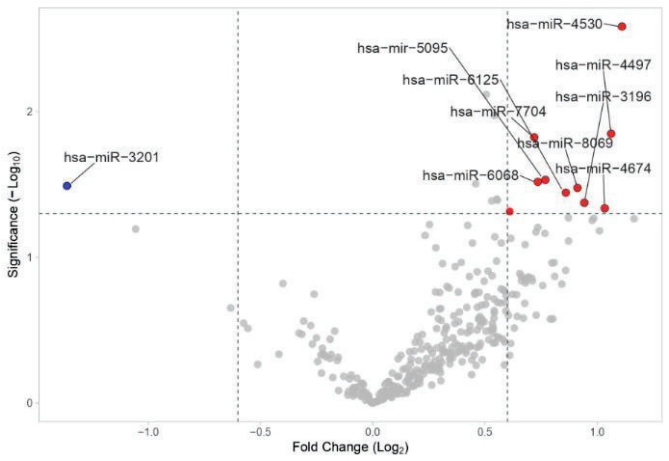
L2PD vs. C
hsa-miR-4530
hsa-mir-5095
hsa-miR-4497
hsa-miR-6125
hsa-miR-3196
hsa-miR-7704
hsa-miR-8069
hsa-miR-3201
hsa-miR-6068
hsa-miR-4674
Significance (−Log10)
Fold Change (Log2)

e

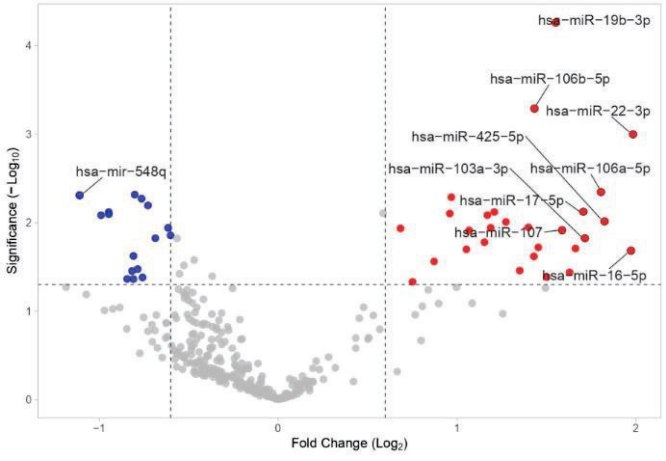
iPD vs. C
hsa-miR-19b-3p
hsa-miR-106b-5p
hsa-miR-22-3p
hsa-miR-425-5p
hsa-mir-548q
hsa-miR-103a-3p
hsa-miR-106a-5p
hsa-miR-17-5p
hsa-miR-107
hsa-miR-16-5p
Significance (−Log10)
Fold Change (Log2)

Fig. 1

a Common and specific candidate DEmiR from array

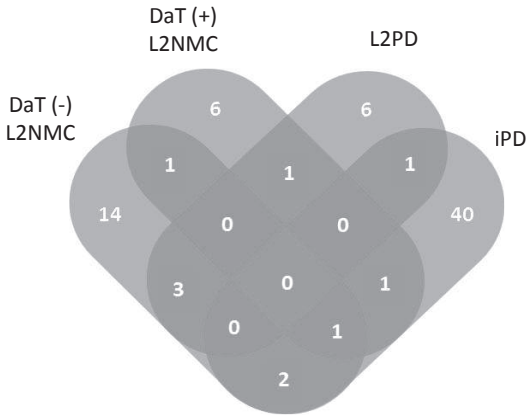

Groups	Total	miRNAs
DaT(+) L2NMC, DaT(-) L2NMC, iPD	1	hsa-miR-4253
DaT(+) L2NMC, DaT(-) L2NMC	1	hsa-miR-4505
DaT(-) L2NMC, L2PD	3	hsa-miR-4749-5p, hsa-miR-7704, hsa-miR-6125
DaT(-) L2NMC, iPD	2	hsa-miR-185-5p, hsa-miR-22-3p
DaT(+) L2NMC, L2PD	1	hsa-miR-3196
DaT(+) L2NMC, iPD	1	hsa-miR-1228-3p
L2PD, iPD	1	hsa-miR-4530
DaT(-) L2NMC	14	hsa-miR-6763-5p, hsa-miR-6860, hsa-miR-455-3p, hsa-miR-4717-3p, hsa-miR-6729-5p, hsa-miR-4459, hsa-miR-4443, hsa-miR-4787-5p, hsa-miR-939-5p, hsa-miR-4454, hsa-miR-4486, hsa-miR-610, hsa-miR-6779-5p, hsa-mir-6776
DaT(+) L2NMC	6	hsa-miR-3921, hsa-mir-3153, hsa-miR-4750-3p, hsa-miR-122-5p, hsa-miR-6075, hsa-miR-1825
L2PD	6	hsa-miR-4674, hsa-miR-8069, hsa-miR-3201, hsa-miR-4497, hsa-mir-5095, hsa-miR-6068
iPD	40	hsa-miR-20b-5p, hsa-miR-25-3p, hsa-miR-5787, hsa-let-7b-5p, hsa-miR-19b-3p, hsa-miR-548aq-3p, hsa-miR-221-3p, hsa-miR-425-5p, hsa-miR-6796-3p, hsa-miR-652-3p, hsa-miR-17-5p, hsa-miR-1263, hsa-miR-181a-5p, hsa-miR-140-3p, hsa-miR-106b-5p, hsa-miR-1273g-3p, hsa-miR-1298-3p, hsa-miR-24-3p, hsa-miR-6797-3p, hsa-miR-93-5p, hsa-miR-3197, hsa-miR-200b-5p, hsa-miR-940, hsa-mir-548q, hsa-miR-548ap-3p, hsa-miR-20a-5p, hsa-miR-106a-5p, hsa-miR-130b-3p, hsa-let-7c-5p, hsa-miR-222-3p, hsa-miR-628-5p, hsa-miR-16-5p, hsa-mir-548a-1, hsa-miR-103a-3p, hsa-miR-423-3p, hsa-miR-151a-3p, hsa-miR-744-5p, hsa-miR-603, hsa-miR-210-3p, hsa-miR-107

b Common and specific validated DEmiR from RT-qPCR

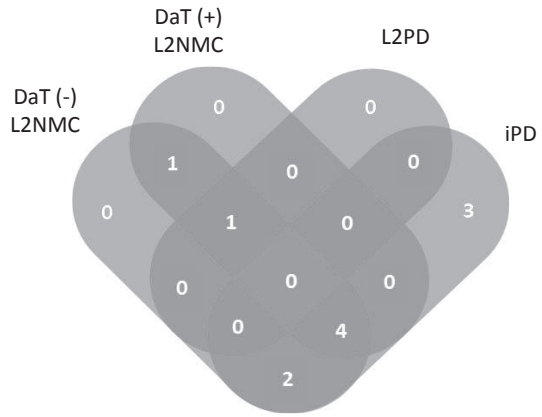

Groups	Total	miRNAs
DaT(-) L2NMC, DaT(+) L2NMC, iPD	4	hsa-miR-122-5p, hsa-miR-16-5p, hsa-miR-185-5p, hsa-miR-451a
DaT(-) L2NMC, DaT(+) L2NMC, L2PD	1	hsa-miR-3196
DaT(-) L2NMC, DaT(+) L2NMC	1	hsa-miR-4505
DaT(-) L2NMC, iPD	2	hsa-miR-221-3p, hsa-miR-8069
iPD	3	hsa-miR-19b-3p, hsa-miR-22-3p, hsa-miR-29c-3p

Fig. 2

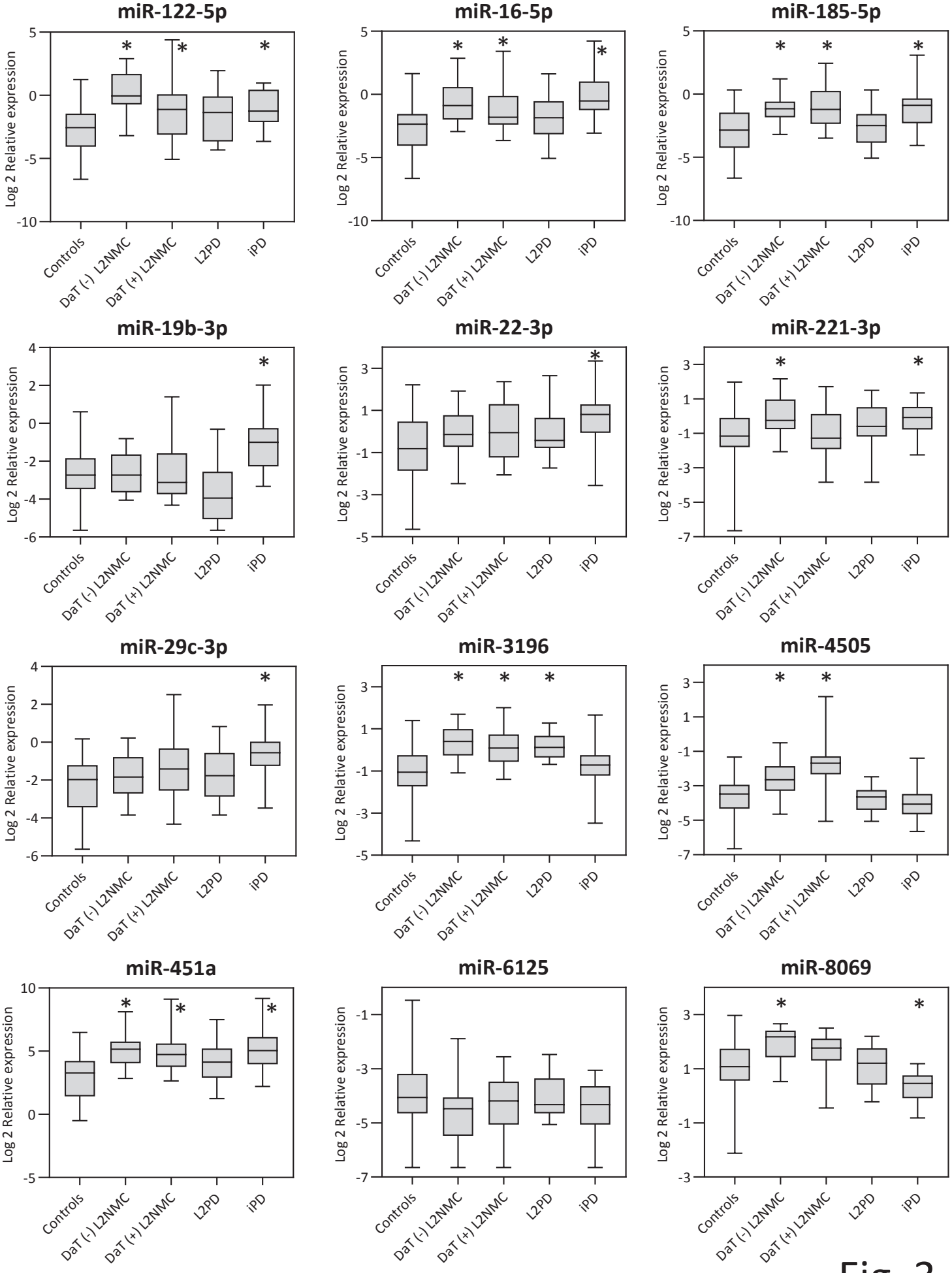
miR-122-5p
miR-16-5p
miR-185-5p
miR-19b-3p
miR-22-3p
miR-221-3p
miR-29c-3p
miR-3196
miR-4505
miR-451a
miR-6125
miR-8069
Log 2 Relative expression
Controls
DaT (-) L2NMC
DaT (+) L2NMC
L2PD
iPD

Fig. 3

a

DaT-negative L2NMC vs. DaT-positive L2NMC

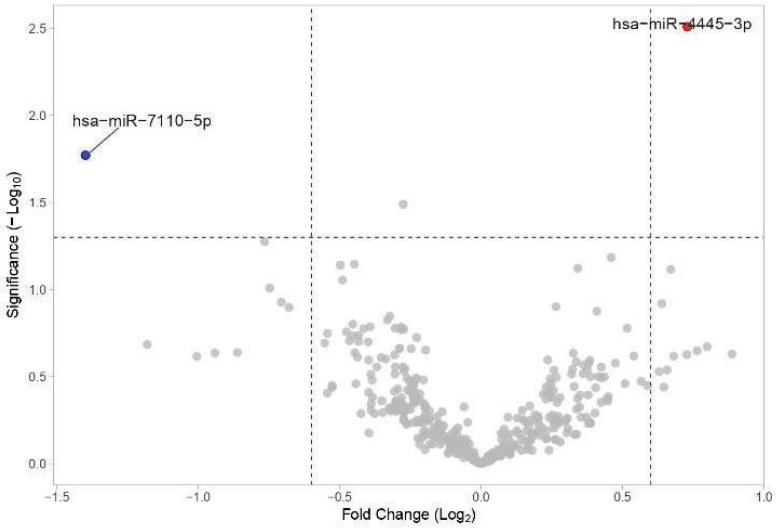

b

DaT-positive L2NMC vs. L2PD

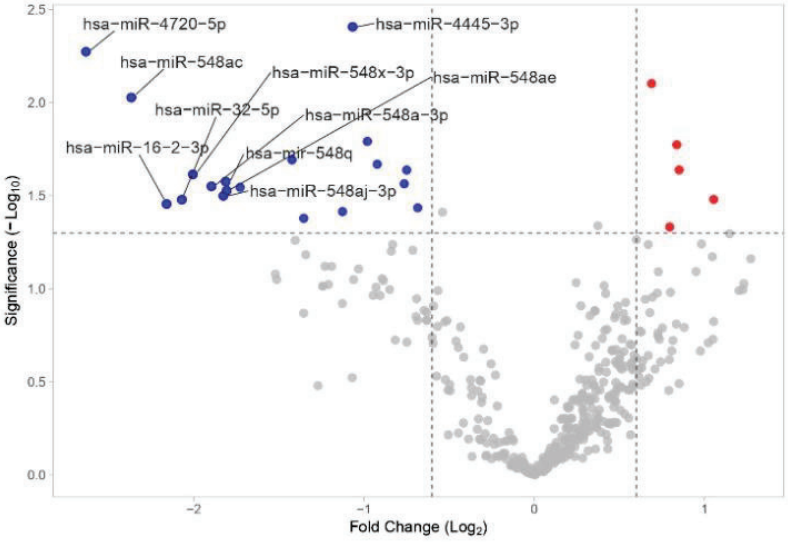

c

L2PD vs. iPD

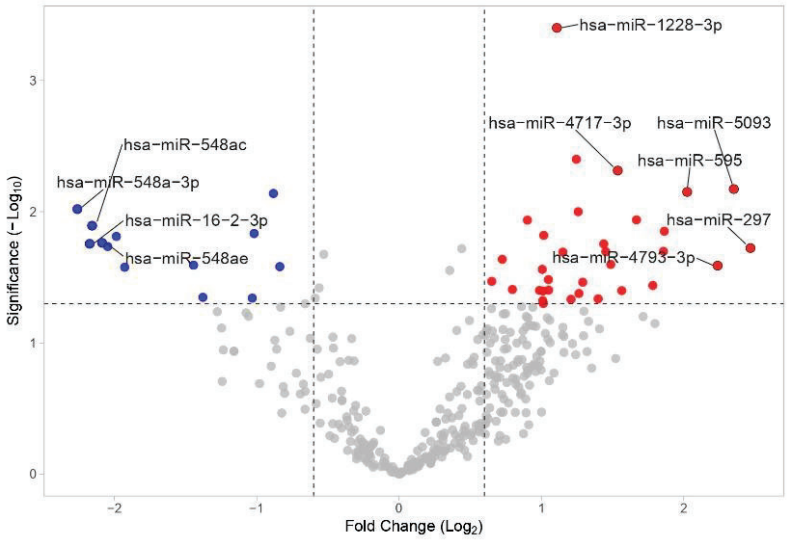

Fig. 4

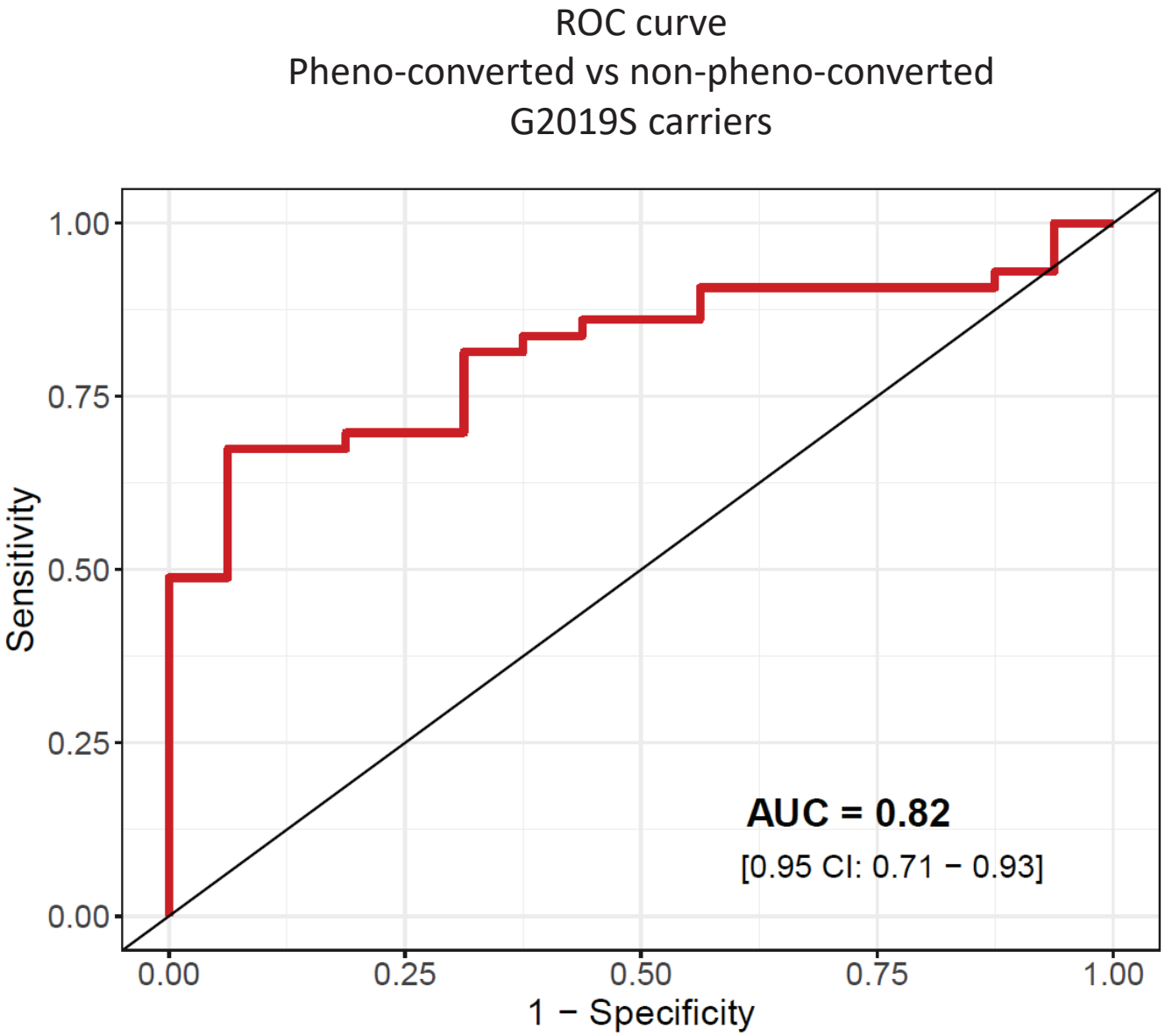
ROC curve
Pheno-converted vs non-pheno-converted
G2019S carriers
Sensitivity
1.00
0.75
0.50
0.25
0.00
0.00
0.25
0.50
0.75
1.00
1 − Specificity
AUC = 0.82
[0.95 CI: 0.71 − 0.93]

Fig. 5

a

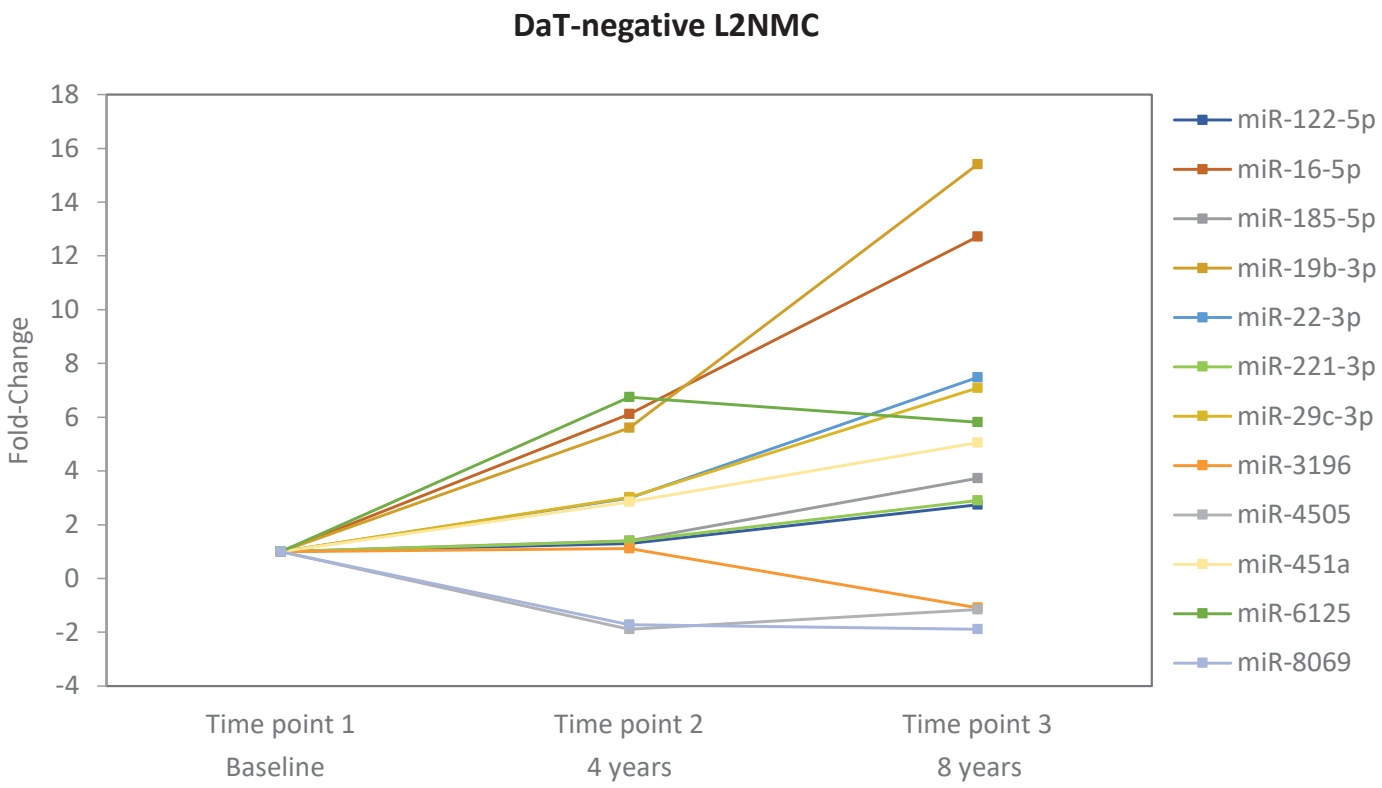
DaT-negative L2NMC
Fold-Change
18
16
14
12
10
8
6
4
2
0
-2
-4
Time point 1
Baseline
Time point 2
4 years
Time point 3
8 years
miR-122-5p
miR-16-5p
miR-185-5p
miR-19b-3p
miR-22-3p
miR-221-3p
miR-29c-3p
miR-3196
miR-4505
miR-451a
miR-6125
miR-8069

b

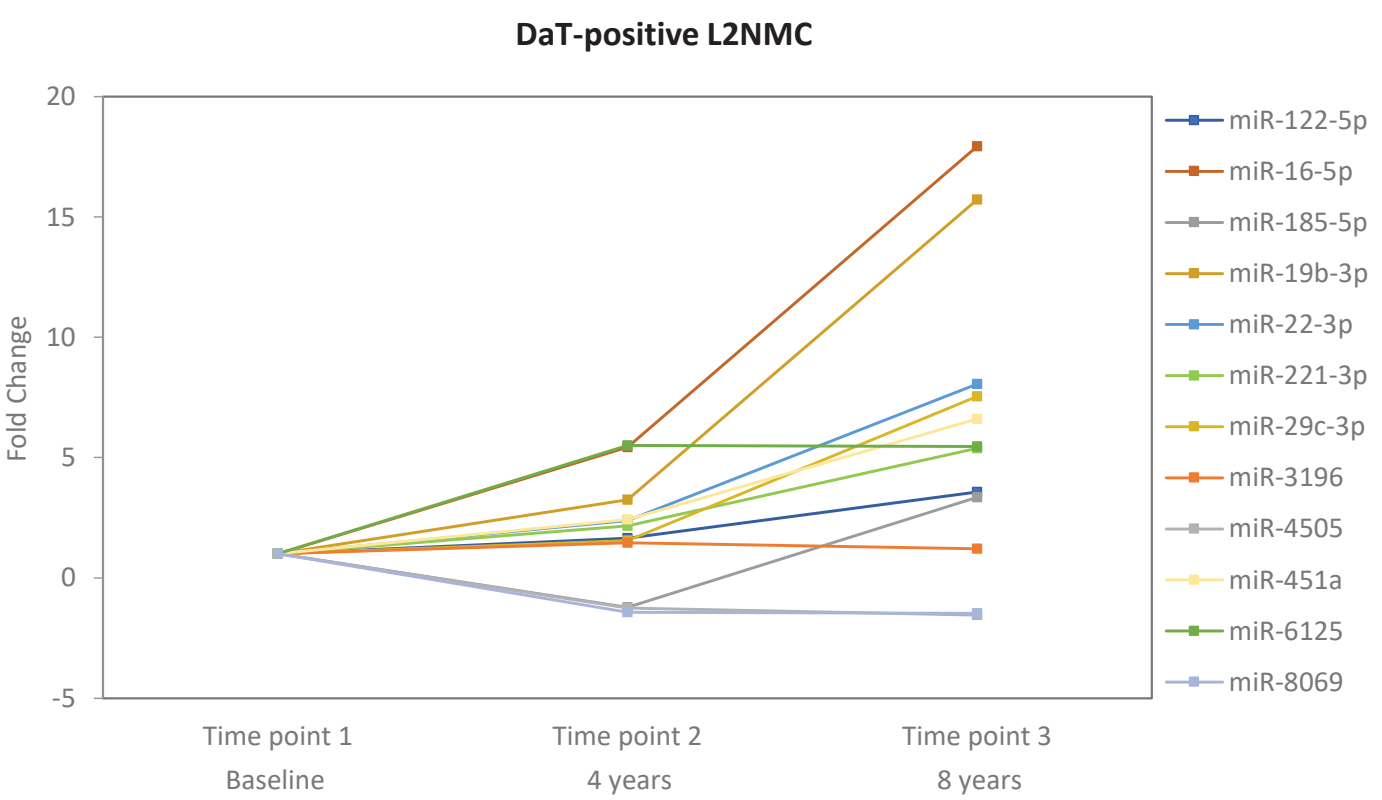
DaT-positive L2NMC
Fold Change
20
15
10
5
0
-5
Time point 1
Baseline
Time point 2
4 years
Time point 3
8 years
miR-122-5p
miR-16-5p
miR-185-5p
miR-19b-3p
miR-22-3p
miR-221-3p
miR-29c-3p
miR-3196
miR-4505
miR-451a
miR-6125
miR-8069

Fig. 6

SUPPLEMENTARY TABLE 1: (A) Candidate differentially expressed miRNAs identified by genome-wide microRNA expression analysis across different contrast
DaT = DaT-SPECT imaging; L2NMC = LRRK2 non-manifesting carriers; L2PD = LRRK2 carrier with symptomatic Parkinson disease; iPD = idiopathic PD; FC = fold change;
Adj. P = FDR multiple-test adjusted P-value

DaT-negative L2NMC vs. C			
Transcript ID	**FC**	**P-value**	**Adj. P**
hsa-miR-4505	2,26	0,0064	0,4108
hsa-miR-4749-5p	1,72	0,0141	0,4108
hsa-miR-4443	2,29	0,0164	0,4108
hsa-miR-6763-5p	1,88	0,0166	0,4108
hsa-miR-455-3p	1,71	0,0174	0,4108
hsa-miR-4253	2,01	0,0175	0,4108
hsa-miR-185-5p	3,05	0,0215	0,4108
hsa-mir-6776	-1,60	0,0232	0,4108
hsa-miR-4486	2,24	0,0286	0,4108
hsa-miR-4454	1,70	0,0297	0,4108
hsa-miR-4459	1,94	0,0312	0,4108
hsa-miR-4717-3p	2,00	0,0340	0,4108
hsa-miR-6860	1,53	0,0376	0,4108
hsa-miR-22-3p	2,22	0,0387	0,4108
hsa-miR-4787-5p	1,54	0,0397	0,4108
hsa-miR-7704	1,67	0,0425	0,4108
hsa-miR-939-5p	1,87	0,0433	0,4108
hsa-miR-6125	1,93	0,0441	0,4108
hsa-miR-610	1,80	0,0457	0,4108
hsa-miR-6729-5p	1,56	0,0462	0,4108
hsa-miR-6779-5p	1,66	0,0498	0,4108

DaT-positive L2NMC vs. C			
Transcript ID	**FC**	**P-value**	**Adj. P**
hsa-mir-3153	-1,66	0,0004	0,1306
hsa-miR-6075	1,57	0,0126	0,7945
hsa-miR-4253	2,48	0,0181	0,7945
hsa-miR-3921	-1,93	0,0184	0,7945
hsa-miR-4750-3p	-1,76	0,0294	0,7945
hsa-miR-1825	-1,77	0,0332	0,7945
hsa-miR-4505	2,26	0,0352	0,7945
hsa-miR-122-5p	3,81	0,0405	0,7945
hsa-miR-3196	2,56	0,0415	0,7945
hsa-miR-1228-3p	-1,69	0,0481	0,7945

L2PD vs. C			
Transcript ID	**FC**	**P-value**	**Adj. P**
hsa-miR-4530	2,16	0,0026	0,7918
hsa-miR-4497	2,09	0,0142	0,7918
hsa-miR-7704	1,65	0,0150	0,7918
hsa-mir-5095	1,70	0,0294	0,7918
hsa-miR-6068	1,67	0,0304	0,7918
hsa-miR-3201	-2,57	0,0323	0,7918
hsa-miR-8069	1,88	0,0335	0,7918
hsa-miR-6125	1,81	0,0360	0,7918
hsa-miR-3196	1,92	0,0424	0,7918
hsa-miR-4674	2,05	0,0461	0,7918
hsa-miR-4749-5p	1,53	0,0484	0,7918

iPD vs. C			
Transcript ID	**FC**	**P-value**	**Adj. P**
hsa-miR-19b-3p	2,93	5,49E-05	0,0182
hsa-miR-106b-5p	2,70	0,0005	0,0857
hsa-miR-22-3p	3,96	0,0010	0,1118
hsa-miR-106a-5p	3,49	0,0045	0,1611
hsa-miR-940	-1,74	0,0048	0,1611
hsa-mir-548q	-2,16	0,0049	0,1611
hsa-miR-181a-5p	1,96	0,0052	0,1611
hsa-miR-1228-3p	-1,70	0,0054	0,1611
hsa-miR-6797-3p	-1,66	0,0064	0,1611
hsa-miR-17-5p	3,26	0,0076	0,1611
hsa-miR-221-3p	2,31	0,0076	0,1611
hsa-miR-4253	-1,93	0,0076	0,1611
hsa-miR-210-3p	1,50	0,0078	0,1611
hsa-miR-423-3p	1,95	0,0079	0,1611
hsa-miR-548aq-3p	-1,93	0,0080	0,1611
hsa-miR-20b-5p	2,25	0,0082	0,1611
hsa-miR-1298-3p	-1,99	0,0082	0,1611
hsa-miR-425-5p	3,54	0,0096	0,1623
hsa-miR-652-3p	2,42	0,0098	0,1623
hsa-miR-20a-5p	2,64	0,0113	0,1623
hsa-miR-25-3p	2,28	0,0114	0,1623
hsa-miR-6796-3p	-1,53	0,0114	0,1623
hsa-miR-130b-3p	1,61	0,0116	0,1623
hsa-miR-107	3,01	0,0122	0,1623
hsa-miR-222-3p	2,10	0,0122	0,1623
hsa-miR-5787	-1,52	0,0139	0,1726
hsa-mir-548a-1	-1,61	0,0150	0,1726
hsa-miR-103a-3p	3,28	0,0151	0,1726
hsa-miR-151a-3p	2,22	0,0166	0,1840
hsa-miR-140-3p	2,74	0,0190	0,2014
hsa-miR-93-5p	3,16	0,0196	0,2014
hsa-miR-744-5p	2,07	0,0200	0,2014
hsa-miR-16-5p	3,93	0,0208	0,2028
hsa-miR-1263	-1,75	0,0238	0,2218
hsa-miR-185-5p	2,69	0,0240	0,2218
hsa-miR-4530	1,83	0,0274	0,2396
hsa-miR-200b-5p	-1,72	0,0335	0,2778
hsa-miR-1273g-3p	2,55	0,0348	0,2782
hsa-miR-3197	-1,76	0,0352	0,2782
hsa-miR-24-3p	3,09	0,0364	0,2814
hsa-let-7b-5p	2,83	0,0411	0,2936
hsa-miR-548ap-3p	-1,69	0,0416	0,2936
hsa-miR-628-5p	-1,79	0,0432	0,2938
hsa-miR-603	-1,75	0,0434	0,2938
hsa-let-7c-5p	1,68	0,0466	0,3093

SUPPLEMENTARY TABLE 1: (B) Candidate differentially expressed miRNAs identified by genome-wide microRNA expression analysis across different G2019S progression stages
DaT = DaT-SPECT imaging; L2NMC = LRRK2 non-manifesting carriers; L2PD = LRRK2 carrier with symptomatic Parkinson disease; iPD = idiopathic PD; FC = fold change;
Adj. P = FDR multiple-test adjusted P-value

DaT-negative L2NMC vs. DaT-positive L2NMC			
Transcript ID	**FC**	**P-value**	**Adj. P**
hsa-miR-4445-3p	1,66	0,0031	0,9978
hsa-miR-7110-5p	-2,64	0,0169	0,9978

DaT-positive L2NMC vs. L2PD			
Transcript ID	**FC**	**P-value**	**Adj. P**
hsa-miR-4445-3p	-2,09	0,0039	0,6714
hsa-miR-4720-5p	-6,21	0,0054	0,6714
hsa-miR-6836-3p	1,61	0,0079	0,6714
hsa-miR-548ac	-5,16	0,0094	0,6714
hsa-miR-3201	-1,97	0,0162	0,6714
hsa-miR-1228-3p	1,79	0,0168	0,6714
hsa-miR-4275	-2,68	0,0203	0,6714
hsa-miR-3128	-1,89	0,0214	0,6714
hsa-miR-1825	1,80	0,0230	0,6714
hsa-miR-3124-5p	-1,68	0,0230	0,6714
hsa-miR-548x-3p	-4,01	0,0244	0,6714
hsa-mir-548q	-3,51	0,0266	0,6714
hsa-miR-6868-5p	-1,70	0,0273	0,6714
hsa-miR-548a-3p	-3,72	0,0282	0,6714
hsa-miR-548aq-3p	-3,31	0,0285	0,6714
hsa-miR-548ae	-3,50	0,0298	0,6714
hsa-miR-548aj-3p	-3,55	0,0318	0,6714
hsa-miR-7844-5p	2,08	0,0331	0,6714
hsa-miR-32-5p	-4,20	0,0332	0,6714
hsa-miR-16-2-3p	-4,47	0,0351	0,6714
hsa-mir-4251	-1,61	0,0368	0,6714
hsa-miR-6800-3p	-2,18	0,0385	0,6714
hsa-miR-4253	-2,56	0,0418	0,6714
hsa-mir-6800	1,74	0,0465	0,6714

L2PD vs. iPD			
Transcript ID	**FC**	**P-value**	**Adj. P**
hsa-miR-1228-3p	2,16	0,0004	0,1412
hsa-miR-127-3p	2,37	0,0040	0,3009
hsa-miR-4717-3p	2,90	0,0049	0,3009
hsa-miR-5093	5,10	0,0067	0,3009
hsa-miR-595	4,07	0,0071	0,3009
hsa-miR-7855-5p	-1,84	0,0073	0,3009
hsa-miR-548a-3p	-4,79	0,0096	0,3009
hsa-miR-3148	2,39	0,0100	0,3009
hsa-miR-4507	3,18	0,0115	0,3009
hsa-miR-1825	1,87	0,0116	0,3009
hsa-miR-548ac	-4,46	0,0128	0,3009
hsa-miR-3907	3,64	0,0141	0,3009
hsa-miR-4708-3p	-2,03	0,0147	0,3009
hsa-miR-1915-3p	2,02	0,0152	0,3009
hsa-miR-32-5p	-3,96	0,0154	0,3009
hsa-miR-548ae	-4,25	0,0173	0,3009
hsa-miR-16-2-3p	-4,51	0,0176	0,3009
hsa-mir-1913	2,71	0,0176	0,3009
hsa-miR-4720-5p	-4,13	0,0184	0,3009
hsa-miR-297	5,54	0,0190	0,3009
hsa-miR-3064-5p	3,63	0,0201	0,3009
hsa-miR-6849-5p	2,74	0,0202	0,3009
hsa-miR-4497	2,22	0,0203	0,3009
hsa-mir-6876	1,65	0,0231	0,3023
hsa-miR-6850-5p	2,80	0,0252	0,3023
hsa-miR-1298-3p	-2,72	0,0256	0,3023
hsa-miR-4793-3p	4,72	0,0258	0,3023
hsa-miR-7154-5p	-1,79	0,0262	0,3023
hsa-miR-548x-3p	-3,81	0,0265	0,3023
hsa-miR-4516	2,01	0,0275	0,3023
hsa-mir-185	2,07	0,0329	0,3334
hsa-miR-6796-3p	1,57	0,0339	0,3334
hsa-mir-297	2,45	0,0345	0,3334
hsa-miR-4701-3p	3,44	0,0365	0,3334
hsa-miR-638	1,74	0,0392	0,3334
hsa-mir-6736	2,07	0,0396	0,3334
hsa-miR-6088	1,98	0,0398	0,3334
hsa-miR-4486	2,96	0,0400	0,3334
hsa-miR-6090	2,02	0,0403	0,3334
hsa-miR-6798-5p	2,40	0,0420	0,3381
hsa-miR-200b-5p	-2,60	0,0450	0,3381
hsa-miR-324-5p	-2,04	0,0456	0,3381
hsa-miR-3124-5p	-1,50	0,0457	0,3381
hsa-miR-1268b	2,64	0,0461	0,3381
hsa-miR-4530	2,31	0,0465	0,3381
hsa-miR-6068	2,01	0,0477	0,3396

SUPPLEMENTARY TABLE 2: Relative fold change expression of 10 selected miRNAs identified by genome-wide miRNA expression analysis and validation by RT-qPCR in DaT-negative L2NMC, DaT-positive L2NMC, L2PD and iPD patients as compared to controls

DaT = DaT-SPECT imaging; L2NMC = LRRK2 non-manifesting carriers; L2PD = LRRK2 carrier with symptomatic Parkinson disease; iPD = idiopathic PD; FC = fold change

DaT-negative L2NMC vs. C				
	Array		RT-qPCR	
Transcript ID	**FC**	**P-value**	**FC**	**P-value**
hsa-miR-4505	2,26	0,0064	1,98	0,0016
hsa-miR-185-5p	3,05	0,0215	3,68	<0.0001
hsa-miR-22-3p	2,22	0,0387	1,66	0,0632
hsa-miR-6125	1,93	0,0441	-1,47	0,1179

DaT-positive L2NMC vs. C				
	Array		RT-qPCR	
Transcript ID	**FC**	**P-value**	**FC**	**P-value**
hsa-miR-4505	2,26	0,0352	3,51	0,0004
hsa-miR-122-5p	3,81	0,0405	3,38	0,0269
hsa-miR-3196	2,56	0,0415	1,98	0,0012

L2PD vs. C				
	Array		RT-qPCR	
Transcript ID	**FC**	**P-value**	**FC**	**P-value**
hsa-miR-8069	1,88	0,0335	1,09	0,7352
hsa-miR-6125	1,81	0,0360	-1,01	0,9535
hsa-miR-3196	1,92	0,0424	2,13	0,0001

iPD vs. C				
	Array		RT-qPCR	
Transcript ID	**FC**	**P-value**	**FC**	**P-value**
hsa-miR-19b-3p	2,93	0,0001	3,04	0,0018
hsa-miR-22-3p	3,96	0,0010	2,67	0,0025
hsa-miR-221-3p	2,31	0,0076	1,93	0,0076
hsa-miR-16-5p	3,93	0,0208	5,21	0,0003
hsa-miR-185-5p	2,69	0,0240	3,60	0,0028

Overall fold-change correlation of fold-changes by array and RT-qPCR:

Pearson's correlation coefficient = 0.703 (P-value=0.003)
Spearman's correlation coefficient = 0.768 (P-value=0.001)

SUPPLEMENTARY TABLE 3: RT-qPCR assessment of miRNA levels in serum samples from a second independent cohort of L2PD patients (n=19) compared to healthy controls (n=20). L2PD = LRRK2 carrier with symptomatic Parkinson disease; FC = fold change; Adj. P = FDR multiple-test adjusted P-value

microRNA	FC	Adj. P
miR-122-5p	4,69	0,0074
miR-16-5p	-1,16	0,9488
miR-185-5p	1,54	0,5539
miR-19b-3p	-1,61	0,5539
miR-22-3p	-1,52	0,5539
miR-221-3p	1,19	0,9488
miR-29c-3p	-1,02	0,9488
miR-3196	1,51	0,5539
miR-4505	1,36	0,5539
miR-451a	1,05	0,9488
miR-6125	-1,02	0,9488
miR-8069	1,05	0,9488

SUPPLEMENTARY TABLE 4: RT-qPCR assessment of miRNA differences between DaT-positive non-pheno-converted L2NMC (n=16) vs all pheno-converted G2019S carriers in the study, i.e., L2PD discovery (n=20) and validation (n=19) sets, and DaT-positive L2NMC which pheno-converted during the study (n=4) (total n=43)
DaT = DaT-SPECT imaging; L2NMC = LRRK2 non-manifesting carriers; L2PD = LRRK2-associated PD patients; FC = fold change; Adj. P = FDR multiple-test adjusted P-value

miRNA	FC*	Adj. P
miR-4505	-3.44	0.0006
miR-8069	-1.87	0.0035
miR-6125	1.92	0.0280
miR-451a	-2.17	0.0828
miR-185-5p	-1.64	0.3631
miR-22-3p	1.48	0.4438
miR-16-5p	1.63	0.4578
miR-3196	1.20	0.5273
miR-19b-3p	-1.29	0.6503
miR-122-5p	-1.28	0.6824
miR-29c-3p	-1.19	0.6824
miR-221-3p	-1.11	0.7216

3.3 Article 3

Parkinsonism and Related Disorders 99 (2022) 33–41

Contents lists available at ScienceDirect

Parkinsonism and Related Disorders

journal homepage: www.elsevier.com/locate/parkreldis

Combined CSF α-SYN RT-QuIC, CSF NFL and midbrain-pons planimetry in degenerative parkinsonisms: From bedside to bench, and back again

Y. Compta [a,b,*,1], C. Painous [a,b,1], M. Soto [a,b,1], M. Pulido-Salgado [a,b], M. Fernández [a,b], A. Camara [a,b], V. Sánchez [c,d], N. Bargalló [c,d], N. Caballol [e,f], C. Pont-Sunyer [g], M. Buongiorno [h], N. Martin [i], M. Basora [i], M. Tio [i], D.M. Giraldo [a,b,j], A. Pérez-Soriano [a,b], I. Zaro [a,b], E. Muñoz [a,b], M.J. Martí [a,b,**], F. Valldeoriola [a,b]

[a] Parkinson's Disease & Movement Disorders Unit, Neurology Service, Hospital Clínic I Universitari de Barcelona; IDIBAPS, CIBERNED (CB06/05/0018-ISCIII), ERN-RND, Institut Clínic de Neurociències (Maria de Maeztu Excellence Centre), Universitat de Barcelona. Barcelona, Catalonia, Spain
[b] Lab of Parkinson Disease and Other Neurodegenerative Movement Disorders: Clinical and Experimental Research; Department of Neurology, Hospital Clínic de Barcelona, Institut D'Investigacions Biomèdiques August Pi I Sunyer (IDIBAPS), Institut de Neurociències, Universitat de Barcelona, Barcelona, Catalonia, Spain
[c] Magnetic Resonance Imaging Core Facility, Institut D'Investigacions Biomèdiques August Pi I Sunyer (IDIBAPS), Barcelona, Spain
[d] Centre de Diagnòstic Per a La Imatge (CDIC), Hospital Clínic, Barcelona, Spain
[e] UParkinson Centro Médico Teknon, Grupo Hospitalario Quirón Salud, Barcelona, Spain
[f] Department of Neurology, Hospital Sant Joan Despí Moisès Broggi and Hospital General de L'Hospitalet, Consorci Sanitari Integral, Barcelona, Spain
[g] Neurology Unit, Hospital General de Granollers, Universitat Internacional de Catalunya, Barcelona, Spain
[h] Movement Disorders Unit. Neurology. University Hospital Mutua de Terrassa, Terrassa, Catalonia, Spain
[i] Department of Anaesthesiology, Hospital Clinic, Barcelona, Spain
[j] Neuroloy Service, Hospital Comarcal Sant Jaume de Calella, Barcelona, Spain

ARTICLE INFO

Keywords:
biomarkers
α-synuclein RT-QuIC
CSF neurofilament Light chain
MRI
Degenerative parkinsonisms

ABSTRACT

Introduction: Differential diagnosis between Parkinson's disease (PD) and atypical parkinsonisms (APs: multiple system atrophy[MSA], progressive supranuclear palsy[PSP], corticobasal degeneration[CBD]) remains challenging. Lately, cerebrospinal fluid (CSF) studies of neurofilament light-chain (NFL) and RT-QuIC of alpha-synuclein (α-SYN) have shown promise, but data on their combination with MRI measures is lacking.
Objective: (1) to assess the combined diagnostic ability of CSF RT-QuIC α-SYN, CSF NFL and midbrain/pons MRI planimetry in degenerative parkinsonisms; (2) to evaluate if biomarker-signatures relate to clinical diagnoses and whether or not unexpected findings can guide diagnostic revision.
Methods: We collected demographic and clinical data and set up α-SYN RT-QuIC at our lab in a cross-sectional cohort of 112 participants: 19 control subjects (CSs), 20PD, 37MSA, 23PSP, and 13CBD cases. We also determined CSF NFL by ELISA and, in 74 participants (10CSs, 9PD, 26MSA, 19PSP, 10CBD), automatized planimetric midbrain/pons areas from 3T-MRI.
Results: Sensitivity of α-SYN RT-QuIC for PD was 75% increasing to 81% after revisiting clinical diagnoses with aid of biomarkers. Sensitivity for MSA was 12% but decreased to 9% with diagnostic revision. Specificities were 100% against CSs, and 89% against tauopathies raising to 91% with diagnostic revision. CSF NFL was significantly higher in APs. The combination of biomarkers yielded high diagnostic accuracy (PD vs. non-PD AUC = 0.983; MSA vs. non-MSA AUC = 0.933; tauopathies vs. non-tauopathies AUC = 0.924). Biomarkers-signatures fitted in most cases with clinical classification.
Conclusions: The combination of CSF NFL, CSF RT-QuIC α-SYN and midbrain/pons MRI measures showed high discriminant ability across all groups. Results opposite to expected can assist diagnostic reclassification.

Abbreviations: MRI, magnetic ressonance imaging; RT-QuIC, real time - quaking induced conversion; CSF, cerebrospinal fluid; NFL, neurofilament light-chain; PD, Parkinson's disease; PSP, progressive supranuclear palsy; MSA, multiple system atrophy; CBD, corticobasal degeneration; AP, atypical parkinsonism.

* Co-corresponding authors. 170 Villarroel street, 08036, Barcelona, Spain.
** Co-corresponding authors. 170 Villarroel street, 08036, Barcelona, Spain.
E-mail addresses: ycompta@clinic.cat (Y. Compta), mjmarti@clinic.cat (M.J. Martí).
[1] These three authors equally contributed.

https://doi.org/10.1016/j.parkreldis.2022.05.006
Received 9 March 2022; Received in revised form 29 April 2022; Accepted 8 May 2022
Available online 13 May 2022

1. Introduction

Neurodegenerative parkinsonisms are classified into synucleinopathies (Parkinson's disease(PD); multiple system atrophy(MSA)), or tauopathies (progressive supranuclear palsy(PSP); corticobasal degeneration(CBD)), depending on the underlying proteinopathy [1]. Despite the use of consensus criteria, differentiating PD from atypical parkinsonisms (APs: PSP, CBD and MSA) remains challenging, even in expert sites [2] as reliable biomarkers are lacking.

Increased cerebrospinal fluid (CSF) levels of neurofilament light chain (NFL) discriminate PD from APs, but are unspecific among APs [3]. Lately, real-time quaking-induced conversion (RT-QuIC) of alpha-synuclein (α-SYN) is being consistently found to be positive in PD and negative in tauopathies, albeit with low sensitivity in MSA [4,5], except for a study with 75% sensitivity, but longer time to positivity and lower amplification than PD [6]. A single published study has reported improved differentiation between PD and APs by combining NFL and α-SYN RT-QuiC, but without other clinical or imaging biomarkers [7]. MRI mid-sagittal planimetry has shown reduced midbrain and pons areas in PSP and MSA, respectively [8,9].

To the best of our knowledge, the combination of CSF NFL (as a biomarker of neuronal/axonal damage and proxy of aggressiveness of neurodegeneration), CSF α-SYN RT-QuiC (as a proxy of underlying abnormal and disease-causing aggregation of α-synuclein) and MRI brainstem planimetry (as indicators of differential predominance of midbrain [PSP] vs. pons [MSA] atrophy) remains unexplored in neurodegenerative parkinsonisms.

Accordingly, we hypothesized that: a) biomarkers-combination yields high diagnostic accuracy allowing for separating parkinsonisms on α-synuclein, aggressiveness, and regional brainstem atrophy axes; b) "biomarker-signatures" relate to clinical diagnoses consistent with different combinations of the aforementioned biomarkers; c) unexpected biomarker findings can, in part of cases at least, relate to phenotypic differences, or guide diagnosis revision. The objectives were thus to explore the combined biomarkers discriminant ability across degenerative parkinsonisms, to assess the association of "biomarker-signatures" with each diagnostic group, and to revisit the clinical features and the diagnosis of cases with unexpected biomarker results.

2. Methods

Design: Multicentre cross-sectional study centralized at the Parkinson's Disease & Movement Disorders Unit of Hospital Clinic Universitari de Barcelona.

Participants: The cohort recruited between 2015 and 2021 consisted of 112 participants: 20PD, 37MSA, 23PSP, 13CBD and 19 control subjects (CSs). Automatized MRI midbrain/pons areas planimetry was available for 74 participants (9PD, 26MSA, 19PSP, 10CBD, 10CSs). All CSF samples were used to set up α-SYN RT-QuIC at our lab. All diseased-participants fulfilled the "probable" (or "clinically established" in PD) category of their respective diagnostic criteria [10–13] upon recruitment, with at least two-year follow-up. CSs were aged>55, with CSF obtained before the injection of spinal anaesthesia for knee surgery, and no neuro-psychiatric condition by clinical history and exam. Secondary parkinsonism and large vascular MRI abnormalities were exclusion criteria, and so was Alzheimer's disease CSF profile [14] in CBD patients. The Ethics Committee approved the study and all participants signed their informed consent.

Clinical assessment: Demographic and clinical variables were sex, age, disease duration at inclusion, the Unified Parkinson's Disease Rating Scale part III (UPDRS-III) [15] and the Hoehn and Yahr (HY) rating scale [16]. Cognition was evaluated with the Montreal Cognitive Assessment (MoCa) [17] in all participants except in MSA patients, whom were assessed by the Mini Mental test (MMSE) [18]. We also administered the PSP rating scale (PSPRS) [19] to PSP, CBD and CSs and the Unified Multiple System Atrophy Rating Scale (UMSARS) [20] in MSA patients.

CSF protocol: All CSF samples were obtained using the protocol published elsewhere [21], via lumbar puncture at the L3-L4 level with a 22-gauge needle, between 8 and 10 a.m. The first 2 mL were used for routine studies. CSF was processed within 30min of obtention, centrifuged 10 min at 2000 rcf and 4 °C, and stored at −80 °C. CSF NFL levels were measured with a commercial ELISA NF-light kit (Umandiagnostics, Sweden) (NF-light datasheet). All samples were run in duplicate together with blank (sample diluent), calibrator solutions, and an internal control sample, evenly distributing all groups among runs. All standard curves fulfilled the quality control criteria established by the manufacturers and R2 values range between 0.999 and 1. For all analysis we used a single concentration value per case in pg/mL (the mean of duplicates; all duplicates had a variation coefficient <20%).

CSF α-SYN RT-QuIC was performed in black 96-well optical bottom plates (Thermo Scientific Nunc MicroWell) measuring all samples in triplicate. Samples from all groups were evenly distributed among runs and an RT-QuIC positive PD sample was added to each plate as positive control. Each well was preloaded with eight 0.5 mm zirconia/silica beads (BioSpec Products) and 85 μl of RT-QuIC reaction mix containing 100 mmol/L phosphate buffer (Ph 8.2), 10 μmol/L Thioflavin T (ThT) and 0.1 mg/ml recombinant human α-synuclein (Sigma-Aldrich). Reactions were seeded with 15 μl of CSF. Plates were then sealed with a sealing tape (Thermo Scientific Nunc) and incubated in a FLUOstar Omega (BMG Labtech) for 120h at 42 °C setting cycles of 90 s shaking at 600 rpm and 14 min resting. Fluorescence was measured at the end of each cycle at an emission wavelength of 482 nm after an excitation at 448 nm. Positivity was defined as ≥2 of 3 replicates over 2SDs above the mean of relative fluorescence units (RFUs) in CSs at 60h and 120h similar to previous studies [4].

MRI planimetry: Brainstem was parcelled using the Brainstem Bayesian FreeSurfer module [22]. First, for each subject, the T1-weighted image was aligned with a template in the MRI to identify the midsagittal plane. To account for variability in the alignment, 10 slices around the central sagittal slice were evaluated to identify the midsagittal slice, which was defined as the one containing the smaller midbrain area. To automatically assess midsagittal midbrain (M_A) and pontine (P_A) areas, the number of voxels segmented as midbrain and pons in the midsagittal slice were counted and multiplied by voxel size. Values are reported in cm^2. M_A and P_A were also manually assessed as previously described [23]. Two independent raters (VS and CP) performed the measurements blinded to the clinical information. To assess the intrarater reliability, a second blinded evaluation was made 1 month after the first evaluation by one of the raters (CP). Intraclass correlation coefficient (ICC) was calculated and considered as poor if ICC <0.40, fair if ICC between 0.40 and 0.59, good if ICC between 0.60 and 0.74, and excellent if ICC between 0.75 and 1.00 [24]. Intra-manual and manual-automatic agreements were excellent and good to excellent, respectively.

Statistical analyses: Statistical power calculation considering prior literature [4–6] resulted in a sample size of at least 80 individuals (20 PD, 20 MSA, 16 PSP, 8 CBD, 16 CSs) to obtain an ≥80% accuracy in the estimation of a proportion by means of a two-tailed 95% confidence interval (95%CI) under a dichotomic assumption (α-SYN RT-QuIC + vs. -, p = 50%). Qualitative variables are presented as absolute and relative frequencies; quantitative data as median and interquartile range (IQR). Non-parametric tests (Fisher's exact test for qualitative variables and Mann Whitney's U or Kruskal-Wallis test for continuous ones) were applied. Non-parametric analysis of covariance with age as covariate was used to compare NFL, M_A and P_A variables across groups. Spearman's correlations (rho), linear regressions and the respective scatter plots were used to evaluate linear correlation across quantitative clinical and biomarker variables.

Univariate binary logistic regression models and receiver operating characteristic (ROC) curves statistics with their area under the curves (AUCs), 95%CIs and sensitivities (Se)/specificities (Sp) were calculated

for discrimination of PD vs. non-PD (CSs + MSA + PSP + CBD), MSA vs. non-MSA (CSs + PD + PSP + CBD) and tauopathies (PSP + CBD) vs. non-tauopathies groups (CSs + PD + MSA). NFL, α-SYN RT-QuiC, M_A or P_A were used as independent variables. Then, multivariate binary logistic regression models combining CSF NFL, α-SYN RT-QuiC, M_A and P_A were calculated, but limiting the number of covariates to minimize the risk of overfitting. The NFL variable was treated as a continuous and binary variable, using as cut-off 1315.40 pg/mL after the ROC curve analysis of CSF NFL levels in APs vs. non-APs (see details in Results).

As a post-hoc exploratory analysis we defined the following biomarkers signatures: "CS signature" = none biomarker altered or no clinical symptoms ± a single altered biomarker; "PD signature" = positive (+) α-SYN RT-QuIC & negative (−) NFL levels and normal MRI values; "tauopathy signature" = + NFL & midbrain atrophy; "MSA signature" = + NFL & pons atrophy. We analysed the proportion of each signature in each diagnostic group.

Finally, and as a "real life" approach to explore the hypothetic post-hoc ability of the studied biomarkers to confirm or challenge the initial diagnosis we revisited all participants' diagnoses according to α-SYN RT-QuIC (positive or negative) and NFL levels (< or >1315.40 pg/mL) results. In Results we summarize cases with unexpected findings and which of them could be reclassified considering both the biomarkers and the clinical follow-up after CSF collection, as in the rest of cases clinical diagnosis and biomarker findings were consistent and did not raise diagnostic doubts. We then accordingly recalculated sensitivities and specificities.

Statistical tests were two-tailed, with significance set at ≤0.05, corrected for multiple comparisons by false-discovery-rate(FDR) [25]. Missing values were not included in the analysis for its outcome. Data analysis was performed with IBM SPSS version 24.0 (Armonk, NY; IBM).

3. Results

Demographic and clinical data: No demographic differences were found except for younger age in MSA. Likewise, UPDRS, PSPRS, MoCa and HY did not significantly differ across parkinsonisms, but were worse in these groups vs. CSs (Table 1).

α-SYN RT-QuIC: In PD patients the proportion of positive seeding was significantly higher than in all other groups (Table 1), with 15/20 of them being positive (sensitivity = 75%). Sensitivity was much lower in MSA (4/33 = 12%). Conversely, none of the CSs and only 4 of 36 tauopathy cases were false positives (Table 1; Fig. 1A–C), resulting in specificities of 100% in PD vs. CSs, and 89% in PD vs. tauopathies. Univariate logistic regression followed by ROC curve analyses demonstrated the following accuracy for the discrimination of: PD vs. non-PD: AUC = 0.832 (95%CI = 0.748–0.895), p < 0.001, Se/Sp: 75.0/91.3; MSA vs. non-MSA: AUC = 0.573 (95%CI = 0.474–0.655), p = 0.06. In the case of PD, since disease duration was significantly longer than in other conditions, we run a binary logistic regression model for PD vs. no-PD with CSF α-SYN RT-QuIC as predictor covaried by disease duration along with the ROC curve resulting from the propensity scores of the regression model, showing that CSF α-SYN RT-QuIC remains an independent significant predictor of PD when adjusting for disease duration (Suppl. Fig 2).

CSF NFL: APs had significantly higher CSF NFL levels than PD and CSs (Table 1). ROC curve analysis of APs vs. non-APs yielded AUC = 0.953 (95%CI = 0.885–0.983), p < 0.0001, with an optimal cut-off of 1315.40 pg/mL (Se = 88%; Sp = 97%). Albeit levels were significantly higher in MSA vs. tauopathies, the difference was marginal with large overlap (AUC = 0.631; 95%CI = 0.504–0.757; p = 0.046; Se/Sp = 25.0/80.4). PD had significant higher NFL vs. CSs (Table 1; AUC = 0.743 (95%CI = 0.577–0.890), p = 0.017, Se/Sp = 58.8/68.8.

MRI planimetry: M_A was significantly smaller in PSP vs. all other

Table 1
Demographic, CSF and MRI measures across the different diagnostic groups.

	CS (n = 19)	PD (n = 20)	MSA (n = 37; 22MSAp [60%], 15MSAc [40%])	PSP (n = 23; Richardson's 15[65%], non-Richardson's 8 [35%])	CBD (n = 13)	p-value *
Age (in years)	72.2 [66.9–74.8]	70.5 [64.9–74.7]	62.5 [55.9–66.8]	74.5 [71.3–79.5]	70.3 [68.3–74.5]	**All groups:** 0.001; **PSP/MSA**: <0.001; **MSA/CS**: 0.006; **MSA/PD**: 0.010; **MSA/CBD**: 0.002;
Female sex (%)	11 (57.9)	11 (55.0)	17 (45.9)	9 (39.1)	10 (76.9)	
Disease duration (in years)	NA	7.8 [4.5–15.6]	4.4 (3.1–6.8)	4.4 (3.1–6.8)	5.1 (3.7–6.8)	
UPDRS	0 [0–2.0]	32 [23–50]	44.5 [42–70]	36 [25.5–45]	48 [42–65]	**PSP/CS**: <0.001; **MSA/CS**: <0.001; **CBD/CS**: <0.001; CBD/PD: 0.254; **PD/CS**: <0.001
PSPRS	0 [0–0]	NA	NA	35 [22–47]	36 [30–43]	**PSP/CS**: <0.001; **CBD/CS**: <0.001
UMSARS	NA	NA	44 [32–69]	NA	NA	
MoCa	26 [26–28]	20.5 [10–27]	NA	22 [16–25]	19 [9.5–26.5]	**PSP/CS**: 0.006
MMSE	NA	NA	28 [28–30]	NA	NA	
HY > 2 (%)	0 (0)	8 (53.3)	25 (69.4)	17 (81.0)	8 (61.5)	**PSP/CS**: <0.001; **MSA/CS**: <0.001; **CBD/CS**: 0.001; **PD/CS**: <0.001
α-SYN RT-QuIC N (+)/N (−)	0/19	15/5	4/33	3/20	1/12	**All groups:** <0.001; **PSP/PD:** <0.001; **MSA/PD:** <0.001; **CBD/PD:** <0.001; **PD/CS:** <0.001
CSF NFL (pg/mL)	656.2 [504.2–867.0]	953.7 [697.4–1237.5]	2879.2 [1939.4–3840.9]	1897.5 [1554.3–2441.2]	2161.5 [1701.6–2330.0]	**All groups:** < 0.001; **AP/PD + CS:** <0.001; **PSP/PD:** < 0.001; **PSP/CS:** <0.001; **MSA/CS:** <0.001; **MSA/PD:** <0.001; **CBD/CS:** < 0.001; **CBD/PD:** <0.001; **PD/CS:** <0.001
M_A (cm^2)	1.1 [1.1–1.2]	1.3 [1.2–1.4]	1.3 [1.2–1.4]	0.9 [0.8–1.0]	1.0 [0.9–1.1]	**All groups:** <0.001; **PSP/MSA**: <0.001; **PSP/PD:** <0.001; **PSP/CS:** 0.013; **MSA/CBD:** 0.004; **CBD/PD:** < 0.001;
P_A (cm^2)	4.6 [4.4–5.6]	4.9 [4.5–5.1]	3.9 [3.4–4.4]	4.7 [4.4–5.2]	4.5 [4.1–4.9]	**All groups:** 0.002; **PSP/MSA:** 0.003; **MSA/CS:** 0.017; **MSA/PD:** 0.008;

Quantitative variables are presented as median [IQR] and compared between groups using Kruskal-Wallis or U Mann Whitney tests as appropriate.
Categorical variables are presented as absolute frequency (proportion) and compared between groups using Fisher's exact test.
*p-values results are presented FDR-corrected. Only significant results are listed.

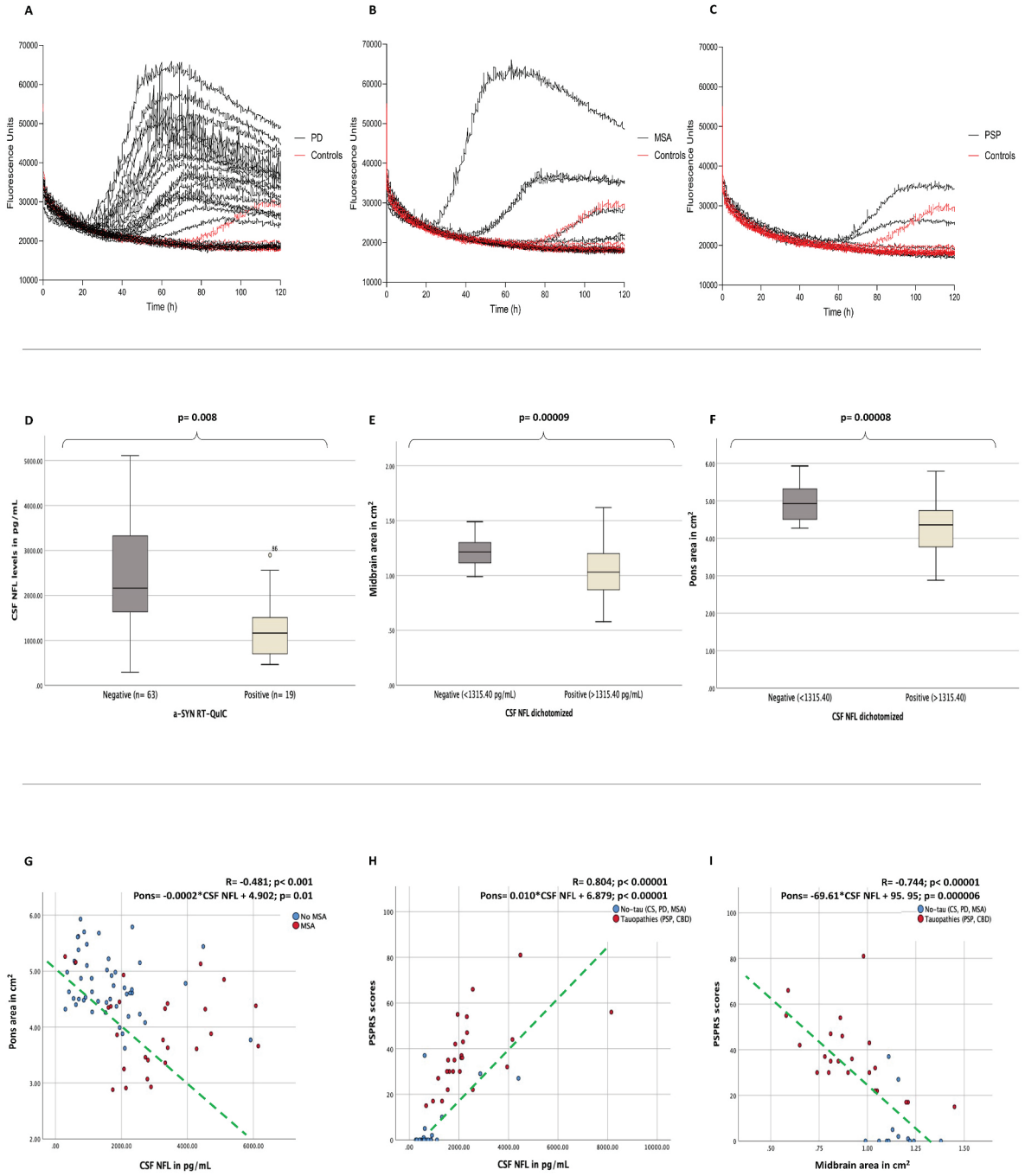

Fig. 1. Representative examples of CSF α-SYN RT-QuIC using FLUOSTAR OMEGA. Examples are from patients studied in the same experiment. Figure legend: A = 7 out of 9 patients PD cases were positive in contrast to none of the 4 CSs; B = 2 of 4 MSA patients were positive compared to the 4 negative CSs; C = 3 of 3 PSP samples did not reach the threshold of 2 of 3 replicates required for positivity as happened with the 4 CSs; D = Significantly Higher CSF NFL levels in participants with negative compared to those with positive α-SYN RT-QuIC; E = significantly smaller midbrain area in participants with positive vs. negative CSF NFL (according to the cut-off with best sensitivity and specificity for differentiating atypical parkinsonisms from PD); F = significantly smaller pons area in participants with positive vs. negative CSF NFl; G = significant negative correlation between pons area and CSF NFL levels driven by MSA cases (the higher the CSF NFL levels, the smaller the pons area); H = significant positive correlation between PSP scores and CSF NFL levels driven by tauopathy-cases (PSP or CBD) (the higher the CSF NFL levels, the higher, thus worse, the PSP scores); I = significant negative correlation between PSP scores and midbrain area driven by tauopathy cases (the smaller the midbrain area, the higher, thus worse, the PSP scores).

groups except CBD, which had smaller M_A than PD and MSA. MSA presented smaller P_A vs. all other groups except CBD (Table 1). ROC curve analyses for M_A were as follows: PD vs. non-PD: AUC = 0.836 (95%CI = 0.734–0.913), p-value<0.001, Se/Sp = 66.7/81.5; tauopathies vs. non-tauopathies: AUC = 0.846 (95%CI = 0.750–0.923), p < 0.001, Se/Sp = 75.9/82.2. For P_A the results were: PD vs. non-PD: AUC = 0.683 (95%CI = 0.571–0.792), p = 0.110; MSA vs. non-MSA: AUC = 0.797 (95%CI = 0.688–0.882), p < 0.001, Se/Sp = 73.1/75.0.

Gender perspective: No significant gender differences were found for positive CSF α-SYN RT-QuIC (22.4% women; 18.5% men; p = 0.65), high CSF NFL (59.3% women; 67.2% men; p = 0.44), midbrain atrophy (48.6% women; 39% men, p = 0.49) and pons atrophy (40% women; 39% men, p = 1.00). ROC analyses yielded significant accuracies for CSF α-SYN in PD, CSF NFL in APs, M_A in tauopathies and P_A in MSA in both

A

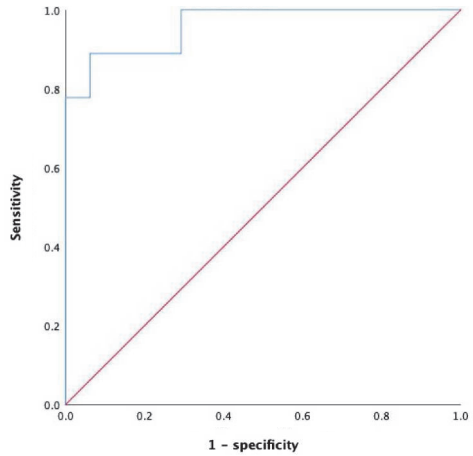

n= 74 (9 PD vs. 65 no-PD)
AUC= 0.961
95%CI= 0.897-1.000
P= 0.000008

ROC curve of PD vs. non-PD groups (propensity scores from binary logistic regression model combining α-SYN RT-QuIC, CSF NFL levels and MRI midbrain area)

B

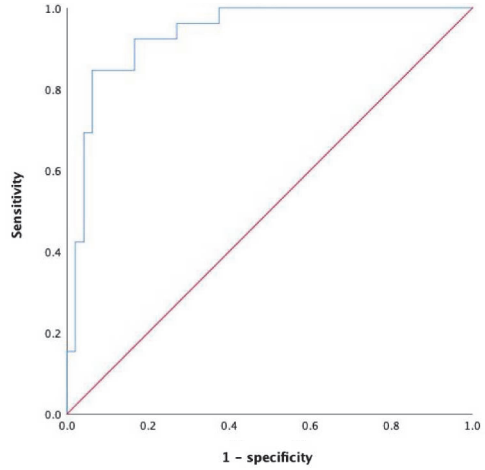

n= 74 (26 MSA vs. 48 no-MSA)
AUC= 0.936
95%CI= 0.881-0.991
P= 0.0000004

ROC curve of MSA vs. non-MSA groups (propensity scores from binary logistic regression model combining α-SYN RT-QuIC, CSF NFL levels, MRI pons area and age)

C

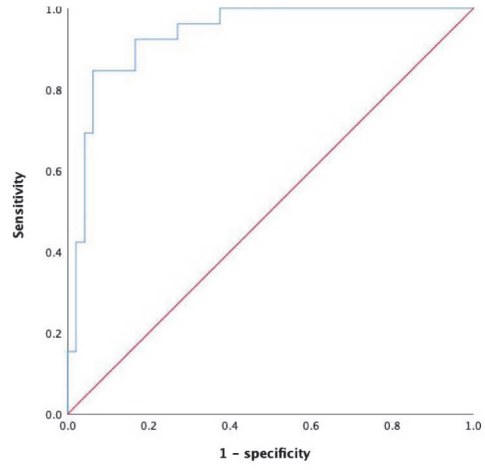

n= 74 (29 tauopathies vs. 45 non-tau participants)
AUC= 0.933
95%CI= 0.875-0.990
P= 0.00000000004

ROC curve of tauopathies vs. non-tau groups (propensity scores from binary logistic regression model combining α-SYN RT-QuIC, CSF NFL & MRI midbrain & pons areas)

Fig. 2. ROC curves of propensity scores from different binary logistic regression models combining biomarkers: [A] model covaried for RT-QuIC, NFL and midbrain area in PD vs. non-PD: AUC = 0.961 (95%CI = 0.897-1.000), $p < 0.0001$, Se/Sp = 78.0/94.0; [B] model covaried for RT-QuIC, NFL, pons area and age in MSA vs. non-MSA: AUC = 0.936 (95%CI = 0.881-0.991), $p < 0.0001$, Se/Sp = 84.0/83.0; [C] model covaried for RT-QuIC, NFL, midbrain and pons areas in tauopathies vs. non-tauopathies: AUC = 0.933 (95%CI = 0.875-0.990), $p < 0.0001$, Se/Sp = 86.0/82.0.

women and men (Suppl. Fig. 1).

Biomarker-biomarker and clinical-biomarker associations: CSF NFL levels were significantly higher in participants with negative α-SYN RT-QuIC (driven by APs) and midbrain and pons areas were significantly smaller in participants with high CSF NFL levels (driven by PSP and MSA cases, respectively) (Fig. 1D–F). Significant negative correlations were found between pons area and CSF NFL levels driven by MSA cases (the higher the CSF NFL levels, the smaller the pons area) and between PSPRS and midbrain area (the smaller the midbrain area, the higher the PSP scores) (Fig. 1G and I). Significant positive correlation was found between PSPRS and CSF NFL levels (the higher the CSF NFL levels, the higher the PSP scores) (Fig. 1H). The proportion of + α-SYN RT-QuIC, + NFL and midbrain/pons atrophy did not significantly differ either between MSA-p and MSA-c, or between Richardson's and non-Richardson's-PSP except for significantly greater midbrain atrophy in Richardson's vs. non-Richardson's-PSP.

Combined biomarkers diagnostic accuracy: The results of ROC curve analyses using propensity scores from binary logistic regression analyses combining biomarkers are shown in Fig. 2A–C and summarized as follows: PD vs. non-PD: AUC = 0.961 (95%CI = 0.897–1.000), p <

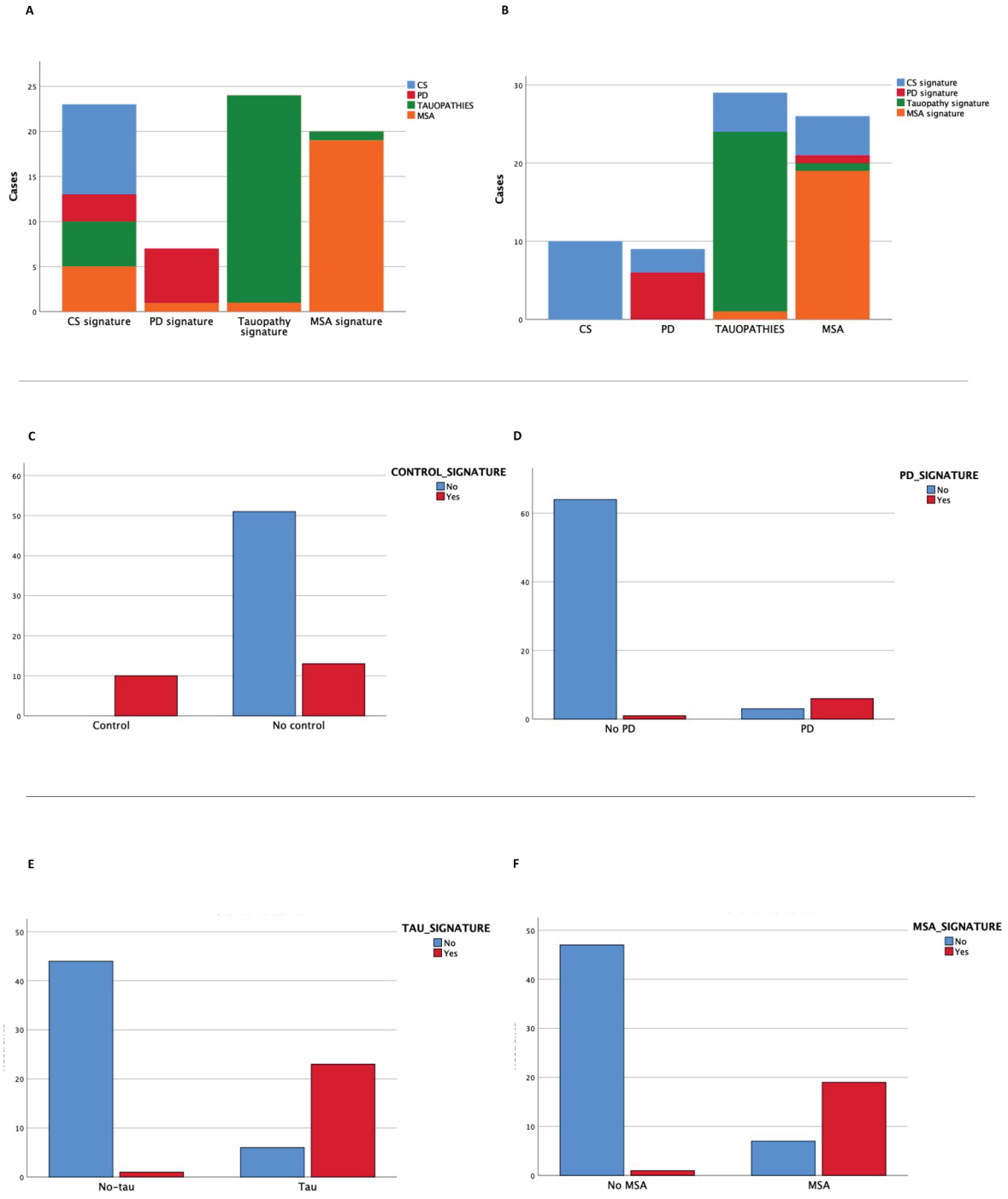

Fig. 3. Biomarkers-signatures association with clinical classification: A = predominance of cases with fitting clinical classification in each biomarkers-signature; B = predominance of cases with fitting biomarkers-signature in each clinical classification; C = predominance of lack of "control-signature" among non-control participants; D = predominance of lack of "PD-signature" among non-PD participants; E = predominance of "tau-signature" among tauopathies (PSP + CBD); F = predominance of "MSA-signature" in MSA.

0.0001, Se/Sp = 78.0/94.0; MSA vs. non-MSA: AUC = 0.936 (95%CI = 0.881–0.991), p < 0.0001, Se/Sp = 84.0/83.0; tauopathies vs. non-tauopathies: AUC = 0.933 (95%CI = 0.875–0.990), p < 0.0001, Se/Sp = 86.0/82.0.

Biomarkers-signatures: All CSs (10/10) had "CS signature". Among PD, 77.7% (7/9) had "PD signature" (the remaining 23.3% (2/9) "CS signature"). In clinically diagnosed tauopathies, 79.8% (23/29) had "tauopathy signature", 17.2% (5/29) "CS signature" and 1 subject "MSA signature". Patients with tauopathy and "CS signature" presented lower PSPRS (17 [15–17] vs. 35.5 [30–47], p = 0.0064) and UPDRS (22 [22–27] vs. 43 [28.5–50] p = 0.0302) scores compared to patients with tauopathy and "non-CS signature. Among MSA 73.1% (19/26) had "MSA signature", 19.2% (5/26) "CS signature", one "tauopathy signature" and another one "PD signature" (Fig. 3A–F).

3.1. Unexpected biomarkers findings: post-hoc diagnostic and Se/Sp revision

α-SYN RT-QuIC: Of the 5 PD cases with negative α-SYN RT-QuIC, one had presented with asymmetrical rigid-akinetic parkinsonism and modest response to levodopa along with vascular risk factors (which are not an exclusion criterion for PD) and mild microvascular damage in brain MRI, thus being classified as PD at the time of obtention of CSF. Thereafter, though, the patient added more vascular lesions on MRI and did not improve with further increase of levodopa, but subsequently stabilized, not progressively worsening in the setting of strict control of vascular risk factors. Of the 4 MSA cases with positive α-SYN RT-QuIC, one had normal CSF NFL values and normal MRI, as well as, eventually, response to high doses of levodopa with typical rest tremor, allowing for reclassifying him as PD. Exclusion of the former case and inclusion of the latter one would increase sensitivity from 75% to 80% (16/20). The other 3 MSA cases with positive α-SYN RT-QuIC had high CSF NFL levels and a clinical picture strongly suggestive and meeting the accepted MSA diagnostic criteria. This along with the fact that the remaining MSA cases with negative α-SYN RT-QuIC also fulfilled the accepted MSA diagnostic criteria, would leave post-hoc sensitivity of α-SYN RT-QuIC for MSA as low as 9% (3/32).

In terms of "false" + for α-SYN RT-QuIC among tauopathies, all 3 PSP participants with positive α-SYN RT-QuIC meet the MDS PSP diagnostic criteria (two with high CSF NFL levels; two with PSP-RS phenotype, one with the PSP-PGF variant). Conversely, the only CBD case with positive α-SYN RT-QuIC presented with asymmetrical parkinsonism with apraxia elements, but at follow-up has a mixed clinical picture including hyposmia, RBD and hallucinations besides parkinsonism which make of PD of the Lewy body dementia variant [16] the most likely diagnosis at last follow-up. This would increase the above recalculated post-hoc sensitivity of α-SYN RT-QuIC for PD from 80% to 81% (17/21), and specificity in PD vs. tauopathies to 91% (32/35).

CSF NFL: Two MSA cases had normal CSF NFL levels, one already has been commented above and has been clinically and paraclinically reclassified as PD; the other one has a diagnosis of MSA-cerebellar type with 11 years of history and mild dysautonomia and still relatively preserved on motor grounds, with negative studies for CAG trinucleotide repeat expansion SCAs. The two PSP cases with low instead of high CSF NFL levels had PSP-P and PSP-PGF phenotypes with long and benign evolution. Likewise, of the two CBD cases with low CSF NFL levels one has 7 years of history with typical corticobasal features, wheelchair-bound and with important left-side apraxia, still cognitively spared; the other one also has parkinsonism and corticobasal features contralateral to the most affected side on presynaptic dopaminergic imaging as the other case, but in this one the follow-up is even longer (9 years) and milder (still able to walk).

4. Discussion

We set up CSF α-SYN RT-QuIC at our site in a cohort of 112 participants ranging from controls to the spectrum of PD and APs (MSA, PSP and CBD). We also report for the first time that the combination of CSF RT-QuIC α-SYN, CSF NFL and midbrain/pons MRI measures in degenerative parkinsonisms yields high accuracy. "Biomarkers signatures" fitted in most cases with clinical classification at recruitment, while part of cases with either false positive or false negative results could be clinically reclassified or their unexpected biomarker findings could be explained by their phenotype and disease progression.

To date several studies have shown high sensitivity and specificity of CSF α-SYN RT-QuIC, particularly for PD, and more inconsistently for MSA. Our results are in keeping with this literature [3–6,26]. Our finding of low sensitivity of α-SYN seeding in MSA deserves further comment. Attempts to detect α-synuclein in MSA have been challenging with most/several studies using CSF RTQuIC reporting low sensitivities, ranging from <10% [5,7] to 35% [26], except in the study of Poggiolini et al. who detected a 75% sensitivity. By contrast, two studies using protein misfolding cyclic amplification (PMCA), a seeding assay similar to RTQuIC, have shown promising results. Shahnawaz and colleagues reported that patients with MSA presented significantly lower fluorescence signal compared to PD, but with 65 out of 75 CSF MSA samples containing α-SYN aggregates. In addition, they demonstrated distinct conformational strains between MSA and PD [27]. The second study [28] also found high sensitivity in two different cohorts (100% and 94% sensitivity). This discrepancy between sensitivity results could be explained by differences in the reaction buffers or recombinant α-SYN used in the different studies suggesting that inherent heterogeneity in α-synuclein seeding occurs in MSA [29].

In terms of combining biomarkers, the combination of CSF RT-QuIC α-SYN and CSF NFL has already been shown to result in improved discriminant ability, with positive CSF RT-QuIC α-SYN among PD and high CSF NFL in APs driving the results [6]. Likewise our MRI findings are in line with previous literature [8,9].

The "biomarkers signatures" we have defined fitted largely with the initial clinical classification. Adding also to the clinical significance of these biomarkers on an individual basis we have seen that in part of patients with unexpected biomarkers findings such results could be attributed to phenotypic peculiarities. Two PSP patients with normal (low) CSF NFL levels have PSP-parkinsonism and PSP-freezing variants, associated with lesser aggressiveness and longer survival [30], which fit with normal (low) CSF NFL levels. Likewise, cases with MSA and CBD with low CSF NFL levels also had longstanding and rather benign disease course. Alternatively, unexpected results in RT-QuIC can be a clue for clinicians to reconsider the diagnosis: one patient initially labelled as PD was reclassified as vascular parkinsonism; another with MSA and positive CSF α-SYN RT-QuIC but normal CSF NFL and MRI was relabelled as PD. Another case with asymmetric apraxia eventually disclosed RBD and presented visual hallucinations and cognitive fluctuations fitting with PD of the dementia with Lewy bodies variant [13]. This post-hoc revision of clinical diagnoses based on biomarkers findings is to be taken with caution, as alternative explanations for false negative or positive results might be failure of the technique itself in some cases, or the presence of co-pathology in false positive cases, as in the case of positive CSF α-SYN RT-QuIC in PSP (13%), which is similar to previously reported postmortem Lewy co-pathology in PSP of 8% [31].

This study is not without limitations. The diagnosis is clinical, not neuropathologically confirmed, limiting the interpretability of the current findings. However, the participants included fulfilled the category of "probable" for their respective diagnosis criteria which provides high diagnostic accuracy and, patients have been systematically examined by neurologists with expertise in parkinsonism. The study findings do not allow for differentiating MSA vs. tauopathies or between tauopathies (PSP vs. CBD) solely relying on CSF α-SYN RT-QuIC or CSF NFl levels. However, and this was one of the goals of the paper, when combining CSF and MRI biomarkers both statistically and under the "profiles" approach there is a hint that these combinations can be helpful, while waiting for more specific CSF α-SYN RT-QuIC and for validated CSF RT-

QuIC for 4r-tau and/or reliable α-synuclein and tau PET tracers. As additional limitations we have not a validation cohort, nor early disease or unclassifiable cases. The sample size is relatively small, particularly in the case of the subgroup with MRI measures available, yet in the range of previous studies [3–6,8,9], and above our sample size calculation. All this along with the fact that we have replicated prior published results gives robustness to our data. However, further studies with larger samples are needed. Our post-hoc recalculation of sensitivities and specificities can be criticized too, but we have done this under the "real clinical practice perspective", in a similar way to when a dopamine imaging scan comes back negative leading to reconsider clinical diagnosis. While obviously this comparison is perhaps premature now, we believe that the section of clinically revisited diagnosis and sensitivities/specificities is of clinical interest. Finally, as mentioned above, we have not assessed RT-QuIC for 4R-tau, expected to mirror in tauopathies the accuracy of RT-QuIC for α-SYN in synucleinopathies, but still needing further validation [32]. Future studies combining CSF α-SYN RT-QUIC with 4R-tau RT-QuIC or PET imaging of 4R-tau [33] might improve diagnosis of tauopathies and even track the effect of potential disease modifying strategies.

In conclusion, the combination of CSF NFL, CSF α-SYN RT-QuIC and midbrain/pons MRI areas yielded high diagnostic accuracy in degenerative parkinsonisms and in most cases the "biomarkers signatures" fitted with the clinical classification. Unexpected results related to phenotypic peculiarities (low CSF NFL in benign phenotypes) or assisted diagnostic reclassification (false + and - CSF α-SYN RT-QuIC). Longitudinal studies of larger cohorts with improved molecular and imaging biomarkers are warranted.

Funding

This work has been funded through Fondo de Investigacion en Salud (Instituto Carlos III) (PI17/00096) in the frame of the European Regional Development Fund (ERDF) and to Fundació la Marató de TV3 (PI043296 and 202009-10). This work has been performed thanks to the 3T Equipment of Magnetic Resonance at IDIBAPS (project IBPS15-EE-3688 co-funded by MCIU and by ERDF). During the study conduction CP was funded through the grant Rio Hortega from Instituto de Salud Carlos III (CM18/00072), and AC through the grant from the PERIS program (SLT008/18/00191). MF is funded through the Maria de Maeztu excellence centre Institut de Neurociències of the University de Barcelona.

Declaration of competing interest

The authors declare that they have no conflict of interest relevant to the current study.

Acknowledgements

We thank all the participants for their generosity as without them none of this research would have been possible. We are grateful to the biomedic diagnostic center (CBD) of our institution for access to, and assistance with, FLUOSTAR Omega equipment and RT-QuIC experiments (Drs. Raquel Ruiz and Laura Naranco). Our institution receives support from the CERCA programme from Generalitat de Catalunya (Catalan government). Our unit and accordingly several authors of this manuscript are members of the European Reference Network for Rare Neurological Diseases - Project ID No 739510, as well as CIBERNED (CB06/05/0018-ISCIII).

YC wants to dedicate this work to, and express his solidarity with, his motherland Ukraine: only construction, never destruction, is the way for humanity to reach progress and prosperity. Слава Україні!

Appendix A. Supplementary data

Supplementary data to this article can be found online at https://doi.org/10.1016/j.parkreldis.2022.05.006.

References

[1] M. Goedert, Filamentous nerve cell inclusions in neurodegenerative diseases: tauopathies and a-synucleonopathies, Phil. Trans. Roy. Soc. Lond. B354 (1999) 1101–1118, https://doi.org/10.1098/rstb.1999.0466.

[2] A.J. Hughes, S.E. Daniel, Y. Ben-Shlomo, A.J. Lees, The accuracy of diagnosis of parkinsonian syndromes in a specialist movement disorder service, Brain 125 (2002) 861–870, https://doi.org/10.1093/brain/awf080.

[3] T.M. Marques, A. van Rumund, P. Oeckl, H.B. Kuiperij, R.A. J Esselink, B.R. Bloem, M. Otto, M.M. Verbeek, Serum NFL discriminates Parkinson disease from atypical parkinsonisms, Neurol. 92 (13) (2019) e1479–e1486, https://doi.org/10.1212/WNL.0000000000007179.

[4] G. Fairfoul, L.I. McGuire, S. Pal, J.W. Ironside, J. Neumann, S. Christie, C. Joachim, M. Esiri, S.G. Evetts, M. Rolinski, F. Baig, C. Ruffmann, R. Wade-Martins, M.T. Hu, L. Parkkinen, A.J. Green, Alpha-synuclein RT-QuIC in the CSF of patients with alpha-synucleinopathies, Ann Clin Transl Neurol 3 (10) (2016) 812–818, https://doi.org/10.1002/acn3.338.

[5] M. Rossi, N. Candelise, S. Baiardi, S. Capellari, G. Giannini, C.D. Orrù, E. Antelmi, A. Mammana, A.G. Hughson, G. Calandra-Buonaura, A. Ladogana, G. Plazzi, P. Cortelli, B. Caughey, P. Parchi, Ultrasensitive RT-QuIC assay with high sensitivity and specificity for Lewy body-associated synucleinopathies, Acta Neuropathol. 140 (1) (2020) 49–62, https://doi.org/10.1007/s00401-020-02160-8.

[6] I. Poggiolini, V. Gupta, M. Lawton, S. Lee, A. El-Turabi, A. Querejeta-Coma, C. Trenkwalder, F. Sixel-Döring, A. Foubert-Samier, A.P. Le Traon, G. Plazzi, F. Biscarini, J. Montplaisir, J.F. Gagnon, R.B. Postuma, E. Antelmi, W.G. Meissner, B. Mollenhauer, Y. Ben-Shlomo, M.T. Hu, L. Parkkinen, Diagnostic value of cerebrospinal fluid alpha-synuclein seed quantification in synucleinopathies, Brain (2021), https://doi.org/10.1093/brain/awab431 awab431.

[8] M. Cosottini, R. Ceravolo, L. Faggioni, G. Lazzarotti, M.C. Michelassi, U. Bonuccelli, L. Murri, C. Bartolozzi, Assessment of midbrain atrophy in patients with progressive supranuclear palsy with routine magnetic resonance imaging, Acta Neurol. Scand. 116 (1) (2007) 37–42, https://doi.org/10.1111/j.1600-0404.2006.00767.x.

[7] C. Quadalti, G. Calandra-Buonaura, S. Baiardi, A. Mastrangelo, M. Rossi, C. Zenesini, G. Giannini, N. Candelise, L. Sambati, B. Polischi, G. Plazzi, S. Capellari, P. Cortelli, P. Parchi, Neurofilament light chain and α-synuclein RT-QuIC as differential diagnostic biomarkers in parkinsonisms and related syndromes, NPJ Parkinsons Dis 7 (1) (2021) 93, https://doi.org/10.1038/s41531-021-00232-4.

[9] A. Quattrone, G. Nicoletti, D. Messina, F. Fera, F. Condino, P. Pugliese, P. Lanza, P. Barone, L. Morgante, M. Zappia, U. Aguglia, O. Gallo, MR imaging index for differentiation of progressive supranuclear palsy from Parkinson disease and the Parkinson variant of multiple system atrophy, Radiology 246 (1) (2008) 214–221, https://doi.org/10.1148/radiol.2453061703.

[10] G.U. Höglinger, G. Respondek, M. Stamelou, C. Kurz, K.A. Josephs, A.E. Lang, B. Mollenhauer, U. Müller, C. Nilsson, J.L. Whitwell, T. Arzberger, E. Englund, E. Gelpi, A. Giese, D.J. Irwin, W.G. Meissner, A. Pantelyat, A. Rajput, J.C. van Swieten, C. Troakes, A. Antonini, K.P. Bhatia, Y. Bordelon, Y. Compta, J.C. Corvol, C. Colosimo, D.W. Dickson, R. Dodel, L. Ferguson, M. Grossman, J. Kassubek, F. Krismer, J. Levin, S. Lorenzl, H.R. Morris, P. Nestor, W.H. Oertel, W. Poewe, G. Rabinovici, J.B. Rowe, G.D. Schellenberg, K. Seppi, T. van Eimeren, G. K. Wenning, A.L. Boxer, L.I. Golbe, I. Litvan, Movement Disorder Society-endorsed PSP Study Group, Clinical diagnosis of progressive supranuclear palsy: the movement disorder society criteria, Mov. Disord. 32 (6) (2017) 853–864, https://doi.org/10.1002/mds.26987.

[11] M.J. Armstrong, I. Litvan, A.E. Lang, T.H. Bak, K.P. Bhatia, B. Borroni, A.L. Boxer, D.W. Dickson, M. Grossman, M. Hallett, K.A. Josephs, A. Kertesz, S.E. Lee, B. L. Miller, S.G. Reich, D.E. Riley, E. Tolosa, A.I. Tröster, M. Vidailhet, W.J. Weiner, Criteria for the diagnosis of corticobasal degeneration, Neurol. 80 (2013) 496–503, https://doi.org/10.1212/WNL.0b013e31827f0fd1.

[12] S. Gilman, G.K. Wenning, P.A. Low, D.J. Brooks, C.J. Mathias, J.Q. Trojanowski, N. W. Wood, C. Colosimo, A. Dürr, C.J. Fowler, H. Kaufmann, T. Klockgether, A. Lees, W. Poewe, N. Quinn, T. Revesz, D. Robertson, P. Sandroni, K. Seppi, M. Vidailhet, Second consensus statement on the diagnosis of multiple system atrophy, Neurol. 71 (9) (2008) 670–676, https://doi.org/10.1212/01.wnl.0000324625.00404.15.

[13] R.B. Postuma, D. Berg, M. Stern, W. Poewe, C.W. Olanow, W. Oertel, J. Obeso, K. Marek, I. Litvan, A.E. Lang, G. Halliday, G.C. Goetz, T. Gasser, B. Dubois, P. Chan, B.R. Bloem, C.H. Adler, G. Deuschl, MDS clinical diagnostic criteria for Parkinson's disease, Mov. Disord. 30 (12) (2015) 1591–1601, https://doi.org/10.1002/mds.26424.

[14] V.C. Constantinides, G.P. Paraskevas, F. Boufidou, M. Bourbouli, L. Stefanis, E. Kapaki, Cerebrospinal fluid biomarker profiling in corticobasal degeneration: application of the AT(N) and other classification systems, Park. Relat. Disord. 82 (2021) 44–49, https://doi.org/10.1016/j.parkreldis.2020.11.016.

[15] S. Fahn, R.L. Elton, Members of the UPDRS development committee, unified Parkinson's disease rating scale, in: S. Fahn, C.D. Marsden, D.B. Calne, A. Lieberman (Eds.), Recent Developments in Parkinson's Disease, McMillan Health Care Information, Florham Park, NJ, 1987, pp. 153–163.

[16] M.M. Hoehn, M.D. Yahr, Parkinsonism: onset, progression and mortality, Neurol. 17 (1967) 427e42, https://doi.org/10.1212/wnl.17.5.427.
[17] Z.S. Nasreddine, N.A. Phillips, V. Bédirian, S. Charbonneau, V. Whitehead, I. Collin, J.L. Cummings, H. Chertkow, The montreal cognitive assessment, MoCA: a brief screening tool for mild cognitive impairment, J. Am. Geriatr. Soc. 53 (4) (2005) 695–699, https://doi.org/10.1111/j.1532-5415.2005.53221.x. Erratum in: J Am Geriatr Soc. 67(9) (2019) 1991.
[18] M.F. Folstein, S.E. Folstein, P.R. McHugh, Mini-mental state". A practical method for grading the cognitive state of patients for the clinician, J. Psychiatr. Res. 12 (3) (1975) 189–198, https://doi.org/10.1016/0022-3956(75)90026-6.
[19] L.I. Golbe, P.A. Ohman-Strickland, A clinical rating scale for progressive supranuclear palsy, Brain 130 (Pt 6) (2007) 1552–1565, https://doi.org/10.1093/brain/awm032.
[20] G.K. Wenning, F. Tison, K. Seppi, C. Sampaio, A. Diem, F. Yekhlef, I. Ghorayeb, F. Ory, M. Galitzky, T. Scaravilli, M. Bozi, C. Colosimo, S. Gilman, C.W. Shults, N. P. Quinn, O. Rascol, W. Poewe, Multiple system Atrophy study group, development and validation of the unified multiple system Atrophy rating scale (UMSARS), Mov. Disord. 19 (12) (2004) 1391–1402, https://doi.org/10.1002/mds.20255.
[21] Y. Compta, T. Valente, J. Saura, B. Segura, A. Iranzo, M. Serradell, C. Junqué, E. Tolosa, F. Valldeoriola, E. Muñoz, J. Santamaria, A. Cámara, M. Fernández, J. Fortea, M. Buongiorno, J.L. Molinuevo, N. Bargalló, M.J. Martí, Correlates of cerebrospinal fluid levels of oligomeric- and total- alfa-synuclein in premotor, motor and dementia stages of Parkinson's disease, J. Neurol. 262 (2) (2015) 294–306, https://doi.org/10.1007/s00415-014-7560-z.
[22] J.E. Iglesias, K. Van Leemput, P. Bhatt, C. Casillas C, S. Dutt S, N. Schuff, D. Truran-Sacrey, A. Boxer, B. Fischl, Alzheimer's disease neuroimaging initiative, bayesian segmentation of brainstem structures in MRI, Neuroimage 113 (2015) 184–195, https://doi.org/10.1016/j.neuroimage.2015.02.065.
[23] V.C. Constantinides, G.P. Paraskevas, G. Velonakis, P. Toulas, E. Stamboulis, E. Kapaki, MRI planimetry and magnetic resonance parkinsonism index in the differential diagnosis of patients with parkinsonism, AJNR Am J Neuroradiol 39 (6) (2018) 1047–1051, https://doi.org/10.3174/ajnr.A5618.
[24] V.D. Cicchetti, Guidelines, criteria, and rules of thumb for evaluating normed and standardized assessment instruments in psychology, Psychol. Assess. 6 (4) (1994) 284–290, https://doi.org/10.1037/1040-3590.6.4.284.
[25] Y. Benjamini, Y. Hochberg, Controlling the false discovery rate: a practical and powerful approach to multiple testing, J. Roy. Stat. Soc. 57 (1995) 289–300, https://doi.org/10.1111/j.2517-6161.1995.tb02031.x.
[26] A. van Rumund, A.J.E. Green, G. Fairfoul, R.A.J. Esselink, B.R. Bloem, M. M. Verbeek, α-Synuclein real-time quaking-induced conversion in the cerebrospinal fluid of uncertain cases of parkinsonism, Ann. Neurol. 85 (5) (2019) 777–781, https://doi.org/10.1002/ana.25447.
[27] M. Shahnawaz, A. Mukherjee, S. Pritzkow, N. Mendez, P. Rabadia, X. Liu, B. Hu, A. Schmeichel, W. Singer, G. Wu, A.L. Tsai, H. Shirani, K.P.R. Nilsson, P.A. Low, C. Soto, Discriminating α-synuclein strains in Parkinson's disease and multiple system atrophy, Nature 578 (2020) 273–277, https://doi.org/10.1038/s41586-020-1984-7.
[28] W. Singer, A.M. Schmeichel, M. Shahnawaz, J.D. Schmelzer, B.F. Boeve, D. M. Sletten, T.L. Gehrking, J.A. Gehrking, A.D. Olson, R. Savica, M.D. Suarez, C. Soto, P.A. Low, Alpha-synuclein oligomers and neurofilament light chain in spinal fluid differentiate multiple system Atrophy from Lewy body synucleinopathies, Ann. Neurol. 88 (2020) 503–512, https://doi.org/10.1002/ana.25824.
[29] I. Martinez-Valbuena, N.P. Visanji, A. Kim, H.H.C. Lau, R.W.L. So, S. Alshimemeri, A. Gao, M.A. Seidman, M.R. Luquin, J.C. Watts, A.E. Lang, G.G. Kovacs, Alpha-synuclein seeding shows a wide heterogeneity in multiple system atrophy, Transl. Neurodegener. 11 (2022) 7, https://doi.org/10.1186/s40035-022-00283-4.
[30] M. Guasp, L. Molina-Porcel, C. Painous, N. Caballol, A. Camara, A. Perez-Soriano, A. Sánchez-Gómez, A. Garrido, E. Muñoz, M.J. Marti, F. Valldeoriola, O. Grau, E. Gelpí, G. Respondek, G.H. Höglinger, Y. Compta, Association of PSP phenotypes with survival: a brain-bank study, Park. Relat. Disord. 84 (2021) 77–81, https://doi.org/10.1016/j.parkreldis.2021.01.015.
[31] M. Jecmenica Lukic, C. Kurz, G. Respondek, O. Grau-Rivera, Y. Compta, E. Gelpi, C. Troakes, J.C. van Swieten, A. Giese, S. Roeber, T. Arzberger, G. Höglinger, Barcelona brain bank collaborative group, the MDS-endorsed PSP study group copathology in progressive supranuclear palsy: does it matter? Mov. Disord. 35 (6) (2020) 984–993, https://doi.org/10.1002/mds.28011.
[32] E. Saijo, M.A. Metrick, S. Koga, P. Parchi, I. Litvan, S. Spina, A. Boxer, J.C. Rojas, D. Galasko, A. Kraus, M. Rossi, K. Newell, G. Zanusso, L.T. Grinberg, W.W. Seeley, B. Ghetti, D.W. Dickson, B. Caughey, 4-Repeat tau seeds and templating subtypes as brain and CSF biomarkers of frontotemporal lobar degeneration, Acta Neuropathol. 139 (1) (2020) 63–77, https://doi.org/10.1007/s00401-019-02080-2. Erratum in: Acta Neuropathol (2019).
[33] M. Song, L. Beyer, L. Kaiser, H. Barthel, T. van Eimeren, K. Marek, A. Nitschmann, M. Scheifele, C. Palleis, G. Respondek, M. Kern, G. Biechele, J. Hammes, G. Bischof, M. Barbe, Ö. Onur, F. Jessen, D. Saur, M.L. Schroeter, J.J. Rumpf, M. Rullmann, A. Schildan, M. Patt, B. Neumaier, O. Barret, J. Madonia, D.S. Russell, A. W. Stephens, A. Mueller, S. Roeber, J. Herms, K. Bötzel, A. Danek, J. Levin, J. Classen, G.U. Höglinger, P. Bartenstein, V. Villemagne, A. Drzezga, J. Seibyl, O. Sabri, G. Boening, S. Ziegler, M. Brendel, Binding characteristics of [^{18}F]PI-2620 distinguish the clinically predicted tau isoform in different tauopathies by PET, 271678X211018904, J. Cerebr. Blood Flow Metabol. 41 (11) (2021), https://doi.org/10.1177/0271678X211018904. Epub ahead of print.

A

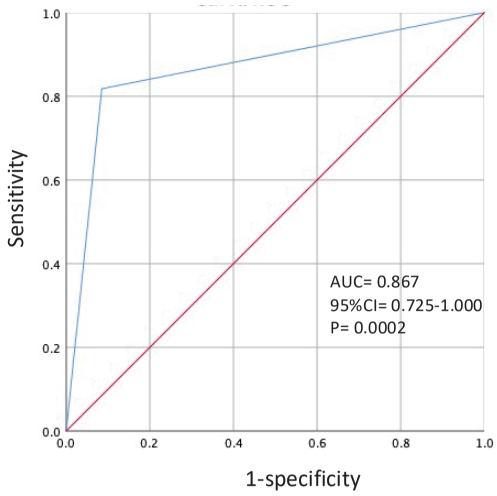

ROC curve of + CSF α-SYN RT-QuIC in PD vs. non-PD in women

B

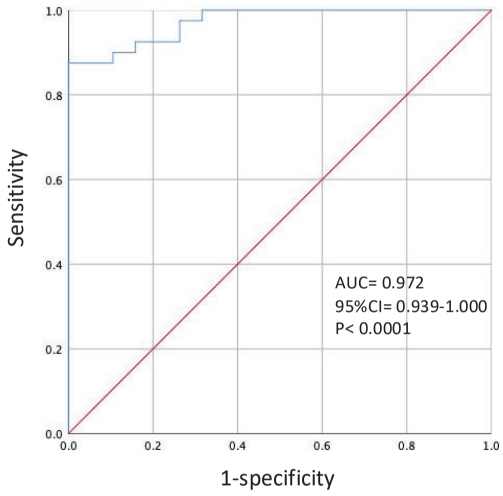

ROC curve of increasing CSF NFL in APs (MSA+PSP+CBD) vs. CSs+PD in women

C

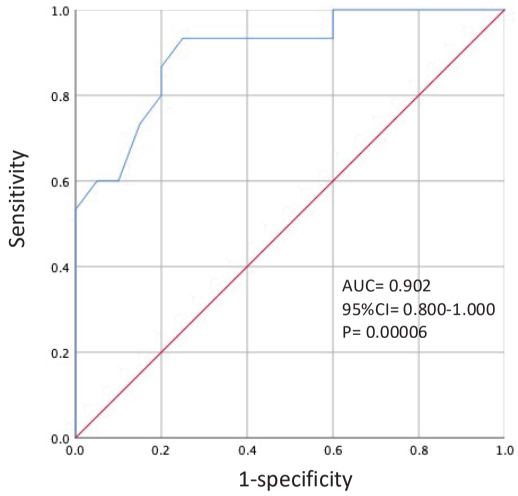

ROC curve of decreasing midbrain area in tauopathies (PSP+CBD) vs. non-tauopathies (CSs+PD+MSA) in women

D

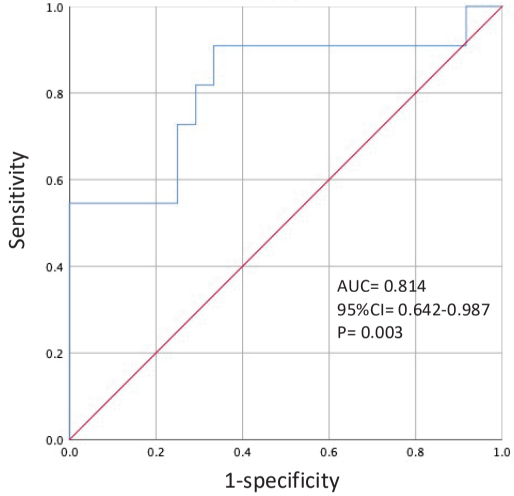

ROC curve of decreasing pons atrophy in tauopathies (PSP+CBD) vs. non-tauopathies (CSs+PD+MSA) in women

E

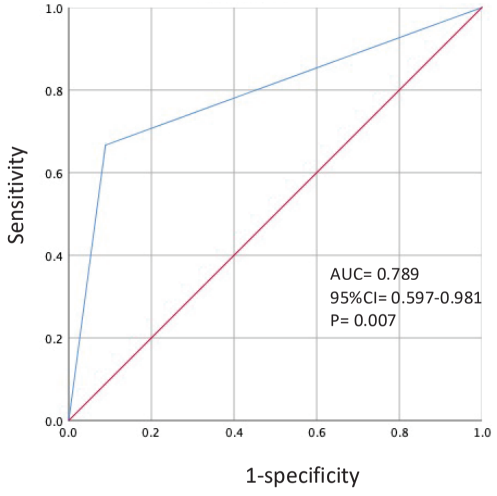

ROC curve of + CSF α-SYN RT-QuIC in PD vs. non-PD in men

F

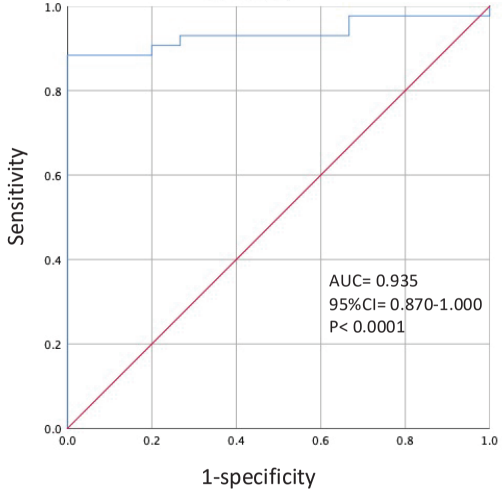

ROC curve of increasing CSF NFL in APs (MSA+PSP+CBD) vs. CSs+PD in men

G

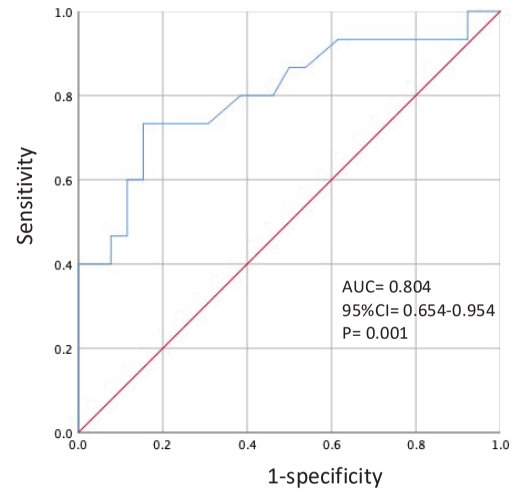

ROC curve of decreasing midbrain area in tauopathies (PSP+CBD) vs. non-tauopathies (CSs+PD+MSA) in men

H

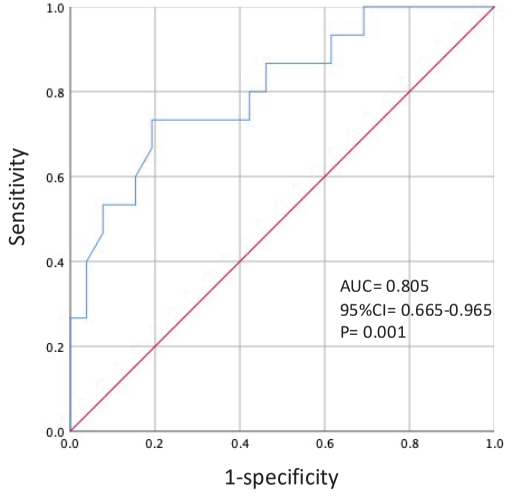

ROC curve of decreasing pons atrophy in tauopathies (PSP+CBD) vs. non-tauopathies (CSs+PD+MSA) in men

Suppl. Figure 2.- Binary logistic regression with PD vs. no-PD as dependent variable and with CSF αSYN RT-QuIC and disease duration as independent variables or predictors along with ROC curve with the propensity scores from the binary logistic regression model.

	OR	*95%CI*	*p*
CSF αSYN RT-QuIC	23.259	5.71-94.62	<0.0001
Disease duration (years)	1.271	1.04-1.55	0.017

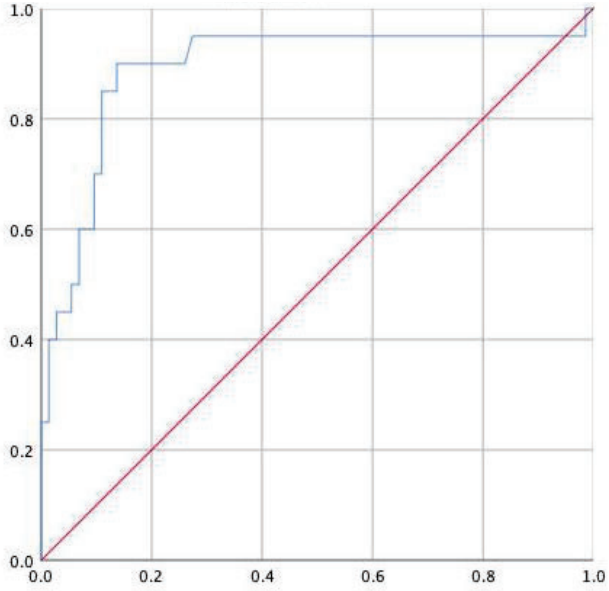

AUC	*95%CI*	*p*
0.89	0.79-0.99	<0.0001

RESULTS SUMMARY

4. RESULTS SUMMARY

In [article 1], using genome-wide miRNA analysis and RT-qPCR validation, we profiled serum miRNA expression levels from DaT-negative iRBD, DaT-positive iRBD, iRBD pheno-converted into PD/DLB, and controls. Longitudinally, we followed up the iRBD cohort at three-time points over 26 months. Overall, we found sustained cross-sectional and longitudinal deregulation of 12 miRNAs across the RBD continuum, including DaT-negative iRBD, DaT-positive iRBD, and PD/DLB pheno-converted iRBD. In addition, we uncovered a 12-miRNA biosignature that alone, without any clinical or imaging input, can discriminate iRBD and PD/DLB from controls (AUC = 0.98; 95% CI = 0.89-0.99). Thus, we identified a specific serum miRNA biosignature capable of discerning iRBD and PD/DLB from controls, and that holds potential as an early disease progression biomarker.

In [article 2], we performed an 8-year longitudinal miRNA assessment of serum samples from *LRRK2* G2019S asymptomatic carriers stratified by DaT-SPECT into DaT-negative and DaT-positive, G2019S *LRRK2*-associated PD, iPD, and controls. We observed dynamic miRNA expression profiles across the progression stages and identified 8 deregulated miRNAs in DaT-negative *LRRK2* asymptomatic carriers, 6 in DaT-positive, and one in *LRRK2*-associated PD. Between groups, the highest differences occurred between DaT-positive *LRRK2* asymptomatic carriers and *LRRK2*-associated PD. By longitudinal follow-up of asymptomatic G2019S carriers, we detected 11 miRNAs with sustained variation compared to baselines. Our study identifies novel miRNA alterations in premotor stages of PD co-occurring with progressive DaT-SPECT decline before motor manifestation, whose deregulation seems to attenuate after the diagnosis of L2PD. Moreover, we found 4 miRNAs with relatively high discriminative ability (AUC=0.82) between non-pheno-converted DaT-positive G2019S asymptomatic carriers and pheno-converted *LRRK2*-associated PD patients (miR-4505, miR-8069, miR-6125, and miR-451a), which hold potential as early progression biomarkers for PD.

In [article 3], we set up the CSF α-synuclein RT-QuIC technique at our laboratory in a cohort including patients with the α-synucleinopathies PD and MSA, the tauopathies PSP and CBD, and neurologically unimpaired controls. Under the criteria of having at least two of the three replicates amplifying above the threshold, we found 15 of the 20 (75%) PD patients positive for RT-QuIC. On the contrary, in MSA, only 4 of the 37 (12%) patients were positive. Moreover, any of the 19 controls and only 4 of the 36 tauopathies exhibited positivity, thus showing an overall specificity of 93%. Other results in the article, particularly the ones concerning the combination of biomarkers, are not included in the present thesis as they are part of the thesis in preparation by the candidate Cèlia Painous.

In addition, during my doctoral thesis, I have also actively contributed to other original research articles in the laboratory as a co-author, as summarised in **Annex 1**.

DISCUSSION

5. DISCUSSION

During my doctoral thesis, I investigated candidate diagnostic and progression biomarkers of PD with a particular focus on the premotor stages of the disease. I explored serum miRNA expression levels as early progression biomarkers in two longitudinal cohorts of premotor PD and PD at-risk subjects, i.e., iRBD and *LRRK2* G2019S asymptomatic carriers, to assess the potential applicability of these biomarkers. In addition, I also set up an α-synuclein RT-QuIC assay as a means to investigate the presence of misfolded α-synuclein aggregates in PD and related α-synucleinopathies.

In [article 1], we performed the first serum miRNA study in a well-established prodromal stage of PD encompassing iRBD patients characterised by DaT-SPECT imaging and with longitudinal follow-up. In line with two previous miRNA studies in iRBD,[176,177] we found deregulation of specific miRNAs in iRBD and PD/DLB pheno-converted patients, confirming that early molecular changes associated with α-synucleinopathies can antedate the clinical manifestation of the disease. More specifically, we defined a 12-miRNA biosignature able to distinguish iRBD and PD/DLB from controls with a high discriminative capacity that accurately classified patients with 98% sensitivity and 86% specificity. This serum miRNA biosignature distinguished premotor and manifest PD/DLB from controls more accurately than other proposed candidate biomarkers but needs independent validation.[117,178–181] Similarly, earlier studies in iRBD observed misfolded α-synuclein in the CSF[182] or phosphorylated α-synuclein aggregates in the minor labial salivary glands[183] before the pheno-conversion. Further studies in longitudinal and larger independent cohorts are needed to validate this signature and explore its ability to discriminate between specific α-synucleinopathies.

Several miRNA studies in blood derivatives have pinpointed specific miRNAs as potential biomarkers in PD cohorts,[172,175,184–187] yet miRNA studies in premotor stages of PD are still scarce.[176,177] In this context, iRBD is a well-established early non-motor PD symptom which presents the highest risk of α-synucleinopathy.[112] Given that hyposmia and constipation are also well-characterised premotor symptoms of PD, evaluating the performance of our miRNA signature in these conditions would allow to expand our findings and assess potential pheno-conversion in other prodromal stages of PD. To achieve this aim, and given the lower specificity of these prodromal signs, performing prospective studies with long-term follow-ups with serial measurements in well-powered cohorts characterised by DaT-SPECT imaging is crucial. Indeed, expanding these studies to other miRNA signatures and candidate biomarkers evaluated simultaneously may lead to the identification of the most accurate disease predictors. Overall, identifying accurate biomarkers in the different PD prodromal stages is needed to anticipate the diagnosis, which could assist in managing patients and developing neuroprotective therapies.

Ours is the first longitudinal serum miRNA study in iRBD characterised by DaT-SPECT status as an indicator of ongoing nigrostriatal DAn loss. Compared to controls, we found longitudinal miRNA expression changes in DaT-negative and DaT-positive iRBD with consistent deregulation in α-synucleinopathy pheno-converted patients. In addition, fold-change expression variation was increased in longitudinal time points compared to baseline and was stronger in DaT-positive than DaT-negative iRBD. Yet, our follow-up period was limited to 26 months. Longer follow-ups, including the pheno-conversion, could enhance our understanding of the miRNA changes through the PD prodromal stage. Indeed, a recent study revealed that the number of circulating miRNAs deregulated in PD is age-dependent.[177] Thus, the additional follow-up of healthy controls and pheno-converted patients would also be helpful in further validation studies of our findings.

In [article 2], we profiled serum miRNAs in PD at-risk asymptomatic *LRRK2* G2019S carriers stratified by DaT-SPECT. We found a more pronounced miRNA deregulation in iPD than in LRRK2-associated PD and specific miRNA profiles for each PD type, as previously reported in monogenic PD with mutations in *LRRK2, SNCA,* or *GBA*.[177,188] Moreover, asymptomatic G2019S carriers exhibited overall more miRNA changes than symptomatic carriers. These results align with studies describing early molecular changes in individuals at-risk of PD that attenuate after motor manifestation. Thus, two transcriptomic studies showed higher deregulation in *LRRK2* asymptomatic carriers (64%)[189] and prodromal PD (32%)[190] than in symptomatic carriers and manifest iPD. One possible explanation is that early molecular changes, such as miRNA deregulation, could reflect potential compensatory mechanisms in PD at-risk subjects.[191,192] In addition, as the LRRK2 protein directly interacts with Argonaute-2, a central component of the miRNA machinery, another possibility is that the G2019S effect on miRNA levels was mediated by the alteration of the miRNA regulation resulting from the pathogenic LRRK2 function.[193,194] Overall, specific miRNA changes in G2019S asymptomatic carriers, specifically those with a dopaminergic deficit, hold the potential as candidate biomarkers of early PD progression before motor manifestation.

To our knowledge, ours is the most comprehensive miRNA study following asymptomatic *LRRK2* mutation carriers. During our 8-year study, 4 out of 20 (20%) DaT-positive G2019S asymptomatic carriers pheno-converted into PD, in line with the penetrance estimates of 26-42% described at ages above 80.[98,99] We exploratorily compared the 16 non-pheno-converted DaT-positive G2019S carriers with all the pheno-converted subjects of the study and found 4 significant miRNAs. These miRNAs showed a relatively high discriminative ability, thus holding potential as pheno-conversion biomarkers in *LRRK2* G2019S carriers. Given that predicting PD development in *LRRK2* asymptomatic carriers is not yet possible, our results, if validated, could have implications for disease prediction, early PD detection in subjects at-risk, and patient stratification for clinical trials.

The discovery of *LRRK2* mutations increasing LRRK2 kinase activity has led to the development of LRRK2 kinase inhibitors as potential disease-modifying therapies for LRRK2-associated PD and potentially iPD,[101] as *LRRK2* variants can increase susceptibility to iPD.[195–197] *LRRK2* mutation carriers represent an ideal target for the initial efficacy trials, particularly the subjects at the prodromal stage. Thus, our findings, if validated, would assist in the identification and clinical follow-up of individuals who will develop PD before their pheno-conversion. Furthermore, it could be a significant step in the field since the early experimental drug administration in asymptomatic carriers who will not develop PD could be avoided, thus avoiding the potential side effects in the lungs and kidneys.[198] Overall, identifying biomarkers able to predict pheno-conversion of *LRRK2* mutation carriers is urgently needed for neuroprotective trials.

Collectively, both [article 1] and [article 2] explore the use of serum miRNAs as disease biomarkers. However, the reproducibility of specific miRNAs in the literature has been limited. This could result from the variety of biospecimens, the different populations, and the techniques used, but also from the need for more standardisation in miRNA normalisation methods.[199] Endogenous miRNA controls are usually selected for each study among the most stable miRNAs among all individuals, yet it hinders inter-laboratory validation. Moreover, finding a universal reference miRNA is difficult as miRNA expression varies among tissues and development stages, the origin of circulating miRNAs needs to be clarified, and the diverse preparation methods may interfere in different ways. Nevertheless, approaches for more accurate case-specific normalisation procedures have been proposed to improve reproducibility.[200,201] In our case, we used the same endogenous controls in both miRNA studies to have consistent results, with the advantage of including an exogenous control for additional technical normalisation in [article 1]. Overall, the accurate selection of the normalisation method is a critical step in miRNA studies, especially when considering its potential application as progression biomarkers.

In addition, *LRRK2* G2019S carriers and iRBD subjects are both at an increased risk of PD,[126,202–205] yet the absence of *LRRK2* mutations in iRBD patients[135,206] suggests that iRBD and *LRRK2* pathogenic mutations represent two independent processes which can ultimately converge into a similar PD phenotype.[207] In line with this idea, comparing data from [article 1] and [article 2], we found overall different miRNA expression in *LRRK2* G2019S carriers and iRBD subjects, as well as between *LRRK2* G2019S carriers and iPD patients. Looking at the candidate miRNAs from the genome-wide discovery analyses (**Annex 2**), we detected that 20 of the 45 (44%) miRNAs identified in iPD were also commonly deregulated in iRBD (including both DaT-positive and DaT-negative). In contrast, only 4 of the 45 (9%) miRNAs were also present in asymptomatic *LRRK2* G2019S carriers. Overall, our findings align with the hypothesis that both iRBD and asymptomatic *LRRK2* G2019S carrier conditions represent two independent forms of PD onset. Recognising the different prodromal PD subtypes and understanding their underlying disease mechanisms would be relevant for identifying and validating efficient biomarkers for each PD subtype and even designing specific mechanism-based treatments. In addition, early identification of the PD subtype could be the first step for implementing personalised medicine strategies in PD, similar to those currently used in other human diseases, such as specific neoplasias.[208–210]

In [article 3], we set up the α-synuclein RT-QuIC to detect the presence of aggregated misfolded α-synuclein in CSF of patients with α-synucleinopathies. We found positive seeding activity in most PD cases (75%) and some MSA cases (12%). In addition, we also tested healthy controls and patients with tauopathies and found specificities of 100% and 89%, respectively (overall 93%). These results align with previous α-synuclein SAA studies showing high sensitivity and specificity in α-synucleinopathies.[39,119,211–213] Yet, 4 of the 36 tauopathies showed unexpected positivity, which could be possibly explained by the presence of co-pathology. Thus, RT-QuIC seems to detect the presence of Lewy body pathology,

which has been shown as co-pathology in non-α-synucleinopathies neurodegenerative disorders such as PSP[214] or AD.[215] After our study, longitudinal studies, including follow-up and autopsy of patients with parkinsonism, are warranted to determine and improve the accuracy of the CSF α-synuclein RT-QuIC. Overall, we found that the CSF α-synuclein RT-QuIC analysis is an informative biomarker that can improve the diagnosis of PD and related parkinsonisms, i.e., MSA, PSP, CBD. Remarkably, driven by our study, CSF α-synuclein RT-QuIC has been introduced in the clinical practice at Hospital Clinic Universitari de Barcelona as an ancillary test in the differential diagnosis of PD compared to other parkinsonisms.

As mentioned above, CSF α-synuclein RT-QuIC holds high promise for the detection of PD, but, as an emerging field, several questions remain to be answered. First, the use of qualitative, instead of quantitative, approaches is partially attributed to the variations observed in seeding activity between biospecimens, plate readers, laboratories, or even experiments depending on the recombinant batch or the reaction environment.[39,160,212,216] Indeed, in our experience and based on the available literature, the CSF α-synuclein RT-QuIC experimental conditions must be specifically set up in each laboratory even using the same recombinant α-synuclein, plate reader, and type of sample. Therefore, future studies should aim at optimising and standardising the assays for more efficient replication of findings across diagnostic laboratories. As a next step, quantitative RT-QuIC methods are currently investigated for α-synucleinopathies using endpoint dilution analyses,[217] as previously shown in prion disease.[213] Thus, the development of quantitative RT-QuIC could improve the stratification of patients in PD subtype populations for more personalised management of the disease and even play a significant role as a drug response biomarker for clinical trials.

Second, the high sensitivity and specificity of α-synuclein RT-QuIC in PD patients with overt disease pave the way out for exploring potential applicability in the early stages of premotor PD or mutation carriers at-high-risk of PD. In this regard, an accurate early PD detection in the premotor phase could help to determine each individual's prognosis and even allow its enrolment in future neuroprotective clinical trials, e.g., anti-α-synuclein immunotherapies.[218] Indeed, the first CSF α-synuclein RT-QuIC studies in iRBD patients have recently provided promising results with sensitivities and specificities of about 90%-100%.[182,212] Contrarily, a CSF α-synuclein RT-QuIC study in *LRRK2* mutation carriers has reported a positive response in only 40% of *LRRK2*-associated PD and 19% of *LRRK2* non-manifesting carriers,[219] thus suggesting that the sensitivity of this technique could depend on the PD subtype. Therefore, early PD detection in different premotor PD subtypes could be informative of the prognosis of the patient and the basis for implementing advanced personalised medicine in PD.[220]

Lastly, the α-synuclein seeding activity is more inconsistent in MSA despite being an α-synucleinopathy.[119,164,212] A possible explanation could involve the neuropathological differences between PD and MSA, recently demonstrated by the discovery of distinct conformational strains of aggregated α-synuclein with different average periodicities of fibrils helical twists.[48,221] Thus, the seeding proprieties could be disease-specific, requiring other experimental conditions for PD and MSA. Studies including different α-synuclein recombinants, different RT-QuIC experimental conditions and inter-laboratory validations should be performed to elucidate potential sources of variation to establish future standardised protocols for MSA. In summary, the CSF α-synuclein RT-QuIC assay set up in our study showed remarkable accuracy for PD detection. Moreover, α-synuclein RT-QuIC can aid in improving clinical PD diagnoses, even at premotor stages, and could help to stratify patients for disease-modifying clinical trials.

Numerous neuroimaging and biofluid measurements have been investigated as potential biomarkers for PD, such as MRI, DaT-SPECT, levels of CSF α-synuclein, CSF NFL or circulating miRNA. However, specificity, sensitivity and/or costs are still not optimal to be applied in clinical practice. Thus, given that finding a single biomarker that discriminates between all parkinsonism or covers all the different PD subtypes alone has proven difficult, a possible strategy may be the use of panels combining multiple biomarkers, either of the same or different types, to improve the predictive value of the model.[222] In this context, in [article 3], we combined different types of measurement, including CSF α-synuclein RT-QuIC, CSF NFL and midbrain/pons planimetry to discriminate parkinsonisms and found that most biomarkers signatures fitted with the clinical classification (these results are part of the thesis in preparation by Cèlia Painous). Thus, encompassing multiple types of measurements could maximise the field of application to diverse parkinsonisms or PD subtypes.[222,223] Yet, new analysis methods able to precisely merge the various criteria are needed. Moreover, in [article 1], we identified a serum miRNA biosignature combining the expression levels of 12 miRNAs that efficiently predicted iRBD and PD/DLB clinical outcomes with high discriminative capacity. These findings represent a proof-of-principle that, beyond clinical or imaging markers, a panel of specific serum miRNAs alone can be informative to predict the presence of iRBD and PD or DLB. Similarly, other groups suggested panels combining five[172] and four[224] serum miRNAs or five CSF miRNAs[117] as potential biomarkers for early PD diagnosis. Finally, in [article 2], we identified a combination of 4 miRNAs with good discriminative ability between G2019S asymptomatic carriers and pheno-converted LRRK2-associated PD patients that hold the potential as candidate pheno-conversion biomarkers.

In summary, the findings uncovered in this thesis advance the current state-of-the-art in the development of early PD biomarkers. Our findings have implications for disease prediction and early detection of α-synucleinopathies, even at prodromal stages.

CONCLUSIONS

6. CONCLUSIONS

1. Dynamic serum miRNA expression changes occur at the iRBD prodromal stage of α-synucleinopathies. Specifically, a 12-serum miRNA biosignature is informative in discriminating iRBD and PD/DLB patients from healthy controls, holding potential as an early progression biomarker for α-synucleinopathies.
2. Specific miRNA changes occur in *LRRK2* G2019S carriers with and without clinical PD and are more prominent in PD at-risk LRRK2 non-manifesting carriers and attenuate in LRRK2-associated PD patients. Specifically, miR-4505, miR-8069, miR-6125 and miR-451a hold potential as pheno-conversion biomarkers and could be prioritised in further validation studies.
3. CSF α-synuclein RT-QuIC was implemented in the laboratory with high diagnostic accuracy for PD and has been introduced as an ancillary test in clinical practice at our university hospital.

REFERENCES

7. REFERENCES

1. Pringsheim T, Jette N, Frolkis A, Steeves TDL. The prevalence of Parkinson's disease: A systematic review and meta-analysis. Mov Disord. 2014;29(13):1583–90.
2. Williams-gray CH. Parkinson's disease Key points. Medicine (Baltimore). 2016;44(9):542–6.
3. Hindle J V. Ageing, neurodegeneration and Parkinson's disease. Age Ageing. 2010;39(2):156–61.
4. Ray Dorsey E, Elbaz A, Nichols E, Abd-Allah F, Abdelalim A, Adsuar JC, et al. Global, regional, and national burden of Parkinson's disease, 1990–2016: a systematic analysis for the Global Burden of Disease Study 2016. Lancet Neurol. 2018;17(11):939–53.
5. Feigin VL, Krishnamurthi R V., Theadom AM, Abajobir AA, Mishra SR, Ahmed MB, et al. Global, regional, and national burden of neurological disorders during 1990–2015: a systematic analysis for the Global Burden of Disease Study 2015. Lancet Neurol. 2017;16(11):877–97.
6. Dorsey ER, Bloem BR. The Parkinson pandemic - A call to action. JAMA Neurol. 2018;75(1):9–10.
7. García-Ramos R, López Valdés E, Ballesteros L, Jesús S, Mir P. The social impact of Parkinson's disease in Spain: Report by the Spanish Foundation for the Brain. Neurologia. 2016;31(6):401–13.
8. Yang W, Hamilton JL, Kopil C, Beck JC, Tanner CM, Albin RL, et al. Current and projected future economic burden of Parkinson's disease in the US npj Park Dis. 2020;6(1):1–9.
9. Parkinson J. An essay on the shaking palsy. 1817. J Neuropsychiatry Clin Neurosci. 2002;14(2):223–36.
10. Goetz CG. The history of Parkinson's disease: Early clinical descriptions and neurological therapies. Cold Spring Harb Perspect Med.

2011;1(1):a008862.

11. Carlsson A, Lindqvist M, Magnusson T. 3,4-Dihydroxyphenylalanine and 5-Hydroxytryptophan as Reserpine Antagonists. Nature. 1957;180(4596):1200.
12. Ehringer H, Hornykiewicz O. Verteilung Von Noradrenalin Und Dopamin (3-Hydroxytyramin) Im Gehirn Des Menschen Und Ihr Verhalten Bei Erkrankungen Des Extrapyramidalen Systems. Klin Wochenschr. 1960;38(24):1236–9.
13. Cotzias GC, Van Woert MH, Schiffer LM. Aromatic Amino Acids and Modification of Parkinsonism. N Engl J Med. 1967;276(7):374–9.
14. Dickson DW, Braak H, Duda JE, Duyckaerts C, Gasser T, Halliday GM, et al. Neuropathological assessment of Parkinson's disease: refining the diagnostic criteria. Lancet Neurol. 2009;8(12):1150–7.
15. Lang AE, Lozano AM. Parkinson's disease. Second of two parts. N Engl J Med. 1998;339(16):1130–43.
16. Jankovic J. Parkinson's disease: Clinical features and diagnosis. J Neurol Neurosurg Psychiatry. 2008;79(4):368–76.
17. Tolosa E, Wenning G, Poewe W. The diagnosis of Parkinson's disease. Lancet Neurol. 2006;5(1):75–86.
18. Cheng HC, Ulane CM, Burke RE. Clinical progression in Parkinson disease and the neurobiology of axons. Ann Neurol. 2010;67(6):715–25.
19. Brooks DJ. Imaging non-dopaminergic function in Parkinson's disease. Mol Imaging Biol. 2007;9(4):217–22.
20. Bonnet AM. Involvement of non-dopaminergic pathways in parkinson's disease: Pathophysiology and therapeutic implications. CNS Drugs. 2000;13(5):351–64.
21. Postuma RB, Berg D, Stern M, Poewe W, Olanow CW, Oertel W, et al. MDS clinical diagnostic criteria for Parkinson's disease. Mov Disord. 2015;30(12):1591–601.

22. Rizzo G, Copetti M, Arcuti S, Martino D, Fontana A, Logroscino G. Accuracy of clinical diagnosis of Parkinson disease. Neurology. 2016;86(6):566 LP – 576.
23. Hughes AJ, Daniel SE, Ben-Shlomo Y, Lees AJ. The accuracy of diagnosis of parkinsonian syndromes in a specialist movement disorder service. Brain. 2002;125(4):861–70.
24. Joutsa J, Gardberg M, Röyttä M, Kaasinen V. Diagnostic accuracy of parkinsonism syndromes by general neurologists. Park Relat Disord. 2014;20(8):840–4.
25. Braak H, Del Tredici K, Rüb U, De Vos RAI, Jansen Steur ENH, Braak E. Staging of brain pathology related to sporadic Parkinson's disease. Neurobiol Aging. 2003;24(2):197–211.
26. Chaudhuri KR, Schapira AH. Non-motor symptoms of Parkinson's disease: dopaminergic pathophysiology and treatment. Lancet Neurol. 2009;8(5):464–74.
27. Burke RE, Dauer WT, Vonsattel JPG. A critical evaluation of the Braak staging scheme for Parkinson's disease. Ann Neurol. 2008;64(5):485–91.
28. Jellinger KA. Is Braak staging valid for all types of Parkinson's disease? J Neural Transm. 2019;126(4):423–31.
29. Venda LL, Cragg SJ, Buchman VL, Wade-Martins R. α-Synuclein and dopamine at the crossroads of Parkinson's disease. Trends Neurosci. 2010;33(12):559–68.
30. Lashuel HA, Overk CR, Oueslati A, Masliah E. The many faces of α-synuclein: from structure and toxicity to therapeutic target. Nat Rev Neurosci. 2013;14(1):38–48.
31. Bartels T, Choi JG, Selkoe DJ. α-Synuclein occurs physiologically as a helically folded tetramer that resists aggregation. Nature. 2011;477(7362):107–11.
32. Li A, Rastegar C, Mao X. α-Synuclein Conformational Plasticity: Physiologic

States, Pathologic Strains, and Biotechnological Applications. Biomolecules. 2022;12(7):994.

33. Spillantini MG, Schmidt ML, Lee VMY, Trojanowski JQ, Jakes R, Goedert M. α-Synuclein in Lewy bodies. Nature. 1997;388(6645):839–40.

34. Recasens A, Dehay B, Bové J, Carballo-Carbajal I, Dovero S, Pérez-Villalba A, et al. Lewy body extracts from Parkinson disease brains trigger α-synuclein pathology and neurodegeneration in mice and monkeys. Ann Neurol. 2014;75(3):351–62.

35. Bernis ME, Babila JT, Breid S, Wüsten KA, Wüllner U, Tamgüney G. Prion-like propagation of human brain-derived alpha-synuclein in transgenic mice expressing human wild-type alpha-synuclein. Acta Neuropathol Commun. 2015;3:75.

36. Kovacs GG, Breydo L, Green R, Kis V, Puska G, Lorincz P, et al. Intracellular processing of disease-associated α-synuclein in the human brain suggests prion-like cell-to-cell spread. Neurobiol Dis. 2014;69:76–92.

37. Danzer KM, Krebs SK, Wolff M, Birk G, Hengerer B. Seeding induced by α-synuclein oligomers provides evidence for spreading of α-synuclein pathology. J Neurochem. 2009;111(1):192–203.

38. Shahnawaz M, Tokuda T, Waraga M, Mendez N, Ishii R, Trenkwalder C, et al. Development of a biochemical diagnosis of Parkinson disease by detection of α-synuclein misfolded aggregates in cerebrospinal fluid. JAMA Neurol. 2017;74(2):163–72.

39. Fairfoul G, McGuire LI, Pal S, Ironside JW, Neumann J, Christie S, et al. Alpha-synuclein RT-QuIC in the CSF of patients with alpha-synucleinopathies. Ann Clin Transl Neurol. 2016;3(10):812–8.

40. Beach TG, Adler CH, Sue LI, Vedders L, Lue LF, White CL, et al. Multi-organ distribution of phosphorylated α-synuclein histopathology in subjects with Lewy body disorders. Acta Neuropathol. 2010;119(6):689–702.

41. Sulzer D, Surmeier DJ. Neuronal vulnerability, pathogenesis, and

Parkinson’s disease. Mov Disord. 2013;28(6):715–24.

42. Sulzer D, Bogulavsky J, Larsen KE, Behr G, Karatekin E, Kleinman MH, et al. Neuromelanin biosynthesis is driven by excess cytosolic catecholamines not accumulated by synaptic vesicles. Proc Natl Acad Sci U S A. 2000;97(22):11869–74.

43. Carballo-Carbajal I, Laguna A, Romero-Giménez J, Cuadros T, Bové J, Martinez-Vicente M, et al. Brain tyrosinase overexpression implicates age-dependent neuromelanin production in Parkinson’s disease pathogenesis. Nat Commun. 2019;10(1).

44. Vila M. Neuromelanin, aging, and neuronal vulnerability in Parkinson’s disease. Mov Disord. 2019;34(10):1440–51.

45. Zucca FA, Segura-Aguilar J, Ferrari E, Muñoz P, Paris I, Sulzer D, et al. Interactions of iron, dopamine and neuromelanin pathways in brain aging and Parkinson’s disease. Prog Neurobiol. 2017;155:96–119.

46. Koga S, Sekiya H, Kondru N, Ross OA, Dickson DW. Neuropathology and molecular diagnosis of Synucleinopathies. Mol Neurodegener. 2021;16(1):1–24.

47. Spillantini MG, Goedert M. The α-Synucleinopathies: Parkinson’s Disease, Dementia with Lewy Bodies, and Multiple System Atrophy. Ann N Y Acad Sci. 2000;920(1):16–27.

48. Shahnawaz M, Mukherjee A, Pritzkow S, Mendez N, Rabadia P, Liu X, et al. Discriminating α-synuclein strains in Parkinson’s disease and multiple system atrophy. Nature. 2020;578(7794):273–7.

49. Williams-Gray CH, Mason SL, Evans JR, Foltynie T, Brayne C, Robbins TW, et al. The CamPaIGN study of Parkinson’s disease: 10-year outlook in an incident population-based cohort. J Neurol Neurosurg Psychiatry. 2013;84(11):1258–64.

50. McKeith I. Dementia with Lewy bodies. 1st ed. Vol. 84, Handbook of Clinical Neurology. Elsevier BV; 2007. 531–548 p.

51. Fanciulli A, Stankovic I, Krismer F, Seppi K, Levin J, Wenning GK. Multiple system atrophy. Vol. 149, International Review of Neurobiology. Elsevier Ltd; 2019. 137–192 p.
52. Wakabayashi K, Takahashi H. Pathological heterogeneity in progressive supranuclear palsy and corticobasal degeneration. Neuropathology. 2004;24(1):79–86.
53. Langston JW. The MPTP story. J Parkinsons Dis. 2017;7:S11–9.
54. Mustapha M, Taib CNM. MPTP-induced mouse model of Parkinson's disease: A promising direction for therapeutic strategies. Bosn J Basic Med Sci. 2021;21(4):422–33.
55. Polymeropoulos MH, Higgins JJ, Golbe LI, Johnson WG, Ide SE, Di Iorio G, et al. Mapping of a Gene for Parkinson's Disease to Chromosome 4q21-q23. Science (80-). 1996;274(5290):1197–9.
56. Polymeropoulos MH, Lavedan C, Leroy E, Ide SD, Dehejia A, Dutra A, et al. Mutation in the α-Synuclein Gene Identified in Families with Parkinson's Disease. Science (80-). 1997 Jun 27;276(5321):2045–7.
57. Tanner CM, Kame F, Ross GW, Hoppin JA, Goldman SM, Korell M, et al. Rotenone, paraquat, and Parkinson's disease. Environ Health Perspect. 2011;119(6):866–72.
58. Olanow CW. Manganese-Induced Parkinsonism and Parkinson's Disease. Ann N Y Acad Sci. 2004;1012(1):209–23.
59. Ascherio A, Schwarzschild MA. The epidemiology of Parkinson's disease: risk factors and prevention. Lancet Neurol. 2016;15(12):1257–72.
60. Lim KL, Ng CH. Genetic models of Parkinson disease. Biochim Biophys Acta - Mol Basis Dis. 2009;1792(7):604–15.
61. Del Rey NLG, Quiroga-Varela A, Garbayo E, Carballo-Carbajal I, Fernández-Santiago R, Monje MHG, et al. Advances in parkinson's disease: 200 years later. Front Neuroanat. 2018;12(December):1–14.
62. Sidransky E, Lopez G. The link between the GBA gene and parkinsonism.

Lancet Neurol. 2012;11(11):986–98.

63. Kitada T, Aakawa S, Hattori N, Matsumine H, Yokochi M, Mizuno Y, et al. Mutations in the parkin gene cause autosomal recessive juvenile parkinsonism. Nat Lett. 1998;169(1993):166–9.

64. Leroy E, Boyer R, Auburger G, Leube B, Ulm G, Mezey E, et al. The ubiquitin pathway in Parkinson's disease. Nature. 1998;395(6701):451–2.

65. Bonifati V, Breedveld GJ, Squitieri F, Vanacore N, Brustenghi P, Harhangi BS, et al. Localisation of autosomal recessive early-onset parkinsonism to chromosome 1p36 (PARK7) in an independent dataset. Ann Neurol. 2002;51(2):253–6.

66. Bonifati V, Rizzu P, Van Baren MJ, Schaap O, Breedveld GJ, Krieger E, et al. Mutations in the DJ-1 gene associated with autosomal recessive early-onset parkinsonism. Science (80-). 2003;299(5604):256–9.

67. Hatano Y, Li Y, Sato K, Asakawa S, Yamamura Y, Tomiyama H, et al. Novel PINK1 mutations in early-onset parkinsonism. Ann Neurol. 2004;56(3):424–7.

68. Valente EM, Abou-Sleiman PM, Caputo V, Muqit MMK, Harvey K, Gispert S, et al. Hereditary early-onset Parkinson's disease caused by mutations in PINK1. Science (80-). 2004;304(5674):1158–60.

69. Paisán-Ruíz C, Jain S, Evans EW, Gilks WP, Simón J, Van Der Brug M, et al. Cloning of the gene containing mutations that cause PARK8-linked Parkinson's disease. Neuron. 2004;44(4):595–600.

70. Zimprich A, Biskup S, Leitner P, Lichtner P, Farrer M, Lincoln S, et al. Mutations in LRRK2 Cause Autosomal-Dominant Parkinsonism with Pleomorphic Pathology. Neuron. 2004;44:601–7.

71. Luoma P, Melberg A, Rinne JO, Kaukonen JA, Nupponen NN, Chalmers RM, et al. Parkinsonism, premature menopause, and mitochondrial DNA polymerase γ mutations: Clinical and molecular genetic study. Lancet. 2004;364(9437):875–82.

72. Strauss KM, Martins LM, Plun-Favreau H, Marx FP, Kautzmann S, Berg D, et al. Loss of function mutations in the gene encoding Omi/HtrA2 in Parkinson's disease. Hum Mol Genet. 2005;14(15):2099–111.
73. Ramirez A, Heimbach A, Gründemann J, Stiller B, Hampshire D, Cid LP, et al. Hereditary parkinsonism with dementia is caused by mutations in ATP13A2, encoding a lysosomal type 5 P-type ATPase. Nat Genet. 2006;38(10):1184–91.
74. Lautier C, Goldwurm S, Dürr A, Giovannone B, Tsiaras WG, Pezzoli G, et al. Mutations in the GIGYF2 (TNRC15) Gene at the PARK11 Locus in Familial Parkinson Disease. Am J Hum Genet. 2008;82(4):822–33.
75. Fonzo A Di, Dekker MCJ, Montagna P, Baruzzi A, Yonova EH, Guedes LC, et al. FBXO7 mutations cause autosomal recessive, early-onset parkinsonian-pyramidal syndrome. Neurology. 2009;72(3):240 LP – 245.
76. Paisan-Ruiz C, Bhatia KP, Li A, Hernandez D, Davis M, Wood NW, et al. Characterisation of PLA2G6 as a locus for dystonia-parkinsonism. Ann Neurol. 2009;65(1):19–23.
77. Vilariño-Güell C, Wider C, Ross OA, Dachsel JC, Kachergus JM, Lincoln SJ, et al. VPS35 mutations in parkinson disease. Am J Hum Genet. 2011;89(1):162–7.
78. Chartier-Harlin MC, Dachsel JC, Vilariño-Güell C, Lincoln SJ, Leprêtre F, Hulihan MM, et al. Translation initiator EIF4G1 mutations in familial parkinson disease. Am J Hum Genet. 2011;89(3):398–406.
79. Edvardson S, Cinnamon Y, Ta-Shma A, Shaag A, Yim YI, Zenvirt S, et al. A deleterious mutation in DNAJC6 encoding the neuronal-specific clathrin-uncoating Co-chaperone auxilin, is associated with juvenile parkinsonism. PLoS One. 2012;7(5):4–8.
80. Krebs CE, Karkheiran S, Powell JC, Cao M, Makarov V, Darvish H, et al. The sac1 domain of SYNJ1 identified mutated in a family with early-onset progressive parkinsonism with generalised seizures. Hum Mutat.

2013;34(9):1200–7.

81. Vilariño-Güell C, Rajput A, Milnerwood AJ, Shah B, Szu-Tu C, Trinh J, et al. DNAJC13 mutations in Parkinson disease. Hum Mol Genet. 2014;23(7):1794–801.

82. Funayama M, Ohe K, Amo T, Furuya N, Yamaguchi J, Saiki S, et al. CHCHD2 mutations in autosomal dominant late-onset Parkinson's disease: A genome-wide linkage and sequencing study. Lancet Neurol. 2015;14(3):274–82.

83. Lesage S, Drouet V, Majounie E, Deramecourt V, Jacoupy M, Nicolas A, et al. Loss of VPS13C Function in Autosomal-Recessive Parkinsonism Causes Mitochondrial Dysfunction and Increases PINK1/Parkin-Dependent Mitophagy. Am J Hum Genet. 2016;98(3):500–13.

84. Deng HX, Shi Y, Yang Y, Ahmeti KB, Miller N, Huang C, et al. Identification of TMEM230 mutations in familial Parkinson's disease. Nat Genet. 2016;48(7):733–9.

85. Sudhaman S, Muthane UB, Behari M, Govindappa ST, Juyal RC, Thelma BK. Evidence of mutations in RIC3 acetylcholine receptor chaperone as a novel cause of autosomal-dominant Parkinson's disease with non-motor phenotypes. J Med Genet. 2016;53(8):559–66.

86. Quadri M, Mandemakers W, Grochowska MM, Masius R, Geut H, Fabrizio E, et al. LRP10 genetic variants in familial Parkinson's disease and dementia with Lewy bodies: a genome-wide linkage and sequencing study. Lancet Neurol. 2018;17(7):597–608.

87. Lee JS, Kanai K, Suzuki M, Kim WS, Yoo HS, Fu YH, et al. Arylsulfatase A, a genetic modifier of Parkinson's disease, is an α-synuclein chaperone. Brain. 2019;142(9):2845–59.

88. Healy DG, Falchi M, O'Sullivan SS, Bonifati V, Durr A, Bressman S, et al. Phenotype, genotype, and worldwide genetic penetrance of LRRK2-associated Parkinson's disease: a case-control study. Lancet Neurol.

2008;7(7):583–90.

89. Gaig C, Ezquerra M, Marti, M J et al. Mutations in Spanish Patients With Parkinson Disease. Arch Neurol. 2006;63:6–11.

90. Stefano G, Sara T, Silvana T, Michela Z, Francesca S, Paola P, et al. Kin-cohort analysis of LRRK2-G2019S penetrance in Parkinson's disease. Mov Disord. 2011;26(11):2144–5.

91. Paisán-Ruiz C, Washecka N, Nath P, Singleton AB, Corder EH. Parkinson's disease and low frequency alleles found together throughout LRRK2. Ann Hum Genet. 2009;73(4):391–403.

92. Aasly JO, Vilariño-Güell C, Dachsel JC, Webber PJ, West AB, Haugarvoll K, et al. Novel pathogenic LRRK2 p.Asn1437His substitution in familial Parkinson's disease. Mov Disord. 2010;25(13):2156–63.

93. Di Fonzo A, Rohé CF, Ferreira J, Chien HF, Vacca L, Stocchi F, et al. A frequent LRRK2 gene mutation associated with autosomal dominant Parkinson's disease. Lancet. 2005;365(9457):412–5.

94. Gilks WP, Abou-Sleiman PM, Gandhi S, Jain S, Singleton A, Lees AJ, et al. A common LRRK2 mutation in idiopathic Parkinson's disease. Lancet. 2005;365(9457):415–6.

95. Ozelius LJ, Senthil G, Saunders-Pullman R, Ohmann E, Deligtisch A, Tagliati M, et al. LRRK2 G2019S as a Cause of Parkinson's Disease in Ashkenazi Jews. N Engl J Med. 2006;354(4):424–5.

96. Lesage S, Dürr A, Tazir M, Lohmann E, Leutenegger AL, Janin S, et al. *LRRK2* G2019S as a Cause of Parkinson's Disease in North African Arabs. N Engl J Med. 2006;354(4):422–3.

97. Lucotte G, David D, Change N. New contribution on the *LRRK2* G2019S mutation associated to Parkinson's disease: age estimation of a common founder event of old age in Moroccan Berbers. Int J Mod Anthropol. 2012;1(5):11–22.

98. Lee AJ, Wang Y, Alcalay RN, Mejia-Santana H, Saunders-Pullman R,

Bressman S, et al. Penetrance estimate of LRRK2 p.G2019S mutation in individuals of non-Ashkenazi Jewish ancestry. Mov Disord. 2017;32(10):1432–8.

99. Marder K, Wang Y, Alcalay RN, Mejia-Santana H, Tang MX, Lee A, et al. Age-specific penetrance of LRRK2 G2019S in the Michael J. Fox Ashkenazi Jewish LRRK2 Consortium. Neurology. 2015;85(1):89–95.

100. Aasly JO, Toft M, Fernandez-Mata I, Kachergus J, Hulihan M, White LR, et al. Clinical features of LRRK2-associated Parkinson's disease in Central Norway. Ann Neurol. 2005;57(5):762–5.

101. Tolosa E, Vila M, Klein C, Rascol O. LRRK2 in Parkinson disease: challenges of clinical trials. Nat Rev Neurol. 2020;16(2):97–107.

102. Ehrminger M, Leu-Semenescu S, Cormier F, Corvol JC, Vidailhet M, Debellemaniere E, et al. Sleep aspects on video-polysomnography in LRRK2 mutation carriers. Mov Disord. 2015;30(13):1839–43.

103. Marras C, Schuele B, Munhoz RP, Rogaeva E, Langston JW, Kasten M, et al. Phenotype in parkinsonian and nonparkinsonian LRRK2 G2019S mutation carriers. Neurology. 2011;77(4):325 LP – 333.

104. Kalinderi K, Bostantjopoulou S, Fidani L. The genetic background of Parkinson's disease: current progress and future prospects. Acta Neurol Scand. 2016;134(5):314–26.

105. Blauwendraat C, Nalls MA, Singleton AB. The genetic architecture of Parkinson's disease. Lancet Neurol. 2020;19(2):170–8.

106. Nalls MA, Blauwendraat C, Vallerga CL, Heilbron K. Identification of novel risk loci, causal insights, and heritable risk for Parkinson's disease: a meta-genome wide association study. Lancet Neurol. 2019;18(12):1091–102.

107. Choi SW, Mak TSH, O'Reilly PF. Tutorial: a guide to performing polygenic risk score analyses. Nat Protoc. 2020;15(9):2759–72.

108. Fernández-Santiago R, Martín-Flores N, Antonelli F, Cerquera C, Moreno V, Bandres-Ciga S, et al. SNCA and mTOR Pathway Single Nucleotide

Polymorphisms Interact to Modulate the Age at Onset of Parkinson's Disease. Mov Disord. 2019;34(9):1333–44.

109. Gayán J, González-Pérez A, Bermudo F, Sáez ME, Royo JL, Quintas A, et al. A method for detecting epistasis in genome-wide studies using case-control multi-locus association analysis. BMC Genomics. 2008;9:1–14.

110. Cope JL, Baukmann HA, Klinger JE, Ravarani CNJ, Böttinger EP, Konigorski S, et al. Interaction-Based Feature Selection Algorithm Outperforms Polygenic Risk Score in Predicting Parkinson's Disease Status. Front Genet. 2021;12:1–9.

111. Dehestani M, Liu H, Gasser T. Polygenic risk scores contribute to personalised medicine of parkinson's disease. J Pers Med. 2021;11(10):1030.

112. Postuma RB, Aarsland D, Barone P, Burn DJ, Hawkes CH, Oertel W, et al. Identifying prodromal Parkinson's disease: Premotor disorders in Parkinson's disease. Mov Disord. 2012;27(5):617–26.

113. Fereshtehnejad SM, Yao C, Pelletier A, Montplaisir JY, Gagnon JF, Postuma RB. Evolution of prodromal Parkinson's disease and dementia with Lewy bodies: A prospective study. Brain. 2019;142(7):2051–67.

114. Postuma RB, Berg D. Prodromal Parkinson's Disease: The Decade Past, the Decade to Come. Mov Disord. 2019;34(5):665–75.

115. Schrag A, Horsfall L, Walters K, Noyce A, Petersen I. Prediagnostic presentations of Parkinson's disease in primary care: A case-control study. Lancet Neurol. 2015;14(1):57–64.

116. Iranzo A, Tolosa E, Gelpi E, Molinuevo JL, Valldeoriola F, Serradell M, et al. Neurodegenerative disease status and post-mortem pathology in idiopathic rapid-eye-movement sleep behaviour disorder: an observational cohort study. Lancet Neurol. 2013;12(5):443–53.

117. Dos Santos MCT, Barreto-Sanz MA, Correia BRS, Bell R, Widnall C, Perez LT, et al. miRNA-based signatures in cerebrospinal fluid as potential

diagnostic tools for early stage Parkinson's disease. Oncotarget. 2018;9(25):17455–65.

118. Mahlknecht P, Iranzo A, Högl B, Frauscher B, Müller C, Santamaría J, et al. Olfactory dysfunction predicts early transition to a Lewy body disease in idiopathic RBD. Neurology. 2015;84(7):654 LP – 658.

119. Poggiolini I, Gupta V, Lawton M, Lee S, El-Turabi A, Querejeta-Coma A, et al. Diagnostic value of cerebrospinal fluid alpha-synuclein seed quantification in synucleinopathies. Brain. 2022;145(2):584–95.

120. Noyce AJ, R'Bibo L, Peress L, Bestwick JP, Adams-Carr KL, Mencacci NE, et al. PREDICT-PD: An online approach to prospectively identify risk indicators of Parkinson's disease. Mov Disord. 2017;32(2):219–26.

121. Chiba Y, Fujishiro H, Iseki E, Ota K, Kasanuki K, Hirayasu Y, et al. Retrospective survey of prodromal symptoms in dementia with lewy bodies: Comparison with alzheimer's disease. Dement Geriatr Cogn Disord. 2012;33(4):273–81.

122. Xia C, Postuma RB. Diagnosing multiple system atrophy at the prodromal stage. Clin Auton Res. 2020;30(3):197–205.

123. Aguirre-Mardones C, Iranzo A, Vilas D, Serradell M, Gaig C, Santamaría J, et al. Prevalence and timeline of nonmotor symptoms in idiopathic rapid eye movement sleep behavior disorder. J Neurol. 2015;262(6):1568–78.

124. Postuma RB, Gagnon JF, Vendette M, Fantini ML, Massicotte-Marquez J, Montplaisir J. Quantifying the risk of neurodegenerative disease in idiopathic REM sleep behavior disorder. Neurology. 2009;72(15):1296–300.

125. Schenck CH, Bundlie SR, Mahowald MW. Delayed emergence of a parkinsonian disorder in 38% of 29 older men initially diagnosed with idiopathic rapid eye movement sleep behavior disorder. Neurology. 1996;46(2):388 LP – 393.

126. Iranzo A, Molinuevo JL, Santamaría J, Serradell M, Martí MJ, Valldeoriola

F, et al. Rapid-eye-movement sleep behaviour disorder as an early marker for a neurodegenerative disorder: a descriptive study. Lancet Neurol. 2006;5(7):572–7.

127. Schenck CH, Mahowald MW. REM sleep behavior disorder: Clinical, developmental, and neuroscience perspectives 16 years after its formal identification in SLEEP. Sleep. 2002;25(2):120–38.

128. Medicine AA of S. The International Classification of Sleep Disorders: Diagnostic & Coding Manual, 2nd edn. Westchester IL: American Academy of Sleep Medicine. 2005.

129. Yao C, Fereshtehnejad SM, Dawson BK, Pelletier A, Gan-Or Z, Gagnon JF, et al. Longstanding disease-free survival in idiopathic REM sleep behavior disorder: Is neurodegeneration inevitable? Park Relat Disord. 2018;54:99–102.

130. Peever J, Luppi PH, Montplaisir J. Breakdown in REM sleep circuitry underlies REM sleep behavior disorder. Trends Neurosci. 2014;37(5):279–88.

131. Boeve BF, Silber MH, Saper CB, Ferman TJ, Dickson DW, Parisi JE, et al. Pathophysiology of REM sleep behaviour disorder and relevance to neurodegenerative disease. Brain. 2007;130(11):2770–88.

132. Scherfler C, Frauscher B, Schocke M, Iranzo A, Gschliesser V, Seppi K, et al. White and gray matter abnormalities in idiopathic rapid eye movement sleep behavior disorder: A diffusion-tensor imaging and voxel-based morphometry study. Ann Neurol. 2011;69(2):400–7.

133. Gan-Or Z, Mirelman A, Postuma RB, Arnulf I, Bar-Shira A, Dauvilliers Y, et al. GBA mutations are associated with Rapid Eye Movement Sleep Behavior Disorder. Ann Clin Transl Neurol. 2015;2(9):941–5.

134. Barber TR, Lawton M, Rolinski M, Evetts S, Baig F, Ruffmann C, et al. Prodromal parkinsonism and neurodegenerative risk stratification in rem sleep behavior disorder. Sleep. 2017;40(8).

135. Fernández-Santiago R, Iranzo A, Gaig C, Serradell M, Fernández M, Tolosa E, et al. Absence of LRRK2 mutations in a cohort of patients with idiopathic REM sleep behavior disorder. Neurology. 2016;86(11):1072 LP – 1073.
136. Krohn L, Wu RYJ, Heilbron K, Ruskey JA, Laurent SB, Blauwendraat C, et al. Fine-Mapping of SNCA in Rapid Eye Movement Sleep Behavior Disorder and Overt Synucleinopathies. Ann Neurol. 2020;87(4):584–98.
137. Brockmann K, Srulijes K, Hauser AK, Schulte C, Csoti I, Gasser T, et al. GBA-associated PD presents with nonmotor characteristics. Neurology. 2011;77(3):276–80.
138. Postuma RB, Gagnon JF, Vendette M, Charland K, Montplaisir J. REM sleep behaviour disorder in Parkinson's disease is associated with specific motor features. J Neurol Neurosurg Psychiatry. 2008;79(10):1117–21.
139. Anang JBM, Gagnon JF, Bertrand JA, Romenets SR, Latreille V, Panisset M, et al. Predictors of dementia in Parkinson disease. Neurology. 2014;83(14):1253 LP – 1260.
140. Atkinson AJ, Colburn WA, DeGruttola VG, DeMets DL, Downing GJ, Hoth DF, et al. Biomarkers and surrogate endpoints: Preferred definitions and conceptual framework. Clin Pharmacol Ther. 2001;69(3):89–95.
141. Strimbu K, Tavel JA. What are biomarkers? Curr Opin HIV AIDS. 2010;5(6):463–6.
142. Emamzadeh FN, Surguchov A. Parkinson's disease: Biomarkers, treatment, and risk factors. Front Neurosci. 2018;12:1–14.
143. Miller DB, O'Callaghan JP. Biomarkers of Parkinson's disease: Present and future. Metabolism. 2015;64(3):S40–6.
144. Saeed U, Compagnone J, Aviv RI, Strafella AP, Black SE, Lang AE, et al. Imaging biomarkers in Parkinson's disease and Parkinsonian syndromes: Current and emerging concepts. Transl Neurodegener. 2017;6(1):1–25.
145. Politis M. Neuroimaging in Parkinson disease: From research setting to clinical practice. Nat Rev Neurol. 2014;10(12):708–22.

146. Brooks DJ, Pavese N. Imaging biomarkers in Parkinson's disease. Prog Neurobiol. 2011;95(4):614–28.

147. Kägi G, Bhatia KP, Tolosa E. The role of DAT-SPECT in movement disorders. J Neurol Neurosurg Psychiatry. 2010;81(1):5–12.

148. Booij J, Speelman JD, Horstink MWIM, Wolters EC. The clinical benefit of imaging striatal dopamine transporters with [123I]FP-CIT SPET in differentiating patients with presynaptic parkinsonism from those with other forms of parkinsonism. Eur J Nucl Med. 2001;28(3):266–72.

149. Sierra M, Martínez- MI, González- I, Palacio E, Carril JM. Olfaction and imaging biomarkers in Parkinson disease. Neurology. 2013;80:621–6.

150. Iranzo A, Valldeoriola F, Lomeña F, Molinuevo JL, Serradell M, Salamero M, et al. Serial dopamine transporter imaging of nigrostriatal function in patients with idiopathic rapid-eye-movement sleep behaviour disorder: A prospective study. Lancet Neurol. 2011;10(9):797–805.

151. Arnaldi D, De Carli F, Picco A, Ferrara M, Accardo J, Bossert I, et al. Nigro-caudate dopaminergic deafferentation: A marker of REM sleep behavior disorder? Neurobiol Aging. 2015;36(12):3300–5.

152. Eisensehr I, Linke R, Tatsch K, Kharraz B, Gildehaus JF, Wetter CT, et al. Increased muscle activity during rapid eye movement sleep correlates with decrease of striatal presynaptic dopamine transporters. IPT and IBZM SPECT imaging in subclinical and clinically manifest idiopathic REM sleep behavior disorder, Parkinson's disease. Sleep. 2003;26(5):507–12.

153. Simuni T, Siderowf A, Lasch S, Coffey CS, Caspell-Garcia C, Jennings D, et al. Longitudinal Change of Clinical and Biological Measures in Early Parkinson's Disease: Parkinson's Progression Markers Initiative Cohort. Mov Disord. 2018;33(5):771–82.

154. Mitchell T, Lehéricy S, Chiu SY, Strafella AP, Stoessl AJ, Vaillancourt DE. Emerging Neuroimaging Biomarkers across Disease Stage in Parkinson Disease: A Review. JAMA Neurol. 2021;78(10):1262–72.

155. Parnetti L, Gaetani L, Eusebi P, Paciotti S, Hansson O, El-Agnaf O, et al. CSF and blood biomarkers for Parkinson's disease. Lancet Neurol. 2019;18(6):573–86.
156. Malek N, Swallow D, Grosset KA, Anichtchik O, Spillantini M, Grosset DG. Alpha-synuclein in peripheral tissues and body fluids as a biomarker for Parkinson's disease - a systematic review. Acta Neurol Scand. 2014;130(2):59–72.
157. Goldman JG, Andrews H, Amara A, Naito A, Alcalay RN, Shaw LM, et al. Cerebrospinal fluid, plasma, and saliva in the BioFIND study: Relationships among biomarkers and Parkinson's disease Features. Mov Disord. 2018;33(2):282–8.
158. Atik A, Stewart T, Zhang J. Alpha-Synuclein as a Biomarker for Parkinson's Disease. Brain Pathol. 2016;26(3):410–8.
159. McGuire LI, Peden AH, Orrú CD, Wilham JM, Appleford NE, Mallinson G, et al. Real time quaking-induced conversion analysis of cerebrospinal fluid in sporadic Creutzfeldt-Jakob disease. Ann Neurol. 2012;72(2):278–85.
160. Manne S, Kondru N, Jin H, Serrano GE, Anantharam V, Kanthasamy A, et al. Blinded RT-QuIC Analysis of α-Synuclein Biomarker in Skin Tissue From Parkinson's Disease Patients. Mov Disord. 2020;35(12):2230–9.
161. Kuzkina A, Bargar C, Schmitt D, Rößle J, Wang W, Schubert AL, et al. Diagnostic value of skin RT-QuIC in Parkinson's disease: a two-laboratory study. npj Park Dis. 2021;7(1):1–11.
162. De Luca CMG, Elia AE, Portaleone SM, Cazzaniga FA, Rossi M, Bistaffa E, et al. Efficient RT-QuIC seeding activity for α-synuclein in olfactory mucosa samples of patients with Parkinson's disease and multiple system atrophy. Transl Neurodegener. 2019;8(1):1–14.
163. Stefani A, Iranzo A, Holzknecht E, Perra D, Bongianni M, Gaig C, et al. Alpha-synuclein seeds in olfactory mucosa of patients with isolated REM sleep behaviour disorder. Brain. 2021;144(4):1118–26.

164. van Rumund A, Green AJE, Fairfoul G, Esselink RAJ, Bloem BR, Verbeek MM. α-Synuclein real-time quaking-induced conversion in the cerebrospinal fluid of uncertain cases of parkinsonism. Ann Neurol. 2019;85(5):777–81.

165. Rossi M, Candelise N, Baiardi S, Capellari S, Giannini G, Orrù CD, et al. Ultrasensitive RT-QuIC assay with high sensitivity and specificity for Lewy body-associated synucleinopathies. Acta Neuropathol. 2020;140(1):49–62.

166. Marques TM, van Rumund A, Oeckl P, Kuiperij HB, Esselink RAJ, Bloem BR, et al. Serum NFL discriminates Parkinson disease from atypical parkinsonisms. Neurology. 2019;92(13):e1479 LP-e1486.

167. Hansson O, Janelidze S, Hall S, Magdalinou N, Lees AJ, Andreasson U, et al. Blood-based NfL: A biomarker for differential diagnosis of parkinsonian disorder. Neurology. 2017;88(10):930–7.

168. Bartel DP. MicroRNAs: Genomics, Biogenesis, Mechanism, and Function. Cell. 2004;116(2):281–97.

169. Chen X, Ba Y, Ma L, Cai X, Yin Y, Wang K, et al. Characterisation of microRNAs in serum: A novel class of biomarkers for diagnosis of cancer and other diseases. Cell Res. 2008;18(10):997–1006.

170. Cardo LF, Coto E, Ribacoba R, Menéndez M, Moris G, Suárez E, et al. MiRNA Profile in the Substantia Nigra of Parkinson's Disease and Healthy Subjects. J Mol Neurosci. 2014;54(4):830–6.

171. Vallelunga A, Ragusa M, Di Mauro S, Iannitti T, Pilleri M, Biundo R, et al. Identification of circulating microRNAs for the differential diagnosis of Parkinson's disease and Multiple System Atrophy. Front Cell Neurosci. 2014;8:1–10.

172. Ding H, Huang Z, Chen M, Wang C, Chen X, Chen J, et al. Identification of a panel of five serum miRNAs as a biomarker for Parkinson's disease. Park Relat Disord. 2016;22:68–73.

173. Ma W, Li Y, Wang C, Xu F, Wang M, Liu Y. Serum miR-221 serves as a biomarker for Parkinson's disease. Cell Biochem Funct. 2016;34(7):511–5.
174. Condrat CE, Thompson DC, Barbu MG, Bugnar OL, Boboc A, Cretoiu D, et al. miRNAs as Biomarkers in Disease: Latest Findings Regarding Their Role in Diagnosis and Prognosis. Cells. 2020;9(276):1–32.
175. Roser AE, Gomes LC, Schünemann J, Maass F, Lingor P. Circulating miRNAs as diagnostic biomarkers for Parkinson's disease. Front Neurosci. 2018;12:1–9.
176. Fernández-Santiago R, Iranzo A, Gaig C, Serradell M, Fernández M, Tolosa E, et al. MicroRNA association with synucleinopathy conversion in rapid eye movement behavior disorder. Ann Neurol. 2015;77(5):895–901.
177. Kern F, Fehlmann T, Violich I, Alsop E, Hutchins E, Kahraman M, et al. Deep sequencing of sncRNAs reveals hallmarks and regulatory modules of the transcriptome during Parkinson's disease progression. Nat Aging. 2021;1(3):309–22.
178. Botta-Orfila T, Morató X, Compta Y, Lozano JJ, Falgàs N, Valldeoriola F, et al. Identification of blood serum micro-RNAs associated with idiopathic and LRRK2 Parkinson's disease. J Neurosci Res. 2014;92(8):1071–7.
179. Mollenhauer B, Caspell-Garcia CJ, Coffey CS, Taylor P, Singleton A, Shaw LM, et al. Longitudinal analyses of cerebrospinal fluid α-Synuclein in prodromal and early Parkinson's disease. Mov Disord. 2019;34(9):1354–64.
180. Chahine LM, Beach TG, Brumm MC, Adler CH, Coffey CS, Mosovsky S, et al. In vivo distribution of α-synuclein in multiple tissues and biofluids in Parkinson disease. Neurology. 2020;95(9):e1267–84.
181. Behbahanipour M, Peymani M, Salari M, Hashemi MS, Nasr-Esfahani MH, Ghaedi K. Expression Profiling of Blood microRNAs 885, 361, and 17 in the Patients with the Parkinson's disease: Integrating Interaction Data to Uncover the Possible Triggering Age-Related Mechanisms. Sci Rep.

2019;9(1):1–11.

182. Iranzo A, Fairfoul G, Na Ayudhaya A, Serradell M, Gelpi E, Vilaseca I, et al. Detection of α-synuclein in CSF by RT-QuIC in patients with isolated rapid-eye-movement sleep behaviour disorder: a longitudinal observational study. Lancet Neurol. 2021;20(3):203–12.

183. Iranzo A, Borrego S, Vilaseca I, Martí C, Serradell M, Sánchez-Valle R, et al. α-Synuclein aggregates in labial salivary glands of idiopathic rapid eye movement sleep behavior disorder. Sleep. 2018;41(8):1–8.

184. Ozdilek B, Demircan B. Serum microRNA expression levels in Turkish patients with Parkinson's disease. Int J Neurosci. 2021;131(12):1181–9.

185. Cao XY, Lu JM, Zhao ZQ, Li MC, Lu T, An XS, et al. MicroRNA biomarkers of Parkinson's disease in serum exosome-like microvesicles. Neurosci Lett. 2017;644:94–9.

186. Uwatoko H, Hama Y, Iwata IT, Shirai S, Matsushima M, Yabe I, et al. Identification of plasma microRNA expression changes in multiple system atrophy and Parkinson's disease. Mol Brain. 2019;12(1):1–10.

187. Botta-Orfila T, Tolosa E, Gelpi E, Sànchez-Pla A, Martí MJ, Valldeoriola F, et al. Microarray expression analysis in idiopathic and LRRK2-associated Parkinson's disease. Neurobiol Dis. 2012;45(1):462–8.

188. Ravanidis S, Bougea A, Papagiannakis N, Maniati M, Koros C, Simitsi AM, et al. Circulating Brain-Enriched MicroRNAs for Detection and Discrimination of Idiopathic and Genetic Parkinson's Disease. Mov Disord. 2020;35(3):457–67.

189. Infante J, Prieto C, Sierra M, Sánchez-Juan P, González-Aramburu I, Sánchez-Quintana C, et al. Comparative blood transcriptome analysis in idiopathic and LRRK2 G2019S-associated Parkinson's disease. Neurobiol Aging. 2015;38:214.e1-214.e5.

190. Craig DW, Hutchins E, Violich I, Alsop E, Gibbs JR, Levy S, et al. RNA sequencing of whole blood reveals early alterations in immune cells and

gene expression in Parkinson’s disease. Nat Aging. 2021;1(8):734–47.

191. Droby A, Artzi M, Lerman H, Hutchison RM, Bashat D Ben, Omer N, et al. Aberrant dopamine transporter and functional connectivity patterns in LRRK2 and GBA mutation carriers. npj Park Dis. 2022;8(1):1–7.

192. Van Nuenen BFL, Helmich RC, Ferraye M, Thaler A, Hendler T, Orr-Urtreger A, et al. Cerebral pathological and compensatory mechanisms in the premotor phase of leucine-rich repeat kinase 2 parkinsonism. Brain. 2012;135(12):3687–98.

193. Gonzalez-Cano L, Menzl I, Tisserand J, Nicklas S, Schwamborn JC. Parkinson's Disease-Associated Mutant LRRK2-Mediated Inhibition of miRNA Activity is Antagonised by TRIM32. Mol Neurobiol. 2018;55(4):3490–8.

194. Gehrke S, Imai Y, Sokol N, Lu B. Pathogenic LRRK2 negatively regulates microRNA-mediated translational repression. Nature. 2010;466(7306):637–41.

195. Simón-Sánchez J, Schulte C, Bras JM, Sharma M, Gibbs JR, Berg D, et al. Genome-wide association study reveals genetic risk underlying Parkinson’s disease. Nat Genet. 2009;41(12):1308–12.

196. Nalls MA, Pankratz N, Lill C, Do C, Hernandez D, Saad M, et al. Large-scale meta-analysis of genome-wide association data identifies six new risk loci for Parkinson’s disease. Nat Genet. 2014;46(9):989–93.

197. Satake W, Nakabayashi Y, Mizuta I, Hirota Y, Ito C, Kubo M, et al. Genome-wide association study identifies common variants at four loci as genetic risk factors for Parkinson’s disease. Nat Genet. 2009;41(12):1303–7.

198. Herzig MC, Kolly C, Persohn E, Theil D, Schweizer T, Hafner T, et al. LRRK2 protein levels are determined by kinase function and are crucial for kidney and lung homeostasis in mice. Hum Mol Genet. 2011;20(21):4209–23.

199. Faraldi M, Gomarasca M, Sansoni V, Perego S, Banfi G, Lombardi G. Normalization strategies differently affect circulating miRNA profile

associated with the training status. Sci Rep. 2019;9(1):1–13.

200. Marabita F, De Candia P, Torri A, Tegnér J, Abrignani S, Rossi RL. Normalisation of circulating microRNA expression data obtained by quantitative real-time RT-PCR. Brief Bioinform. 2016;17(2):204–12.

201. Vigneron N, Meryet-Figuière M, Guttin A, Issartel JP, Lambert B, Briand M, et al. Towards a new standardised method for circulating miRNAs profiling in clinical studies: Interest of the exogenous normalisation to improve miRNA signature accuracy. Mol Oncol. 2016;10(7):981–92.

202. Sánchez-Rodríguez A, Martínez-Rodríguez I, Sánchez-Juan P, Sierra M, González-Aramburu I, Rivera-Sánchez M, et al. Serial DaT-SPECT imaging in asymptomatic carriers of LRRK2 G2019S mutation: 8 years' follow-up. Eur J Neurol. 2021;28(12):4204–8.

203. Sierra M, Martínez-Rodríguez I, Sánchez-Juan P, González-Aramburu I, Jiménez-Alonso M, Sánchez-Rodríguez A, et al. Prospective clinical and DaT-SPECT imaging in premotor LRRK2 G2019S-associated Parkinson disease. Neurology. 2017;89(5):439 LP – 444.

204. Artzi M, Even-Sapir E, Shacham HL, Thaler A, Urterger AO, Bressman S, et al. DaT-SPECT assessment depicts Dopamine depletion among asymptomatic G2019S LRRK2 mutation carriers. PLoS One. 2017;12(4):1–13.

205. Schenck CH, Boeve BF, Mahowald MW. Delayed emergence of a parkinsonian disorder or dementia in 81% of older men initially diagnosed with idiopathic rapid eye movement sleep behavior disorder: A 16-year update on a previously reported series. Sleep Med. 2013;14(8):744–8.

206. Ouled Amar Bencheikh B, Ruskey JA, Arnulf I, Dauvilliers Y, Monaca CC, De Cock VC, et al. LRRK2 protective haplotype and full sequencing study in REM sleep behavior disorder. Park Relat Disord. 2018;52:98–101.

207. Berg D, Borghammer P, Fereshtehnejad SM, Heinzel S, Horsager J, Schaeffer E, et al. Prodromal Parkinson disease subtypes — key to

understanding heterogeneity. Nat Rev Neurol. 2021;17(6):349–61.

208. Schilsky RL. Personalised medicine in oncology: the future is now. Nat Rev Drug Discov. 2010;9(5):363–6.

209. Drescher CW, Shah C, Thorpe J, O'Briant K, Anderson GL, Berg CD, et al. Longitudinal screening algorithm that incorporates change over time in CA125 levels identifies ovarian cancer earlier than a single-threshold rule. J Clin Oncol. 2013;31(3):387–92.

210. O'Dwyer ME, Druker BJ. Status of bcr-abl tyrosine kinase inhibitors in chronic myelogenous leukemia. Curr Opin Oncol. 2000;12(6):594–7.

211. Hall S, Orrù CD, Serrano GE, Galasko D, Hughson AG, Groveman BR, et al. Performance of αSynuclein RT-QuIC in relation to neuropathological staging of Lewy body disease. Acta Neuropathol Commun. 2022;10(1):1–13.

212. Rossi M, Candelise N, Baiardi S, Capellari S, Giannini G, Orrù CD, et al. Ultrasensitive RT-QuIC assay with high sensitivity and specificity for Lewy body-associated synucleinopathies. Acta Neuropathol. 2020;140(1):49–62.

213. Groveman BR, Orrù CD, Hughson AG, Raymond LD, Zanusso G, Ghetti B, et al. Rapid and ultra-sensitive quantitation of disease-associated α-synuclein seeds in brain and cerebrospinal fluid by αSyn RT-QuIC. Acta Neuropathol Commun. 2018;6:1–10.

214. Jecmenica Lukic M, Kurz C, Respondek G, Grau-Rivera O, Compta Y, Gelpi E, et al. Copathology in Progressive Supranuclear Palsy: Does It Matter? Mov Disord. 2020;35(6):984–93.

215. Robinson JL, Lee EB, Xie SX, Rennert L, Suh E, Bredenberg C, et al. Neurodegenerative disease concomitant proteinopathies are prevalent, age-related and APOE4-associated. Brain. 2018;141(7):2181–93.

216. Bargar C, Wang W, Gunzler SA, LeFevre A, Wang Z, Lerner AJ, et al. Streamlined alpha-synuclein RT-QuIC assay for various biospecimens in

Parkinson’s disease and dementia with Lewy bodies. Acta Neuropathol Commun. 2021;9(1):1–13.

217. Wilham JM, Orrú CD, Bessen RA, Atarashi R, Sano K, Race B, et al. Rapid endpoint quantitation of prion seeding activity with sensitivity comparable to bioassays. PLoS Pathog. 2010;6(12):e1001217.

218. Weihofen A, Liu YT, Arndt JW, Huy C, Quan C, Smith BA, et al. Development of an aggregate-selective, human-derived α-synuclein antibody BIIB054 that ameliorates disease phenotypes in Parkinson’s disease models. Neurobiol Dis. 2019;124:276–88.

219. Garrido A, Fairfoul G, Tolosa ES, Martí MJ, Green A. α-synuclein RT-QuIC in cerebrospinal fluid of LRRK2-linked Parkinson’s disease. Ann Clin Transl Neurol. 2019;6(6):1024–32.

220. Marras C, Chaudhuri KR, Titova N, Mestre TA. Therapy of Parkinson’s Disease Subtypes. Vol. 17, Neurotherapeutics. Neurotherapeutics; 2020. p. 1366–77.

221. Ayers JI, Lee J, Monteiro O, Woerman AL, Lazar AA, Condello C, et al. Different α-synuclein prion strains cause dementia with Lewy bodies and multiple system atrophy. Proc Natl Acad Sci U S A. 2022;119(6):1–9.

222. Li T, Le W. Biomarkers for Parkinson’s Disease: How Good Are They? Neurosci Bull. 2020;36(2):183–94.

223. Mollenhauer B, Zimmermann J, Sixel-Döring F, Focke NK, Wicke T, Ebentheuer J, et al. Monitoring of 30 marker candidates in early Parkinson disease as progression markers. Neurology. 2016;87(2):168 LP – 177.

224. Dong H, Wang C, Lu S, Yu C, Huang L, Feng W, et al. A panel of four decreased serum microRNAs as a novel biomarker for early Parkinsons disease. Biomarkers. 2016;21(2):129–37.

ANNEX

ANNEX 1. Contribution to other projects of our laboratory during my doctoral thesis

Pérez-Soriano, A., Bravo, P., **Soto, M**., Infante, J., Fernández, M., Valldeoriola, F., Muñoz, E., Compta, Y., Tolosa, E., Garrido, A., Ezquerra, M., Fernández-Santiago, R., Martí, M.-J. and the Catalan MSA registry (CMSAR). (2020) MicroRNA Deregulation in Blood Serum Identifies Multiple System Atrophy Altered Pathways. *Mov Disord*, 35: 1873-1879. DOI: 10.1002/mds.28143 (JCR'20 IF: 10.338 Q1)

Garrido, A., Pérez-Sisqués, L., Simonet, C., Campoy-Campos, G., Solana-Balaguer, J., Martín-Flores, N., Fernández, M., **Soto, M.**, Obiang, D., Cámara, A., Valldeoriola, F., Muñoz, E., Compta, Y., Pérez-Navarro, E., Alberch, J., Tolosa, E., Martí, M.-J., Ezquerra, M., Malagelada, C. and Fernández-Santiago, R. (2022), Increased Phospho-AKT in Blood Cells from LRRK2 G2019S Mutation Carriers. *Ann Neurol*, 92: 888-894. DOI: 10.1002/ana.26469 (JCR'21 IF: 11.274 Q1)

Garrido, A., Santamaría, E., Fernández-Irigoyen, J., **Soto, M.**, Simonet, C., Fernández, M., Obiang, D., Tolosa, E., Martí, MJ., Padmanabhan, S., Malagelada, C., Ezquerra, M., Fernández-Santiago, R. (2022) Differential Phospho-Signatures in Blood Cells Identify LRRK2 G2019S Carriers in Parkinson's Disease. *Mov Disord*. 37: 1004-1015. DOI: 10.1002/mds.28927 (JCR'21 IF: 9.698 Q1)

ANNEX 2. Common and specific differentially expressed miRNAs compared to controls from the discovery analyses of [article 1] and [article 2].

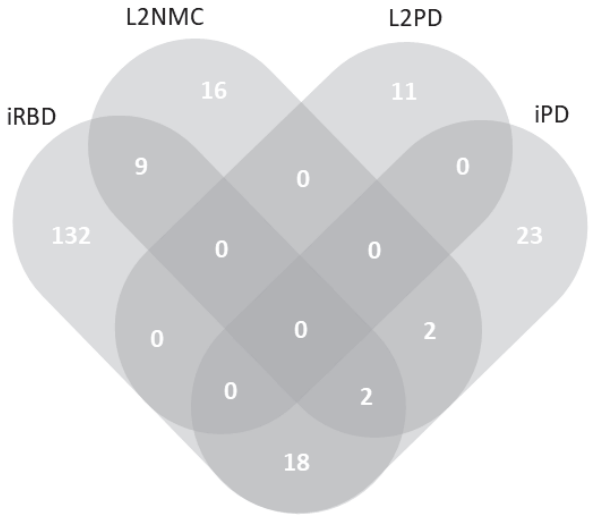

iRBD and L2NMC groups include both DaT-negative and DaT-positive results. iRBD = idiopathic REM-sleep behaviour disorder; L2NMC = LRRK2 non-manifesting carriers; L2PD = LRRK2-associated PD; iPD idiopathic Parkinson's disease